Dissertation

NEW ACTUATION WAVEFORM DESIGN OF DOD INKJET PRINTER FOR SINGLE AND MULTI-DROP EJECTION METHOD

(インクジェットプリンタの高画質化のためのマルチドロップ駆動波形設計に関する研究)

OKE OKTAVIANTY

Graduate School of Science and Engineering
Yamaguchi University
Japan

September 2017

CONTENTS

LIST OF FIGURES

LIST OF TABLES

ACKNOWLEDGEMENT

Oke Oktavianty

Ube City, September 2017

ABSTRACT

The Drop-on-Demand (DoD) inkjet printer that mostly used for the commercial printer is still being developed to improve the performance. The requirements related to the jetting performance, such as drop velocity, volume, and shape become more challenging. The jetting performance needs to be efficiently controlled to make it viable in various applications. Currently, it is necessary to substitute the print-head if using the different fluid. Hence, finding the best operating parameter that can be used in a wider range of fluid properties is necessary to improve its ability in market customization.

The droplet size and shape performance are strongly related to the print quality. The clear spherical droplet without satellite and ligament is required. There are two techniques for improving the print quality related to the resolution, namely binary and greyscale techniques. Recently, the binary technology that generates one smaller drop with the same size is mostly used instead of greyscale technology. The greyscale technology with multi-drop method to generate the different droplet size is still become a big challenge in inkjet printer development. It is difficult to synchronize the multi-pulse in waveform design for getting the optimum result of the droplet performance. The poor droplet performance such as satellite, ligament and weeping occurrence also still become a big problem. The main issue in causing satellite is residual vibration which is unacceptable in some inkjet printer applications and needs to be eliminated. For reducing the residual vibration and obtaining the good droplet performance related to shape, velocity and volume, the actuating waveform to eject the droplet must be properly designed. The comparison with previous study shows that the study using negative pulse and multi-drop ejection method is very limited. Therefore, in this study, the negative pulse of actuation waveform was designed and applied in single and multi-drop concept (Chapter 1).

Theoretical approach concurrently with experimental approach was conducted to design the waveform. The conceptual system model by wave superposition principle was also conducted to predict the total response of waveform (Chapter 2). The good experiment system is important in product development process. Hence, as the beginning step of this research, the measurement method for droplet weight and speed was examined. The experiment standard was determined and used for the next step of this study. In addition, the nozzle checking was also conducted to ensure the properly result of data was obtained from the established experiment system (Chapter 3).

The experimental study using Dowanol as the operating liquid was done to examine the effect of preliminary and suppressing vibration. The basic concept in controlling the droplet behavior was revealed. Furthermore, the simple conceptual system model by wave superposition principle was used to explain the droplet behavior. However, the result still showed an unexpected droplet performance (Chapter 4). The new actuation waveform design was made by using two overlapped pulse as preliminary vibration so-

called "W" waveform. An additional suppressing vibration at the end of pulse and suitable t_{wait} between each pulse is important for the multi-drop design. It was found that the new design in this study is effective to generate clear spherical droplet without satellite, ligament and weeping occurrence. The new waveform design in this study also can deliver the droplet such as push-pull method. It generates the droplet with a bigger volume and lower speed so then called as "push-pull reflection method". However, the droplet speed in single drop can be increased by applying the larger applied voltage. In multi-drop method, it controlled by the suitable adjusted voltage of each pulse. The proposed design is evidently effective until 5 main pulses for two operating liquids namely Dowanol and UV ink (Chapter 5). The edible ink with lower viscosity than Dowanol and UV ink was also used for verifying the effectiveness of waveform design. The modification of "W" waveform was made to improve the droplet performance from the lower viscosity of fluid in multi-drop method. The residual vibration was reduced by rear-ramp deduction of "W" waveform as the preliminary vibration. It was proofed to be effective to avoid the satellite and weeping occurrence and generate the clear spherical droplet. The waveform design is also viable and more flexible to be used for other liquid with different viscosity (Chapter 6). Good performance in droplet shape without satellite, ligament and weeping occurrence give a big contribution in inkjet printer technology and intended to achieve high print quality. The basic concept of controlling the droplet behavior particularly in multi-drop method was summarized. The process of designing the waveform will be easier by using the simple conceptual model of wave superposition principle. As a future challenge, it is important to examine the waveform design in different voltage direction (polar) and different apparatus. (Final Chapter).

CHAPTER I

INTRODUCTION

1.1. Background

One of four components of monozukuri strategy to improve company's profitability is implicit competitiveness. An implicit competitiveness is the factor that cannot be viewed directly by customer. The competitiveness factors are quality, production cost, product development lead time, etc. Enhancing quality and product development productivity is one of an important strategy in improving the company's implicit competitiveness. In this study, the quality issue become our research target with the join research company which has one of substantial products namely Drop-on-Demand (DoD) Inkjet printer [89].

The wide range of application from inkjet printer offers the big opportunities in expanding market [2], [27] & [46], for increasing the company's profitability. However, the customization of current print-head technology is still limited. There is a necessity to develop the print-head technology that can be much more tolerant with the fluid properties [111]. At present, it is necessary to substitute the print-head if using the different fluid. On the other side, for the different model of print-head, requiring the fluid formulation adjustment to get a good result. Therefore, without changing the print-head design, it is very challenging to find the best operating parameter that can be used in a wider range of fluid properties.

The inkjet microdroplets experimental investigation is challenging, because of tiny drop sizes and high speeds of droplets [1] & [3]. The good experiment system is important in product development process. At beginning step of this research, it was found that there is no standardization in fire limitation number to measure the droplet weight in previous research. For droplet weight measurement, it was stated in the previous study that the fire limitation number using 1 million droplets for one data. Nevertheless, it was found that some data using different drops number. In addition, the droplet speed measurement was using 500 μm as the observation distance (droplet stand-off distance). Therefore, the evaluation of previous measurement method for droplet weight and speed was became the first stage to determine the experiment standard for the next step of this study.

As stated before, in this study, we concerned about the print quality from DoD inkjet printer. The printing quality is closely related to quality of the ejected droplet.

Printing quality is influenced by droplet performance related to the droplet speed, shape and volume [1], [2], [6], [16] & [39]. Printing speed and droplet size control still become a big challenge for jet-printing techniques. The other challenge is, to generate the wider range in droplet volume from same print-head [2], [4] & [5]. There are two techniques to generate the droplet size and increase the print resolution. The most of today's technology using binary technology which generate a single size of droplet. Another technology, sometimes called as grey-scale printing with multi-drop concept, could improves print quality and flexibility without changing the print resolution [5]. In this case, each nozzle is used to print a range of different drop sizes. A variety of techniques have been proposed to implement this technology, such as by changing in the shape of the driving pulse. However, this technique can also produce unwanted drop velocity changes and is very dependent on the nozzle geometry and ink properties.

The other big challenges are to generate the droplet shape with good performance, a clear spherical droplet without satellite and ligament. The optimal droplet is the droplet without satellite [6], [13], [22] & [39] which is unacceptable in some inkjet printer application and necessary to eliminate for high print quality [7]. Satellite is a main drop followed by one or more smaller drops. For controlling the droplet satellite is not easy but necessary for generate high-quality printing [31]. Many studies observed the satellite formation [8] – [16], [23] – [26], [31], [48], [71], [73], [93] & [103]. However, the study about eliminating the satellite effect is still limited.

Chung Wu et. al. deployed the numerical analysis study for investigate the effect of actuating pressure waveform on the droplet behavior include the factors that could influenced the satellite formation. The simulation using triangle bipolar waveform and changed the pressure waveform by applying different voltage. The simulation results showed that the higher amplitude of positive pressure caused the longer tail, higher speed and larger volume of droplet. In contrary, the higher amplitude of negative pressure caused the shorter tail, lower speed and smaller volume of droplet [16].

The other research for satellite observation was conducted by Khalate et.al, who proposed a robust feedforward control by using bipolar waveform. The experiment in that study used 2 mm for paper surface distance from the nozzle. The distance used may allow the satellite to merge with the main drop. In addition, the variation of velocity for each drop still reach 2 m/s and most of the drops have different velocities [14].

One of the requirements of droplet shape performance from PZT inkjet printer particularly in industrial applications are the spherical droplet. The drop-shape performance is also influenced negatively by the formation of tails (ligament) or satellite drops. In this dissertation, the clear spherical droplet without satellite, ligament and weeping occurrence is become the main target to be obtained for achieving high quality of printing result. The drop shape performance with good quality and poor quality (satellite, ligament and weeping occurrence) is shown in Fig. 1.1. This figure shows the spherical droplet for good shape, and the droplet with satellite and ligament for the bad one. The other figure shows the ligament with weeping occurrence. If the satellite and ligaments are formed during the process and it cannot merge to the main drop, then it may impact to the misshaping the printed dot on the substrate. The misshaping of the printed dot is described in Fig. 1.2. It shown that the main droplet that is followed by satellite and ligament, or when there is weeping occurrence, will affect to the final shape of the drop on the substrate. It will influence the final print quality, especially for the fine image that need high accuracy. Figure 1.3 presents the illustration of satellite effect on the substrate.
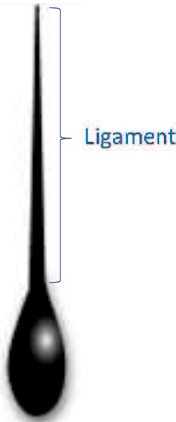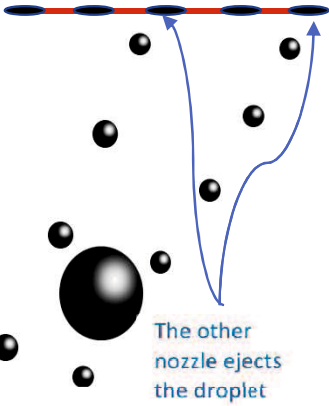
Clear Spherical	With satellite	With ligament	Weeping
GOOD	NOT GOOD		

Fig. 1.1 Droplet shape performance

The preliminary observation for droplet shape that was generated from basic actuation waveform showed that the droplet shapes were not as the expectation. Figure 1.4 shows that the clear spherical droplet was only generated from low applied voltage (14V). The single drop ejection with applied voltage > 14V was the droplets with ligament. Furthermore, it is impossible to deploy the basic waveform from print-head supplier in

multi-drop concept because of weeping occurrence. The comparison between good performance of droplet (small speed variation of droplet from different nozzle) and bad performance (large speed variation) is shown in Fig. 1.5.
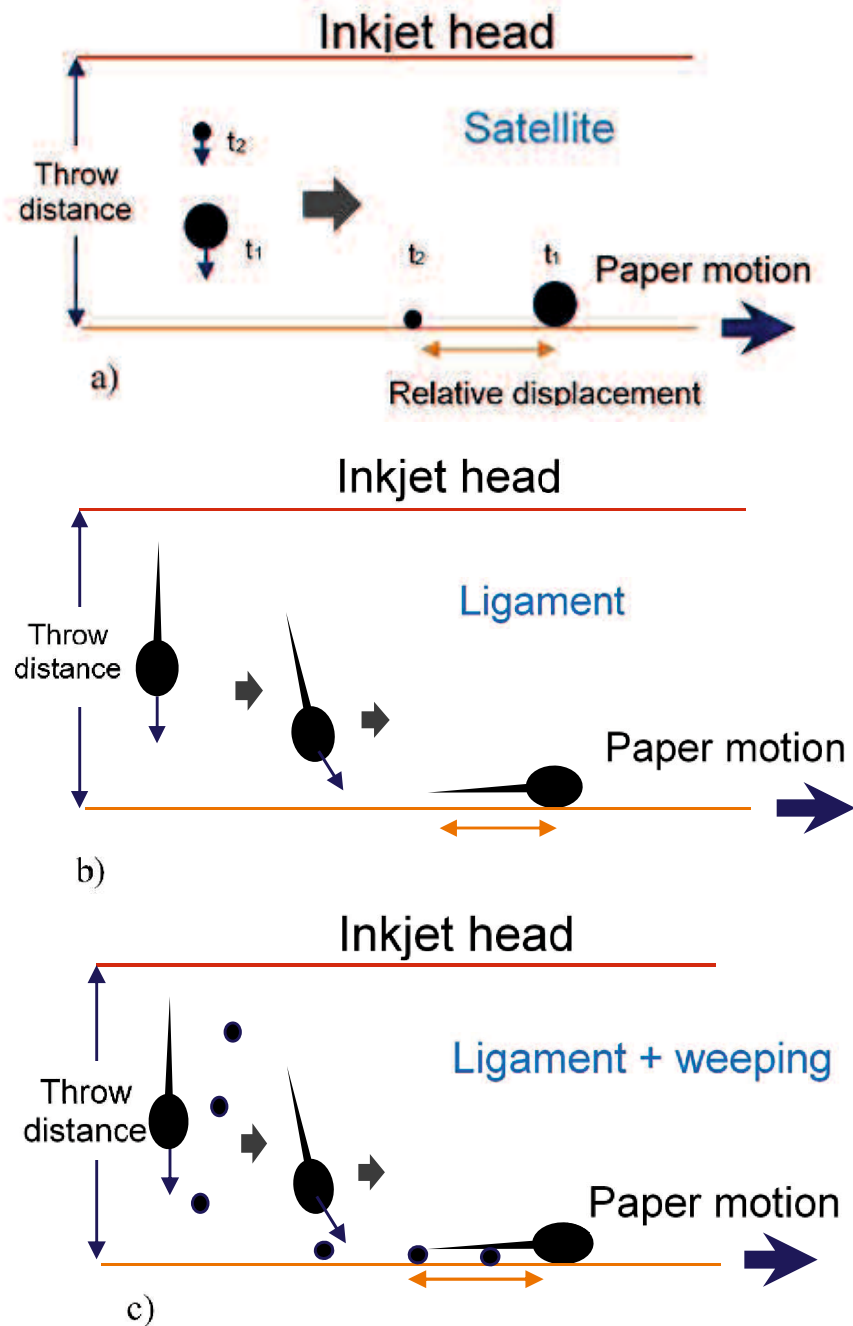
Fig. 1.2 Description of droplet misshaping effect on the paper

(a) satellite   (b) ligament   (c) ligament + weeping

Meeting these performance requirements is severely hampered by the following operational issues that are associated with the waveform design and operation of nozzle heads. For good performance of droplet, the satellite drop and ligament of an ink droplet must be suppressed during the jetting process.
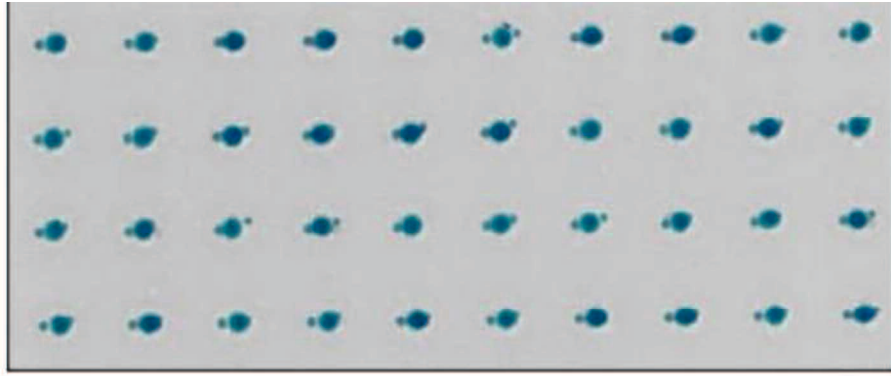
Fig. 1.3 Illustration of satellite effect on substrate
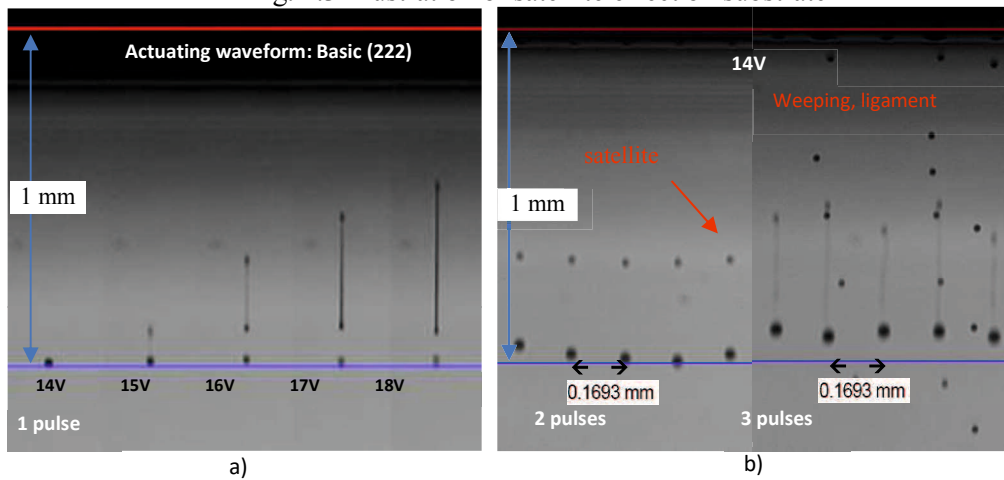
Fig. 1.4 Droplet shape from basic waveform (1- 3 pulse)
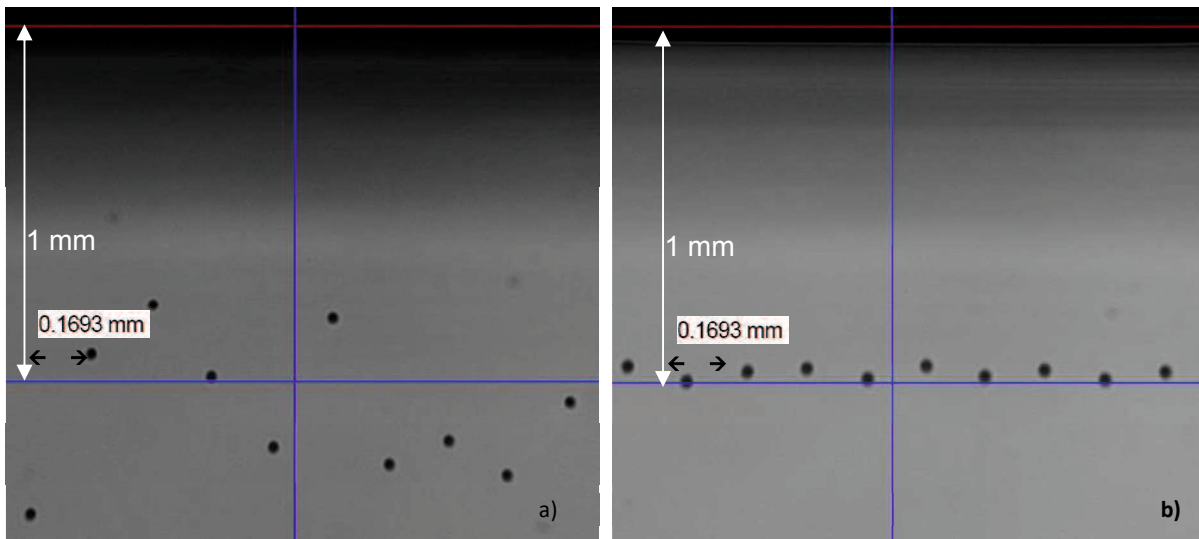
Fig. 1.5 Droplet speed variation (a) Large variation   (b) Small variation

It was stated that the performance of inkjet print-head is mainly affected by residual vibration occurrence [15], [17], [34], [40], [55] & [107]. The residual vibration and crosstalk influence each other particularly in high drop repetition rate. This problem can cause the very large difference in droplet speed [18] & [39]. The actuation waveform of the

piezoelectric element has a strong influence on the droplet ejection process, controlling both the size and velocity of the ejected droplets [22]. For reducing the residual vibration that caused satellite, the actuating waveform to eject the droplet must be properly designed [17], [19], [81] & [82].

It is important to have a good understanding about basic concept of inkjet printer, how it works and how to control it. Many efforts in product research and development were conducted to investigate the responds of droplet formation due to different piezoelectric actuation waveform. Some studies discussed about the droplet formation with different parameters [13], [28] – [30] & [99]. There are two methods to control inkjet drop formation. One method is to modify the jetting material properties such as surface tension and viscosity [13]. The other method is to modify waveform for the driving inkjet head [19], [27], [34], [40], [41] & [93].

In relation with binary technique that mostly used by commercial inkjet printer, it is necessary to generate the single droplet with the smaller size for high print resolution. DoD inkjet print-head generate the droplet with similar diameter to the nozzle orifice [11] & [20]. The droplet volume can be reduced by decreasing the nozzle size [101]. However, the small nozzles are easy to clog [20], [21]. Many studies concerned in controlling or the droplet size or volume [11], [20], [23], [28], [42], [44], [57] & [72]. Gan et al. reported and demonstrated about droplet size reduction by using different actuation waveform. The effect of positive unipolar waveform (until 2 pulses), 2 pulses bipolar (positive-negative) and 3 pulses bipolar (negative-positive-negative) were investigated with different liquid. Gan et.al. stated that the unipolar waveform is the simplest form to generate the droplet and the droplet volume distinctly varied due to different dwelling time and applied amplitude.

Most of the other studies using push pull (positive waveform) and bipolar method as their actuating waveform [8] - [11], [14], [17], [20], [23], [25], [28], [29], [44], [47], [57], [58], [71], [72], [76], [81], [94], [95] & [108]. The bipolar waveform was recommended to reduce the droplet volume particularly in Newtonian fluid. The bipolar waveform was used to remove the residual vibration that affect satellite formation, but the discussion about the effectiveness of the waveform is still limited. The waveform design of previous study is shown in table 1.1. From this table, we can see that most of the study were investigated the single ejection, and few study maximums used 2 main pulses. Furthermore, it also stated that the negative waveform research is still limited [81]. In this

study, we designed the unipolar negative waveform in single and multi-drop ejection, deployed it until 5 main pulses or 5 drops ejection to generate the grey-scale technology.

The effect of applied voltage and head temperature was also investigated to determine the optimum applied voltage that can generate good performance of droplet [11], [15], [20], [23], [29], [71] & [72]. Xu et.al. investigated the effect of high voltage on the charged density, droplet velocity and size, and pinch-off position of single droplet in DoD inkjet Printing [11]. It was stated that the waveform used in this study (positive-negative-positive polar) with higher applied voltage will generate the higher speed and smaller volume of ejected droplet. The result about correlation of applied voltage and droplet size is in contrary with the other researches. On another side, the other research concluded that the higher applied voltage generated the larger volume and speed [15], [20], [23], [29], [95], [98] & [102]. The result of droplet size could be decrease because it only measured the main droplet without observed the ligament or satellite. Noted that the higher voltage could generated the longer ligament and resulted the smaller main droplet size. Therefore, in this study, the optimum applied voltage for generating the good performance of ejected droplet was also investigated, particularly in multi-drop generation.

The way to control the droplet could be easier to know if we have an understanding in the inkjet system for generating the droplet. Many studies developed the simulation model of droplet ejection [16], [24], [25], [42], [43], [44], [45], [46], [48], [49], [56] & [92]. The others simulation model is for modelling the droplet formation process. As mentioned before, the main problem that should be done to improve the droplet performance is by reducing the residual vibration. The mechanism in reducing residual vibration could be known by the wave superposition concept. Therefore, in this study, the simple simulation model was built to predict the response of wave characteristic from different actuating waveform. Subsequently, the wave response from each waveform design was used to explain the mechanism of wave superposition from preliminary and suppressing vibration. The development in simulation model was determined from the experiment result to improve the system model, using modelica software.

1.2 Research Objectives

The inkjet printer quality is related to the print-head performance. The performance of an inkjet print-head is limited by residual vibrations, cross-talk and jet instability that generated the droplet with ligament, satellite or even weeping, particularly in multi-drop.

Those both residual vibrations and cross-talk can be minimized by the properly waveform design [19] & [57]. However, the waveform design that given by the nozzle head supplier in this research still could not as expected.

Therefore, during this research, the basic concept in controlling droplet and finding the key concept to control the droplet, was investigated. It was also focussed to investigate how the design of actuating waveform can help to improve jet stability without weeping occurrence particularly in multi-drop ejection or known as grey-scale technique.

The important aspect from throughout all considerations defined as problem statement:

Propose the experiment standard and new actuating waveform design particularly in multi-drop concept to generate the clear spherical shape of droplet without satellite, ligament and weeping occurrence and improve the droplet performance and quality.

The problem statement can be translated to the following research objectives:

- Evaluate the previous experiment measurement method and determine the experiment standardization for inkjet printer research and development such as actual natural period, fire limitation number for droplet weight measurement and droplet distance from the nozzle for droplet velocity. The correlation between applied voltage and print head temperature are also investigated to determine the optimum operating parameter.

- Investigate the basic concept in controlling droplet velocity and volume by preliminary and suppressing vibration, and propose the optimum parameter and observed the droplet behavior by different input parameter.

- Testing the hypothesis on how to withstand the "water gun" effect in pull-push method of PZT print-head, and how to reduce the residual vibration that generated the droplet with satellite, ligament and weeping occurrence. Propose the new waveform design from combination of preliminary and suppressing vibration in previous method in single droplet and multi-drop ejection. The main target in designing the actuating waveform is "the new actuation waveform design that is able to be applied in multi-drop ejection without weeping occurrence, and generate the clear droplet without satellite and ligament".

- Verified the proposed waveform design with different operating liquid.

- Improve the conceptual system model on inkjet printer to increase the development productivity and easily explain the mechanism of proposed waveform design.

1.3. Outline

The dissertation is organized in the remaining eight chapters:

- Chapter I, is the description about the introduction, related to motivation, previous studies and background of the research. The comparison with other studies including the waveform design. The research objectives and the outline of this dissertation also included in this chapter.

- Chapter II, is about the literature review that related to the research. Start from description about inkjet printing technology and its application, inkjet printer classification, DoD inkjet printer and piezoelectric print-head inkjet printer. The comparison of pull-push and push pull method as a driving pulse mode in PZT print-head was also discussed. The comparison of binary technology for single drop and greyscale technology for multi drop, the requirement of droplet performance and waveform design method by previous studies was used for theoretical approach. The introduction about system model with FEM approach using modelica is also revealed. The conceptual model of print-head with wave superposition principle is explained at the end section of this chapter.

- Chapter III, is about the experiment apparatus that used in this study and IPO (input-Process-Output) od the experiment system. The standardization in inkjet printer experiment as an initial step for conducting the next experiment was discussed. The sub chapter is the experimental study of actual natural period, droplet formation process that related to the droplet observation distance from the nozzle head for velocity measurement, and the fire limitation number experiment for determining the standard of droplet volume measurement. Three basic concepts of waveform namely basic waveform, preliminary vibration waveform and suppressing vibration waveform is explained in detail. The preliminary experiment for obtaining the percentage of base voltage for the preliminary vibration and suppressing vibration pulse is also discussed in this chapter. The conclusion of this chapter is used as standard for subsequent experiment in this study and as proposal for company to improve their experiment system.

- Chapter IV is the preliminary experimental study in building the concept of waveform design. The chapter is discussion about effect of preliminary vibration and suppressing vibration on droplet behavior. The effect of applied voltage and head temperature was also discussed, including the explanation of experiment result phenomenon with wave

superposition concept and mechanism in reducing the residual vibration. The conceptual system model was used to explained the response of each pulse in the waveform design.

- Chapter V is contained of the main concept in controlling the droplet behavior that proposed in this study, as a new waveform design especially in multi-drop concept. The design of actuating waveform in this study is using two overlapped waveforms so called "W" waveform as preliminary vibration, with an additional suppressing vibration at the end pulse of multi-drop concept. The function of "W" pulse as preliminary vibration is to create a large back pressure and functioned as a "soliton", whereas the suppressing will reduce the residual vibration. The comparison between basic waveform from supplier for single and multi-drop concept was discussed. The experiment results show that the proposed waveform design used particularly "W" waveform is effective to determine the high quality of printing result with no satellite, ligament and weeping occurrence even in 5 pulses of actuating waveform. In this chapter, we used two kinds of operating liquids, namely Dowanol and UV ink. The improved droplet controlling method was introduced in UV ink section, by adjusting the percentage of suppressing vibration in higher applied voltage.

- Chapter VI discussed the other improvement of proposed waveform design, introduced the modified "W" design with deducted rear-ramp of original "W" design from previous chapter. The "W" waveform that assumed in two wave-ramps namely front-ramp and rear-ramp. It allows the concept improvement with modified waveform from its original "W" by adjusted rear-ramp to reduce the residual vibration and avoid the satellite and weeping occurrence. A clear and brief concept to control the droplet behavior including velocity and volume particularly in multi-drop ejection intended the high quality and performance of droplet without satellite and ligament. The operating liquid that used in this chapter is Edible ink. The wave superposition principle in reducing the residual vibration and voltage adjustment in designing the actuation waveform can be explained briefly and easier with the simulation model using modelica.

- Chapter VII is conclusion of the whole chapter in this study including the illustration of the actuation waveform design mechanism in multi-drop ejection. The future challenge in optimization of waveform to drive to inkjet printer was also stated.

Table 1.1 Waveform design of previous studies (examples)

No	Author	Title	Observed Parameter	Waveform	Remark
1	Khalate, A.A., et.al, 2011	Performance Improvement of a Drop-on-Demand Inkjet Printhead using an Optimization-based Feedforward Control Method	- Droplet velocity variation (objective is to reduce the variation) - Droplet satellite comparison between standard and actuation pulse	(1) (2)	- There is no clear explanation of the mechanism for effect of each waveform to the satellite formation. - Single droplet only.
2	Shin, P, et.al, 2011	Control of Droplet Formation for Low Viscosity Fluid by Double Waveforms Applied to a Piezoelectric Inkjet Nozzle	Droplet formation with different waveform (single and double) with low viscosity liquid		In single waveform, the satellite and long liquid thread was caused by excessive ejection due to non-damped oscillating pressure. In double waveform, the separating time is an important parameter to eliminate the satellite. - Single droplet only
3	Chung Wu, H., et.al, 2004	Development of a Three-Dimensional Simulation System for Micro-inkjet and its experimental Verification	Droplet morphology, break-up time, flying distance, droplet volume (comparison between simulation and experiment)		If the surface tension of liquid is decrease, the break-up time is longer, length is longer, higher speed, longer tail and the liquid droplet is relatively unstable (vice versa). Single droplet only.
4	Kwon, et.al, 2010 [13]	Experimental analysis of waveform effects on satellite and ligament behavior via in situ measurement of the drop-on-demand drop formation curve and the Instantaneous jetting	Effect of waveform to droplet formation (satellite)		dwell time > efficient dwell time can reduce the satellite. Single droplet only.
5	Jo, B.W. et.al, 2009 [10]	Evaluation of Jet Performance in Drop-on-Demand (DoD) Inkjet Printing	Jet retraction speed at different voltage and different liquid include the satellite observation		Both the optimal dwell time and the maximum stable jetting frequency were affected by viscosity. More viscous liquid is stable up to a higher frequency. single droplet only.

Table 1.1 (continued). Waveform design of previous studies (examples)
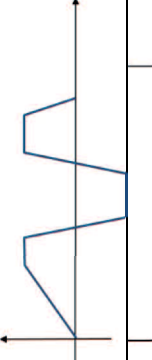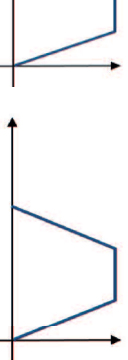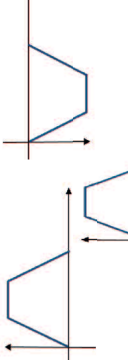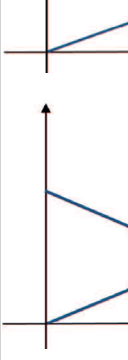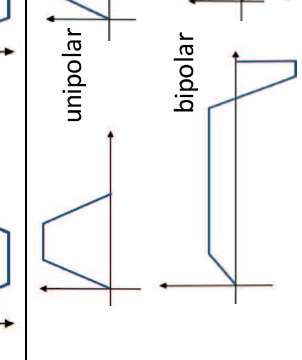
No	Author	Title	Observed Parameter	Waveform	Remark	
6	Xu, C., et. al, 2014	Electric Field-assisted Droplet Formation using Piezoactuation-based Drop-on-Demand Inkjet Printing	Droplet formation, velocity, volume and pinch off location		stated that the increase of applied voltage, droplet speed will increase but droplet size decreased (not in agreement with the other studies	Only measure the main droplet without tail (ligament)
7	Kwon, et.al, 2007	A Waveform Design Method for High Speed Inkjet Printing Based on Self-Sensing Measurement	Jetting performance of different waveform by self-sensing signal		two pulse waveform to suppress the residual vibration, the optimal starting time of 2nd waveform is 1.5x from 1st waveform	Single droplet only.
8	Kwon, et.al, 2009 [81]	Waveform Design Method for Piezo Inkjet Dispenser Based on Measured Meniscus Motion	Meniscus motion comparison from different waveform		Concluded the optimal value of dwell time for each waveform based on maximum meniscus motion for jetting and minimum residual meniscus motion after jetting	the jetting condition such as satellite and volume is beyond the scope and requires further research.
9	Kim, B.H et al., 2012	Dynamic characteristics of a piezoelectric driven inkjet printhead fabricated using MEMS technology	Droplet volume and velocity with different voltage, droplet formation comparison between different waveform		suppressing waveform for reduce the residual vibration related to eliminating the satellite	Single droplet only.
10	Gan, H.Y., et.al., 2009	Reduction of droplet volume by controlling actuating waveforms in inkjet printing for micro-pattern formation	Droplet volume of different liquid and different actuating waveform, and also satellite formation.		The unipolar waveform is simplest but still lead to satellite. M & W shape was designed to minimized the satellite, but the effectiveness of this waveform is not clearly stated.	Single droplet only.

Table 1.1 (continued). Waveform design of previous studies (examples)
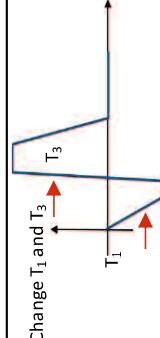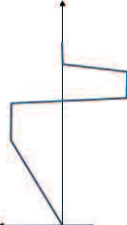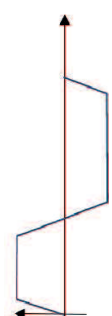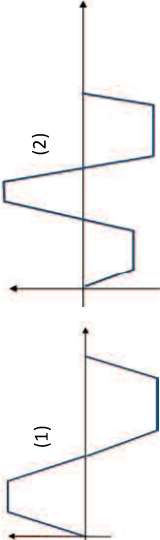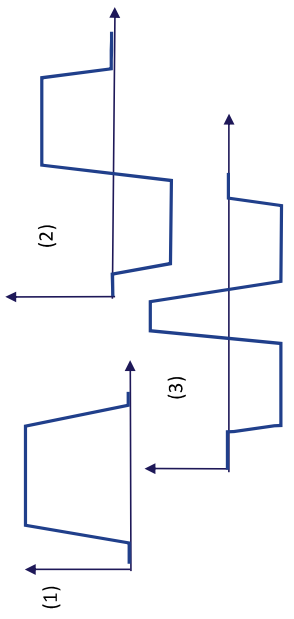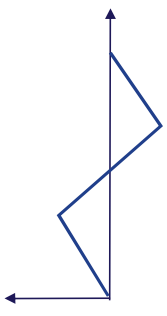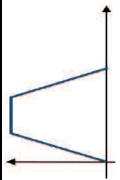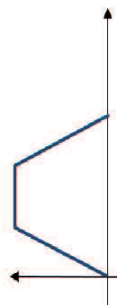
No	Author	Title	Observed Parameter	Waveform	Remark
11	Hsiu, M and Hwang W. S., 2008 [8]	Effects of Pulse Voltage on the Droplet Formation of Alcohol and Ethylene Glycol in a Piezoelectric Inkjet Printing Process with Bipolar Pulse	Droplet formation and satellite occurrence of different fluid and applied voltage		It is concluded that the velocities of the main droplet and satellite droplet in the different voltage ranges are responsible for whether the multiple initial droplets can be recombined. Single droplet only.
12	Miin Liou, T. et.al, 2010 [9]	Effect of Actuating Waveform, Ink Property, and Nozzle Size on Piezoelectrically Driven Inkjet Droplets	Droplet configuration, volume and velocity of different fluid, voltage, waveform and nozzle size	Change T_1 and T_3 $\quad T_3 \quad T_1$	Single droplet only.
13	Lin Tsai, H., et.al, 2015 [28]	Fabrication of Microdots Using Piezoelectric Dispensing Technique for Viscous Fluids	Droplet dimensions by dispensing gap control		Single droplet only.
14	Jiuan Lin, H., et al., 2006 [29]	The Effects of Operating Parameters on Micro-Droplet Formation in a Piezoelectric Inkjet Printhead Using Double Pulses Voltage Pattern	Droplet velocity and volume with different applied voltage, operating frequencies and T_{keep} for different liquid		Single droplet only.
15	Herran, C.L., et.al., 2012 [108]	Performance Evaluation of Bipolar and Tripolar Excitations during Nozzle-jetting-based Alginate Microsphere Fabrication	Comparison of bipolar and tripolar for alginate microsphere fabrication	(1) (2)	The bipolar (1) is more robust in making spherical drop than tripolar particularly for high viscosity fluid (2). The relatively long third dwell time facilitates the spherical drop. Single droplet only. The optimum third dwell time was not defined briefly.
16	Ezzeldin M. et al, 2013 [39]	Experimental-based Feedforward Control for a DoD inkjet Printhead	Design the actuation waveform to reduce the speed variation (objective is less than 1 m/s)		Using negative waveform in second pulse to damp the residual vibration and control the droplet velocity Single droplet only.

Table 1.1 (continued). Waveform design of previous studies (examples)

No	Author	Title	Observed Parameter	Waveform	Remark
17	Chen, A.U., and Basara, O.A, 2002 [42]	A New Method for Significantly Reducing Drop Radius without Reducing Nozzle Radius in Drop-on-Demand Drop Production	Effect of waveform to reduce the Droplet radius (size)	(1) (2) (3)	result: 3) is best, reduce size, but slower. Single droplet only.
18	Chung Wu, H., et.al, 2010 [16]	Effect of Actuating Pressure Waveform on the Droplet Behavior in a Piezoelectric Inkjet	Simulation for investigate the factors that influence the satellite formation		Increasing the amplitude of positive pressure cause the longer tail, larger speed and volume. Increasing the amplitude of negative pressure will cause the shorter tail and smaller volume. There is no verification by experiment
19	Van der Meulen, 2014	Meniscus motion and drop formation in inkjet printing	Meniscus motion and position and droplet formation process, and asymmetries in inkjet system.		The less velocity variation of the larger drops than the smaller one. Only observed the single droplet formation by experiment and simulation.
20	Wei, H., et.al., 2017 [56]	A Waveform Design Method for High DPI Piezoelectric Inkjet Print-head Based on Numerical Simulation	Jetting behavior by different parameter of trapezoidal waveform (by simulation and experiment).	Different dwell time: (1). 3_10_3 (2). 3_16_3 (3). 3_25_3	Using different dwell time to find the optimized driving waveform. Input parameter (2) can successfully jet droplets. Single droplet only. There is no clear explanation about the parameter of optimized waveform

CHAPTER II

LITERATURE STUDY

2.1. Inkjet Printing Technology

Inkjet technology is a family of multidiscipline or different technologies that have a similar function with the precise generation of free-flying fluid droplets. The "precise" term are referring to the droplet volume, the time, the droplet velocity, and the direction of travel. The range of diameter, velocity, and frequency of generation of the droplet obtained, along with the precision, will be varies depending on the specific technology employed [33].

Many application of inkjet technology offered a good opportunity and commercial benefit in expanding market. The example of various inkjet technology implementations namely automotive coatings, plastic part decoration, conductive pattern, Printed Circuit Board (PCB), active Electronics, Radiofrequency Identification (RFID), biopolymers and Cell printing and tissue Engineering [5], [32] and [33]. In Micro-manufacturing, there are chemical sensor, Optical and Bio MEMS (Micro-Electro-Mechanical Systems) devices and assembly and Packaging. The use of inkjet in terms of graphics is the largest application area. The application of inkjet printing was also structured into three main material applications: organic, inorganic and biological area [73]. In 2013, the other author classified current printing business category as shown in Fig. 2.1 [37].
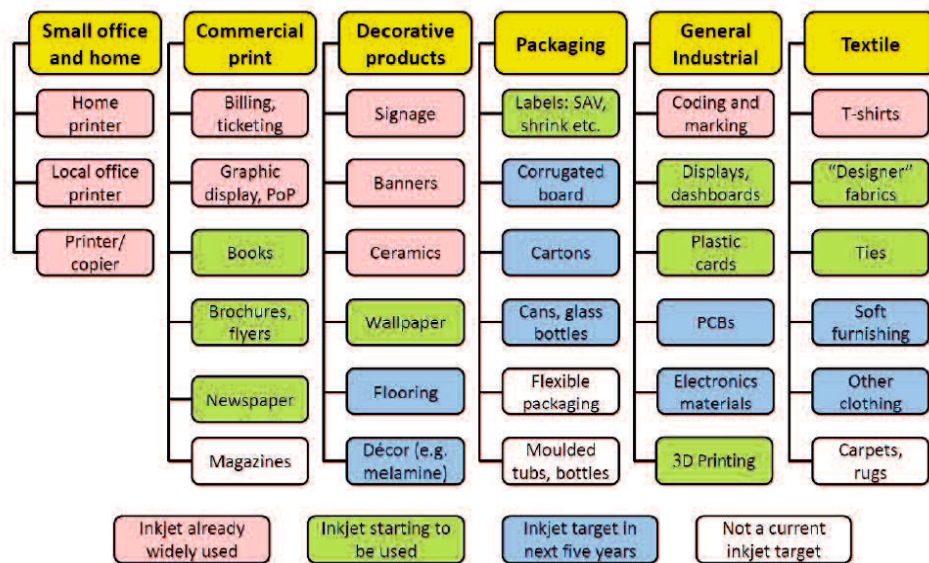
Fig. 2.1 Current classification of the printing business (adopted from [37])

Ink-jet is a printing technology in which tiny droplets are ejected from a small aperture directly to a specified position on a substrate to create an image [32] and [36]. Many different techniques fall under the generic title "inkjet". The most basic common feature is that liquid (possibly also containing particles) is transported from a print-head, across a gap, to a receiving substrate [37].

The inkjet printer can transfer materials as liquid drops without any mechanical contact between the print head and the substrates. The sciences of Inkjet and Droplet are concerned far more about droplet formation from fluid into jets and drops, which travel to and impact the substrate. The droplet then spread and dry or cure [2].

An inkjet system in printer is basically consists of three fundamental components:

- Print engine (print-head)

- Inks

- Imaging medium (e.g., paper, glass, plastics, etc).

Inks produce color by absorbing it selectively and scattering the light. The print engine (print head) operates under digital control and projects the ink droplet with different diameter (depending on the technology), onto the imaging medium to form an image. The modern inkjet systems utilize micro-fabricated print-heads that contain hundreds to thousands of integrated micro-nozzles. A print-head can produce millions of droplets of ink per second with remarkable uniformity in both volume and velocity. The droplets are projected onto the imaging medium with precision placement to render high quality images. The classification of inkjet printing technologies is shown in Fig. 2.2. Inkjet systems broadly fall into two categories, namely Continuous Inkjet (CIJ) Drop-on-Demand (DoD) inkjet. In CIJ, continuous jets of inks are produced at each nozzle by applying pressure in a common ink reservoir. The jets are inherently unstable (Rayleigh instability) and can be modulated using a periodic stimulus to break up into a stream of uniformly spaced droplets.

In DoD system, the droplets are generated by applying a pulse within an ejection chamber that feeds a nozzle. In this study, we use DoD with PZT print-head and push mode of PZT print-head. The comparison of inkjet printing method is shown in Figure 2.3 [54].
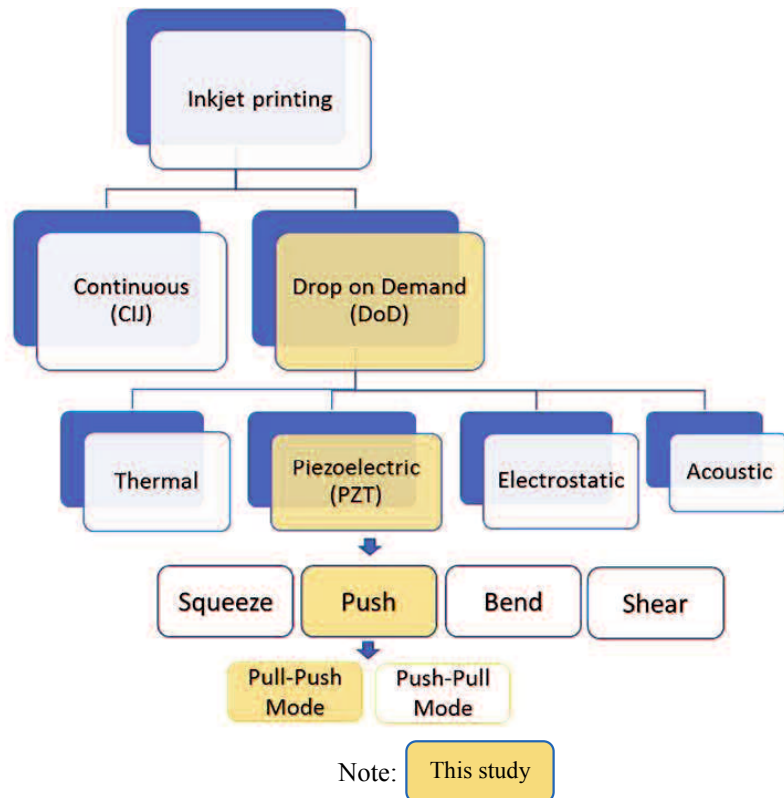
Fig. 2.2 The classification of inkjet printing technology (adopted from [35], [50])
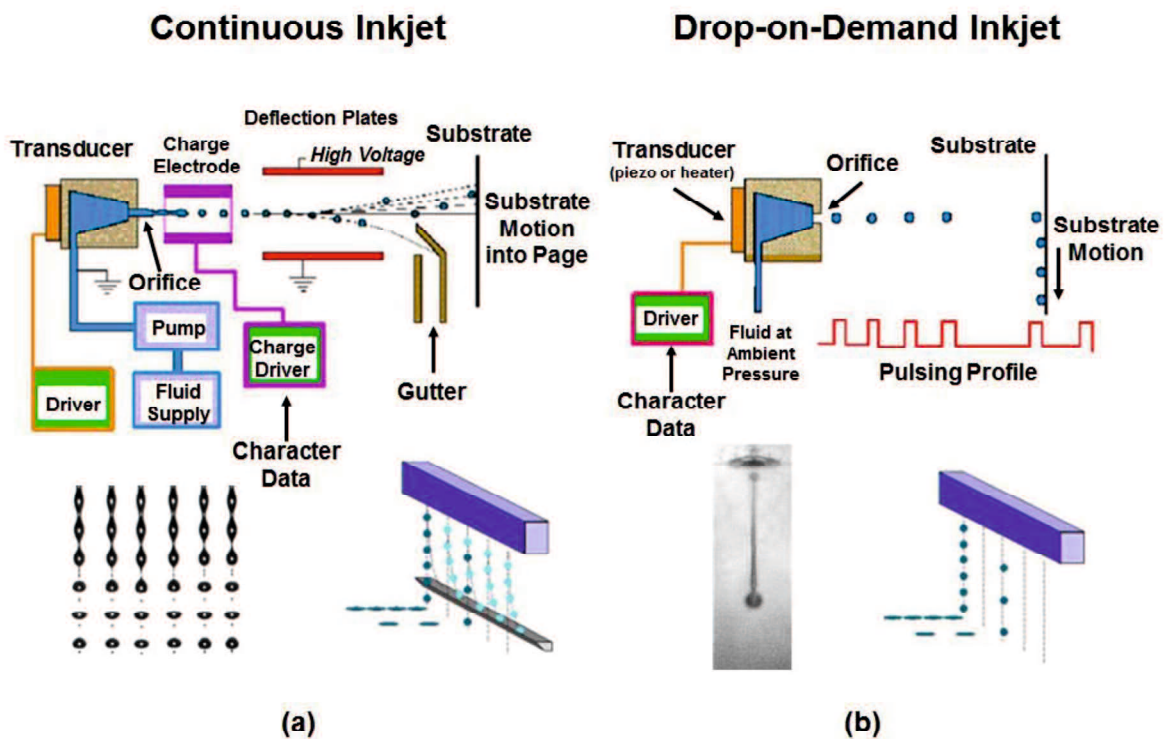
Fig. 2.3 Inkjet printing methods (a) CIJ   (b) DoD
(adopted from [54])

In both the CIJ and DoD methods, the liquid ink flows through a small hole namely "nozzle". The fundamental difference between two methods is about the nature of the flow through the nozzle. In CIJ, the flow is continuous, produces a continuous stream of drops. In DoD, the flow is impulsive, the ink is emitted through the nozzle when it is required. The example of types of flow is shown in Fig. 2.4.

1 mm

(a)

200 μm

(b)
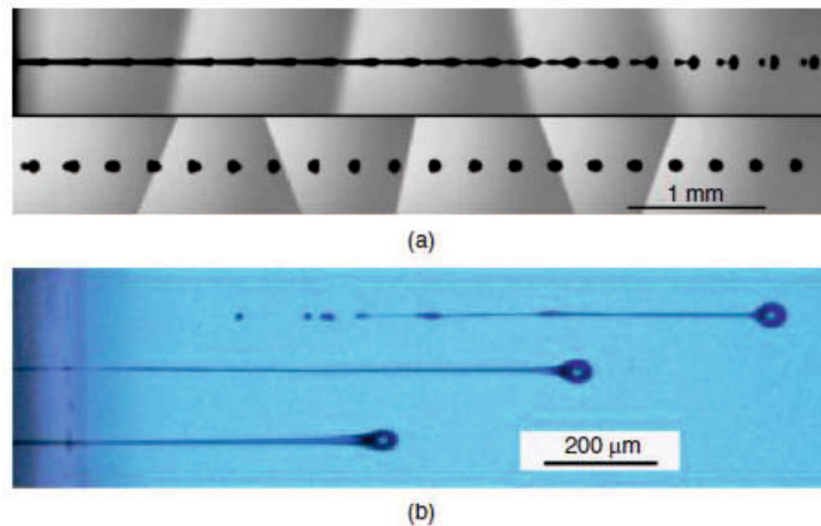
Fig. 2.4 Images of liquid jets moving from left to right adapted from [2]
(a) The break-up of CIJ to form drops (the lower image is a continuation of the upper image
(b) Jet and drop formation in DoD.

From Fig. 2.4., we can see that the main droplet is followed by a long ligament of liquid, which eventually detaches from the nozzle and is pulled toward the head of jet, while, at the same time becoming thinner and, in this case, forming a series of "satellite" drops.

Drop on Demand means that the drop of ink only generated when it needed [105]. Actuation mechanism required with enough energy to generate drop at required velocity to eject and reach substrate successfully. The main advantages of DoD printers compared to CIJ are, in DoD, there is no electrodes charging and deflection, guttering, re-circulation system and break off synchronization [5]. In addition, DoD was stated as the more economical printer than CIJ [99]. DoD method in inkjet technology then classified into 4 techniques;

- Thermal
- Piezo
- Electro Static
- Acoustic

The principle of electrostatic DoD was not used anymore because of its poor quality and reliability. The thermal inkjet has a critical problem such as spreading and bleeding with water-based ink. On the other hand, the main advantages of Piezo Inkjet (PIJ) are its wide variety of material and application [35].

2.2. Piezo Inkjet Print-head

Piezoelectric transducer with a voltage-driven is used to mechanically deform the ejection chamber's wall for ejecting the droplet. When the voltage is applied, it will produce an electric field across layer of piezoelectric material that made the transducer deform [2]. The deformation of transducer causes the volume of ejection chamber to contract or expand, depending on the polarity of the applied voltage. The higher pressure is needed when the chamber contracts, and the lower pressure when it expands.

The development of piezo inkjet print-head was firstly pioneered by C.W. Hanslell of the Radio Corporation of America (RCA) in the late 1940s. He also invented the first Drop-on-Demand (DoD) device. DOD print-heads are categorized according to the mechanism used for droplet ejection. The most of commercial DOD printers utilize either piezoelectric or thermal-based droplet generation [2] & [100]. The categorization of piezo inkjet print-head configurations are as follows:

- Push Mode
- Shear Mode
- Bend Mode
- Squeeze Mode

Piezo DOD print-heads use a voltage-induced deformation of a piezoelectric transducer to produce the pressure pulse needed to eject a droplet [5], [36]. In thermal inkjet (TIJ) printers (also referred to as bubble jet), a resistive heating element is used to superheat the ink within the ejection chamber to generate a homogenous vapor bubble that expands rapidly and provides the pressure needed to eject a droplet.

Push-piezo actuators of PIJ rely directly on the expansion and contraction of a piezoelectric (PZT) rod pushing a membrane, which changes the volume of an ink-filled reservoir behind a nozzle. A cylinder of PZT with a field directed from the outside to the inside will contract radially (squeeze mode). Shear-mode structures have been used to

actuate inkjets. Figure 2.5 shows an arrangement where the fields are arranged so as to cause two regions of shear, creating a wall movement above an ink channel.
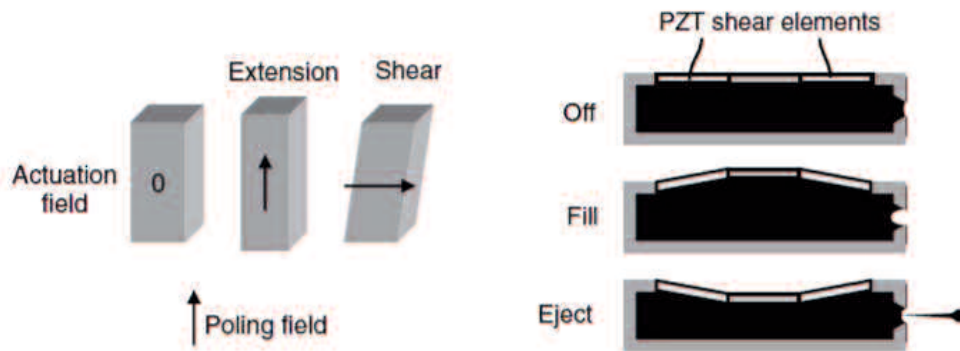
Fig. 2.5 Phases of wall movement in the actuation of shear-mode piezoelectric
(adopted from [5])

The Push-mode and bend-mode of PZT mechanism is shown in Fig. 2.6.
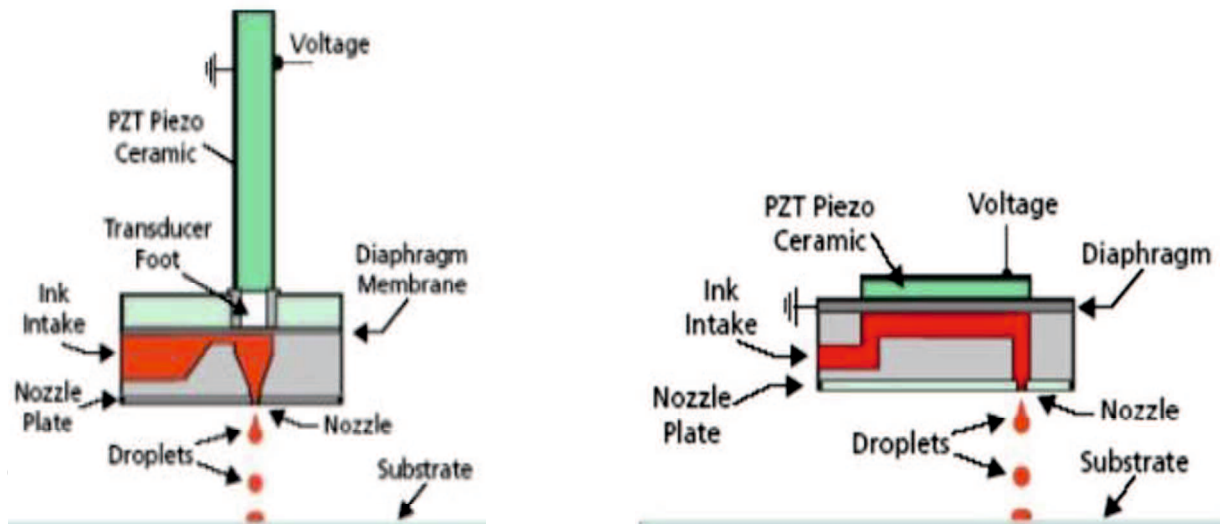
Fig. 2.6 (a) Push-Mode (b) Bend-Mode of PZT (adopted from [87])

2.2.1 Working principle of piezo inkjet printer (PIJ)

The schematic diagram of Piezo inkjet working principle is shown in Fig. 2.7. To fire a droplet, an electric voltage is applied, and the channel cross section will be deformed by the inverse piezoelectric effect. This results in pressure waves inside the channel. The charging of the piezo element enlarges the channel cross section, and the resulting negative pressure wave will be reflected at the reservoir on the left (b). The large reservoir acts as an open end, and the acoustic wave returns as a positive-pressure wave (c). The discharging of the piezo element reduces the channel cross section to its original size. This will amplify the positive pressure wave when tuned to the travel time of this acoustic wave (d). The

channel structure and driving pulse are designed to obtain a large incoming positive pressure peak at the nozzle (e), which drives the ink through the nozzle. Acceleration of the ink movement in the small cross section of the nozzle (conservation of mass and incompressibility) results in drop formation.
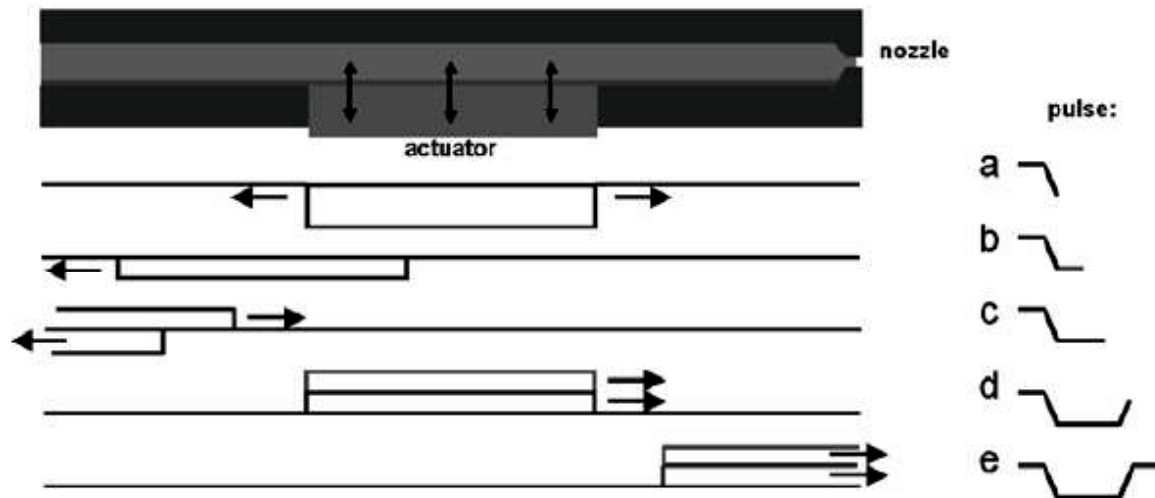
Fig. 2.7 The schematic drawing of the actuation principle (adopted from [35], following [74])

2.2.2 Classification of basic drive pulse in piezoelectric inkjet

The classification of basic drive pulse in piezoelectric inkjet is shown in Fig. 2.8, according to voltage direction and pulse width. There are two main categories of piezoelectric element driving method, namely pull-push method and push-pull method. The third category is the combination of basic drive pulse. According to the voltage direction, forward or positive for push-pull method and backward or negative for pull-push mode, so then the push-pull mode sometimes called as positive waveform whereas the pull-push mode called as negative waveform.

Voltage Pulse width	Voltage change direction		
	Forward voltage direction	*	Reverse voltage direction
Natural period of the liquid room	First basic drive pulse (Push-Pull drive pulse) (maximum mass) (soliton, stable discharge)		Currently ⇒ Not available new proposal Resonance oscillation excavational pulse (Push-Pull reflection drive pulse) (soliton, no-discharge)
Half of the natural period of the liquid room	Third basic drive pulse (Pull-Push-Pull drive pulse) or (Push-Pull-Push)		
	Not available (Excitation of unnecessary vibration）		Second basic drive pulse (Pull-Push drive pulse) (maximum speed)

Fig. 2.8 Classification of the basic drive pulse in piezoelectric

2.2.3 Comparison between Pull-Push Mode and Push-Pull Mode

Yamaguchi et.al. described the comparison of two methods for driving the piezoelectric element [53] & [91]. In Pull-Push method, first stage is the pull mode, when the signal to eject the droplet is received, the applied voltage becomes zero, and piezoelectric element return to its original condition. Then, the negative pressure is generated inside the liquid chamber to increase the volume. This pressure wave at sequent process will be reflected, become a positive pressure to eject the droplet. The second stage, push mode when in one cycle of its operation, the positive pressure wave reflected by the negative pressure that generated inside the chamber, overlapped with positive pressure wave to resonate and eject the droplet. This method produces the higher pressure and generate the droplet with long and narrow droplet with higher speed.

In Push-Pull method, when the signal to eject the droplet is received, the applied voltage will enter the push mode, and the positive pressure will be generated to compress the liquid chamber, and eject the droplet. After the droplet ejection, the piezoelectric element is going to the pull mode, back to the standby mode.

Figure 2.9 shows the difference between pull-push method and push-pull method. Push-Pull method will produce bigger droplet, resulted lower speed with wider column of liquid droplet, whereas pull-push method produces smaller droplet with higher speed and narrow column of liquid droplet.
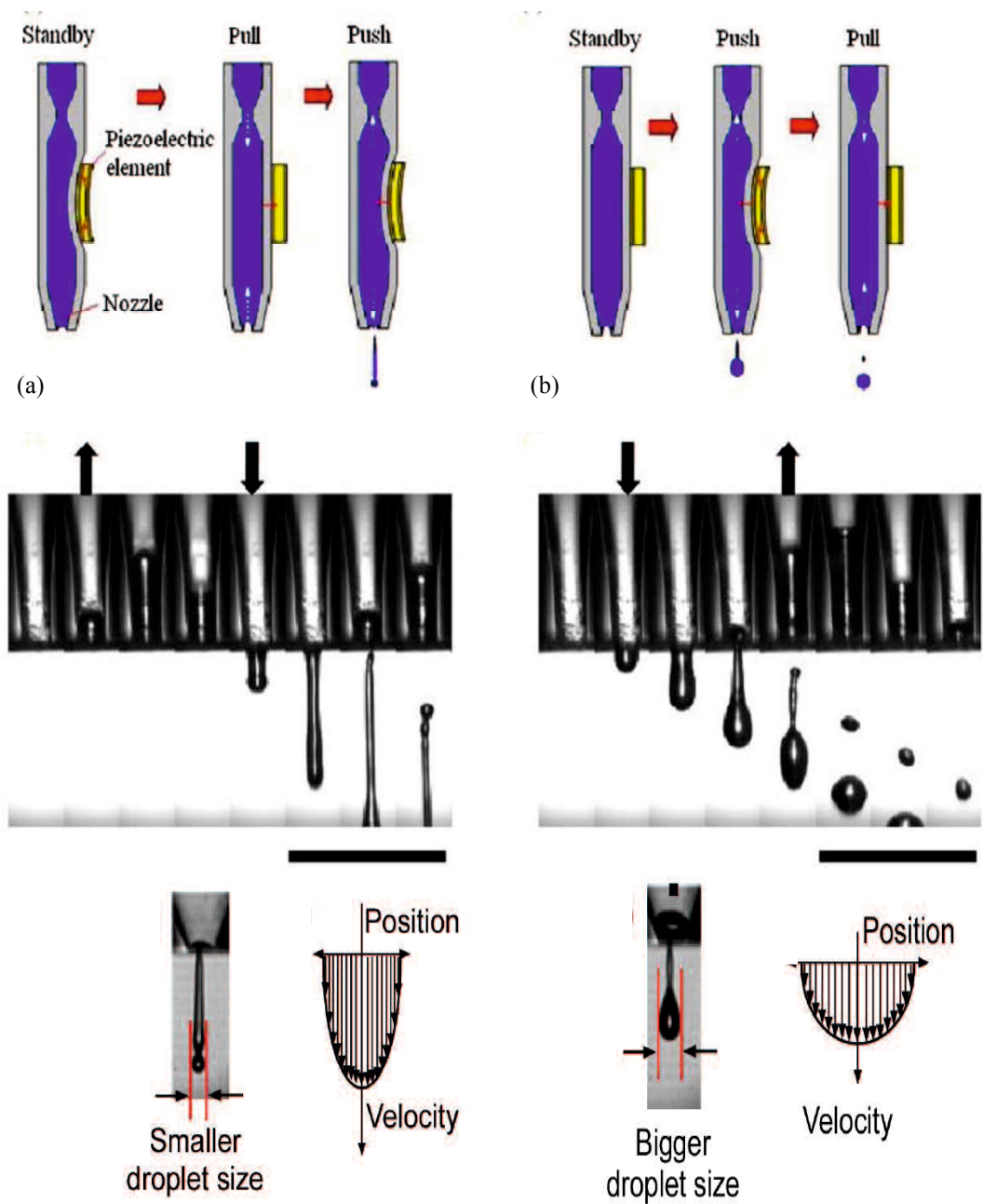
Fig. 2.9 The comparison of piezoelectric element driving method,
a) Pull-push method b) Push-pull method. (Adapted from [53])

2.3 Operational Issue of PIJ Print-head

There are two operational issues that are generally encountered the print-head performance [15], [17], [34], [40], [55]:

2.3.1 Residual vibrations

After a drop ejected from the nozzle, the fluid-mechanics within an ink channel are not at rest immediately: apparently traveling pressure waves are still present. These are

referred to as residual vibrations. The impact of residual vibrations on the drop properties is also influenced by cross-talk effects. The residual vibrations and cross talk do influence each other at high drop repetition rates. This can result in very large differences in drop speed between a single actuated channel and the same channel with the neighboring channels are firing as well [35] & [52].

2.3.2 Cross talk in piezo-inkjet

Cross talk is the effect that neighboring channels can also be influenced by the actuation of a channel. Cross-talk effects via the structure of the print-head are electrical cross talk, direct cross talk, and pressure-induced cross talk. The latter cross-talk effect goes also through the ink domain and another ink-domain-related cross-talk effect is acoustic cross talk via the ink supply. Furthermore, disturbing resonances in the print-head structure can be excited. Finally, the variations in drop properties can become very large when cross-talk effects interfere with residual vibrations in the ink domain. The drop velocity variation that caused by crosstalk is less significant than residual vibration [55]. Crosstalk in piezo-inkjet types are as follows:

- Electrical cross talk

It is obvious that only the channel to which a driving voltage is supplied should be deformed by the piezo-element. However, in many cases some of the neighboring channels are also deformed. When the electric field expands to other channels, an electric cross-talk effect is generated.

- Pressure-induced cross talk

The actuation of a channel results in pressure waves with an amplitude of at least 1–2 bar. These pressure waves will also deform the structure, especially with a soft channel plate material such as graphite. In the third example in Figure 2.10, the deformation is shown of 220 μm wide channels in graphite, covered with a 25-μm tantalum foil. A positive pressure inside the actuated channel results in a deformation of all channels, which is called the *pressure-induced cross-talk effect*.
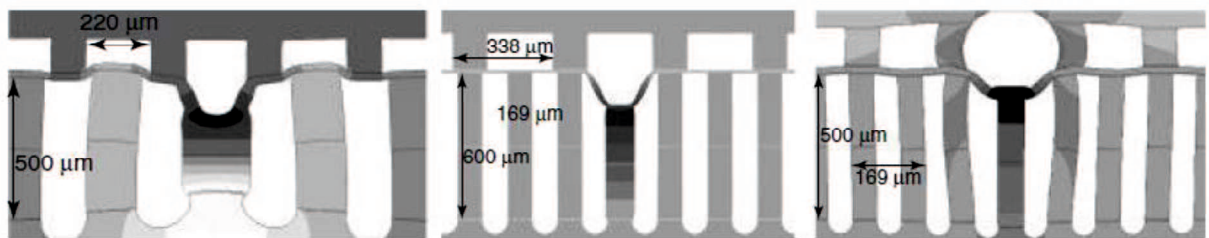
Figure 2.10 Pressure-Induced Cross Talk (adopted from [55])

- Acoustic cross talk

A complete reflection of the pressure waves inside the ink channel at the ink supply or reservoir is very important. Without a complete reflection of the pressure waves, a part of the pressure waves will travel through the supply and the reservoir. The transmitted part of the pressure waves from the actuated channels will enter all other channels as a traveling wave from the supply side of the channels, leading to an acoustic cross-talk effect throughout the whole print-head.

2.4 The Requirement of Droplet Performance

The requirements of droplet performance in Piezo-electric inject printer particularly in industrial applications are as follows [1], [2], [6], [16], [39] & [96];

- Drop-shape.

The drop-shape is influenced negatively by the formation of tails (ligament) or satellite drops. Satellites are the additional drops which are smaller than the main drop that often produced during process of inkjet printing. If the satellite cannot merge with the main drops by the time they reach the substrate as the deflecting field, it will cause the poor print quality or inkjet device part. In this thesis, the clear droplet without satellite and ligament is become the target to be obtained for achieving high quality of printing result. For ligament, if long ligaments are formed during the process and it also cannot merge to the main drop, then the ligament may impact to the misshaping the printed dot. The good spherical droplet shape and bad droplet shape (with satellite, ligament and weeping occurrence) is shown in Fig. 2.11.
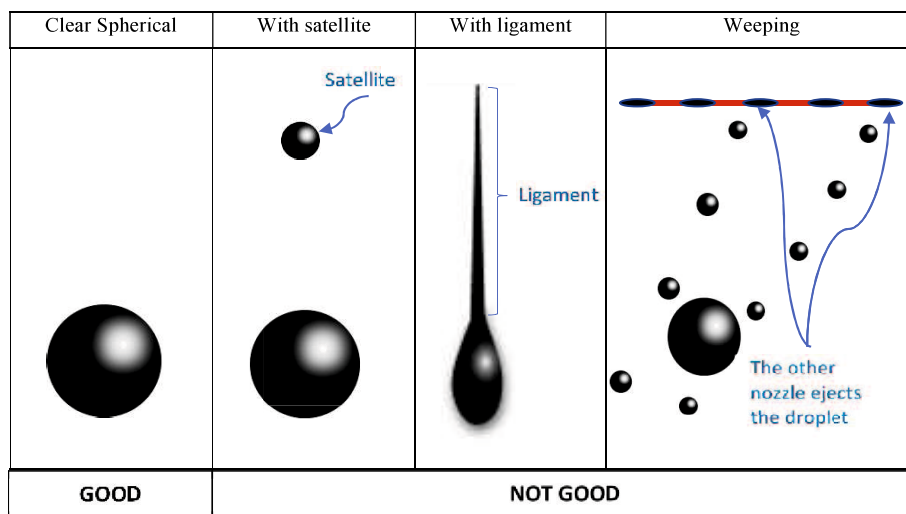
Fig. 2.11 Droplet shape performance

- Droplet velocity.

The requirement of droplet speed is depending on the application. The resulting droplets are required to have a certain speed, typically around several m/s.

- Droplet volume.

The requirement of droplet volume in inkjet printer are typically varies from 5 to 15 picoliter, depending on the application. For some applications, it is required that the drop-size can be varied during operation. For example, for large areas that need to be covered large drops are desired, whereas for high resolution printing small drops are desirable. This is referred to as drop-size modulation. Controlling and generating the wide range of droplet volume by the same nozzle head is one of objectives of this thesis.

- Drop-speed and -volume consistency.

The variations in drop-volume and drop-speed between successive drops and between the nozzles must stay within a certain percentage band, typically ranging from 2 to 15 percent. This is to avoid irregularities in the printed object.

- Jet straightness.

The droplets must be deposed in a straight line to the substrate.

2.5. Resolution and print quality

In graphical inkjet image, the print quality is determined by many factors, such as resolution, drop size, drop shape, ink density, ink color, substrate reflectivity, substrate color, substrate texture, drop position accuracy, type of image and image processing itself. Those factors then can be categorized into 4 following main factors;

- Droplet performance (shape and size)
- Ink
- Substrate
- Image

Print quality related to the droplet size can be improved by using 2 techniques, as shown in Fig. 2.12.

- Using a larger number of smaller drops at a higher resolution (the droplet is only produced in one size, called as binary printer or binary printing technique). The

smaller droplet can improve the resolution by higher dpi (dot per inch) as describe in Fig. 2.13.

- Using grey-scale printing technique, each nozzle is used to print a range of different droplet sizes.
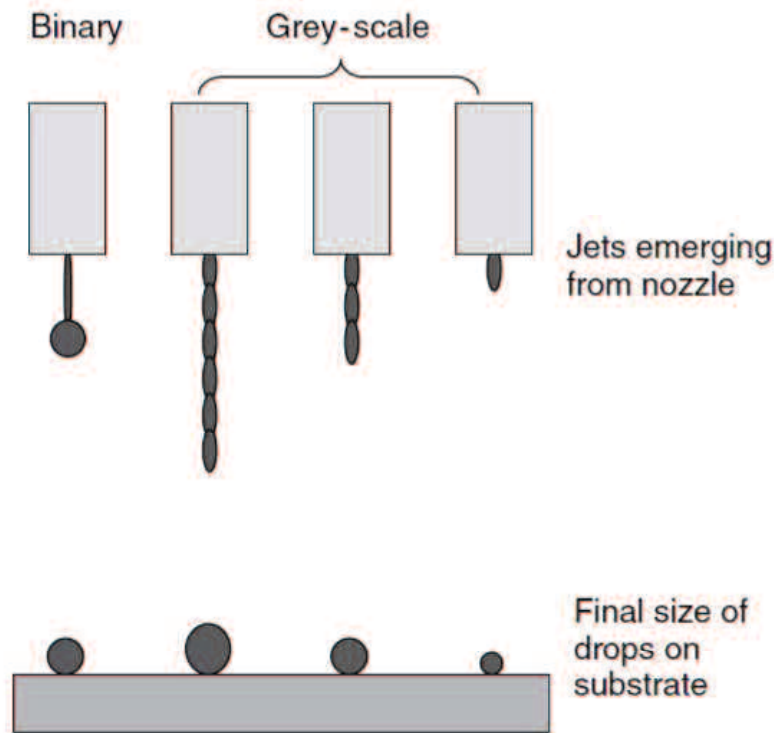
Figure 2.12 Comparison between Binary and grey-scale printing (adopted from [74])

The edges of an image can be formed more precisely with a higher resolution. The higher resolution with binary technique provides the drop positioned flexibility, but need a higher nozzle density. Grey-scale printing technique can improve print quality and flexibility without changing the print resolution. The limitation of this technique is in the number of unique drop sizes which can be obtained and unwanted drop velocity changes [74].

Figure 2.12 describes the grey-scale technique in inkjet printing. The drops commonly following the initial drop and then emerge before the ligament of the first drop had broken off from the nozzle, until the last drops. The velocity of subsequent pulses that used to produce these drops can be adjusted so that the following drops would quickly catch up and merge with the initial drop to form a single drop, before it reaches the substrate. This technique provides a useful to maintain the nozzle densities, potential ink coverage and print speeds, with an ability to considerably improve print quality. The illustration of binary and grey-scale technique farther shown in Fig. 2.14. and 2.15.
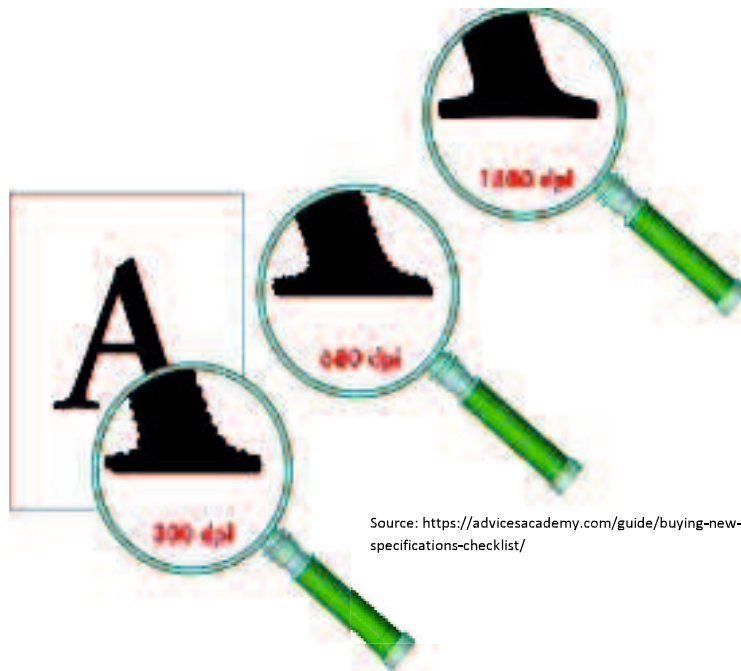
Fig. 2.13 Illustration of different dot per inch (dpi) on printing result
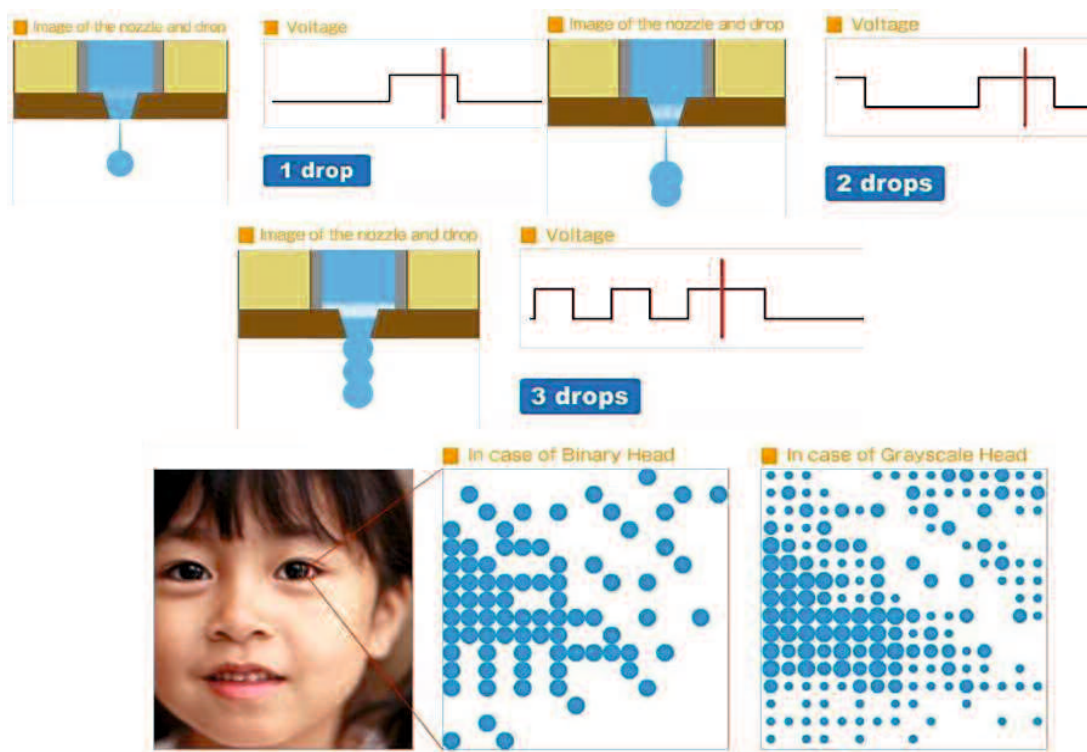
Fig. 2.14 Binary – Grayscale ilustration in inkjet printing (adopted from [87])
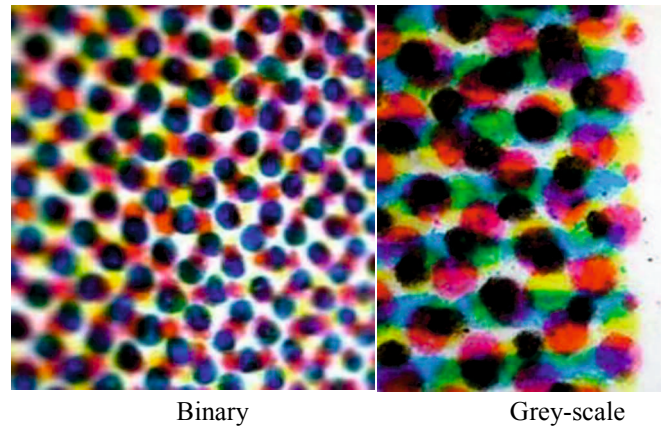
Binary   Grey-scale

Fig. 2.15 Illustration of binary and grey-scale technique

2.6 The Actuation Waveform Design

The actuation pulses are designed to provide an ink drop of a specified volume and velocity under the assumption that the ink channel is in steady state. The inkjet print-head performance is mainly limited due to the residual pressure vibrations. Once the ink drop is jetted, the pressure oscillations inside the ink channel take several microseconds to decay. If the next ink drop is jetted before the residual pressure oscillations have settled, the resulting drop properties will be different from the ones of the previous drop.

2.6.1 Unipolar pulse

To increase the jetting performance and avoid the residual vibration, the input waveform voltage driving the print-head must be properly designed [13, 17, 19]. There are two categories of actuation pulses to damp the residual vibration, namely unipolar and bipolar actuation pulse. The unipolar pulse consists of the jetting pulse for the droplet and an additional trapezoidal pulse of the same polarity as the jetting pulse to damp the residual vibrations. There are two unipolar pulse, with positive polar (push-pull method) and negative polar (pull-push method), as shown in Fig. 2.14. We refer the additional pulse as the quenching pulse due to its objective to reduce the residual vibration by using negative polar. The bipolar pulse consists of the jetting pulse for the ink droplet, and the residual vibration are damped by an additional trapezoidal pulse with opposite polarity to that of the jetting pulse. The parameterization of a unipolar waveform (positive and negative pulse) is shown in Fig. 2.16.

(a) positive (push-pull) waveform

(b) negative (pull-push) waveform
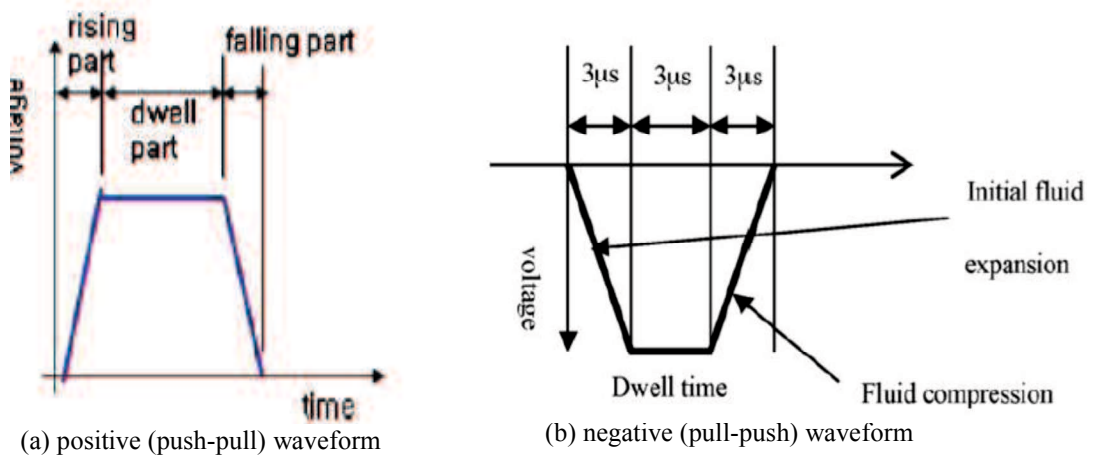
Fig. 2.16 Unipolar waveform (adapted from [13] & [19])

Many studies using the positive (push-pull) waveform design in the inkjet printer research and development [1], [10], [13], [20], [23], [25], [40], [42] and [56]. Most study observed the effect of applied voltage, dwell time and fluid properties with different voltage, frequency, nozzle diameter, etc. It was stated that the unipolar waveform is simplest but still lead to satellite problem. In addition, the dwell time must be carefully selected for optimum result.

Shin et.al compared the single waveform and double waveform in single droplet ejection method as shown in Fig. 2.17. The second pulse in the double waveform design play a role in sucking the liquid thread to reduce the volume, as well the suppressing vibration in this study. In single waveform, several satellites were found by the capillary wave on a long liquid thread but also the successive ejection due to un-damped oscillating pressure wave inside the nozzle. It was concluded that the double waveform is more stable. The separating time between waveform influenced the droplet formation. The suitable time separation between waveform will generate the droplet without satellite. Furthermore, it was found that the droplet size and transient satellite velocity of the low viscosity fluid will behave oppositely to the change of time separation. This study also discussed about the proportional correlation between driving voltage with the droplet size and velocity.
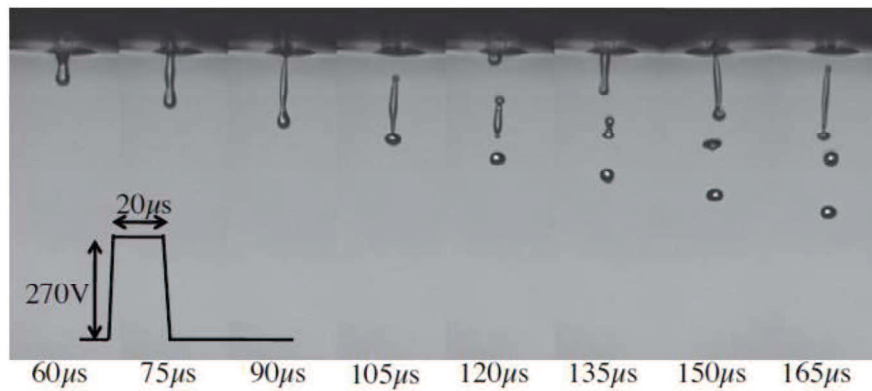
(a) single waveform
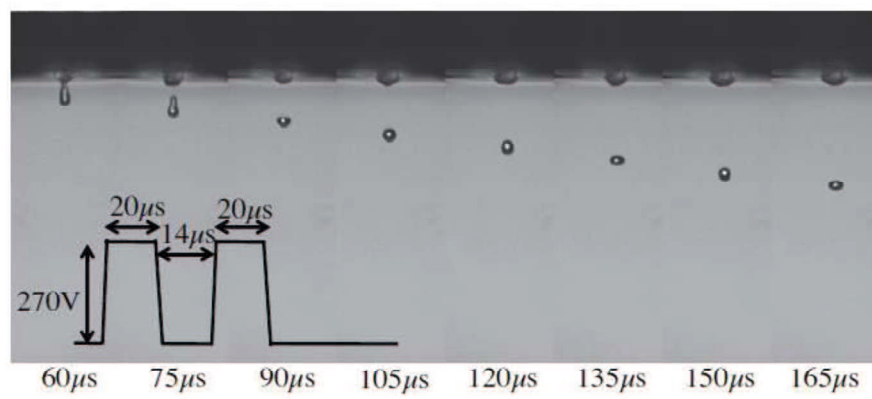
(b) double waveform

Fig. 2.17. Comparison of single and double waveform (adopted from [23])

2.6.2. Bipolar and tripolar pulse

Figure 2.18 shows the comparison of trapezoidal pulse with same polar (positive) is in bipolar (positive and negative). The crucial information in quenching pulse design is the fundamental mode frequency of the inkjet print-head. The fundamental period is possible to measure by measuring the channel pressure with piezo self-sensing, or by observing the meniscus position displacement. It is also possible to measure the period of ink channel by conducting a series of experiments where the droplet velocity is measured as a function of the dwell time of the jetting pulse (t_{rR} + t_{wR} + t_{fR}) is approximately equal to $T_f/2$.   If fundamental period or natural period of the device is known, computation of the time parameters of the actuation pulse can be simplified.
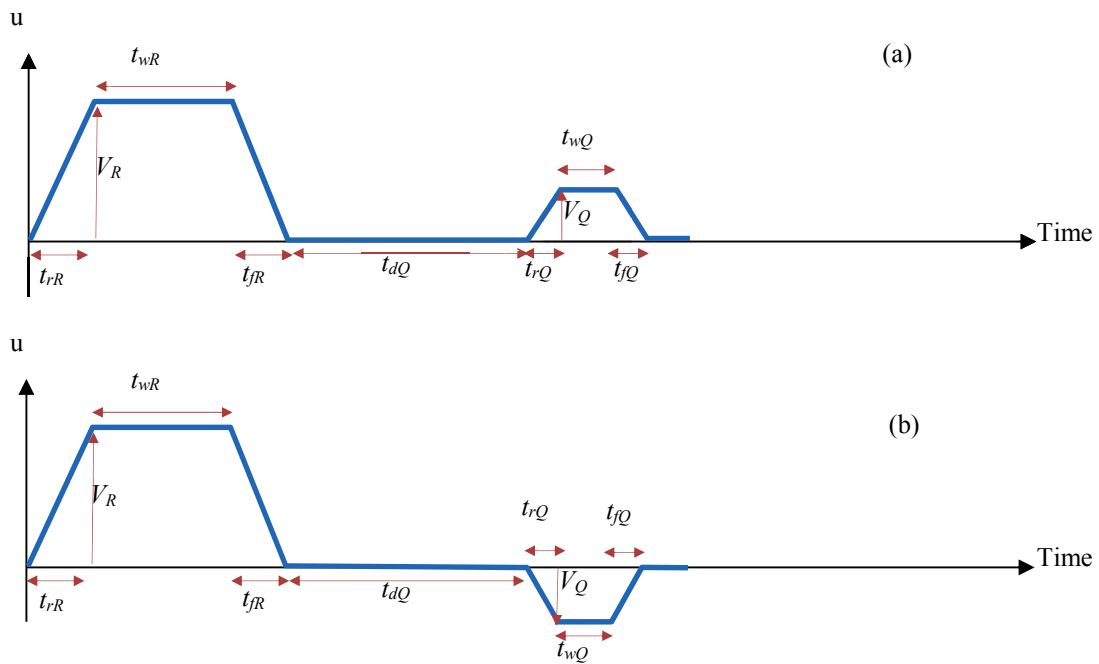
Fig. 2.18. Parameterization of (a) unipolar and (b) bipolar pulse (adopted from [2])

Some researchers using bipolar waveform as the actuation waveform [8], [9], [14], [16], [28], [29] and [39]. The negative pulse is used for damping the residual vibration and control the droplet volume and velocity. Chen et.al compared three waveform designs namely waveform 1 (unipolar positive), 2 (bipolar) and 3 (tripolar), for reducing the droplet size (see Fig. 2.19). The waveform 3 (tripolar) was concluded as the most effective waveform in reducing the droplet size. The third negative pulse will suppress the droplet ejection from second pulse and effective to reduce the droplet size until 45%. The velocity of droplet that was generated from this waveform also lower [42].

Waveform 1)
Unipolar positive

Waveform 2)
Bipolar

Waveform 3)
Tripolar
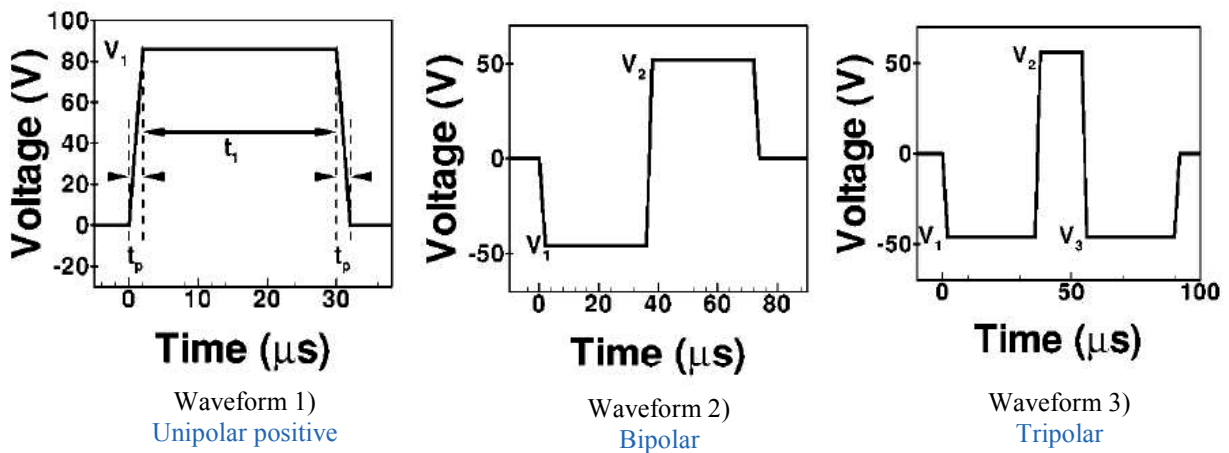
Fig. 2.19. The comparison of waveform (unipolar, bipolar and tripolar)

The other research investigated the effect of waveform design to the droplet behavior, and for reducing the droplet volume [20]. In this study, the bipolar waveform is more recommended due to its relative simplicity compare to the tripolar waveform. The second pulse in bipolar waveform has a function to generate the "suction" effect immediately after jetting (from first pulse), and eliminate the satellite. There is no discussion related to the droplet velocity comparison from each waveform. The bipolar waveform was also recommended by other study as a more robust waveform than tripolar, in making the spherical droplet. This author also discussed about the difficulties to synchronized the multi pulse for resulting the optimum acoustic wave in generating the droplet [108]. The mechanism of tripolar waveform in droplet ejection is shown in Fig. 2.20. It present that the first negative pulse provides the initial energy to "pull" back the liquid inside the chamber, then push out the liquid with the second positive pulse. Subsequently, the third negative pulse play role in pull back the liquid for the final state in one excitation period, before the next firing process. It was stated that the long third dwell time facilitates the spherical droplet formation.
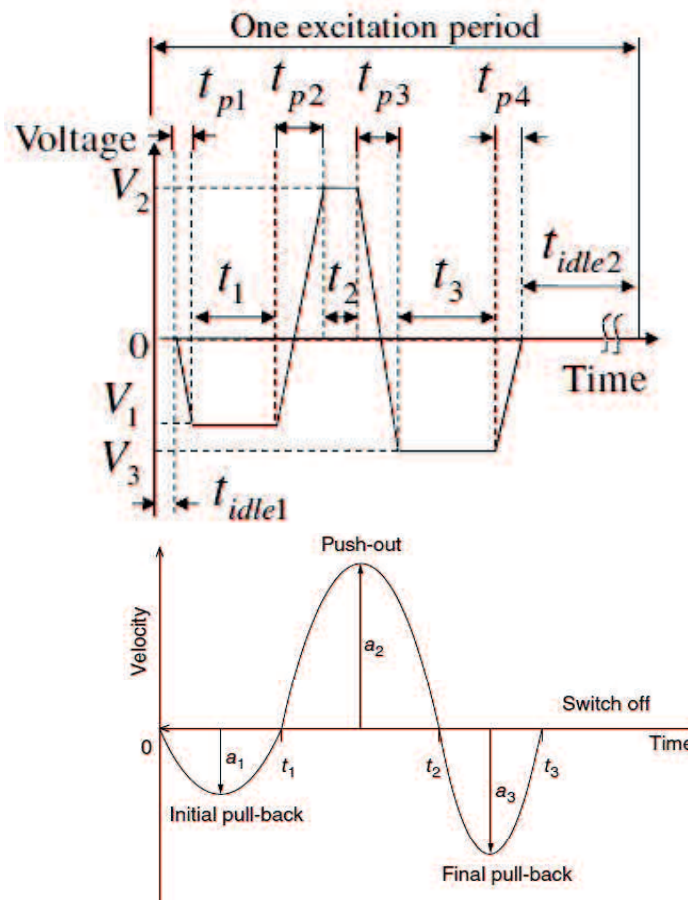
Fig. 2.20 The mechanism of tripolar waveform in droplet ejection (adopted from [108])

33

2.6.3 Jetting speed measurement

The relationship between dwell time (in this study: t_{keep}) and jetting speed is frequently used to determine the optimal jetting waveform [88]. For determining the relationship between dwell time and jetting speed, the others input parameter such as rising time (t_{up}), falling time (t_{down}), voltage, operating liquid and head temperature was set as fixed value. Then, the droplet speed was measure in the experiment. A dwell time that results the highest drop speed is recommended for driving the inkjet print-head. The typical experiment results for jetting speed-dwell time relationship is shown in Fig. 2.21.
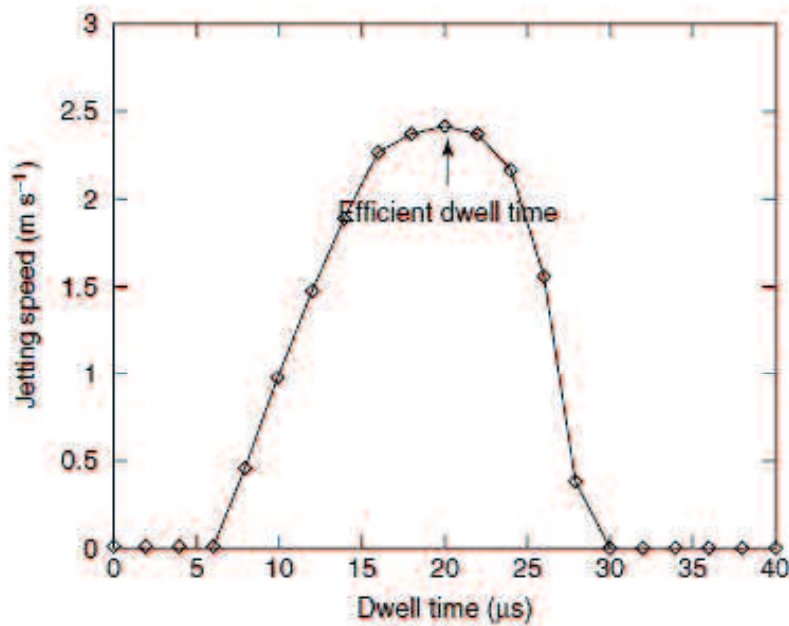
Fig. 2.21 Jetting speed-dwell time relationship (adopted from [13])

2.6.4 Waveform effect on satellite droplets

Kwon, K.S. studied about the waveform effect on the satellite formation in inkjet printing. This study used simplest unipolar positive waveform (push-pull method) as shown in Fig. 2.14 (a). It was stated that the dwell time is a critical parameter and the common method to understand the jetting behavior and its relationship with respect to the waveform uses [13]. The effect of dwell time to droplet shape in droplet formation process is shown in Fig. 2.22.

Kwon, K.S. concluded that the longer dwell time than the efficient dwell time (in natural frequency) is the most effective waveform to suppress the satellite effect. The mechanism of different dwell time compared to the efficient dwell time is shown in Fig. 2.23. The efficient dwell time, in this study, called as natural period). In Fig. 2.23 (b), the

jetting pressure is maximized if the positive pressure waves from both the rising and falling sections are in phase. On the other hand, the dwell time for 180° out-of-phase pressure waves can result in minimizing the positive pressure waves, and there will no droplet ejection in this condition. Note that the first rising section of the waveform generates a negative pressure wave and it takes some time to reach positive pressure at the nozzle.

In Fig. 2.23 (a), when the dwell time is shorter then efficient dwell time, then the falling section will produce the stronger pressure then the rising section. The faster jetting speed will become a main drop while the later of slow speed due to the weaker pressure will become a satellite. If the dwell time use is slightly longer than the efficient dwell time as shown in Fig. 2.23 (c), then the main droplet will be slower than the second droplet as satellite. Therefore, two drops are likely to merge into one drop and produce the final droplet without satellite.
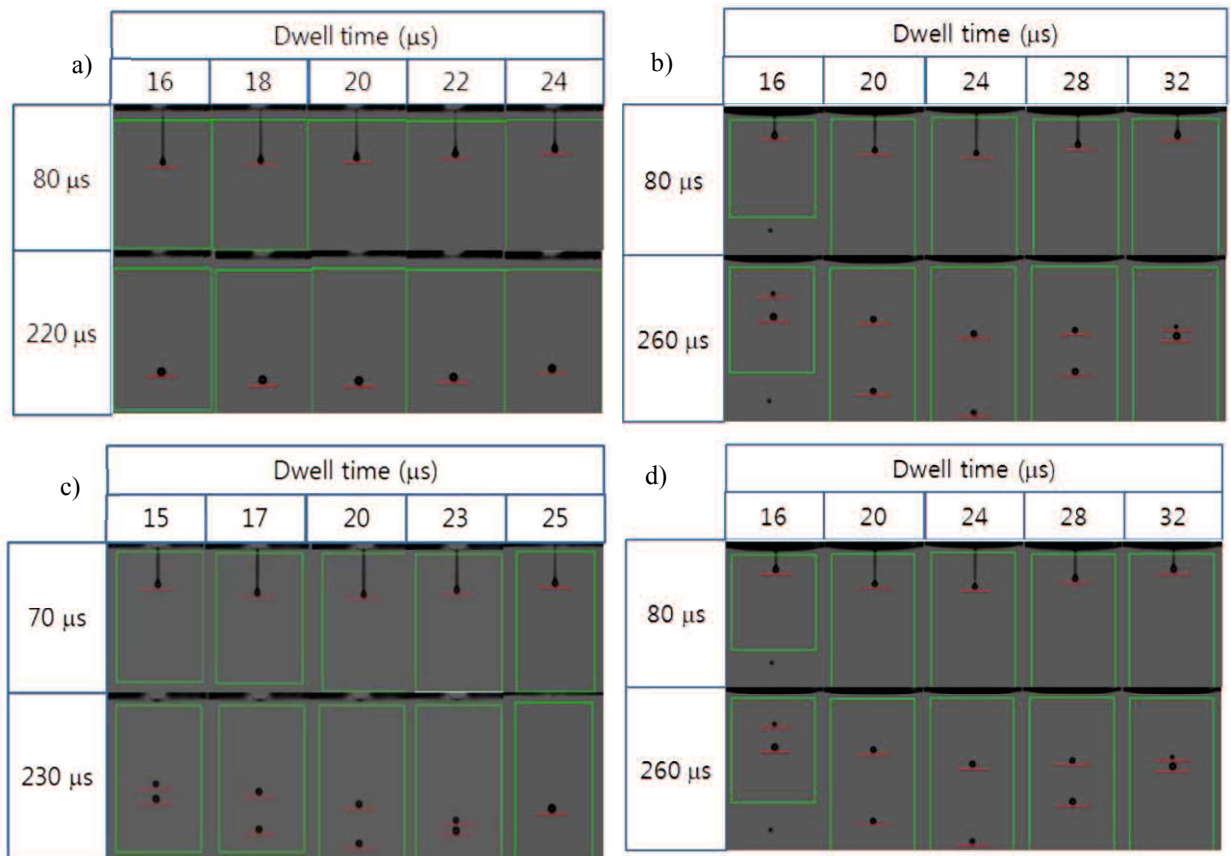
Fig. 2.22 Droplet shape with different dwell time (t_{keep}) and viscosity (adopted from [13])

a)

$t_{dwell} < t_{dwell\_efficient}$

b)

$t_{dwell} = t_{dwell\_efficient}$

c)

$t_{dwell} > t_{dwell\_efficient}$
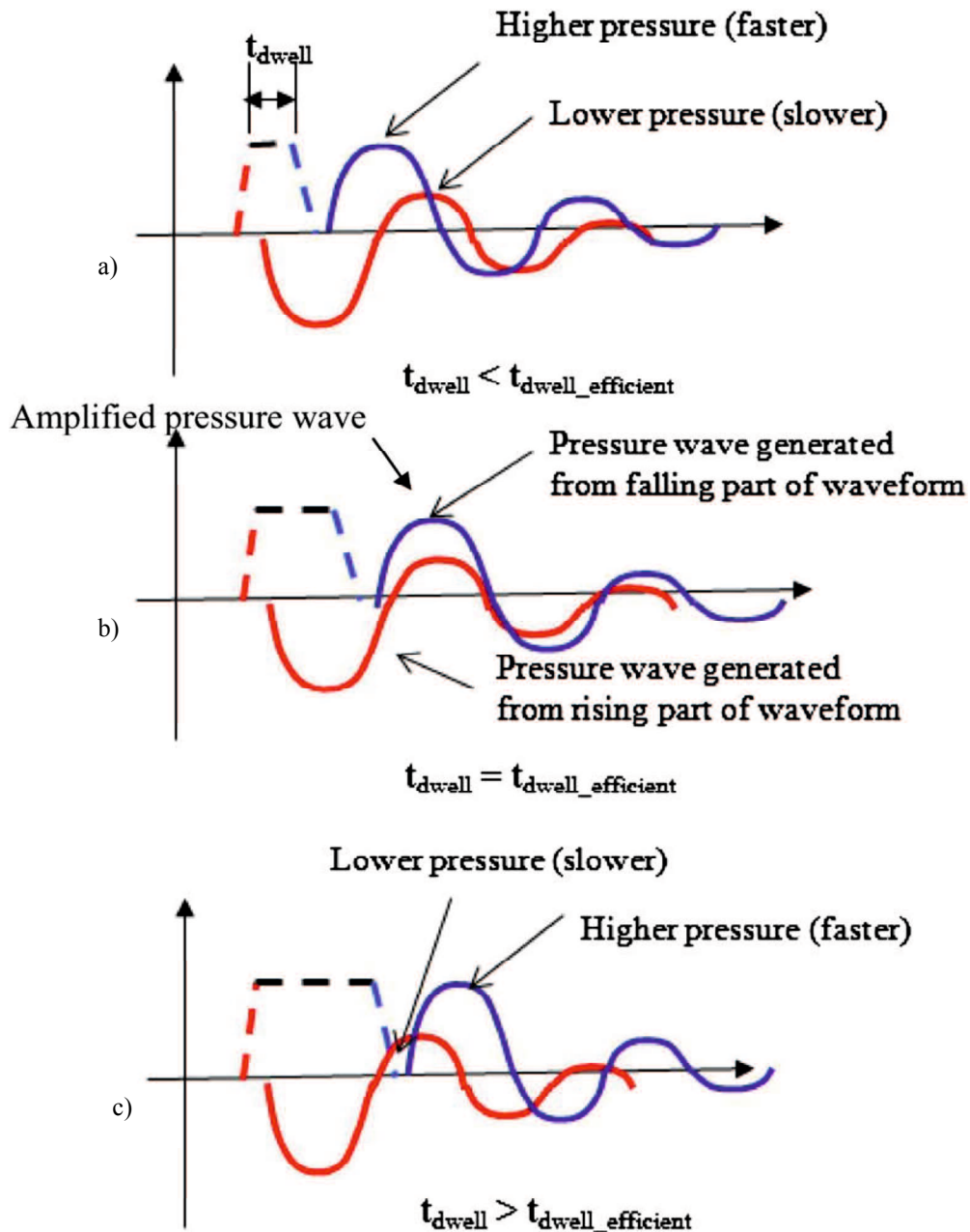
Fig. 2.23 Waveform effect on positive pulse (adopted from [13])

2.7. Droplet speed measurement methods

The shadowgraph technique is primarily used to get the inkjet droplet imaging [70]. The shadowgraph technique is using bright background from light source which is blocked by droplets in the magnified of view. The different parameter in droplet observation must be considered to obtain the precisely data. The droplet image in single nozzle of DoD inkjet printer with different frequency is shown in Fig. 2.24. The measurement approach comparison of droplet speed is shown in Fig. 2.25.
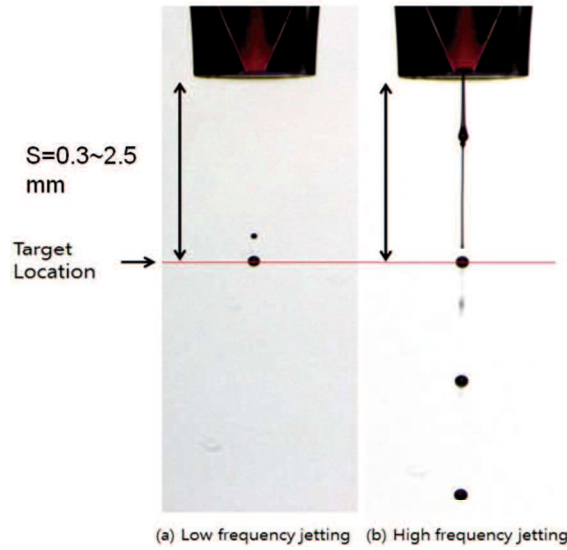
Fig. 2.24 The droplet image from single nozzle of DoD inkjet printer at low and high jetting frequencies (adopted from [71])

Approach 1	Approach 2	Approach 3	Approach 4	Approach 5
Elapsed time T between trigger from print head and droplet reaching specific stand-off distance D	Elapsed time T after jet tip emerges from nozzle until jet tip reaches stand-off D	"Instantaneous speed" determined from distance drops move in short time: U=(D2-D1)/(T2-T1)	Distance D between successive drops at jet frequency F=1/T gives U=D×F	High speed videos of droplet motion
U=D/T usually under-estimates average velocity over flight path	Better estimate, but nozzle plane often not observable for industrial print head	U is tracked with distance from nozzle so is a measure of impact speed at Ď; ΔT strobe: not small	Jetting (or strobe) frequency sufficient for > 1 drop in view. centroid (precision); edges (less precise)	Used for academic studies of droplet trajectories
Early method: for easy comparisons, but low accuracy	Academic method: inkjet trajectory by strobe, video, flash	Edges cope with any ligament; strobed drops (less precise)	Approximate speed for different drops; Double flash precise	HS cameras are too expensive for quite lo spatial resolution

Fig. 2.25 The measurement approach comparison of droplet speed (adopted from [71])

Hoath, S.D. [71] describes the 5 possible approaches for droplet speed measurement standard. The drop speed for approach 1 is obtained from the ratio between stand-off distances (D) with flight time (T) as formula: $U = D/T$. This is the simplest method and the lowest level. This approach is not recommended for high jetting frequency. In approach 2, using the average of droplet speed $U = D/T$ where T is the elapse time between the tip emergence at "zero" distance and the tip reaching D. This approach assuming that the nozzle plane is visible and the emergence time of the jet tips can be established. The speed uncertainties in approach 3 can be found directly from the variance of the double flash

measurements that taken over many drops, whereas the strobe method automatically gives the average speed including this variation (which extends the image length). In order to determine the speed uncertainty for double strobe measurements, the extra analysis could be used by determining the gradients of grayscale profiles for the drop edges in the jetting (length L) and transverse (width W) directions, or from aspect ratio (L/W).

Approach 4 using the distance between the successive drops at f = 1/T. So then the droplet speed become U = Df, used for sufficiently high printing frequencies or relatively slow drops. For double flash measurements, where the same drop can be reliably identified and tracked, direct measurements of position change could offer highest precision speeds provided the timing interval is great enough and the slowing down in air is negligible. This method for speed measurement is a "precision grade" because the variation between the speeds of different drops is eliminated.

Approach 5 is using the high speed and resolution videos to record the droplet motion. This approach is recommended for determining the drop positions or size. Where the inkjet jetting behavior is repeatable, e.g. jet emergence before break-off from the nozzle, single shot image sequences at short regular delay intervals (1-2 μs) are very commonly used to construct "videos" illustrating such jetting behavior with high resolution.

2.8 Ink Classification and the Influence on Print-head and Jetting

The acoustic wave in DoD Inkjet printer are affected by ink properties such as ink viscosity. High viscosity will dampen the acoustic waves that used to generate the drop ejection. On the other side, low viscosity can reduce the damping factor [75] & [76]. Some studies observed the effect of ink viscosity to the droplet behavior [72], [76] - [80], [94], [97] & [99]. Jang et.al. investigated the relationship between physical fluid properties and inkjet printability, stated that the low viscosity fluid is easier to eject the droplet without a significant viscous dissipation but the high surface tension will be detached the retreating filament from the main droplet, forming satellite [76]. Wijshoff concluded that the pinch off time and the shape of droplet's tail is not influenced by the actuating waveform, but by the ink properties [106]. The classification of ink that is used for inkjet printer applications are as follows [5]:
- Water-based ink (aqueous ink)
- Oil-based ink
- UV-currable ink

- Solvent-based ink
- Hot-Melt Ink (Phase-Change ink)

2.9 Inkjet System Simulation Model

There are three techniques for building the system model as shown in Fig. 2.26, namely:

a. White box modeling (deductive modeling), when the whole structure of system is defined clearly and the model can be described by mathematical expression.

b. Black box modeling (inductive modeling), if the whole structure of system is unknown. The input and output data is obtained from experiment. It is impossible to indicate the exact value.

c. Grey box modeling, is the modeling which structure of whole system is partly known and some parameters are unknown. It is still possible to approach the real system by increase the known parameters.
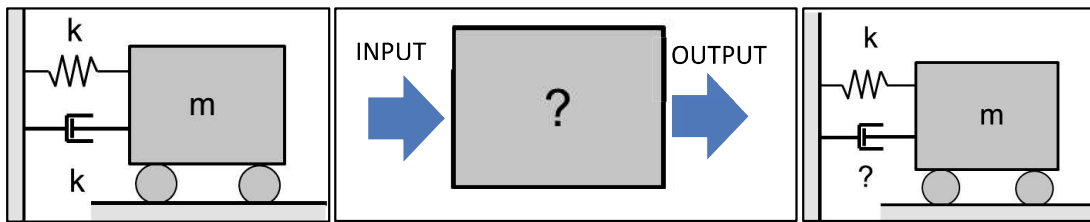
Fig. 2.26 The modeling techniques
(a)   Black box modeling (b) white box modeling (c) grey box modeling

The comparison of white and black box modeling approach is shown in table 2.1 [59].

Table 2.1 Advantage-disadvantage of white and black box modeling

	WHITE BOX MODELING	BLACK BOX MODELING
ADVANTAGE	Potentially more accurate than black box modeling (due to better insight internal circuit operation). It is easier to develop scalable models. For years, the focus of industry and academia (with respect to behavioral modeling) was on the white box modeling approach and therefore, this approach is (usually) more developed (resulting in increased robustness and stability)	Models can be made from measurements (or simulations). Potentially are able to cover a broader spectrum of circuits and systems due to the fact that in black box modeling, they are observed only by analysis of input-output signals. It is not necessary to know circuit / system schematic to model it. Core procedures and methods are the same for all circuits. Hides the circuit details (i.e. it can be sold to customers without revealing (almost) any details about the circuit structure). Developed core modeling procedures and methods can be used on other types of modeling problems.
DISADVANTAGES	Full circuit / system schematic must be known. All device models must be available (if a circuit or system is simulated). It can't be used on measurements. White box model, in general, require more information to build the model.	Complexity of the model is relatively high. Stability and robustness are potentially not as good as in other approaches. Potentially less accurate (due to no actual insight into internal circuit operation). Changes in circuit or device properties necessitate a complete reconstruction of the model.

2.9.1 Physical modeling by Modelica

An important property of systems is that they should be observable. Some systems, but not large natural systems like the universe, are also controllable in the sense that we can influence their behavior through inputs, that is:

- The inputs of a system are variables of the environment that influence the behavior of the system. These inputs may or may not be controllable by us.

- The outputs of a system are variables that are determined by the system and may influence the surrounding environment.

Modelica is an object-oriented equation-based programming language with the ability for defining model libraries with re-usable components and complex applications involving parts from several application domains make it powerful [60], [61]. Modelica is open source software which allows additional tools and algorithm development. It is especially appropriate for academic users [65].

Many advantages of modelica mentioned by some researchers on their paper such as:

‒ Interface is user-friendly, simple and efficient [62].

‒ Well suited for multi domain modeling of large, complex and heterogeneous technical system [63].

‒ A declarative mathematical description in Modelica has simplifier further analysis and the code is become concise and easier to change without introducing error [60].

‒ No particular variable needs to be solved for manually [64], etc.

An article discussed about reasons why most people in their laboratory not using modelica. The reasons are most people that mainly work on control system design think that using other software is a right and sufficient choice, so no need to switch to Modelica. The other reason is, it is much easier to detect and solve numerical problems (example: with Simulink). In addition, even though modelica should be a very appropriate tool, they found that it is difficult to understand. This article also discussed about particular danger when using sophisticated library that occasionally make users forget some basic modeling principles [65]. Hopefully with this paper we can refresh our knowledge in basic modeling principle.

Some difficulties that can be found in understanding Modelica concept is discussed and compared with FEM approach. We propose new approach with FEM concept in textual modeling using Modelica. Many engineers are familiar with this method in the modeling and simulation of advanced engineering systems [66]. FEM has developed into a

key, indispensable technology in various fields. With this study, we expect the right ALD practice (Analysis LED Design) by detailed design engineer who get used with causal model construction (for example: FEM) for learning the acausal model construction technology (for example: Modelica). We want to show that using FEM approach it is easier for beginner to make textual modeling and it also can be used with Modelica software. Comparison between original concept and FEM approach using acausal and causal model is discussed with simulation's result.

2.9.2 Hand translation of simple circuit model with solver ordering system

On this section, some additional explanations about give detail steps for solving the algebraic transformation and sorting procedure [68]. We also propose some revision for making it easier to understand, how to extract the equation from simple circuit model and compare the modelica concept with FEM. In Modelica, process of translation and execution of model sketched in Fig 2.27. Modelica model is change to flat model by translator then using horizontal and vertical sorting as analyzer. The result of sorted equation is optimized by state-space representation. Next stage is Code generator and C compiler and the final is simulation. For Modelica concept, simple circuit model with explicitly labeled connection nodes N1, N2, N3, and N4 and wires 1 to 7 shown on Fig. 2.28.

Depending on whether the variables in connected connector using flow prefix or nonflow (default), there are two types of coupling in Modelica:

- Equality coupling for nonflow variables according to Kirchoff's first Law.
- Sum-to-zero coupling for flow variables according to Kirchoff's current Law.

It is difficult for student to understand the way to extract the equation without any explanation about ordering system and get the extracted result. For making it easier to understand, we make the ordering system to provide variable extracting steps. For modeling a circuit, we must transform the implicit differential algebraic system of equations (DAE system) become explicitly formulated algebraic and differential equations. There are 3 following steps or processes:

1. Horizontal sorting
2. Vertical sorting
3. State space representation

Rules for horizontal sorting:

- The state variables (variables that appear in differentiated form) may be assumed as known variable.
- Equations that contain only one unknown must solved for first. The solved variables then become known variable.
- Solve unknown variable one by one until all variable become known variable.
- Variables that show up in only one equation must be solved for using that equation.
- All rules may be used recursively.
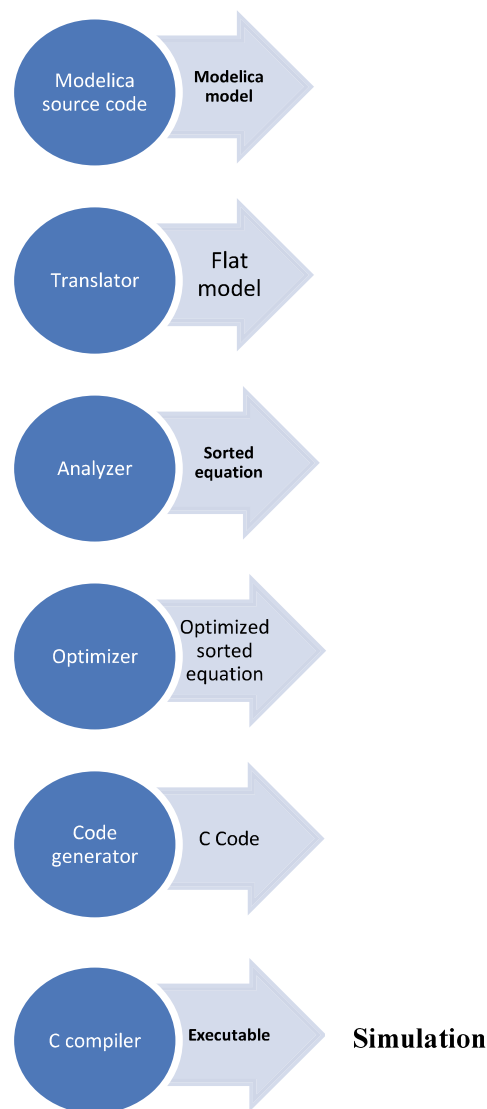
Fig. 2.27 Stages of translating and executing a modelica model
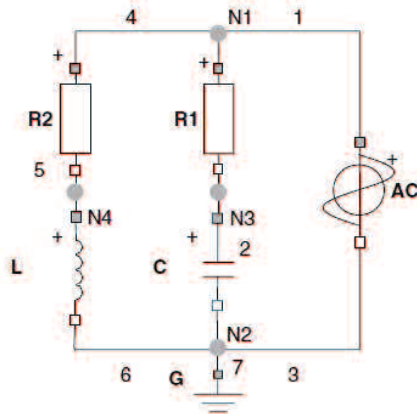
Fig. 2.28 Simple circuit model with explicitly labeled connection for Modelica Concept

- Rules for Vertical Sorting:

We can do vertical sorting for the equations that have become assignment such that no variable is being used before defined. First step, we assume that C.v and L.i as a known variable (temporarily), and algebraically extracting the variables in the vector as equation (1) and (2):

$$C.i = C.C * der\ (C.v) \tag{2.1}$$

$$L.v = L.L * der\ (L.i) \tag{2.2}$$

- Horizontal Sorting

An example for solver ordering system shown on Table 2.2.

Assume that C.v and L.i is available at t = 0 when we start the simulation (t as input and L.i, C.v as state variable). Our horizontal sorting steps are as follow:

- Horizontal sorting is conduct by input (time) and initial value of state variable (L.i and C.v).
- Next target is unknown variable (C.i , L.v), are the variables in the State-space representation.
- We may divide the Horizontal Sort using a middle variable ($R_2.v$, $R_1.v$, $R_1.p.v$) as needed.
- Finally reverse sort and arrange it as an expression chain from the target unknown variable (C.i , L.v).

1) C.i   = C.p.i

2) 0   = R_1.n.i + C.p.i   → C.p.i = - R_1.n.i

3) 0   = R_1.p.i + R_1.n.i   → - R1.n.i   = R_1.p.i

4) R_1.i   = R_1.p.i   → R_1.p.i = R_1.i

5) R_1.v   = R1.R*R1.i   → R1.i = R_1.v / R_1.R

    Then C.i   = R_1.v / R_1.R

Result of Horizontal Sort using a middle variable:

C.i $\quad$ = $R_1.v/R_1.R$ $\qquad$ (2.3)

$R_1.v$ $\quad$ = $R_1.p.v - R_1.n.v$ $\quad$ = $R_1.p.v - C.v$ $\qquad$ (2.4)

$R_1.p.v$ $\quad$ = $AC.VA*\sin(2*AC.f*AC.PI*t)$ $\qquad$ (2.5)

L.v $\quad$ = $L.p.v - L.n.v$ $\quad$ = $R_1.p.v - R_2.v$ $\qquad$ (2.6)

$R_2.v$ $\quad$ = $R_2.R*L.i$ $\qquad$ (2.7)

Table 2.2. An Example for Horizontal Sorting Order for C.i

1) $\quad$ **C.i= C.p.i = -R1.n.i = R1.p.i =R1.i =R1.v/R1.R (Reverse Horizontal sort)**

AC	0	= AC.p.i + AC.n.i	**L**	0	= L.p.i + L.n.i
	AC.v	= AC.p.v – AC.n.v		L.v	= L.p.v – L.n.v
	AC.i	= AC.p.i		L.i	= L.p.i
	AC.v	= AC. VA*sin (2*AC.PI*AC.f * time);		L.v	= L.L*der(L.i)
R1	0	= R1.p.i + R1.n.i ③	**G**	G.p.v = 0	
	R1.v	= R1.p.v – R1.n.v			
	R1.i	= R1.p.i ④			
	R1.v	= R1.R*R1.i ⑤			
R2	0	= R2.p.i + R2.n.i	**wires**	R1.p.v = AC.p.v	// wire 1
	R2.v	= R2.p.v – R2.n.v		C.p.v = R1.n.v	// wire 2
	R2.i	= R2.p.i		AC.n.v = C.n.v	// wire 3
	R2.v	= R2.R*R2.i		R2.p.v = R1.p.v	// wire 4
				L.p.v = R2.n.v	// wire 5
				L.n.v = C.n.v	// wire 6
				G.p.v = AC.n.v	// wire 7
C	0	= C.p.i + C.n.i	**Flow**	0 = AC.p.i + R1.p.i + R2.p.i	// N1
	C.v	= C.p.v + C.n.v	**at**	0 = C.n.i + G.p.i + AC.n.i + L.n.i	// N2
	C.i	= C.p.i ①	**node**	0 = R1.n.i + C.p.i ②	// N3
	C.i	= C.C*der(C.v)		0 = R2.n.i + L.p.i	// N4

Total: 32 equations

- Vertical Sorting

Next step is vertical sorting. The sorting order is shows on Fig. 2.29. The result of extracted variable shown on Table 2.2. The equation then converted to Block Lower Triangular (BLT) as shown on Table 2.3

Result from horizontal sorting

L.i , C.v , t

C.i	= R1.v/R1.R
R1.v	= R1.p.v-C.v
R1.p.v	= AC.AV*sin(2*AC.f*AC.PI*t)
L.v	= R1.p.v - R2.v
R2.v	= R2.R*L. i
der(L.i)	= L.v/L.L
der(C.v)	= C.i/C.C

I

	C.i	= R1.v/R1.R
	R1.v	= R1.p.v-C.v
②	R1.p.v	= AC.AV*sin(2*AC.f*AC.PI*t)
	L.v	= R1.p.v - R2.v
①	R2.v	= R2.R*L. i
	der(L.i)	= L.v/L.L
	der(C.v)	= C.i/C.C

IV

①	R2.v	= R2.R*L. i
②	R1.p.v	= AC.AV*sin(2*AC.f*AC.PI*t)
③	L.v	= R1.p.v - R2.v
④	R1.v	= R1.p.v-C.v
	C.i	= R1.v/R1.R
	der(L.i)	= L.v/L.L
	der(C.v)	= C.i/C.C

V

①	R2.v	= R2.R*L. i
②	R1.p.v	= AC.AV*sin(2*AC.f*AC.PI*t)
③	L.v	= R1.p.v - R2.v
④	R1.v	= R1.p.v-C.v
⑤	C.i	= R1.v/R1.R
⑥	der(L.i)	= L.v/L.L
	der(C.v)	= C.i/C.C

II

①	R2.v	= R2.R*L. i
②	R1.p.v	= AC.AV*sin(2*AC.f*AC.PI*t)
	C.i	= R1.v/R1.R
	R1.v	= R1.p.v-C.v
	L.v	= R1.p.v - R2.v
	der(L.i)	= L.v/L.L
	der(C.v)	= C.i/C.C

III

①	R2.v	= R2.R*L. i
②	R1.p.v	= AC.AV*sin(2*AC.f*AC.PI*t)
	C.i	= R1.v/R1.R
④	R1.v	= R1.p.v-C.v
③	L.v	= R1.p.v - R2.v
	der(L.i)	= L.v/L.L
	der(C.v)	= C.i/C.C

VI

①	R2.v	= R2.R*L. i
②	R1.p.v	= AC.AV*sin(2*AC.f*AC.PI*t)
③	L.v	= R1.p.v - R2.v
④	R1.v	= R1.p.v-C.v
⑤	C.i	= R1.v/R1.R
⑥	der(L.i)	= L.v/L.L
	der(C.v)	= C.i/C.C

VII

①	R2.v	= R2.R*L. i
②	R1.p.v	= AC.AV*sin(2*AC.f*AC.PI*t)
③	L.v	= R1.p.v - R2.v
④	R1.v	= R1.p.v-C.v
⑤	C.i	= R1.v/R1.R
⑥	der(L.i)	= L.v/L.L
⑦	der(C.v)	= C.i/C.C

Summary of verical sorting

Fig. 2.29 Vertical sorting order

Table 2.3 Variable Extracted from Simple Circuit Model for Modelica

Total 32 variables	connector				In component	
State variable : L.i ,C.v	Pin. p		Pin. n		flow	nonflow
R_1	$R_1.p.i$	$R_1.p.v$	$R_1.n.i$	$R_1.n.v$	$R_1.i$	$R_1.v$
R_2	$R_2.p.i$	$R_2.p.v$	$R_2.n.i$	$R_2.n.v$	$R_2.i$	$R_2.v$
C	C.p.i	C.p.v	C.n.i	C.n.v	C.i	C.v
L	L.p.i	L.p.v	L.n.i	L.n.v	L.i	L.v
AC	AC.p.i	AC.p.v	AC.n.i	AC.n.v	AC.i	AC.v
G	G.p.i	G.p.v				

(component — label for the leftmost column group)

Matrix of vertical sorting result is:

$$\begin{Bmatrix} R2.v \\ R1.p.v \\ L.v \\ R1.v \\ C.i \\ der(L.i) \\ der(C.v) \end{Bmatrix} = \begin{bmatrix} 1 & & 1 & & & & \\ & & & 1 & 1 & & \\ & & & & 1 & 1 & 1 \\ 1 & & & 1 & & 1 & \\ & & & & & 1 & 1 \\ 1 & & & & 1 & & 1 \\ 1 & & & & & 1 & 1 \end{bmatrix} \begin{Bmatrix} L.i_0 \\ C.v_0 \\ AC.VA \cdot \sin(\ ) \\ R2.v \\ R1.p.v. \\ L.v \\ R1.v \\ C.i \\ L.i \\ C.v \end{Bmatrix}$$

(2.8)

- State-Space Representation

Next step is make state-space representation. From BLT form, we make state-space representation with 2 cases:

a. Theoretical Case

C.i   =   C.C*der (C.v)

L.v   =   L.L*der (Li)

$$\begin{Bmatrix} \dfrac{dC.v}{dt} \\ \dfrac{dL.i}{dt} \end{Bmatrix} = \begin{bmatrix} \dfrac{1}{C.C} & 0 \\ 0 & \dfrac{1}{L.L} \end{bmatrix} \begin{Bmatrix} C.i \\ L.v \end{Bmatrix} = \begin{bmatrix} \dfrac{1}{C.C} & 0 \\ 0 & \dfrac{1}{L.L} \end{bmatrix} \left(\begin{bmatrix} \dfrac{1}{R1R} & 0 \\ 0 & 1 \end{bmatrix} \begin{Bmatrix} R1.v \\ R1.p.v - R2.v \end{Bmatrix} \right)$$

$$= \begin{bmatrix} \dfrac{1}{C.C}\dfrac{1}{R1R} & 0 \\ 0 & \dfrac{1}{L.L} \end{bmatrix} \left(\begin{bmatrix} 1 & -1 & 0 \\ 1 & 0 & -1 \end{bmatrix} \begin{Bmatrix} R1.p.v \\ C.v \\ R2.v \end{Bmatrix} \right) = \begin{bmatrix} \dfrac{1}{C.C}\dfrac{1}{R1R} & -\dfrac{1}{C.C}\dfrac{1}{R1.R} & 0 \\ \dfrac{1}{L.L} & 0 & -\dfrac{1}{L.L} \end{bmatrix} \begin{bmatrix} 1 & 0 & 0 \\ 0 & 1 & 0 \\ 0 & 0 & R2.R \end{bmatrix} \begin{Bmatrix} R1.p.v \\ C.v \\ L.i \end{Bmatrix}$$

$$= \begin{bmatrix} \dfrac{1}{C.C}\dfrac{1}{R1R} & -\dfrac{1}{C.C}\dfrac{1}{R1.R} & 0 \\ \dfrac{1}{L.L} & 0 & -\dfrac{R2.R}{L.L} \end{bmatrix} \begin{Bmatrix} R1.p.v \\ C.v \\ L.i \end{Bmatrix}$$

$$= \begin{bmatrix} -\dfrac{1}{C.C}\dfrac{1}{R1.R} & 0 \\ 0 & -\dfrac{R2.R}{L.L} \end{bmatrix} \begin{Bmatrix} C.v \\ L.i \end{Bmatrix} + \begin{Bmatrix} \dfrac{1}{C.C}\dfrac{1}{R1R} \\ \dfrac{1}{L.L} \end{Bmatrix} \{ AC.AV * \sin(2 * AC.f * AC.PI * t) \}$$

(2.9)

b. Practical Case

From horizontal result in (3) until (7), we can get the practical case of state-space representation as equation (10).

$R_1.v = R_1.p.v - C.v$

$R_1.p.v = AC.VA*\sin(2*AC.f*AC.PI*t)$

$R_2.v = R_2.R*L._i$

$L.v = L.p.v - L.n.v = R_1.p.v - R_2.v$

$C._i = R_1.v / R_1.R$

$$\begin{Bmatrix} \dfrac{dL.i}{dt} \\ \dfrac{dC.v}{dt} \end{Bmatrix} = \begin{bmatrix} \dfrac{1}{L.L} & 0 \\ 0 & \dfrac{1}{C.C} \end{bmatrix} \begin{Bmatrix} L.v \\ C.i \end{Bmatrix}$$

(2.10)

Table. 2.4 Block lower triangular form of the simple circuit model

	R₂.v	R₁.p.v	L.V	R₁.v	C.i	L.i	C.v
R₂.v	1						
R₁.p.v		1					
L.v	1	1	1				
R₁.v		1		1			
C.i				1	1		
del(L.i)		1				1	
del(C.v)					1		1

2.9.3 Acausal and causal model construction with fem approach using Modelica

a. Comparison between original concept in Modelica and FEM approach

The differences between modelica original concept and FEM approach in stages of translating and executing a modelica model was discussed in accordance with Figs. 2.28 and 2.29. As explained before, in modelica concept, we must conduct the horizontal and vertical sorting as analyzer and get sorted equation. According to FEM approach, it is not necessary to do this stage and make the process become simpler. By using the simple circuit problem as example, it found that in modelica, first model includes all variable

(both known and unknown variables) and difficult to separate. With FEM approach, it is easier to separate known and unknown variable after building the system model.

Problem for beginner in modelica concept is about connector. Particularly in multi domain, it is difficult to understand connector concept because in different domain we must use different connector e.g. in electrical we use pin while in mechanical domain using flange. To connect different domain, we must utilize the special connector. In FEM approach, there is no connector concept, make it easier to understand.

Furthermore, the other difference is we could not use graphical modeling in FEM approach and this matter can be one disadvantages. Admittedly it can sometimes be rather convenient to use graphical modeling compared to textual modeling especially for beginner. Nevertheless, for practical use it is difficult to define connector in multi domain as mentioned before. In FEM approach, we only use textual modeling to solve the problem. However, this approach has superiority in language using for different software. The previous study introduced the semi-Acausal system model using scilab [69]. From this study, we can use the same language or same textual modeling for the other software with acausal model such as acausal model in scilab.

b. FEM approach using Modelica

In this section, we propose Finite Element Methode (FEM) approach as causal model construction for learning acausal model construction technology using modelica. We also show the causal model construction with FEM approach. Graphical modeling with original concept in modelica shows on Fig. 2.30.
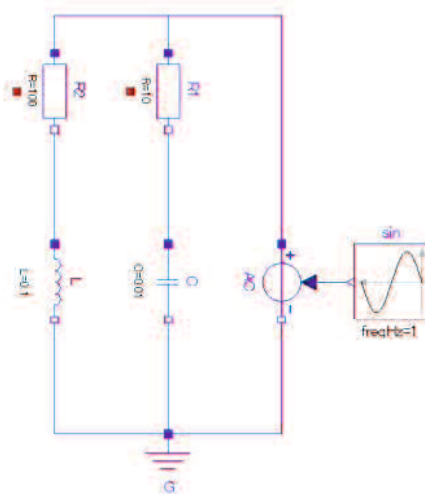
Fig. 2.30 Graphical modeling in modelica (orginal)
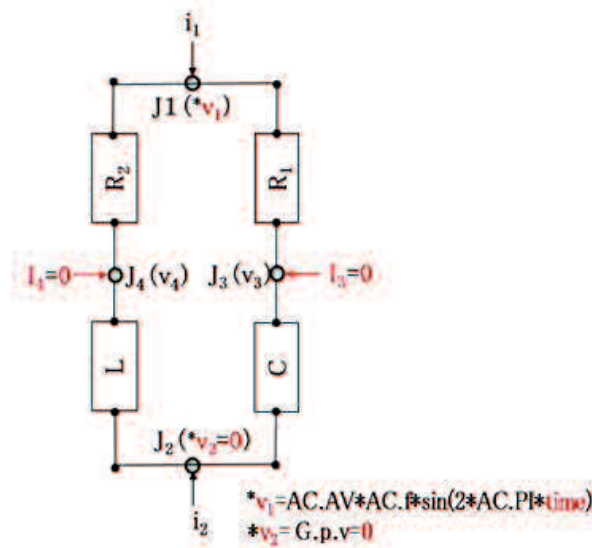
Fig. 2.31 Graphical modeling in modelica (FEM approach)

In Modelica, we must draw all known variables (such as a ground or a voltage source) on the graph model from beginning, so it may be said that in a sense it has already become the causal model. Whereas characteristic of our modeling technique suggesting that we made a truly acausal model, because we make all node-equilibrium equations without the distinction of known and unknown variable (v_j, i_j). Later then we set a value in the known variable. As a result, the necessarily unknown variable (node voltage and addition electric current) will be found.

For making it easier to understand, we make graphical modeling in FEM approach that use 4 joints namely J_1, J_2, J_3 and J_4. FEM approach graphical modeling shown on Fig. 2.31. Compare with original table in Modelica for equation extracted from simple circuit model shown on Table I, we provide FEM approach. Component in Modelica is named as element in FEM approach i.e. AC, R_1, R_2, C and L. In Modelica, each component defined at first step and then connector. In FEM, each element is already connected and variable at joint are named as v_1, v_2, v_3 and v_4. So that the other difference between original Modelica and FEM approach is in naming rule.   In FEM, it is not only scalar variable is available but also vector and we can combine different domain. Internal variable definitions for FEM are $R_1.i_1$ and $R_1.i_3$ for R_1, $R_2.i_1$ and $R_2.i_4$ for R_2, $C.i_4$ and $C.i_2$ for C, $L.i_3$ and $L.i_4$ for L. Node variable definitions at joint are v_1, v_2, v_3, v_4 for voltage and i_1, i_2, i_3, i_4 for current. We can make system model for simple circuit model (internal variable representation) from Fig. 2.31 as equation 2.11.

$$\begin{cases} R1.i_1 + R2.i_1 = i_1 \\ L.i_2 + C.i_2 = i_2 \\ R1.i_3 + C.i_3 = i_3 \\ R2.i_4 + L.i_4 = i_4 \end{cases}$$

(2.11)

Table. 2.5. FEM Approach for Equations Extracted from Simple Circuit Model

AC	$0 = \{1 \quad -1\}\begin{Bmatrix} AC.p.i \\ AC.n.i \end{Bmatrix}$ $AC.AV * \sin(\ ) = \{1 \quad -1\}\begin{Bmatrix} v_1 \\ v_2 \end{Bmatrix} = \{1 \quad -1\}\begin{Bmatrix} v_1 \\ 0 \end{Bmatrix}$ $\therefore \quad v_1 = AC.AV * \sin(\ )$	L	$\begin{Bmatrix} v_2 \\ v_4 \end{Bmatrix} = L.L * del\left(\begin{bmatrix} 1 & -1 \\ -1 & 1 \end{bmatrix}\begin{bmatrix} L.p.i \\ L.n.i \end{bmatrix}\right)$ $\therefore \quad \{v_2 - v_4\} = L.L * del(L.p.i)$
R_1	$\begin{Bmatrix} R1.p.i \\ R1.n.i \end{Bmatrix} = \frac{1}{R1.R}\begin{bmatrix} 1 & -1 \\ -1 & 1 \end{bmatrix}\begin{Bmatrix} v_1 \\ v_3 \end{Bmatrix}$	G	$v_2 = 0$ =constant G.p.i = Unknown variable (reaction electric current)
R_2	$\begin{Bmatrix} R2.p.i \\ R2.n.i \end{Bmatrix} = \frac{1}{R2.R}\begin{bmatrix} 1 & -1 \\ -1 & 1 \end{bmatrix}\begin{Bmatrix} v_1 \\ v_4 \end{Bmatrix}$	wires	v_1, v_2, v_3, v_4
C	$\begin{Bmatrix} C.p.i \\ C.n.i \end{Bmatrix} = C.C * del\left(\begin{bmatrix} 1 & -1 \\ -1 & 1 \end{bmatrix}\begin{Bmatrix} v_3 \\ v_2 \end{Bmatrix}\right)$ $= C.C * \begin{bmatrix} 1 & -1 \\ -1 & 1 \end{bmatrix}\begin{Bmatrix} \dot{v}_3 \\ \dot{v}_2 \end{Bmatrix}$	Flow at node	$0 = AC.i + R_1.p.i + R_2.p.i$ //J_1 $0 = C.n.i + G.p.i + AC.n.i + L.n.i$ //J_2 $0 = R_1.n.i + C.p.i$ //J_3 $0 = R_2.n.i + L.p.i$ //J_4

By input the component, element and internal variable definition on Tables IV and V, we can get flow variable equilibrium equation with node variable representation as equation 2.12.

(2.12)

$$\begin{bmatrix} 0 & 0 & 0 & 0 \\ 0 & C.C & -C.C & 0 \\ 0 & -C.C & C.C & 0 \\ 0 & 0 & 0 & 0 \end{bmatrix}\begin{bmatrix} \dot{v}_1 \\ \dot{v}_2 \\ \dot{v}_3 \\ \dot{v}_4 \end{bmatrix} + \begin{bmatrix} \frac{1}{R1.R}+\frac{1}{R2.R} & 0 & -\frac{1}{R1.R} & -\frac{1}{R2.R} \\ 0 & 0 & 0 & 0 \\ -\frac{1}{R1.R} & 0 & \frac{1}{R1.R} & 0 \\ -\frac{1}{R2.R} & 0 & 0 & \frac{1}{R2.R} \end{bmatrix}\begin{bmatrix} v_1 \\ v_2 \\ v_3 \\ v_4 \end{bmatrix} + \begin{bmatrix} 0 & 0 & 0 & 0 \\ 0 & \frac{1}{L.L} & 0 & -\frac{1}{L.L} \\ 0 & 0 & 0 & 0 \\ 0 & -\frac{1}{L.L} & 0 & \frac{1}{L.L} \end{bmatrix}\begin{bmatrix} \int v_1 dt \\ \int v_2 dt \\ \int v_3 dt \\ \int v_4 dt \end{bmatrix} = \begin{bmatrix} i_1 \\ i_2 \\ i_3 \\ i_4 \end{bmatrix}$$

In FEM approach, we can separate the known variable on left side and unknown variable on right side easily as follow:

- known variable:

  v_1 = sin (2*pi*time)"AC.VA"

  v_2 = 0 " G.p.v "

  i_3 = 0;

  i_4 = 0;

- Then unknown variable: i_1, i_2, v_3, v_4 can be solved.

Afterward we can build textual modeling with modelica software and make comparison between textual modeling in original concept with FEM approach. It is not difficult for simple circuit model to make textual modeling. For more complex system, it is become more complicated to make so many connectors between all components exist in modelica concept. Perhaps the FEM approach can be another alternative for user to utilize Modelica. We make two models with FEM approach, acausal model and causal model

construction. Causal model construction with FEM approach only need 2 equations while acausal model need 4 equations. The simulation results for all approaches are same, as shown in Fig. 2.32.

(a) Original   (b) FEM approach
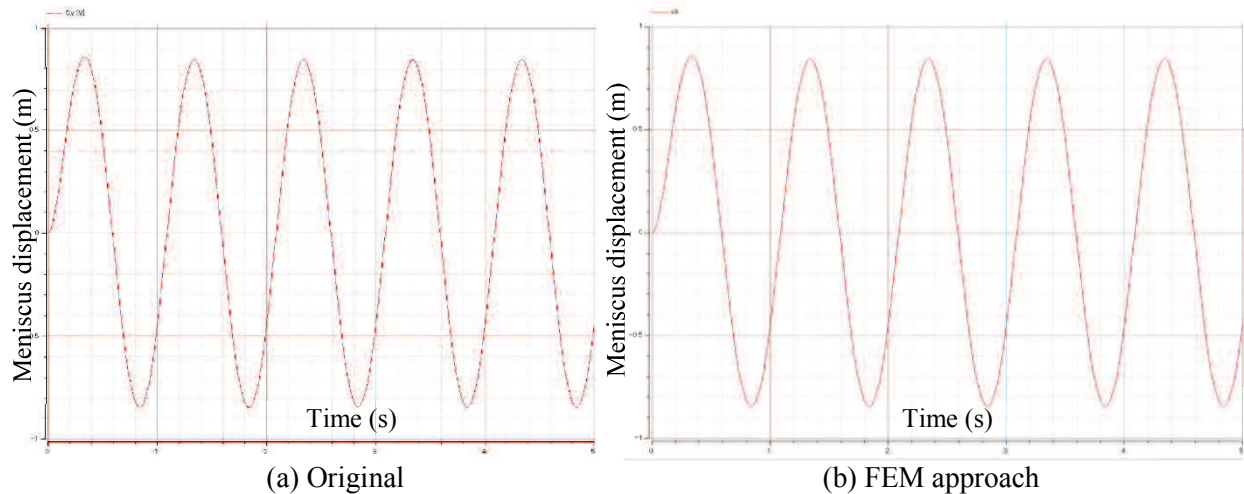
Fig. 2.32 The simulation results with different approaches

2.9.4 Conceptual system model of Ink-Jet Print-head

The understanding and prediction of system behavior could be predicted by simulation model. It also could be used as a substitute of real experiment that costly and need a longer time [1,2]. However, the accuracy of simulation result is limited by the power of the computer used for the simulation, and complete information about the real system is important which occasionally are not available.

The development of inkjet system model simulation particularly to understanding the jetting condition from nozzle print-head in this study is a difficult process because of the limited information about the real system. Furthermore, it is difficult to determine the possible cause in no jetting condition so then a trial-error approach has been the only option to understand [81]. It was stated that using the experimental result is easier to develop a model of inkjet system [96]. Therefore, many experiments that were conducted in finding the optimum waveform design was used to modelling the basis of droplet meniscus behavior and take the measured data into models. The experiment result was used as information in improving the simulation model. The improved model then used for explaining the conceptual mechanism of the experimental result. The conceptual model for inkjet system was established by using Modelica. With the inkjet simulation model, the

optimization of waveform design in the future will be easier, and will reduce the trial-error experiment to improve the inkjet printer performance.

In this study, the simple conceptual system model of actuation waveform is used to predict wave response from each input parameter. By using basic model with basic waveform, the combination of different pulse response is predicted by using wave superposition principle. This conceptual model is only used to make it easier to understand the mechanism of wave superposition particularly in multi-pulse input parameter of waveform, and for predicting the droplet velocity and volume before and after wave superposition. The model cannot estimate the droplet shape.

The laws of physics are used in physical modelling to describe the behavior of inkjet system. In the conceptual model of droplet control, it is common to adopt forced vibration model of single mass point, damper and spring system. It is also common to adopt transient response of one-mass system forced vibration to a concept (first approximation) simulation model shown in Fig. 2.33.
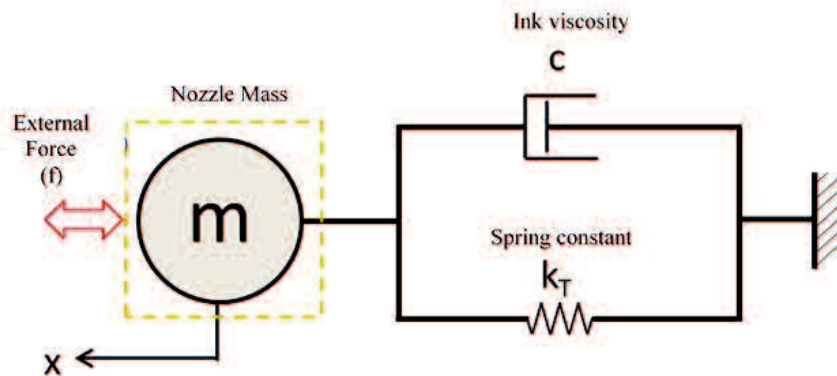
Fig. 2.33 The conceptual system model

The formulation of the conceptual system model in Fig. 2.33 is as follows:

$$m\ddot{x} + c\dot{x} + k_T x = f$$

Where:
m : mass of fluid in nozzle

k_T : composite spring (spring in nozzle and liquid chamber)

c : viscosity coefficient of ink

f : Exciting force by driving voltage

51

$$m\ddot{x} + c\dot{x} + kx = f \quad \Rightarrow \quad \ddot{x} + \frac{c}{m}\dot{x} + \frac{k}{m}x = \frac{f}{m} \quad \Rightarrow \quad \ddot{x} + 2h\omega_0\dot{x} + \omega_0^2 x = \frac{f}{m}$$

$$\omega_0 = \sqrt{\frac{k}{m}} \quad , \quad T_0 = \frac{2\pi}{\omega_0} \quad , \quad \omega_d = \omega_0\sqrt{1-h^2} \quad , \quad T_d = \frac{2\pi}{\omega_d} = \frac{2\pi}{\omega_0\sqrt{1-h^2}}$$

$$\omega_0 = \frac{2\pi}{T_d\sqrt{1-h^2}} \quad \therefore \quad m = \frac{k}{\omega_0^2} = \frac{kT_d^2(1-h^2)}{(2\pi)^2}$$

$$c = 2h\omega_0 m = 2h\frac{2\pi}{T_d\sqrt{1-h^2}}\frac{kT_d^2(1-h^2)}{(2\pi)^2} = \frac{hkT_d\sqrt{1-h^2}}{\pi}$$

2.13)

Where h: damping coefficient

The first model assumed that there is no damping in the inkjet system. The basic model without damper for basic waveform is shown in Fig. 2.34, with the response of simulation result is shown in Fig. 2.35.
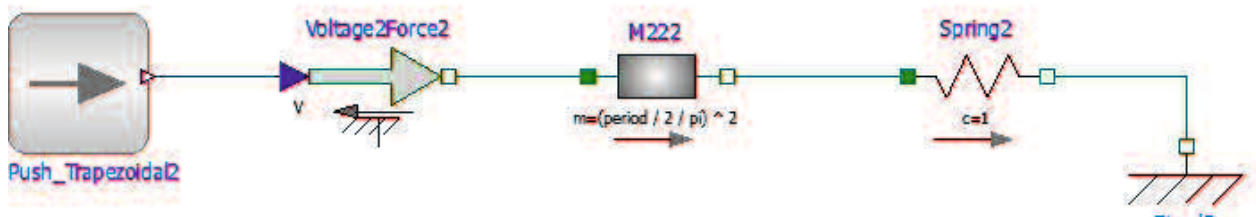
Fig. 2.34. Basic model of inkjet print-head without damper
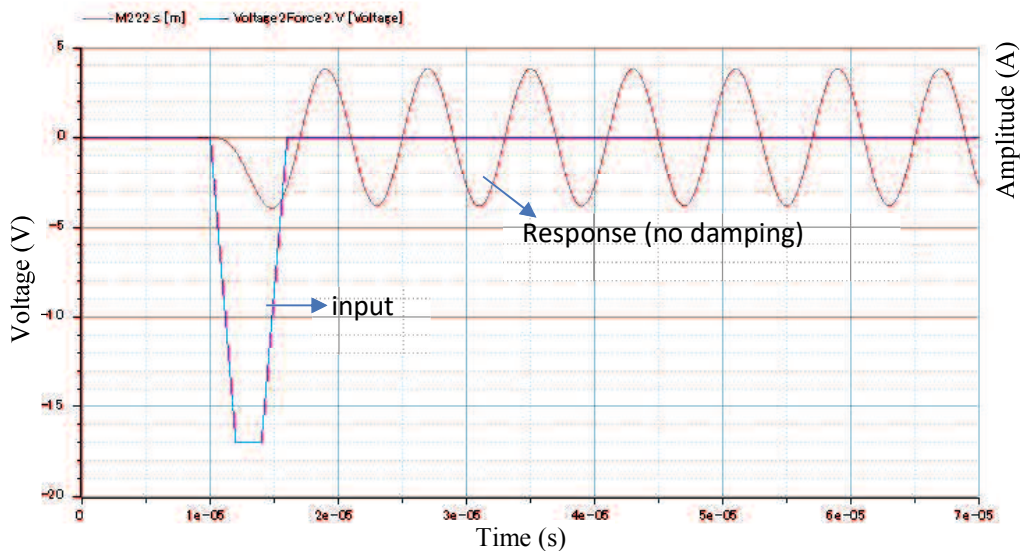
Fig. 2.35. The conceptual simulation model of basic waveform without damper

In real condition, the system in inkjet printer are with the damping factor. The viscosity of operating liquid will damp the vibration inside the liquid chamber. Therefore,

52

the simulation model of basic waveform was developed by considering damper as shown in Fig. 2.36 with simulation response shown in Fig. 2.37.
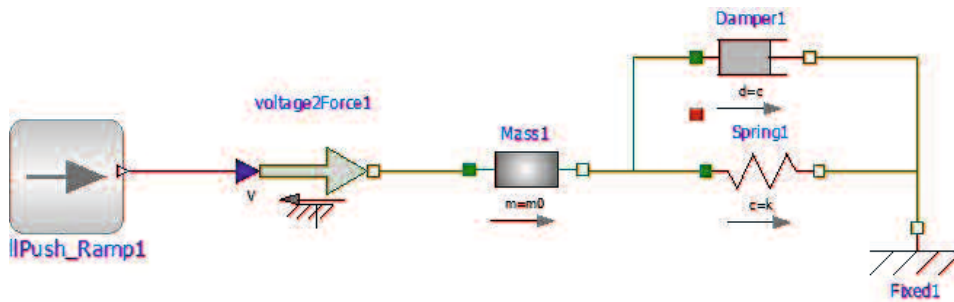
Fig. 2.36 Diagram of basic waveform model with damper
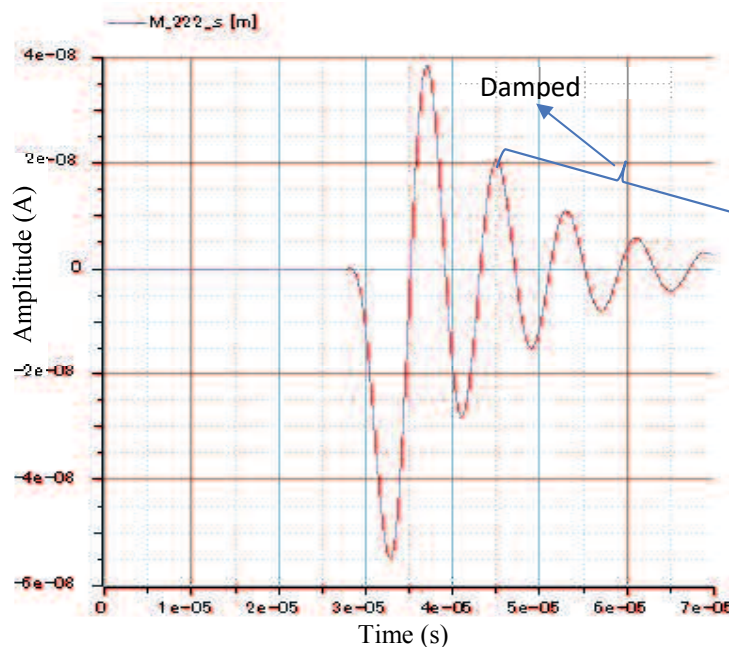
Fig. 2.37 Response of basic waveform model with damper

If using more than one pulse, the solution is obtained by multi-step synthesis with sum of the solutions that added separately. The features of the basic drive waveform are for easier to understand. The input parameter can be changed for the simulation. An example of solution combined addition of the two steps load for the first and second basic waveform below. The example conceptual model of two wave superposition with input parameter 222_6_222, the simulation result for input waveform and the response is shown in Figs. 2.38.

$$m\ddot{x}_T + kx_T = f_a + f_b$$

$$\Updownarrow$$

$$\begin{cases} m\ddot{x}_a + kx_a = f_a \quad , \quad m\ddot{x}_b + kx_b = f_b \\ x_T = x_a + x_b \end{cases}$$

2.14)

Input parameter for main pulse (1)

Input parameter for main pulse (2)

```
extends Modelica.Icons.Example;
import pi = Modelica.Constants.pi;
import SI = Modelica.SIunits;
//
// m*x" + c*x' + k*x = f  ,  x" + 2*h*w0*x' + w0^2 = f/m
//
parameter SI.Frequency Td = 8e-006;
parameter SI.DampingCoefficient h = 0.2;
parameter SI.TranslationalSpringConstant k = 1;
//
parameter SI.AngularFrequency w0 = 2 * pi / Td / sqrt(1 - h * h);
parameter SI.Mass m0 = k / w0 ^ 2;
parameter SI.AngularFrequency wd = 2 * pi / Td;
parameter SI.DampingCoefficient c = 2 * h * w0 * m0;
//
```

Fig. 2.38. The example conceptual model of two wave superposition
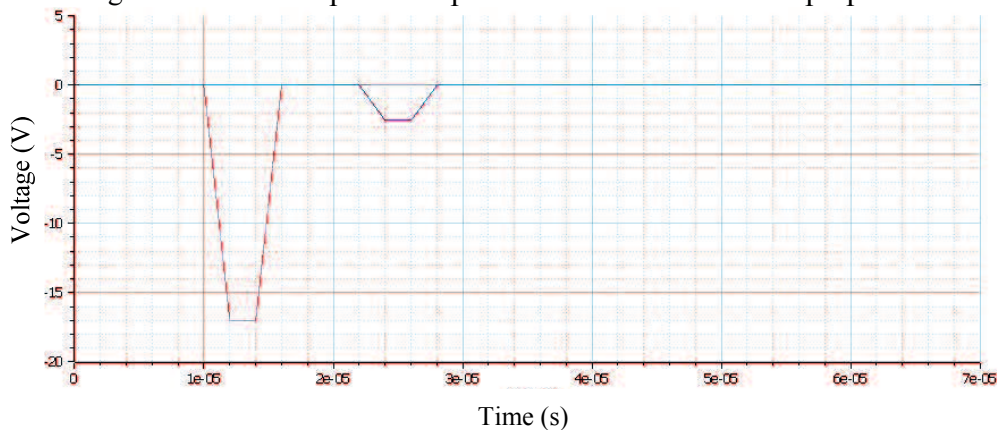
Fig. 2.39 The example of simulation result from input waveform in Fig. 2.38
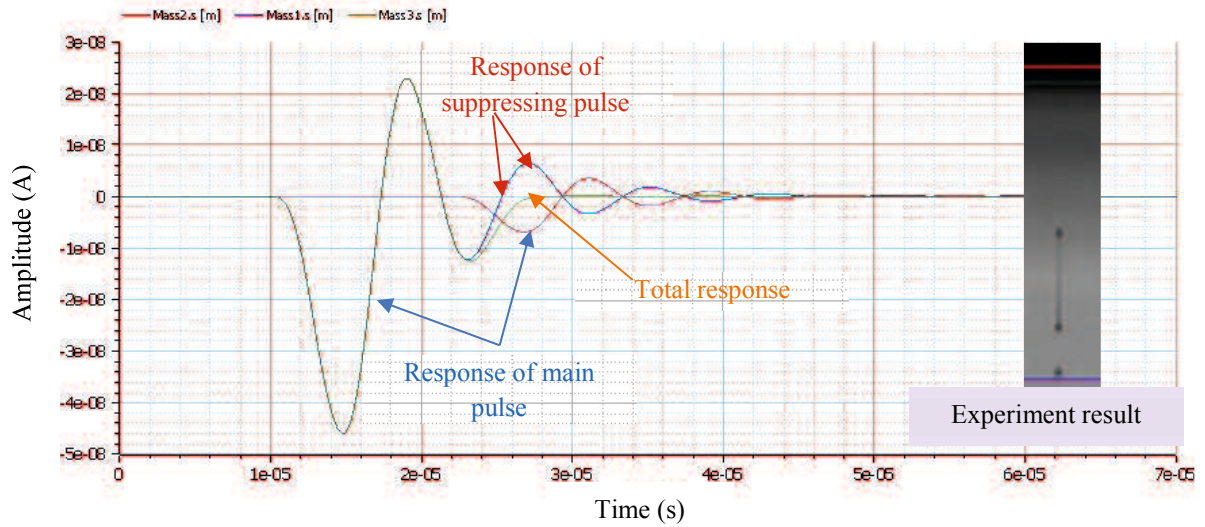
Fig. 2.40. The example output (response) of waveform from Fig. 2.39 and the experiment result

Figure 2.40 shows the response of wave superposition between main pulse 222 with separating time (t_{keep}) 6μs so then the starting time difference in the input parameter is set as 12 μs later from the main pulse starting time. Because of the same phase of each response but in different direction (positive and negative), so then the destructive superposition is occurred to eliminate the residual vibration. The final wave from wave superposition result should be without any residual vibration. The volume and velocity of the total response should be same. Noted that the result only shown the wave response for predict the droplet volume and velocity. The droplet shape cannot be estimated by this simulation. From experiment result, the droplet shape that generated from this input parameter is the droplet with long ligament.

CHAPTER III
EXPERIMENT STANDARD OF INKJET PRINTER

3.1 Introduction

Research development in inkjet printing experiment system is being carried out to increase the inkjet printer performance and its printing result. A good understanding of the drop formation process and droplet behavior is important for the next step in improving the print quality of inkjet systems. In addition, the measurement standard of experiment in the process of product development, should be established for a good experiment system.

In inkjet printer experiment, the droplet performance is investigated from some parameters, such as droplet shape, velocity and volume. For droplet volume, the data that we get from the experiment is the droplet weight from number of droplet that is discharged from the selected nozzle. The number of droplet that we want to discharge is set with fire limitation number.

Currently, there is no standardization in fire limitation number to measure the droplet weight in the previous research. The previous study with the same device was usually using 1.000.000 drops in the droplet weight measurement. It need more than 20 minutes to gather 1 data with this amount as shown in table 3.1. On the other side, 500 μm of nozzle distance was used to measure the droplet speed. From prior observation with different distance, it was found the droplet shape could change, as shown in Fig. 3.1. Therefore, in this study, we evaluated the fire limitation and distance setting for measuring the droplet speed to determine the experiment system standard that will be used on the next experimental study.

The other objective of this study is to determine the actual natural period of ink jet printer by experiment, compared to the previous natural period used by the company based on supplier specifications. The computation of time parameters of the actuation pulse can be simplified if natural period is known [2]. In addition, t_{keep} (dwell time) in input parameter of the actuation waveform that results the highest drop speed is recommended for driving the inkjet print-head [13]. Therefore, the actual natural period from this experiment result is used as recommendation to the company for generating the optimum speed of droplet.

The droplet ejection process, shape, volume and speed are influenced by actuating waveform of the piezoelectric element [2], [7], [19], [27], [34], [40], [41], [81] & [93].

Some studies were conducted to investigate the droplet formation process [1] − [12], [17], [19] & [27]. Most of that studies using positive (trapezoidal) waveform or positive-negative (bipolar) waveform. The simplest waveform for driving the piezoelectric actuator to generate a droplet is unipolar waveform [7]. In this research, we used the negative unipolar waveform with pull-push method for the piezoelectric element. The comparison of the droplet formation process for negative basic waveform with the preliminary vibration waveform was also conducted.

Table 3.1 Fire limitation number for droplet weight measurement data

No	Fire Limitation Number	Weight (gr) (10 Nozzles)	Time (minutes)	No	Fire Limitation Number	Weight (gr) (10 Nozzles)	Time (minutes)
1	50,000	0.00437	<1	16	450,000	0.04117	± 10
2	100,000	0.00937	± 1	17	475,000	0.04202	± 10
3	125,000	0.01087	± 2	18	500,000	0.04554	± 11
4	150,000	0.01347	± 2	19	525,000	0.04640	± 12
5	175,000	0.01548	± 4	20	550,000	0.05025	± 12
6	200,000	0.01900	± 4	21	575,000	0.05221	± 13
7	225,000	0.01987	± 5	22	600,000	0.05464	± 13
8	250,000	0.02245	± 5	23	650,000	0.05951	± 14
9	275,000	0.02407	± 6	24	700,000	0.06415	± 15
10	300,000	0.02780	± 6	25	750,000	0.06868	± 16
11	325,000	0.02849	± 7	26	800,000	0.07174	± 17
12	350,000	0.03224	± 7	27	850,000	0.07525	± 18
13	375,000	0.03390	± 8	28	900,000	0.08221	± 19
14	400,000	0.03659	± 9	29	950,000	0.08432	± 20
15	425,000	0.03692	± 9	30	1,000,000	0.08951	± 23
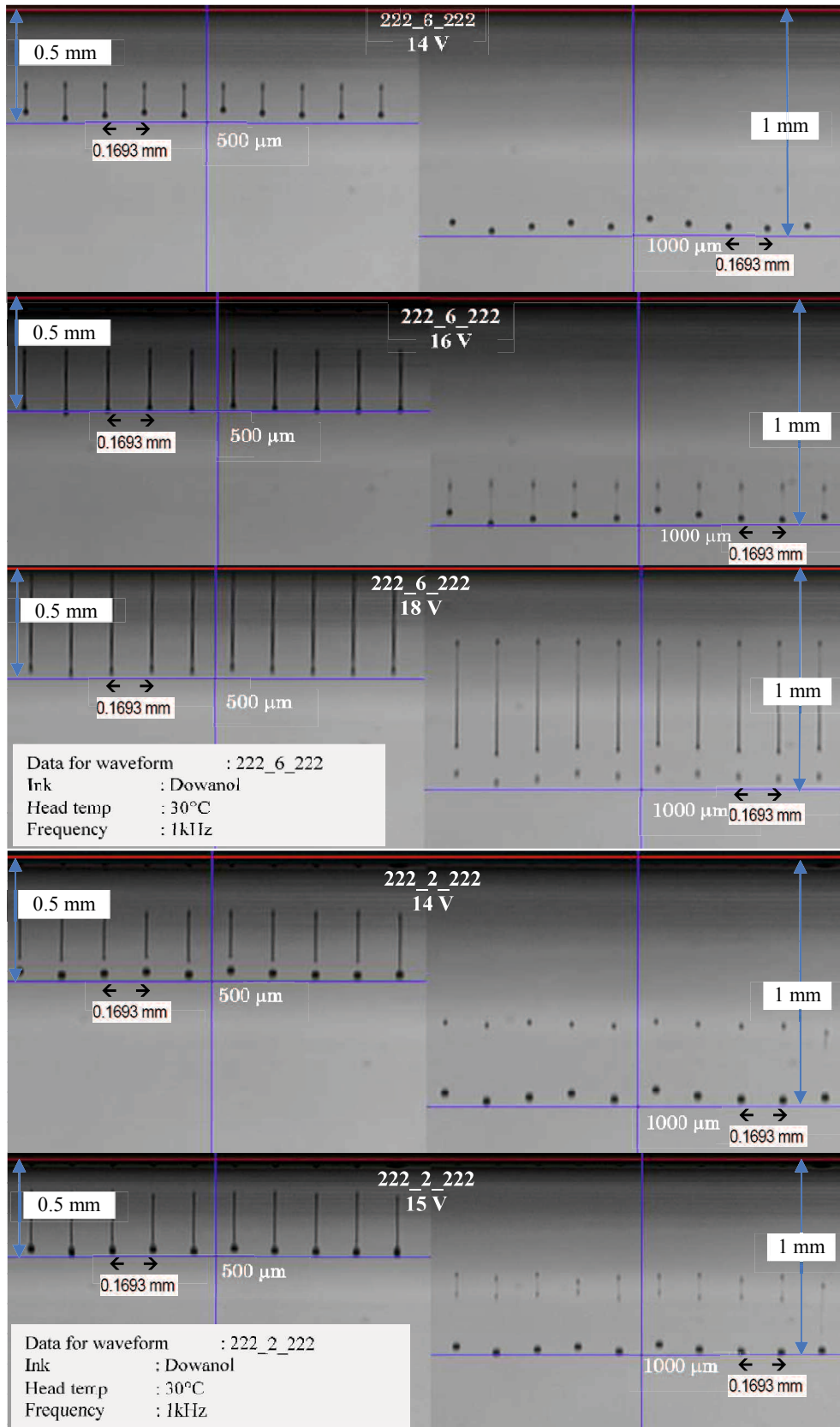
Fig. 3.1 Initial random observation of droplet shape in different observation distance

3.2 Description of Experimental Setup

3.2.1 Experiment IPO Diagram

The Input-Proses-Output (IPO) diagram of experiment in this research is shown in Fig. 3.2. For ensuring the experiment system work properly, the room temperature is set at 27°, and monitor the humidity. Furthermore, the print-head nozzle checking was also conducted. The preliminary data gathering was done to check that the data is in the normal distribution. The bell curve of probability density is shown in Fig. 3.3.

As the experiment input are applied voltage and time for down, keep, up and wait in the waveform design. The droplet ejection is the experiment process using the waveform design to drive the piezoelectric print-head. As an output of the experiment, we obtain the results of firing drops weight that measured by digital balance. In addition, we get the droplet image and the delay time of the droplet from the distance off from the nozzle.
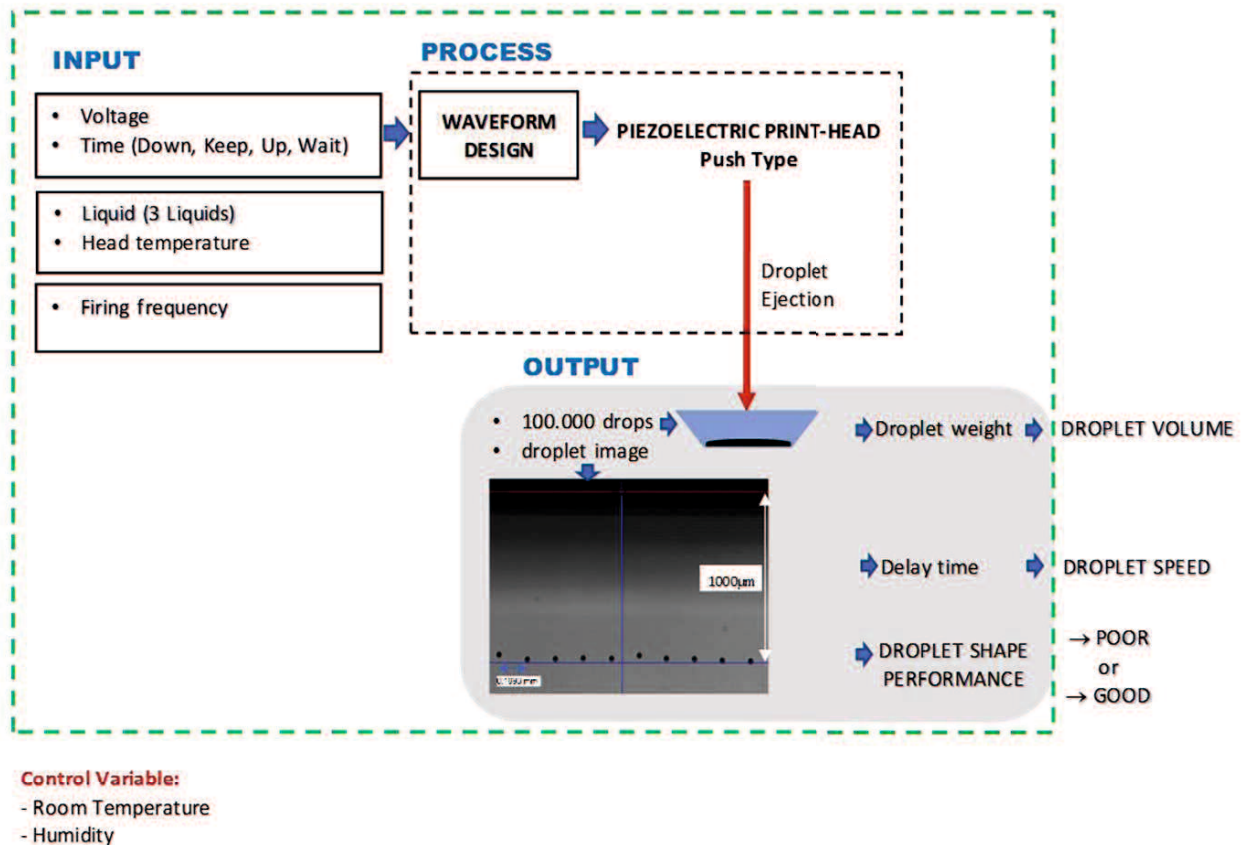
Fig. 3.2 Experiment IPO diagram
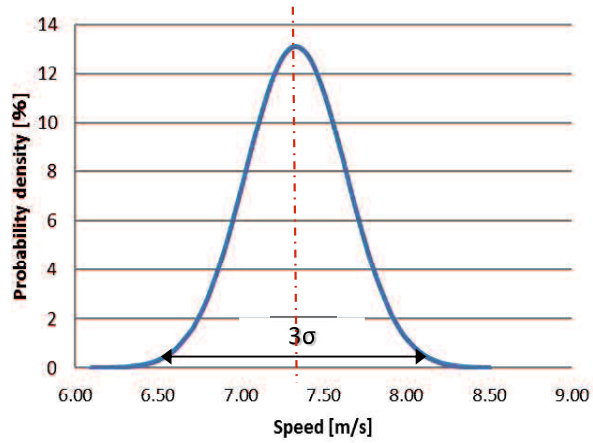
Fig. 3.3 Probability density of nozzle checking

The apparatus (IJ-DOT-R5) that used to measure the droplets shape, speed and volume is shown in Figure 3.2. The experiment set up diagram is shown in Figure 3.4.
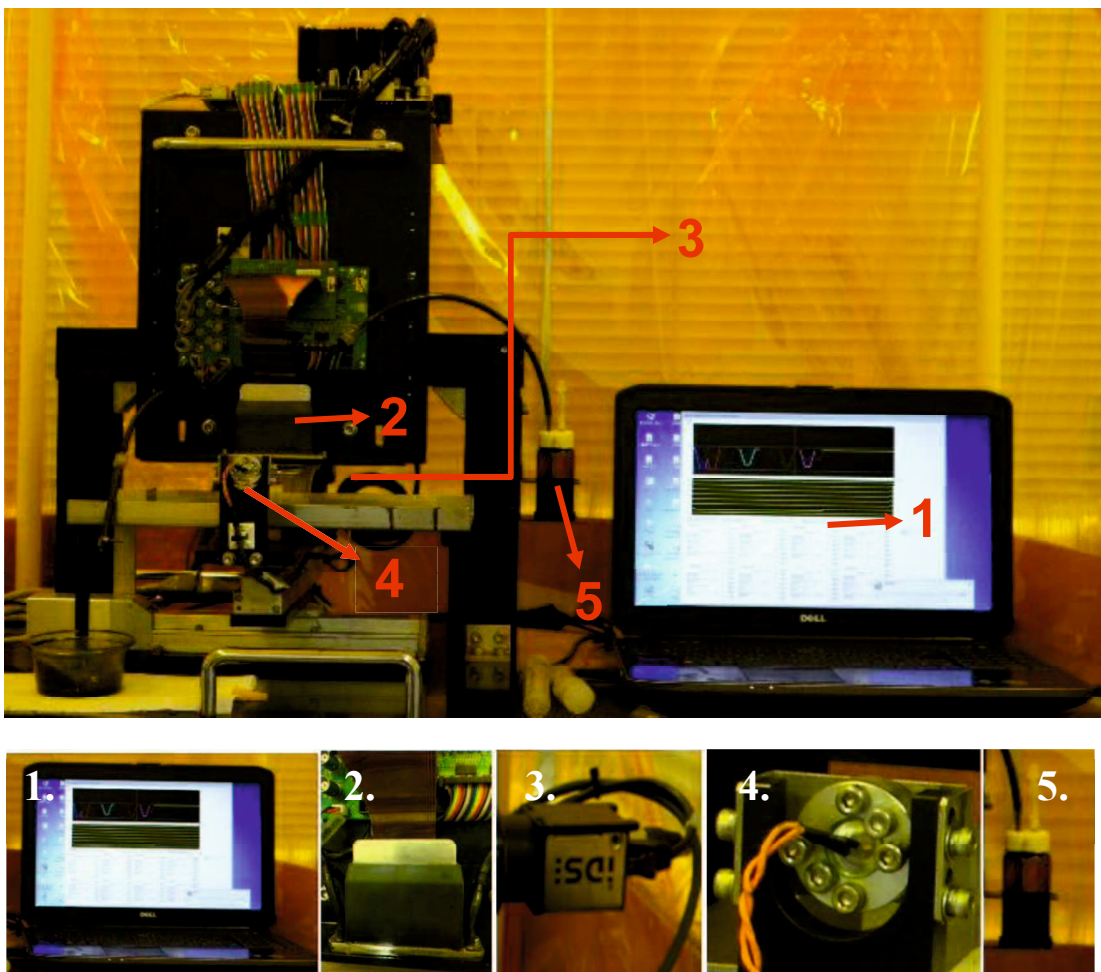
Figure 3.4 Experiment apparatus (IJ-DOT-R5)

It consists of 5 fundamental elements namely:

1. Waveform controller and drop observation.
2. Print-head GEN 5 using piezoelectric type D33 stacked PZT
3. CCD (Charged-Coupled Device) Camera type UI - 5240CP - M - GL
4. Light source (Strobe LED)
5. Liquid

The experiment schematic diagram is shown in figure 3.5.
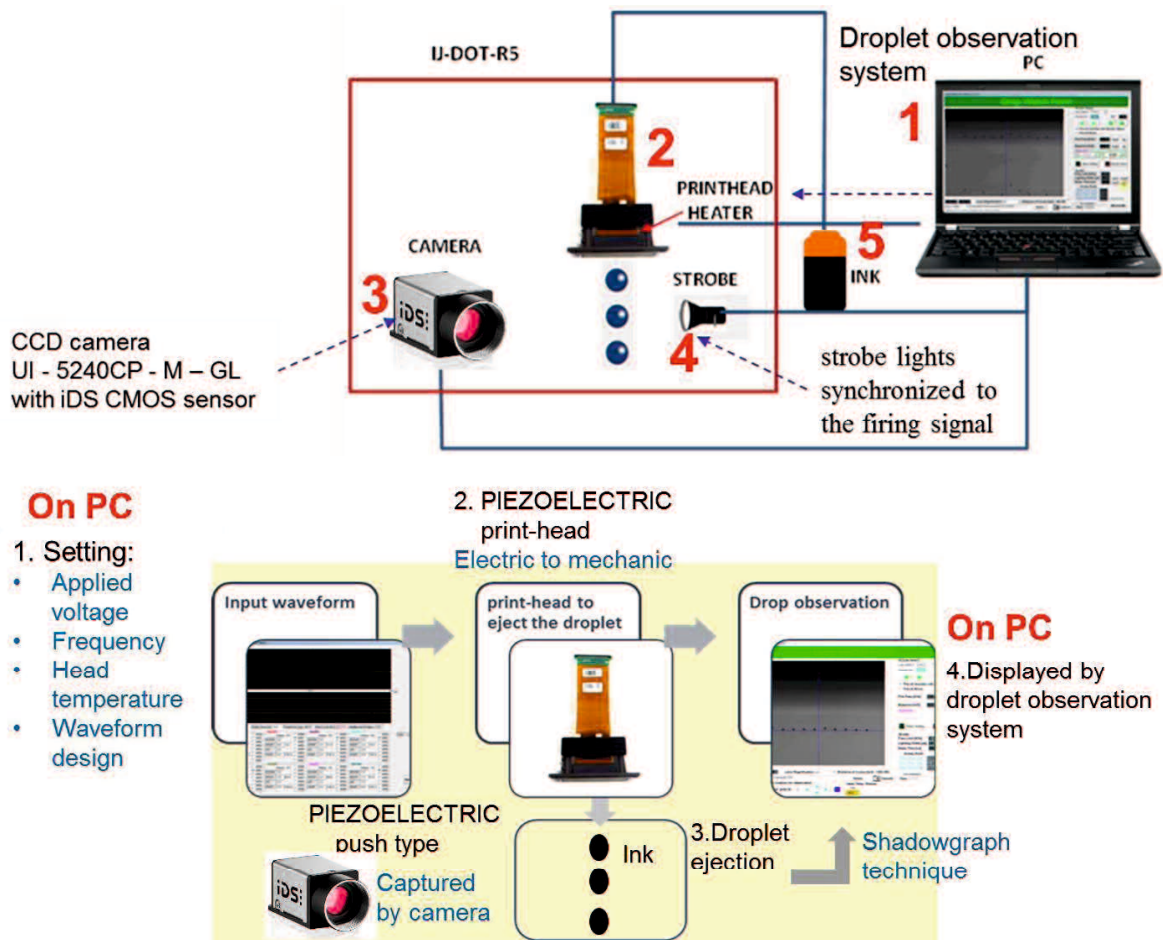
Fig. 3.5 Experiment schematic diagram

When a driving voltage is used to drive piezo actuators in an inkjet head, it will result in expansion or contraction of the piezo actuator. Piezo actuator generates a pressure in the ink chamber. Proper driving voltage amplifies the pressure wave such that a droplet of ink can be jetted from the inkjet head. A driving voltage and waveform design was input using a droplet observation system "drop station for print-head GEN 5 (2.1.5.0)" on a personal computer. The signal was sent from a personal computer to the print-head, to eject the droplet. The droplet observation system software that connected to the print-head GEN 5 using piezoelectric type D33 stacked PZT that is installed in PC to input the

actuation waveform for driving the print-head. The print-head configuration is shown in Fig. 3.6 with specification shown in Fig. 3.7.

The shadowgraph technique is used to get the ink-jetting droplet imaging. The shadowgraph technique is using bright background from light source which is blocked by droplets in the magnified of view. The droplet image was taken by CCD camera type UI - 5240CP - M - GL that equipped with iDS CMOS sensor. By using strobe lights synchronized to the firing signal, droplet images appear to be frozen in the acquired CCD camera image. The droplet image then will be displayed in the PC at drop watch form.
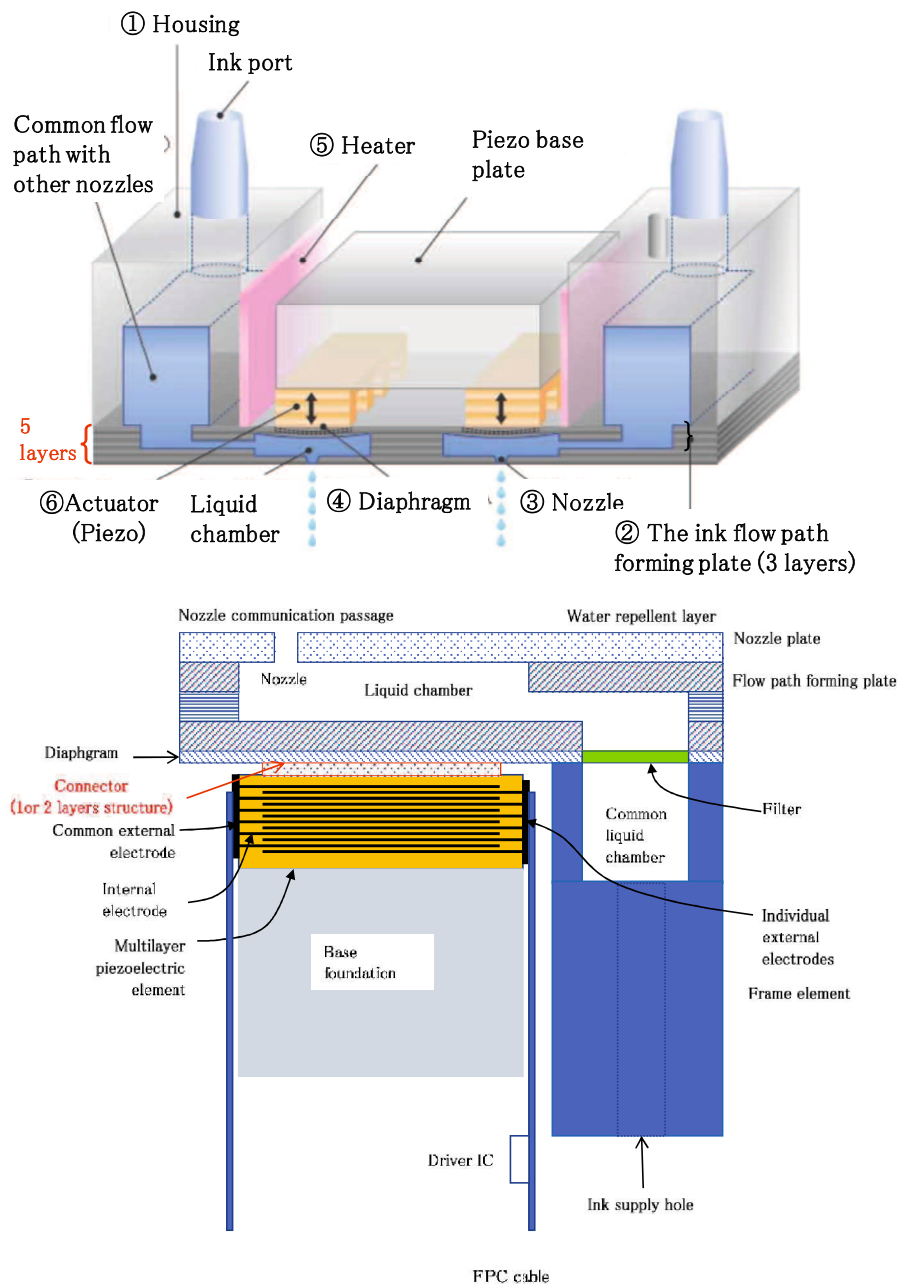
Fig. 3.6 Print-head configuration

GEN-5 Printhead Series Preliminary Specification

DESIGN FEATURES

- 1,280 channels
- Two color and four color support
  - Single color: 600npi
  - Two color: 300npi
  - Four color: 150npi
- 8 level grey scale capability
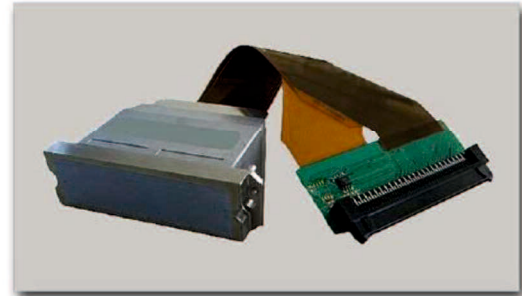
SPECIFICATION
PHYSICAL:

Size	89(W) x 25(D) x 69(H) mm (excluding cables & connectors)
Head materials	SST, Nickel alloy & Epoxy adhesive (Direct contact with ink)
Compatible jetting fluids	Compatible with water, solvent, oil, UV curable inks
Nozzle plate surface	Coated SST
Number of nozzles	4 x 320 channels
Nozzle spacing A: Within a single row B: Within a color C: Single pass D: Row to row distance E: Color to color	0.1693 mm (1/150") 0.0847 mm (1/300") 0.0423 mm (1/600") 0.55 mm 11.811 mm
Ink inlet port	2 x dual ports
Piezo type	D33 stacked PZT
Drop ejection mode	Piston pusher with metallic diaphragm plate
Integrated electronics	Low-voltage serial to high-voltage parallel converter; 3-bit shift resistors; transmission gate outputs
Temperature control	Integrated heater and thermistor
Viscosity	11 cP (at operating temp.)
Surface tension	32 dynes/cm
Native drop volume	7 pico-liter
Drop volume range / variation	7– 35 pico-liter with grey-scale / ±10%
Drop velocity nominal / variation	7 m/sec / ±15%
Crosstalk	10% or less with all channels firing
Jet straightness 1 sigma	< 3.5 milli-radian from nozzle centerline
Native drop operating frequency	60kHz (Higher burst possible under ideal condition)
Life	100 billion actuation's per nozzle

Fig. 3.7 Print-head specification

3.2.2 Experiment step for droplet speed and weight measurement

The input parameter of experiment, observation of droplet shape, measurement of droplet speed and droplet volume was conducted by droplet observation software that was installed in the PC connected to the experiment apparatus. The experiment was conducted as following steps:

1) Turn on the droplet observation program, click on the Heater control form (Fig. 3.10).

2) Set the heater to the needed temperature, click close after the temperature needed to be achieved (Fig. 3.11).

3) Click Drop watch to display the control display for droplet observation (Fig. 3.10).

4) Click on the nozzle select for selecting the observation nozzle (Fig. 3.12).

5) Click on wave setting for input parameter of waveform (Fig. 3.12).

6) Set the input parameter for time for DOWN, KEEP, UP and WAIT for each wave according to the waveform design (Fig. 3.13).

7) Select MN (1 ~ 7) for selecting the wave (pulse) (Fig. 3.13).

8) Click save and back (Fig. 3.13).

9) Set the fire frequency (Fig. 3.12).

10) Set the applied base voltage (Fig. 3.12).

11) Click on fire all nozzle on nozzle select (Fig. 3.12).

12) Click on "start" to view the ejection and check the starting point of ejected droplet (Fig. 3.12).

13) Set the red line at the starting point of ejected droplet (Fig. 3.12).

14) Set the blue line until the distance of cursor reach 1000μm as standard of observation distance (Fig. 3.12).

15) Click "start" button (Fig. 3.12).

16) For Speed Measurement:

Check the delay time for each droplet (Fig. 3.12).

Speed Formula: Observation distance / average of delay time.

This formula is based on approach 2 for standard of speed measurement methods by IEC TC119 [70]. The illustration of speed measurement method is shown in Fig. 3.8.
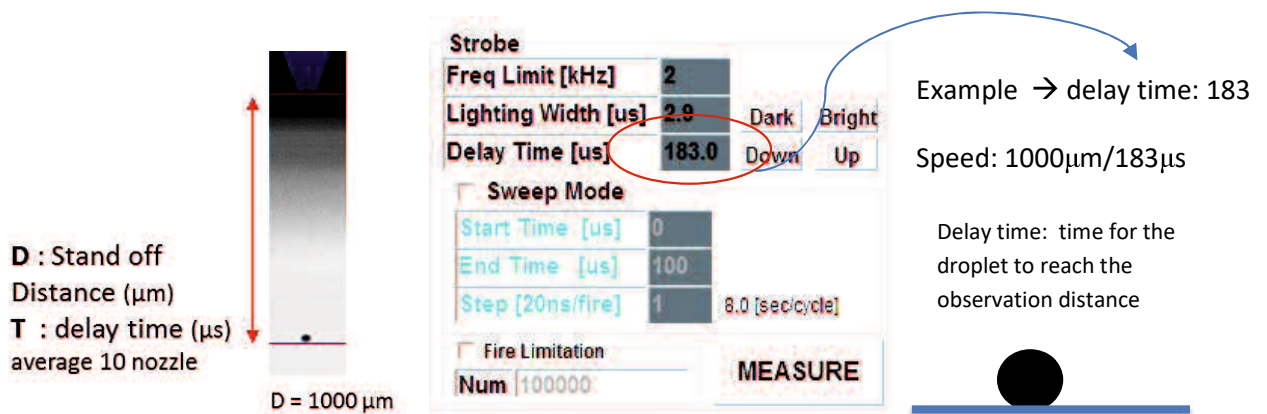
Fig. 3.8 Speed measurement method

17) Unselect the Set the button (11) "fire all nozzle on nozzle select", and click and set the fire limitation number (standard: 100.000), then put the container to collect the ink then click start (Fig. 3.12).

18) Measure the droplet weight by using the Digital scales (in this study using series AUW220D as shown in Fig. 3.9). The measured weight is for 100.000 drops from 10 nozzles.

Fig. 3.9 Digital scales AUW220D

19) The formula of droplet volume using $\rho = \dfrac{m}{v}$, then volume $= \dfrac{m}{\rho}$ divided by 100.000 drops. The result then divided by 10 for obtain the droplet volume per one drop.

The description of experiment step for obtaining the data of droplet speed and volume is shown in Figs. 3.10-3.13.
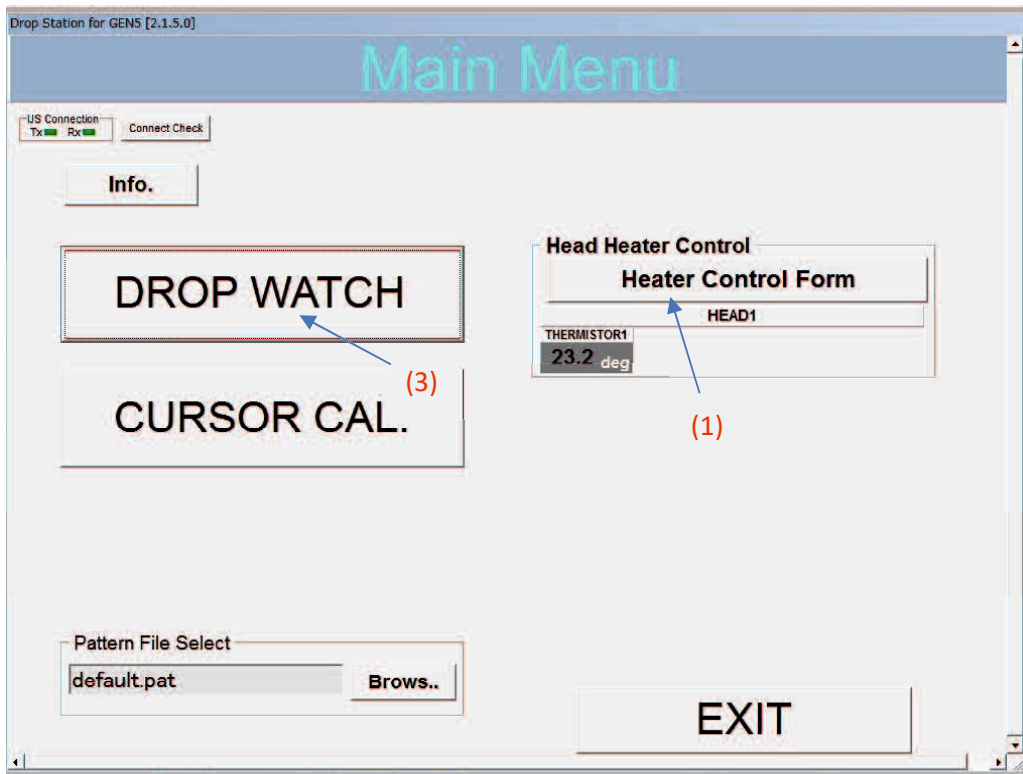
Fig. 3.10 Step 1 and 3
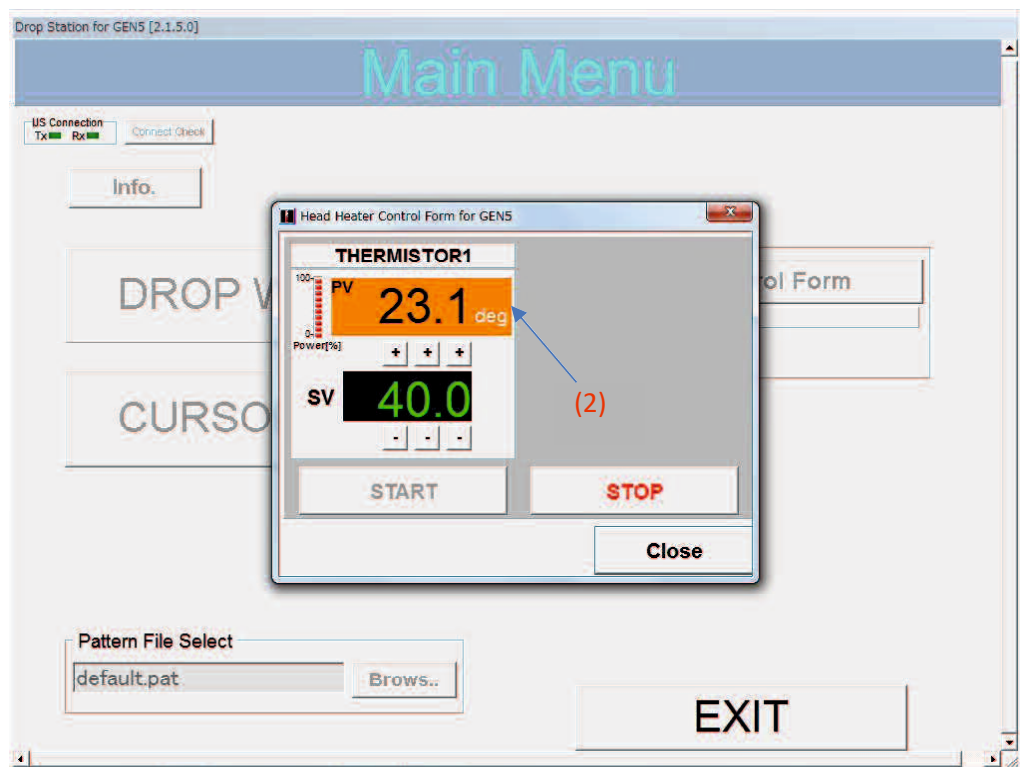
Fig. 3.11. Setting the head temperature (Step 2)
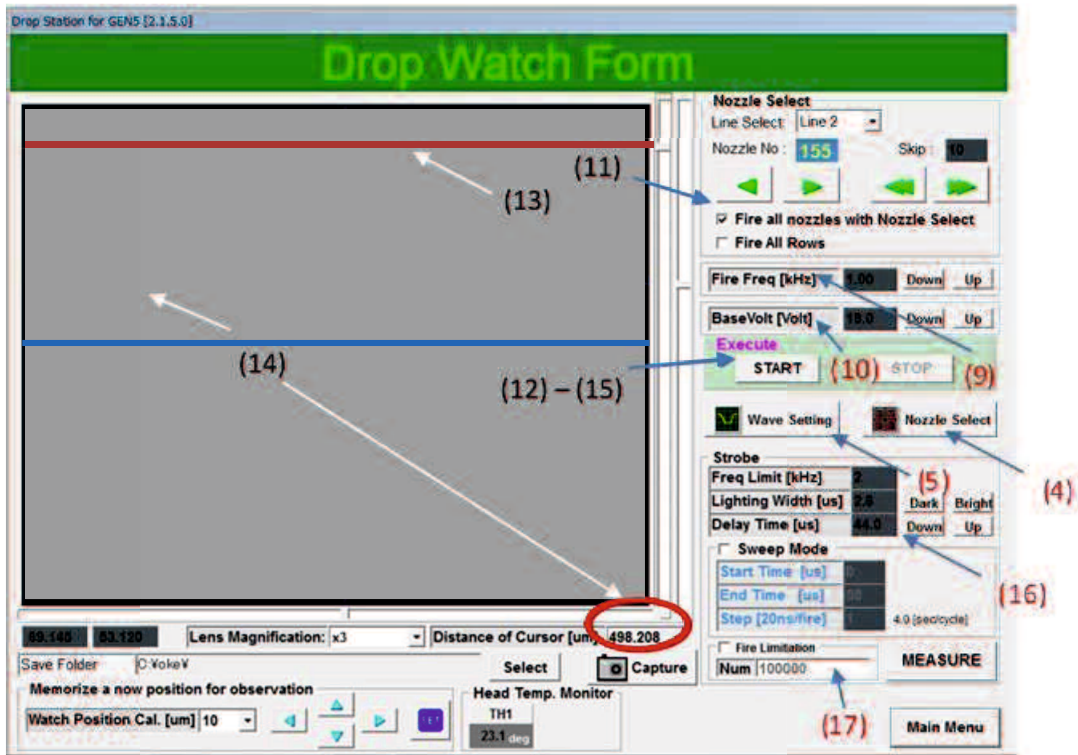
Fig. 3.12. Step 4 - 17. Setting the input parameter
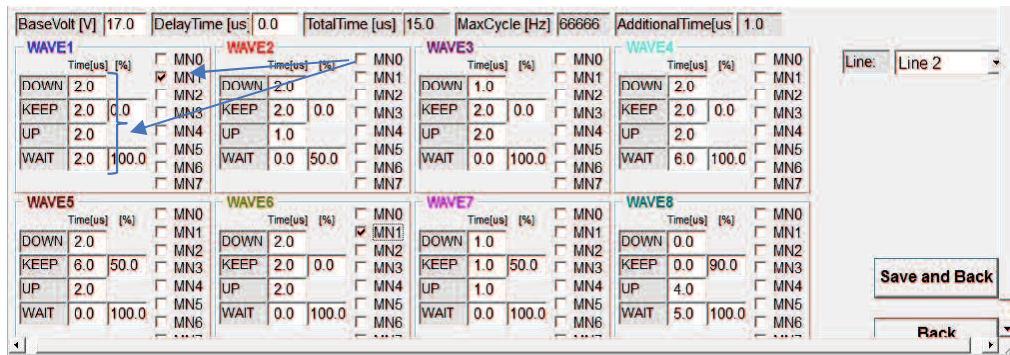
Fig. 3.13. Step 6-8. Setting the input waveform

3.3 Droplet Ejection Process by Input Waveform

The basic waveform profile with input parameter time for down, keep, up and waut is shown in Fig. 3.14. The illustration of droplet ejection with print-head mechanism is shown in Fig. 3.15.
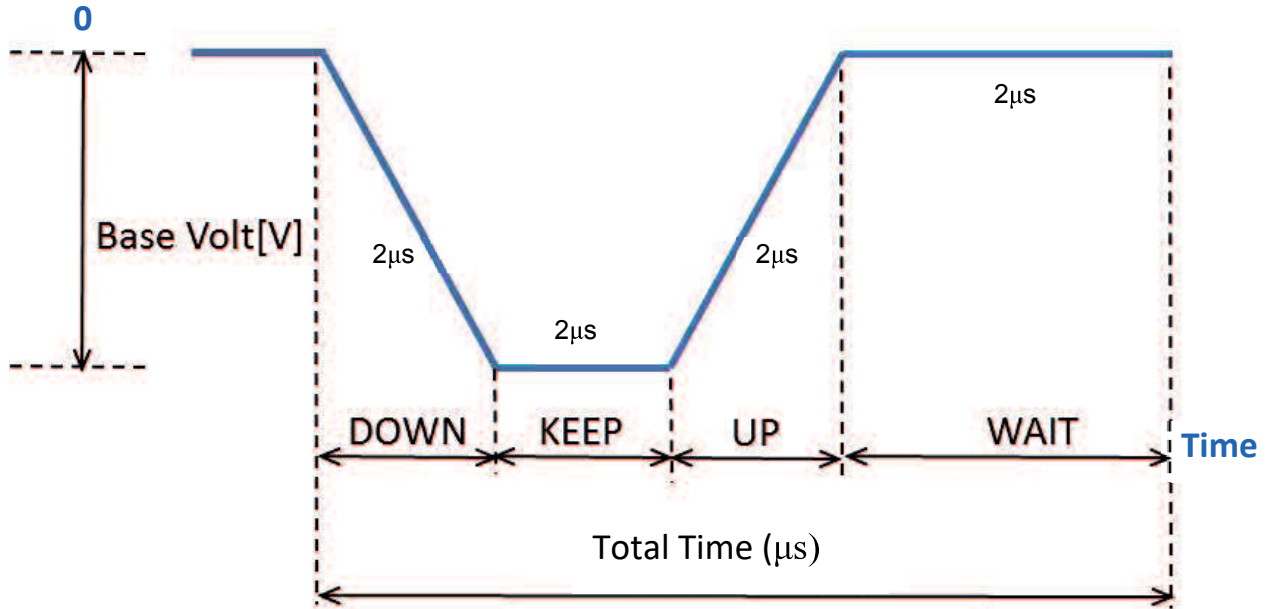
Fig. 3.14 The basic waveform profile
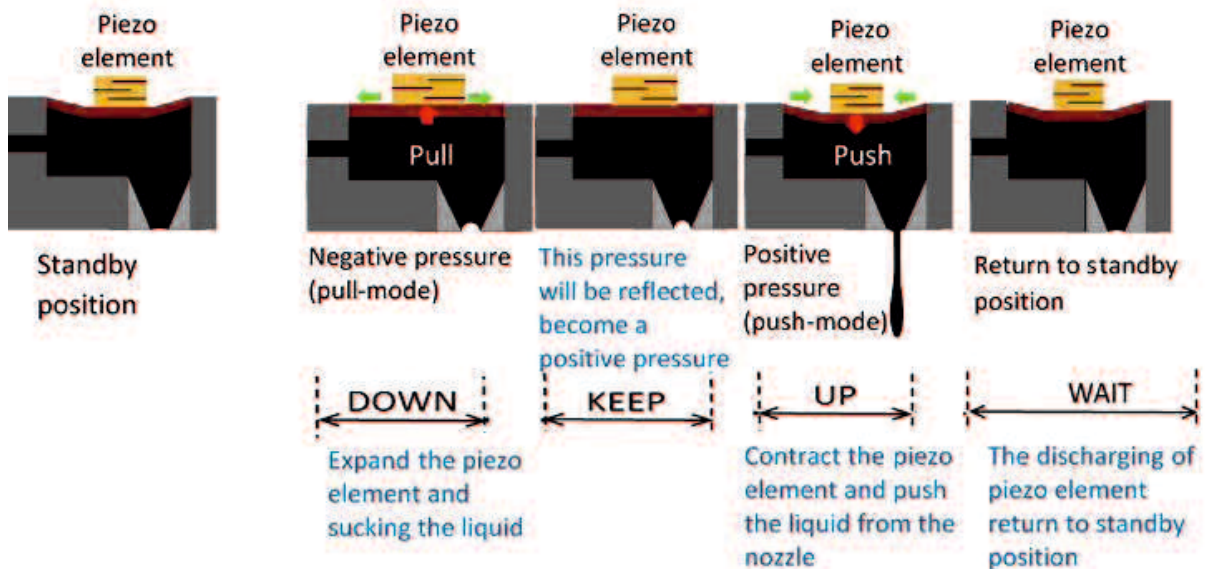
Fig. 3.15 The illustration of droplet ejection with print-head mechanism

The explanation for each input parameter of the actuation waveform for ejecting one single droplet are as following step:

1. The standby position of the PZT is shown at the left side of the figure. The first stage is the pull mode, when the signal to eject the droplet is received, the applied voltage becomes zero, and piezoelectric element return to its original condition. Then, the negative pressure is generated to expand and increase the volume of the liquid chamber, by sucking the liquid inside the chamber (DOWN).

2. This pressure wave at sequent process will be reflected, become a positive pressure to prepare ejecting the droplet (KEEP).

3. The second stage, push mode when in one cycle of its operation, the positive pressure wave reflected by the negative pressure that generated inside the chamber, overlapped with positive pressure wave to resonate, contract the liquid chamber and eject the droplet (UP). This method produces the higher pressure and generate the droplet with long and narrow droplet with higher speed.

4. After ejection, the position of piezo element is return to its standby position, prepare for the next firing process (WAIT).

3.4 Research Methodology

The methodology of this study was conducted by using "PDCA (Plan-Do-Check-Action) cycle, as shown in Fig. 3.16. As a "PLAN" step of this study, the literature review and evaluation of current experiment system was conducted for arranging the problem formulation and the research purpose. The experiment standard was determined and used in the next step of the experimental study. The nozzle checking must be done beforehand. The hypothesis and basic concept of controlling the droplet behavior as "DO" step by the theoretical and experimental approaches. It also starting from the study about print-head mechanism and the effect of the driving pulse mode for the droplet behavior. The process of designing the waveform was conducted by the literature study concurrently with the simulation model with wave superposition principle. The experiment approaches were used as the "CHECK" step during the process design for determine the optimum waveform design in generating the best droplet performance. The improvement of waveform design was put as the "ACTION" in this research, to obtain the final design of new actuation waveform.
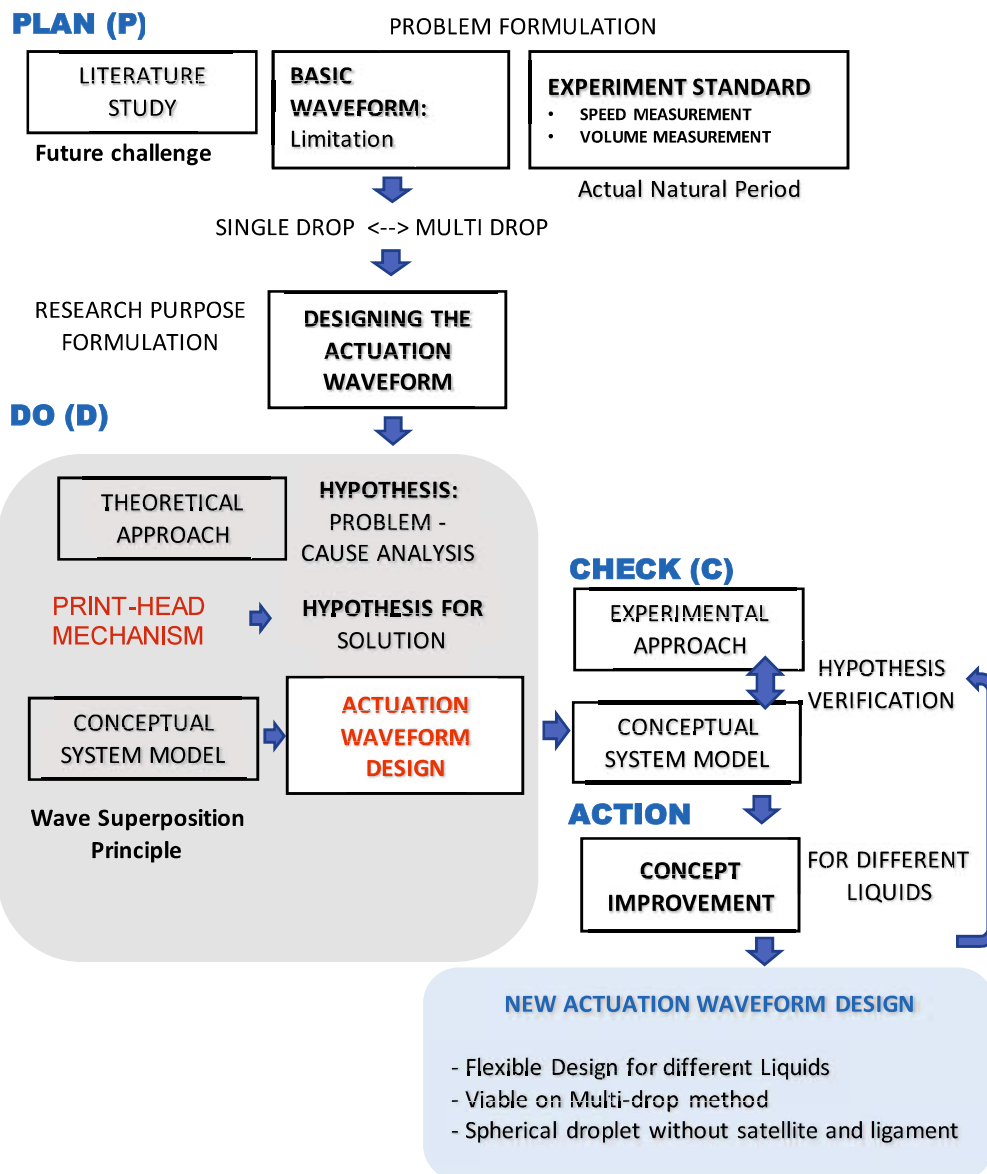
Fig. 3.16 Research methodology with PDCA cycle

3.5 Experiment of Actual Natural Period

Natural period in inkjet printer is the time in which a freely oscillating system completes one cycle of oscillation to eject the droplet. The frequency (or period) at which the drop reaches the highest speed corresponds to the "channel resonance frequency". The specification of the basic waveform from the supplier for the actuation parameters; time for down, keep, and up is respectively 2 μs with total period 8 μs. Hereafter, in this study, this period referred as natural period. The objective of this section is to determine the actual natural period that can give the highest value of drop speed at basic waveform for the inkjet device used in this study [88]. For determining the relationship between dwell time

and jetting speed, the others input parameter such as rising time (t_{up}), falling time (t_{down}), voltage, operating liquid and head temperature was set as fixed value. Then, the droplet speed was measure in the experiment. Thus, the experiment was conducted with different period as shown in Table 3.2. In this experiment, we used 28°C as head temperature.

Table 3.2. Input parameter for actual natural period experiment

No	Down (μs)	Keep (μs)	Up (μs)	Period (μs)
1	1	2	1	6
2	1	2.5	1	7
3	1	3	1	8
4	1	3.5	1	9
5	1	4	1	10
6	1	4.5	1	11

The experiment results for input parameter in table 3.2 is shown in Fig. 3.12. We can see that the data for droplet speed with different period formed the quadratic function. From the pattern of experimental curve, the maximum value is in the vicinity of period 8 μs and 9 μs. In other words, parameter value for t_d, t_k, t_u, t_w should be more than 2 μs. In order to determine the exact value of natural period, the quadratic function $y = ax^2 + bx + c$, is used to obtained the maximum number of x, which is represent the actual natural period.

$$y = -0.7994x^2 + 13.213x - 36.777$$
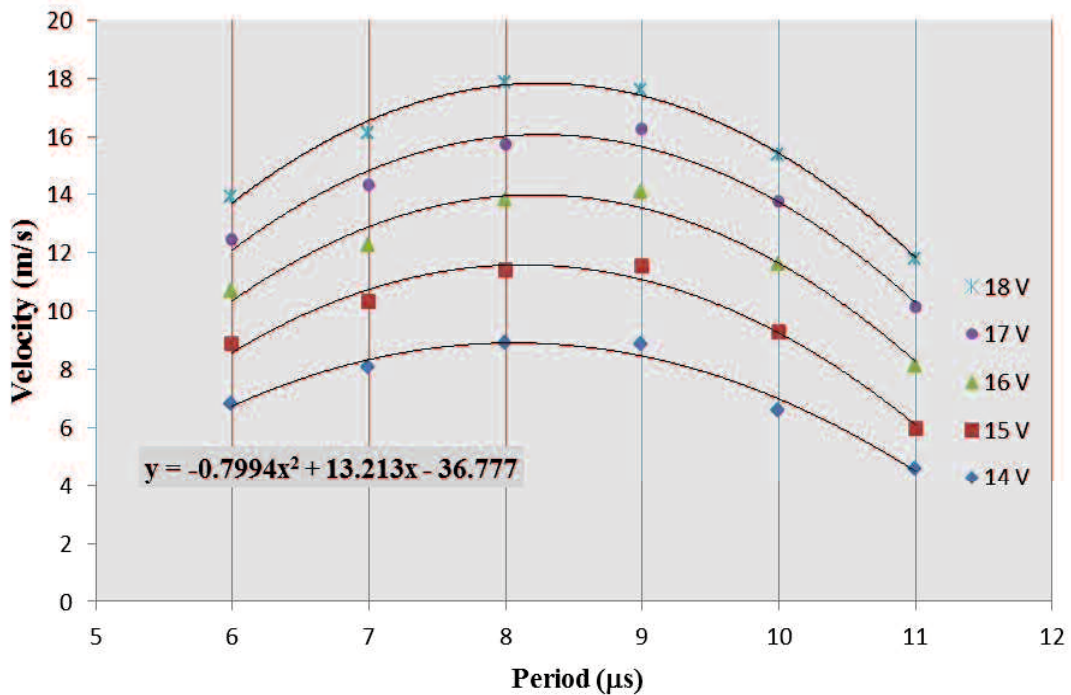
Fig. 3.17 Droplet speed on different t_{keep}

From that equation, we can determine the estimated actual natural period from maximum value of axis, with formula as follows:

$$x = \frac{-b \pm \sqrt{b^2 - 4ac}}{2a} \qquad \qquad 1)$$

$$x\ max = \frac{-b}{2a} \qquad \qquad 2)$$

The quadratic function obtained from experimental data is: $y = -0.7994x^2 + 13.213\ x - 36.777$ When $a = -0.7994$ and $b = 13.213$ Then

$$x\ max = \frac{-\ .}{2(-0.7994)} = 8.2643\mu s$$

It is determined that the estimated actual natural period of the inkjet device is 8.2643μs. Hereafter, this actual natural period symbolized by T_{an}. From this result, we can propose 8.26 μs as the natural period and 2.066 μs as input parameter of t_d, t_k, t_u, t_w in the inkjet printer device to obtain the higher droplet speed with basic waveform.

3.6 Experiment Standard of Fire Limitation Number

The purpose of this experiment is to determine the correlation between amounts of fire limitation with droplet weight. Fire limitation number is set up in the experiment input parameter for the droplet weight measurement. Then, to obtain one droplet weight, we divide the total weight with the number of fire limitation. Currently, there is no experiment standardization of fire limitation number for weight measurement in the join research company. The experiment frequently uses 1 million droplets for each weight measurement data. It takes about 23 minutes for 1 data only, so then the data can be collected is limited. The null hypothesis is, the difference fire limitation number of droplet do not show the different weight of one droplet. The parameters used in this experiment based on standard from supplier for input waveform are as follows:

Table 3.3 Input parameter for fire limitation number experiment

t_{Keep}	t_{Down}	t_{Up}	Voltage	Fire Frequency	Head Temperature
2	2	2	14V – 18V	1 kHz	27°C

The fire limitation number were starting from 50.000 until 1.000.000 (with interval 25.000). The hypothesis that there is no difference on droplet weight if using the

different fire limitation number was tested by regression analysis. The hypothesis testing results is shown in Fig. 3.13. This figure presents the regression result of droplet weight with different fire limitation number. We can see that the R square (R^2) value for that experiment is very small, only 0.0034. $R^2 = 0.0034$ means that the percentage of droplet weight movement is only 0.34% caused by fire limitation number.

Analysis Result

Regression statistics	
Multiple correlation R	0.057964427
R square R2	0.003359875
Adjusted R square R2	-0.032234415
Standard Error	2.06989E-10
Observations	30

Analysis of variance table

	df	SS	MS	F	significant F
Regression	1	4.04425E-21	4.04425E-21	0.094393644	0.76093766
Residual	28	1.19965E-18	4.28445E-20		
Total	29	1.20369E-18			
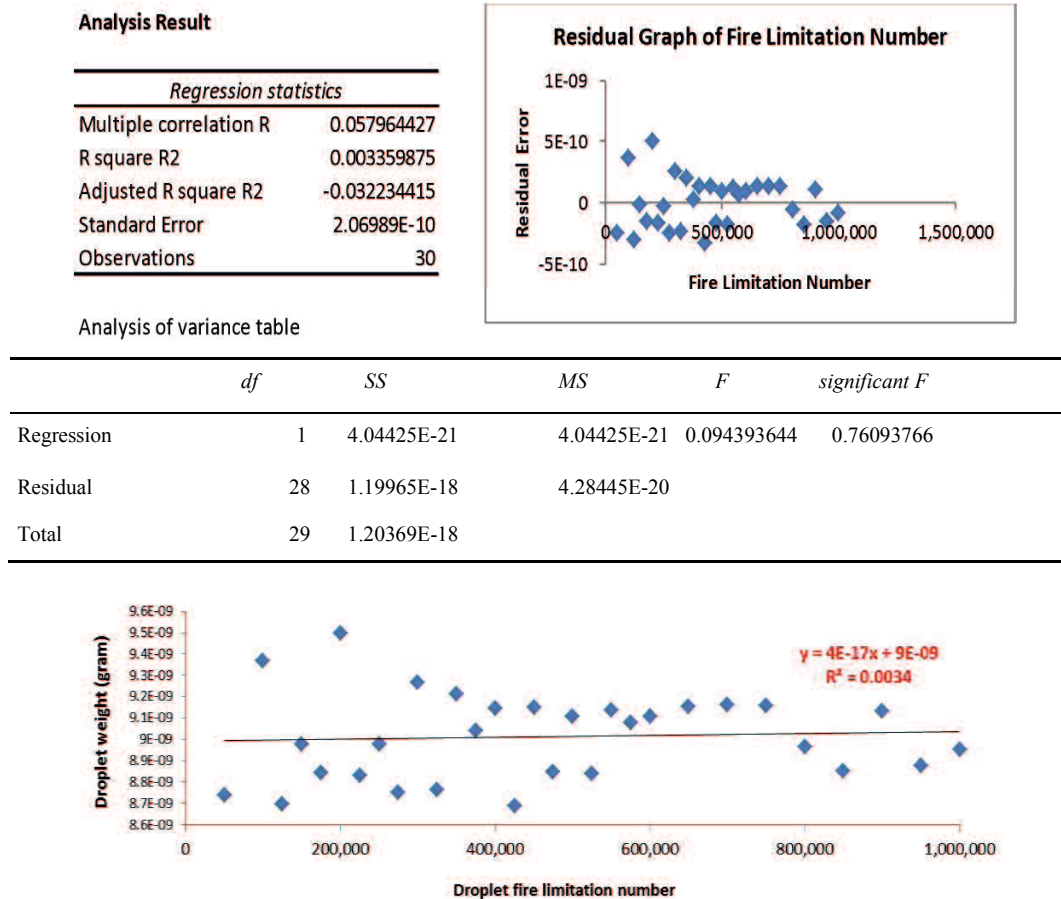
Fig. 3.18 Regression result of fire limitation number experiment

From significant F value, the result is 0.76093766, more than 0.05. It means that input is not significant to output. In other words, we can say that there is no significant effect for using different number of fire limitation with the droplet weight. If we compare the time needed for 100.000 with 1.000.000 fire limitation, there is significant difference of it. It need over than 20 minutes to take one data of droplet weight for 1.000.000 fire limitation number whereas only ± 1 minute for 100.000 drops.

Furthermore, the evaporated droplets during firing process could be more when using 1.000.000 fire limitation number. The partial evaporation of the droplet during their travel from the nozzle may influence the mass measurement [104]. Even though the evaporation

effect cannot be neglected [102], however, by using 100.000 drops the evaporation effect during firing process could be reduced. Hence, it is recommended for using 100.000 drops for fire limitation number, to reduce time in the measurement process of droplet weight.

3.7 Actuation Waveform

3.7.1 Basic Waveform

Waveform profile for basic waveform without preliminary or suppressing vibration is shown in Fig. 3.19. This is the waveform standard from the print-head supplier with time for down, keep and up (t_d, t_k, t_u) respectively 2μs.

$$t_d = t_k = t_u = \frac{T_{an}}{4} \approx 2$$
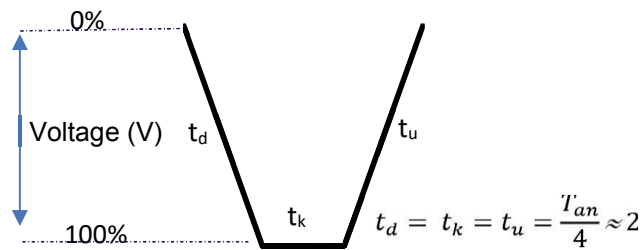
Fig. 3.19 Profile of Basic Waveform

3.7.2 With preliminary vibration waveform

The preliminary vibration serves to accelerate the droplet velocity and increase the volume with one pulse addition in front of the main pulse. The additional front pulse as a preliminary vibration such as the main pulse was using basic waveform but with a different voltage. This concept can be explained easier by the conceptual model with wave superposition principle as shown in Fig. 3.20. The input parameter from two pulses (preliminary and main) with time for down, keep and up (t_d, t_k, t_u) respectively 2μs. The input parameter of the actuation waveform with preliminary vibration then represents by 222_2_222. The constructive wave superposition delivers to the higher amplitude. It implies that it will generate the droplet with higher pressure and larger droplet volume.

Since the model is only predict the wave response from the input pulse, we cannot predict the droplet behavior in the real system. Furthermore, the applied voltage for first pulse as the preliminary vibration must be verified by experiment to ensure that it will not cause the droplet ejection as well multi drop method (ejecting 2 drops). Therefore, prior experiment was conducted to determine the voltage percentage of first pulse to ensure that the vibration will not cause the droplet ejection to generate the single droplet as shown in Fig. 3.21. This experiment used the different base voltage start from 10% of base voltage

until the droplet is really dripped from the nozzle. The input parameters of t_d, t_k, t_u are equal to basic waveform.
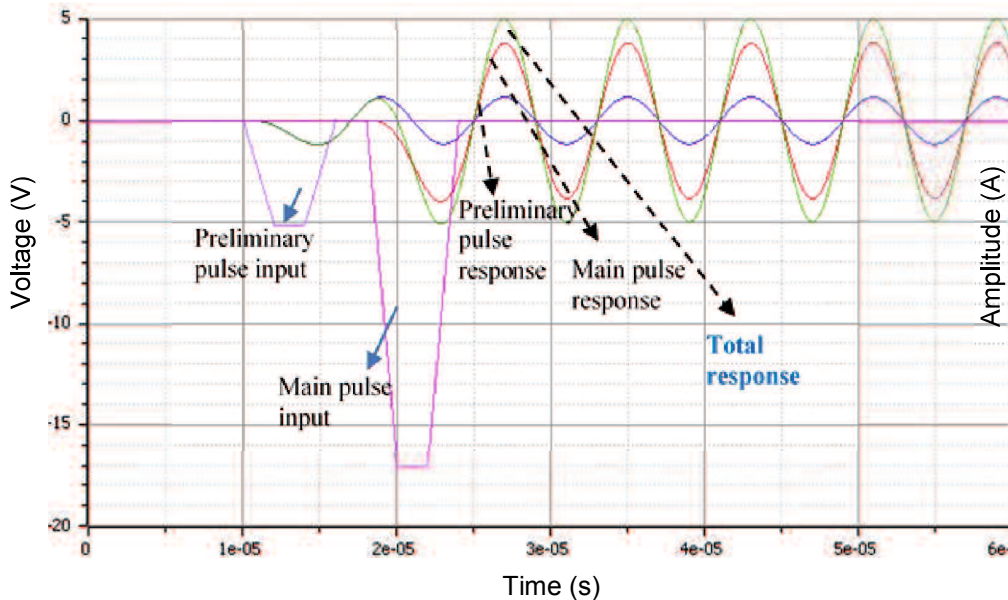
Fig. 3.20 Wave superposition principle as conceptual model of actuation waveform with preliminary vibration
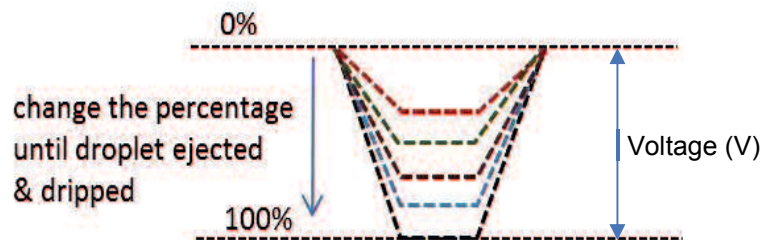
Fig. 3.21 Prior experiment to determine preliminary vibration

Figure 3.22 shows the experiment result from previous study with the same experiment device and operating liquid. It presents the droplet ejection behavior for different period and applied voltage. It is shown at $T_1 = 2\mu s$ (was used in this study), with head temperature 28°C and Dowanol as operating liquid, the stable voltage with droplet ejection was occurred at 11-13V. Therefore, since this 30°C was used as the head temperature, the base voltage is used base voltage for determining the preliminary vibration pulse is start from 10- 18V.
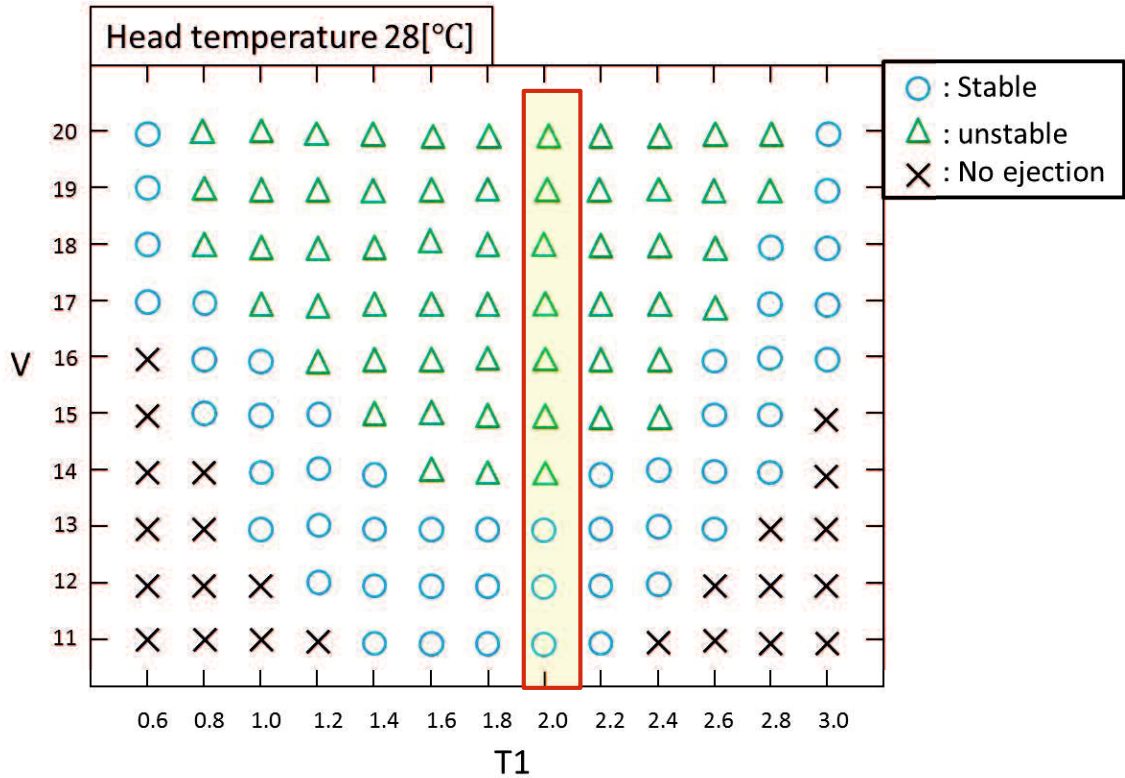
Fig. 3.22 Droplet ejection mapping (V = voltage, T1 = time (down, keep, up, wait))

The illustration of prior experiment result for preliminary vibration is shown in Fig. 3.23. There are four conditions of the droplet ejection process that shown in the figure. First condition id when there is no ejection. There is no enough energy to push the droplet out from the nozzle orifice. The next condition is when the droplet appear outside the nozzle. The smaller voltage will generate the shorter ink released by the nozzle head without breakup. The droplet will break up from the nozzle and then dripped when it has enough energy. The percentage of base voltage with droplet totally ejection (until totally breakup or dripped from the nozzle) is shown in table 3.4.
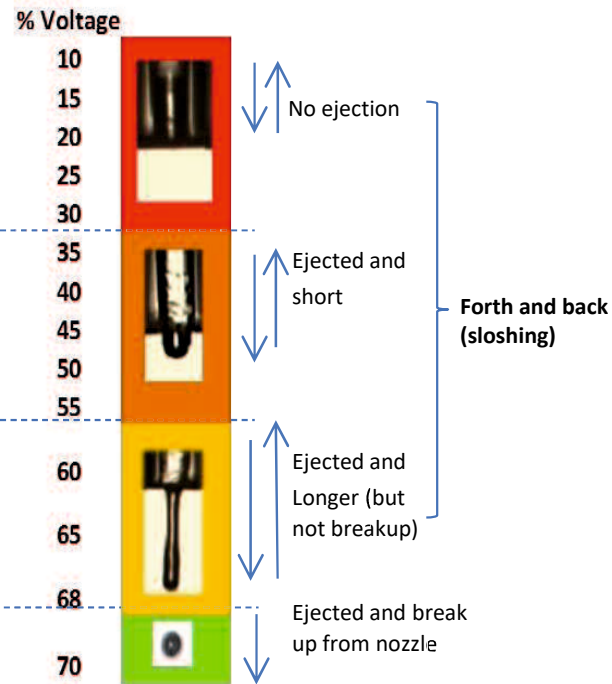
Fig. 3.23 The illustration of prior experiment result for droplet ejection
(At base voltage 14 V, Head temp: 30°C, frequency: 1 kHz)

Table 3.4. Percentage of base voltage for droplet ejection

Base Voltage (Volt)	The starting ejection (% of Voltage)	
10	100	= 10V
11	90.9	≈ 10V
12	83.3	≈ 10V
13	76.9	≈ 10V
14	71.5	≈ 10V
15	66.7	≈ 10V
16	62.5	≈ 10V
17	58.8	≈ 10V
18	55.6	≈ 10V

Table 3.4 shows that for all base voltage, the droplet will totally be ejected and break up from the nozzle at applied voltage 10V. Accordingly, the appropriate voltage percentage for base voltage 14V until 18 Volt is less than 55% of base voltage. Hence, if using input parameter for time of down, keep and up 2 μs respectively, as the second actuating waveform, we used 30% - 50% from base voltage as applied voltage of

preliminary vibration. The profile of actuation waveform with preliminary vibration is shown in Fig. 3.24.

$$t_{dp} = t_{kp} = t_{up} = t_{wp} = t_d = t_k = t_u = \frac{T_{an}}{4} \approx 2$$
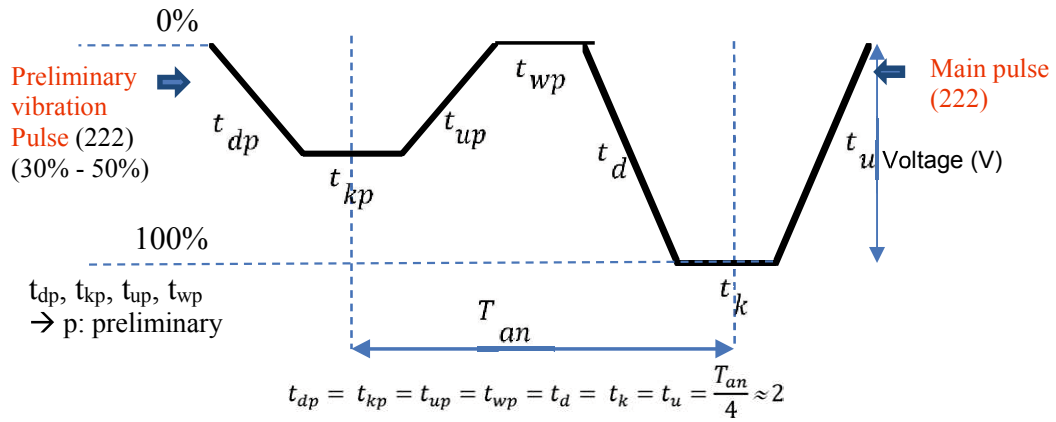
Fig. 3.24 Profile of waveform with preliminary vibration

3.7.3. With suppressing vibration waveform

The function of suppressing vibration is for damping the residual vibration and suppressing the droplet speed and volume. Suppressing vibration in this experiment is applied by the addition of pulse after main pulse. The idea of this suppressing vibration was to shift the t_{keep} and reduce the residual vibration of main pulse or suppress the positive waveform to reduce the droplet volume.

The first idea to reduce the residual vibration is by using the half-shifted period wave as shown in Fig. 3.25(a). The input parameter for down, keep, up, and wait 222_6_222, hereafter called "Suppress A". The percentage of suppressing vibration was determined by pre-experiment, using 30%, 50% and 100% from base voltage 14v – 18 V.

The second idea of suppressing vibration used half period of actual natural period (T_{an} /2) with input parameter 222_0_111 as shown in Fig. 3.25 (b). This period of second pulse waveform is shifted 4 μs to reduce the residual vibration of main pulse. This original overlapped waveform then modified, transformed into the right image to make it easier to input. The applied voltage of this pulse using 30%, 40% and 50% from base voltage 14 – 18 V.
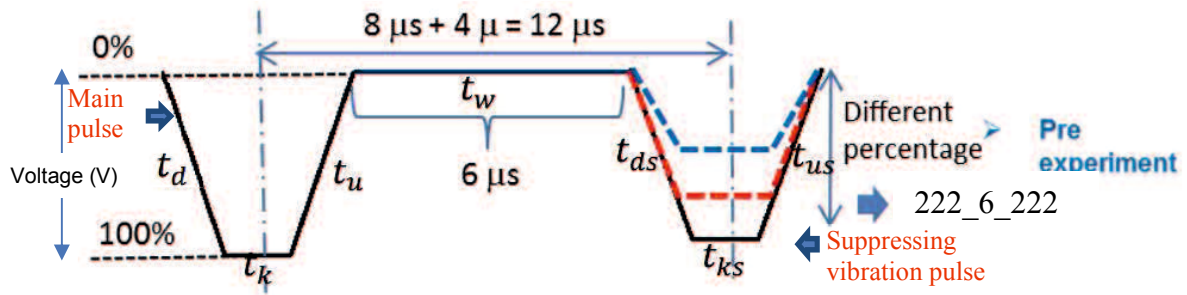
Fig. 3.25 (a) Profile of waveform with suppressing vibration
(Suppress A)

$$t_d = t_k = t_u = \frac{T_{an}}{4} \approx 2, \qquad t_{ds} = t_{ks} = t_{us} = \frac{T_{an}}{8} \approx 1$$
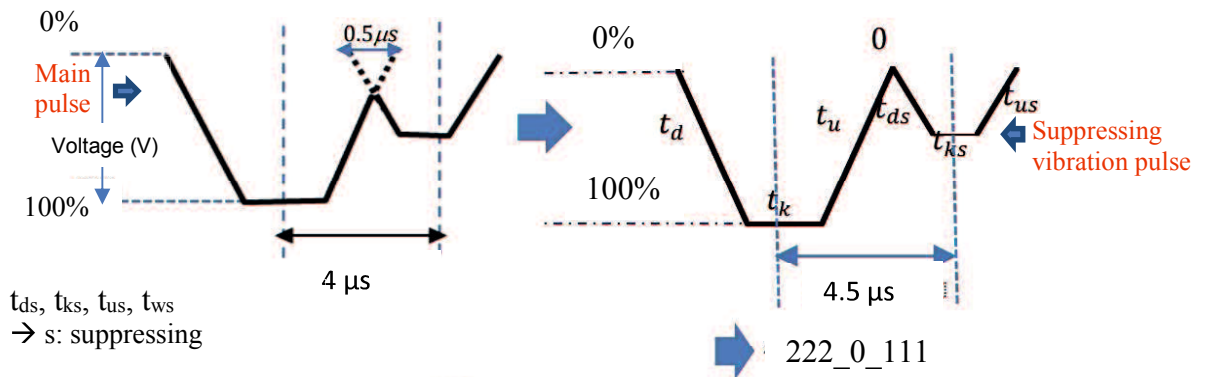
Fig. 3.25 (b) Profile of waveform with suppressing vibration
(Suppress B)

The conceptual model of this actuation waveform is shown in Fig. 3.26 (a) and (b). It presents the total response from wave superposition principle is lower amplitude than basic waveform. It means that the predicted pressure and mass of the final droplet will be lower and smaller than the basic waveform.
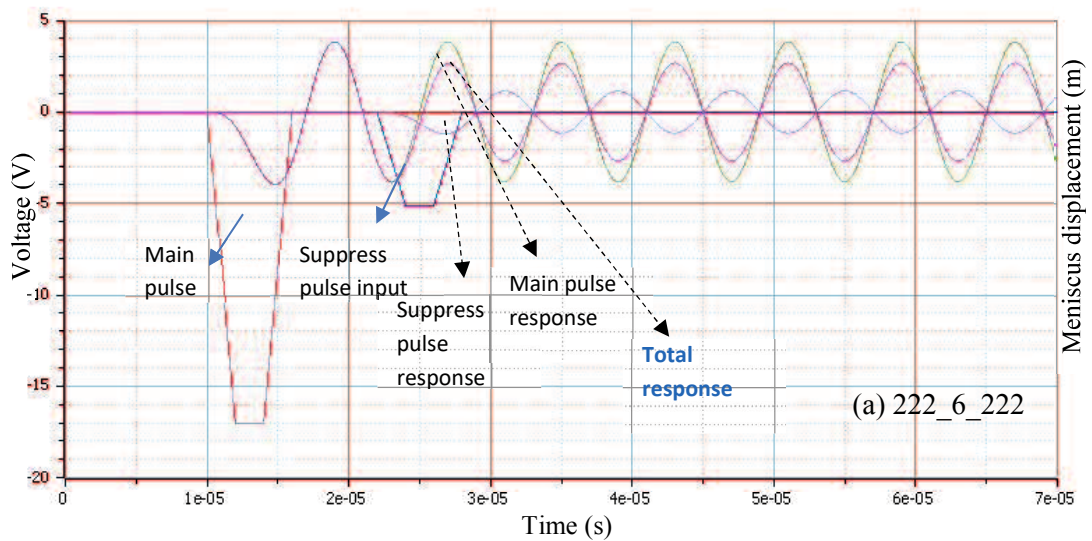
(a) 222_6_222

Fig. 3.26 (a) Wave superposition principle as conceptual model of actuation waveform with suppressing vibration 222_6_222
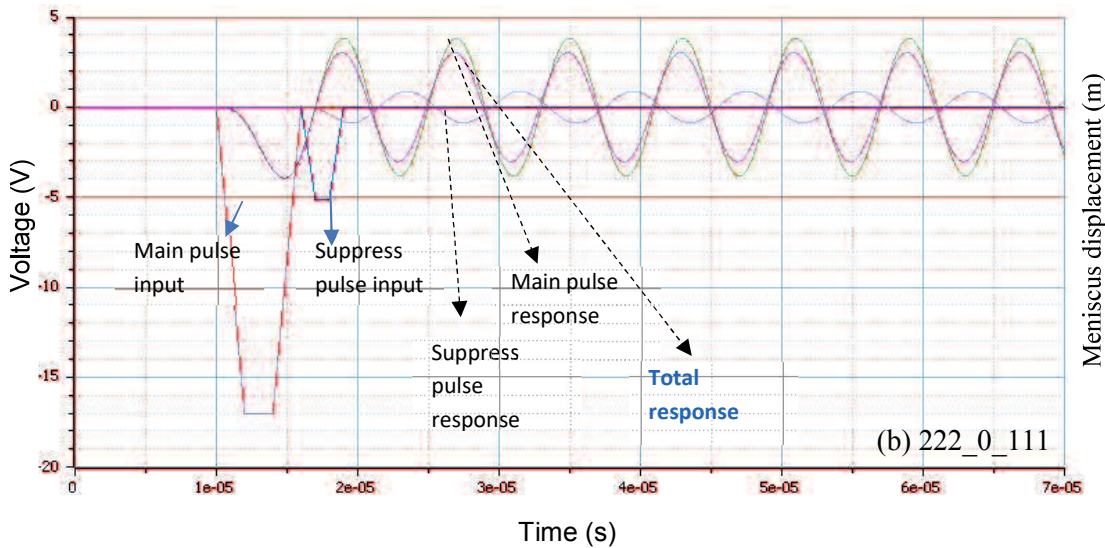
Fig. 3.26(b) Wave superposition principle as conceptual model of actuation waveform with suppressing vibration 222_0_111

3.8 Droplet Formation Process and Speed Measurement Standard

The objective of this section is for investigate the droplet formation process and observe the droplet shape and speed at different distance from nozzle. The other purpose is to decide the experiment standard for distance of droplet observation from Nozzle head to take the speed. Currently, the experiment applies 500 μm as setting distance from nozzle head to measure the droplet speed. In this experiment, we observed the droplet shape and speed at the different distance from nozzle head, start from 200 μm until 1000 μm. The different voltage was applied in the experiment, respectively. The droplet formation process and speed is shown in Fig. 3.27. This figure presents the droplet formation process for the distance from nozzle at 200 μm until 1000 μm. There are three stages of droplet speed when it ejected from nozzle. First stage is when the droplet still connected to the nozzle, at 200 μm for base voltage 14V and 200-400 μm for 15-18 V. At this stage, the droplet speed is still affected by the actuating waveform and generated the higher droplet speed.

The next stage is when the droplet had breakup from the nozzle and still in a shrinking process of ligament or in necking process. The speed at this stage is gradually decreased because of air resistance. The third condition is when the droplet became a

single clear droplet or split off and became two drops (main drop and satellite or main drop and ligament drop) which have two different velocities that are head and tail speed. The speed at this stage is more constant than other stages. Based on this condition, we recommend to using 1000 μm for the observation distance of droplet from nozzle and as standard distance in inkjet printer experiment system for speed measurement. The speed measurement concept is shown in Fig. 3.28. The other reason, this distance is also the distance standard of printing surface from the nozzle head. With same distance, the droplet shape in our experiment is equal to the droplet shape when reach the print surface. The drop speed is obtained from the average of distance (D) from nozzle divided by elapsed time between the nozzle head until reaching D (T), appropriate to approach 2 in droplet speed measurement [13].
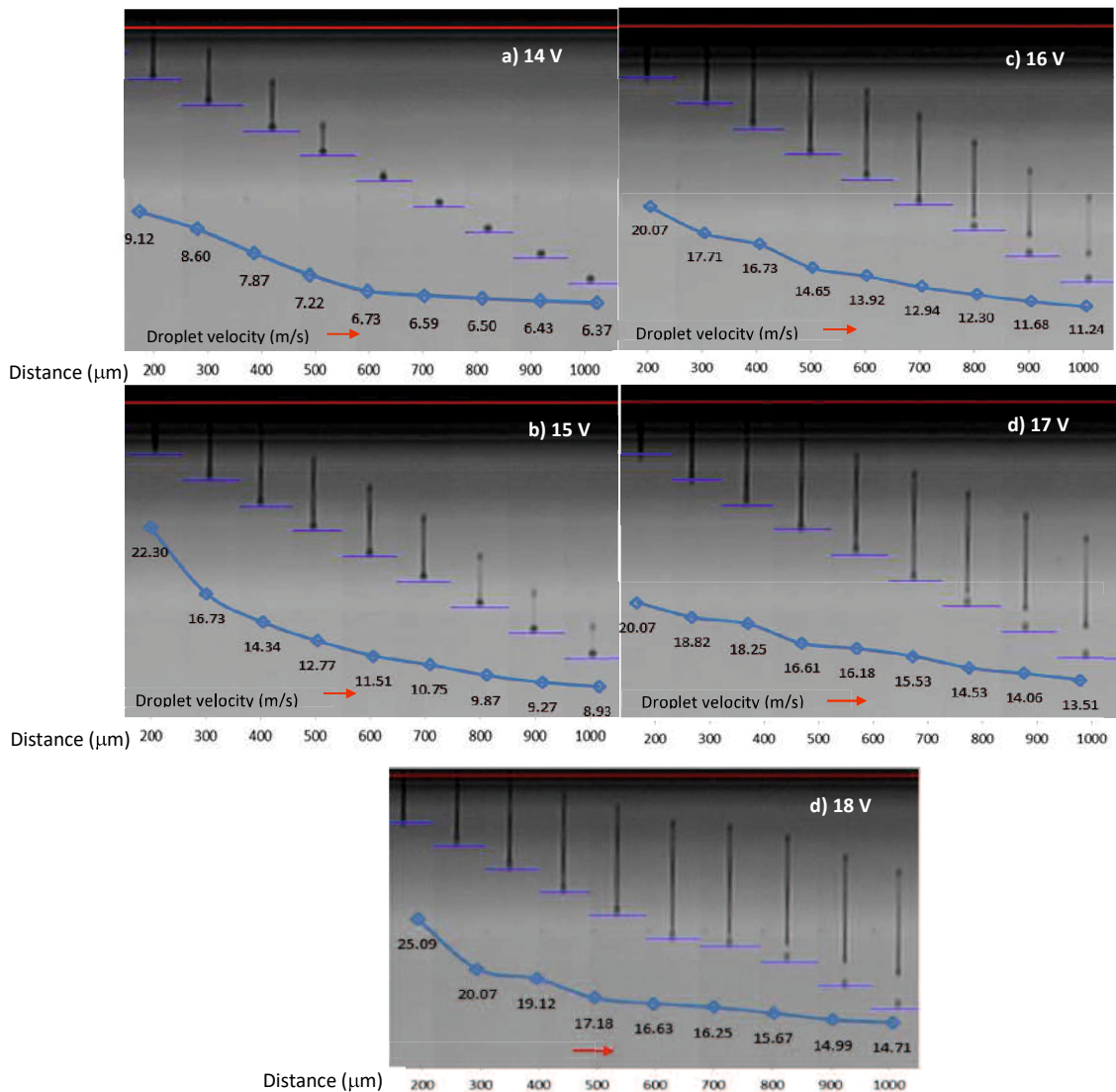
Fig. 3.27. Droplet formation process and speed
(Basic waveform)

Speed = D / T (m/s)

D : Distance from nozzle (μm)

T : elapsed time (μs)

D = 1000 μm
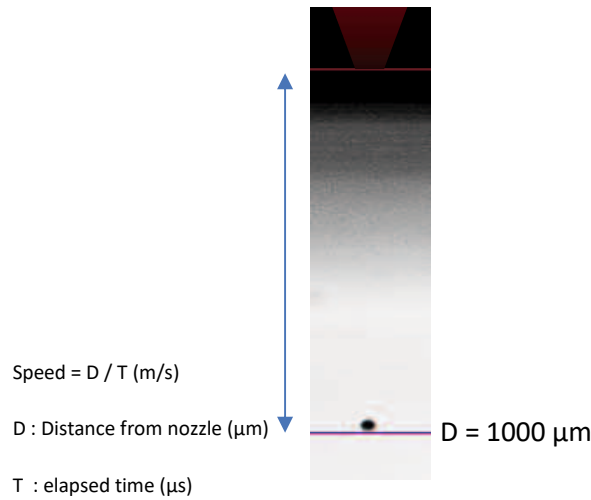
Fig. 3.28. Droplet speed measurement method

BASIC WAVEFORM

14V   15V   16V   17V   18V
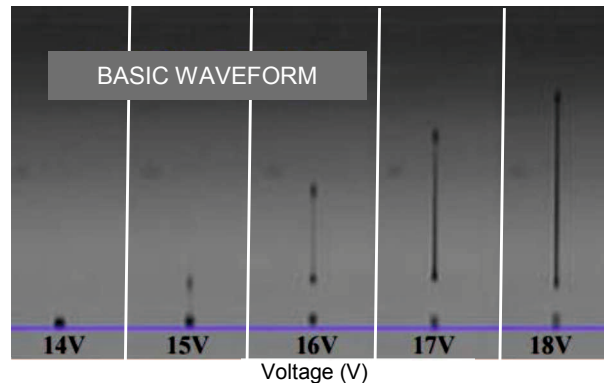
Voltage (V)

Fig. 3.29 Droplet shape for basic waveform at 1000 μm from nozzle

Fig. 3.29 shows the final droplet shape (at 1000 μm from the nozzle). It shows the clear droplet was only generated in applied voltage 14V. Furthermore, the larger applied voltage will cause the longer ligament. The different droplet formation process that was generated from the actuating waveform with preliminary vibration is shown in Fig. 3.30. It shows the different kind of droplet shapes; droplet with short-connected ligament (a), satellite that joins with the main droplet and then became a clear droplet (b), droplet with long-split ligament (c), and main droplet with satellite (d). We can see the clear droplets without ligament or satellite is at 14V for 50% preliminary vibration waveform. This figure shows that the droplet shape with the higher voltage in the different actuating waveform will generate the longer ligament, severed ligament or more than one drop.

The larger voltage applied to the actuation waveform, the longer ligament will be generated. The larger voltage means the higher amplitude or higher pressure to eject the

droplet, so then make the head droplet has such a higher speed and make the tails droplet cannot reach the head droplet. It will generate the longer ligament. If the short tail combined, then the droplet will become 2 drops, the big droplet is head droplet, with a small droplet from tail droplet so called "satellite".
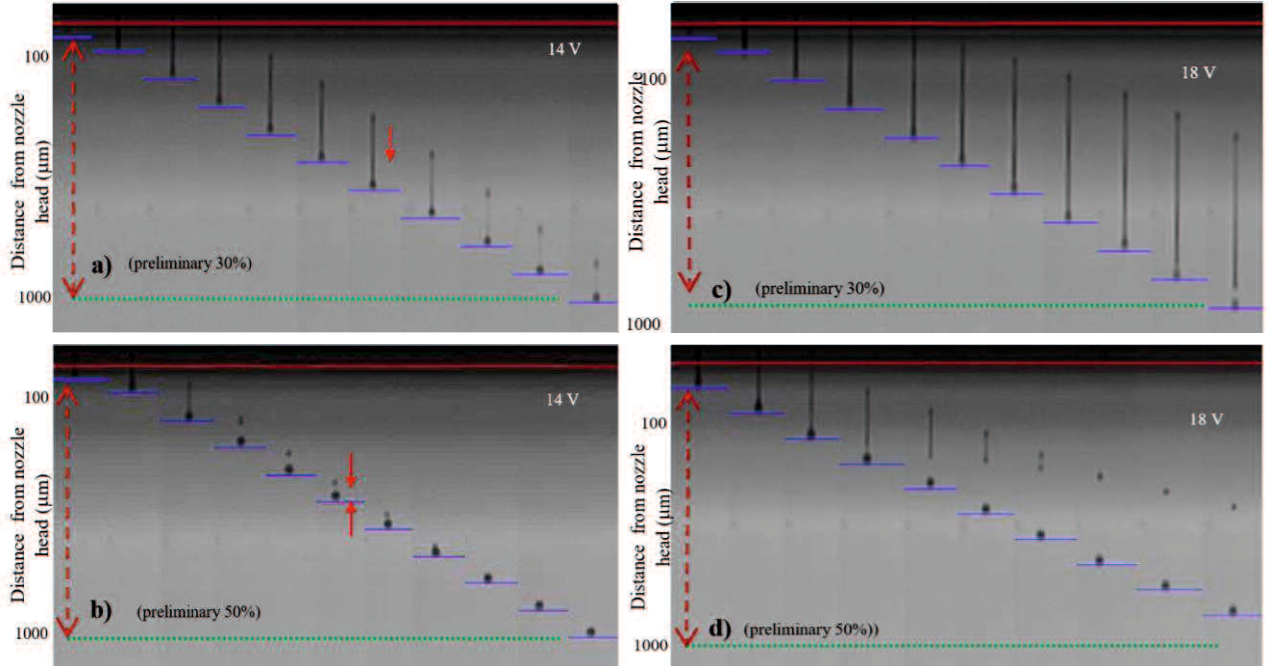
Fig. 3.30 Droplet formation process for preliminary vibration

3.9 Conclusion

This chapter contain the explanation about the experiment set up, and the step of obtaining the data for droplet speed measurement and volume measurement. The actuation waveform that will be used in the next chapter was also discussed with the prior experiment and conceptual system model for determining the optimum applied voltage of preliminary and suppressing vibration. The percentage of base voltage for preliminary and suppressing vibration is 30%, 40% and 50%. The experimental study was conducted to obtain the actual natural period of experiment device and other parameter as experiment standard. The actual natural period that determined for inkjet printer experiment with Dowanol ink is 8.2643 μs. This result is used to propose 2.066 μs as t_d, t_k, t_u and t_w input parameter for the actuation basic waveform in the experiment system. The experiment was also done for determining the standard of fire limitation number and droplet distance from nozzle on droplet weight and speed measurement method. The recommendation of fire limitation number standard is 100.000 drops for droplet weight measurement and 1000 μm distance from the nozzle for droplet speed measurement. This standard is necessary to be implemented for improve the inkjet printer experiment system.

CHAPTER IV

EFFECT OF ACTUATING WAVEFORM WITH PRELIMINARY AND SUPPRESSING VIBRATION

4.1. Introduction

Inkjet printing research and development is being carried as continuous improvement to increase the inkjet printer performance and its printing result. The droplet ejection process, shape, volume and velocity are influenced by actuating waveform of the piezoelectric element [1] – [3]. The properly design of input waveform must be made to get the optimum result [17], [19], [81] & [82]. Some studies were conducted to design the actuating waveform. Kwon et al. discussed about waveform design method for high speed inkjet printing based on self-sensing measurement. A two pulses waveform was design with pull-push system based on the33 measured pressure wave to effectively suppress the residual pressure wave after jetting. In that study, the waveform design is not verified by real inkjet printer experiment to check the actual result on droplet shape, velocity and volume for actual condition [19].

The other study by same author was conducted to propose the method on designing an efficient waveform. In this study, three different types of waveform using positive (trapezoidal) waveform as basic waveform, high-speed jetting waveform using positive and negative (bipolar) waveform, and negative waveform, is compared and designed to determine the optimal value of dwell time [81]. Shin et al. using double positive waveform to observe its effect to droplet formation [23], while Kim et al. using double piezo-actuators with bipolar waveform and investigated the effect to ejected droplet speed [15].

The droplet ejection process, shape, volume and velocity are influenced by actuating waveform of the piezoelectric element [2], [4] & [10]. Some studies were conducted to investigate the droplet behavior [1] - [13], [18], [23] & [76] – [83]. Most of studies were using positive (trapezoidal) waveform or positive and negative (bipolar) waveform [3], [5], [6], [10], [16], [17] & [19] – [22].

The applied voltage effect to the droplet speed were discussed by some studies [11], [15], [20], [23], [29], [71] & [72]. Xu et.al. investigated the effect of high voltage on the charged density, droplet velocity and size, and pinch-off position of single droplet in DoD inkjet Printing [11]. It was stated that the waveform used in this study (positive-negative-

positive polar) with higher applied voltage will generate the higher speed and smaller volume of ejected droplet. The result about correlation of applied voltage and droplet size is in contrary with the other researches. On another side, the other study concluded that the higher voltage that applied for ejecting the droplet will generate the larger size and volume of droplet [6], [15] − [18], [22], [24], [27] & [32]. Logically, the result of droplet size could be decrease because it only measured the main droplet without observed the ligament or satellite.

In this study, we investigated the effect of different applied voltage in the actuating waveform design that using preliminary and suppressing vibration and determine the optimum parameter of each waveform. The comparison of actuating waveform design with preliminary and suppressing vibration to basic waveform was discussed in detail. Dowanol ink was used as operating liquid and tested by different nozzle head temperature and applied voltage from 14 V until 18 V. By observing the droplet shape, volume and velocity, the optimum base voltage for each actuating waveform could be determined and proposed.

4.2 Input Parameter and Actuation Waveform

The input parameter of the experiment in this chapter is shown in table 4.1.
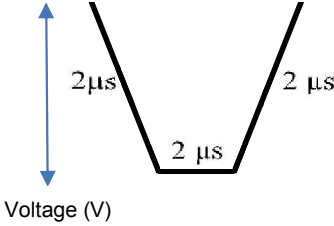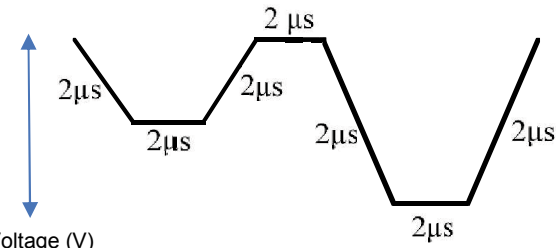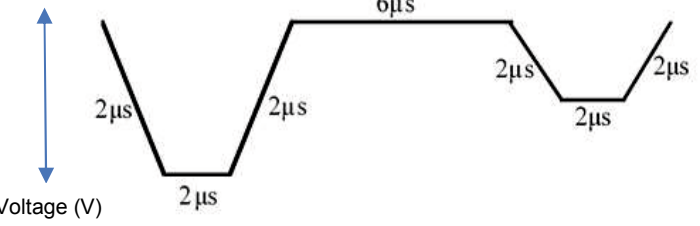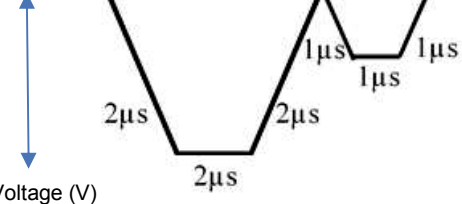
Table 4.1 Input parameter

Liquid	**: Dowanol**
Applied voltage	: 14 – 18 V
Fire frequency	: 1 kHz
Head Temperature	: 30 - 45°C

As discussed in chapter III, the idea of each actuating waveform is for generating the total response that able to control the droplet velocity and volume. It was assumed that by the additional pulse before or after the main pulse, we can improve the droplet velocity and volume, or reducing it. In this chapter, we examine the concept by experiment and investigate the effect of different percentage of the preliminary and suppressing vibration.

The actuation waveform profile shown in table 4.2. The detail information about the actuation waveform profile is discussed in the previous chapter (Chapter III). In this chapter, the measurement of droplet velocity, volume and shape observation was conducted. The comparison of the experiment result was done and analized for understanding the droplet behavior in related with each actuation waveform.

Table 4.2 Actuation waveform profile

Actuation waveform type	Actuation waveform profile
(a) Basic (222)	
(b) Preliminary vibration (222_2_222)	 Percentage of preliminary vibration: 30%, 40% and 50%
(c) Suppressing vibration (222_6_222) → "Suppress A"	 Percentage of suppressing vibration: 30%, 50% and 100%
(d) Suppressing vibration (222_0_111) → "Suppress B"	 Percentage of suppressing vibration: 30%, 40% and 50%.

4.3. The Effect of Voltage in Different Actuation Waveform on Droplet Velocity and Volume

The discussion of this section is divided into two subsections according to different actuating waveform. The preliminary vibration and suppressing vibration effect compared to basic waveform with different condition is discussed and analyzed.

4.3.1 Preliminary vibration

The basic idea of preliminary vibration in actuating waveform is for generate the initial vibration before actual vibration to eject the droplet by generating the constructive wave superposition to eject the larger and faster droplet. This idea can be explained by wave superposition principle, similar with measured meniscus motion concept in other study to design waveform [81]. The conceptual model of the actuation waveform with preliminary vibration is shown in Fig. 4.1. The illustration of wave mechanism by different percentage of preliminary vibration is shown in Figure 4.2.
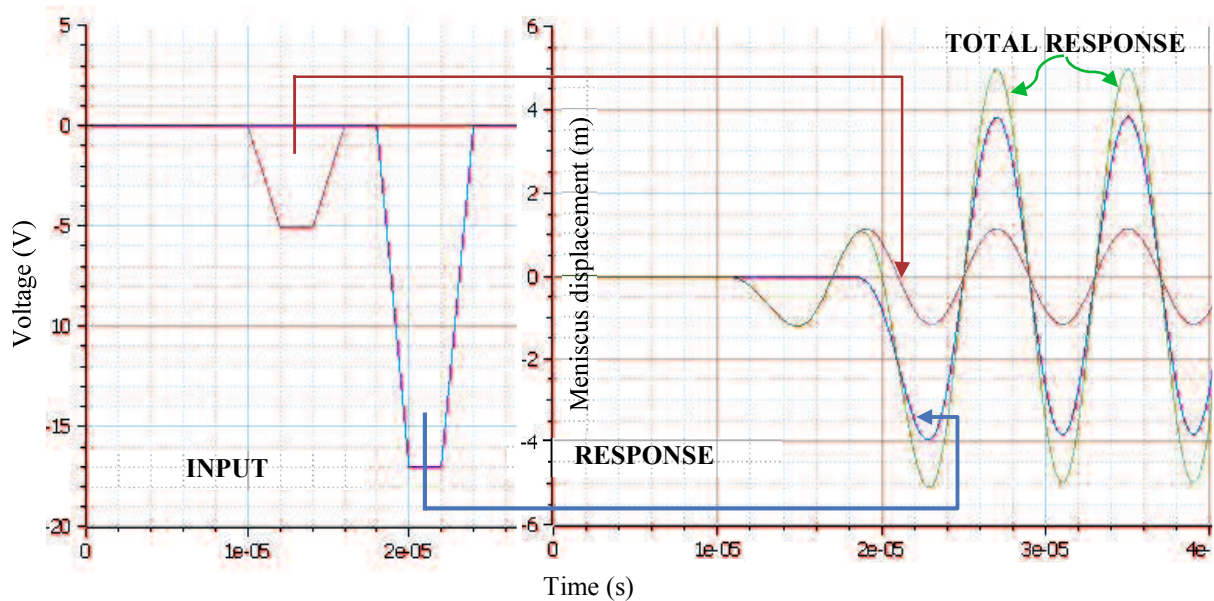
Fig. 4.1 The conceptual model by wave superposition principle of actuation waveform by preliminary vibration
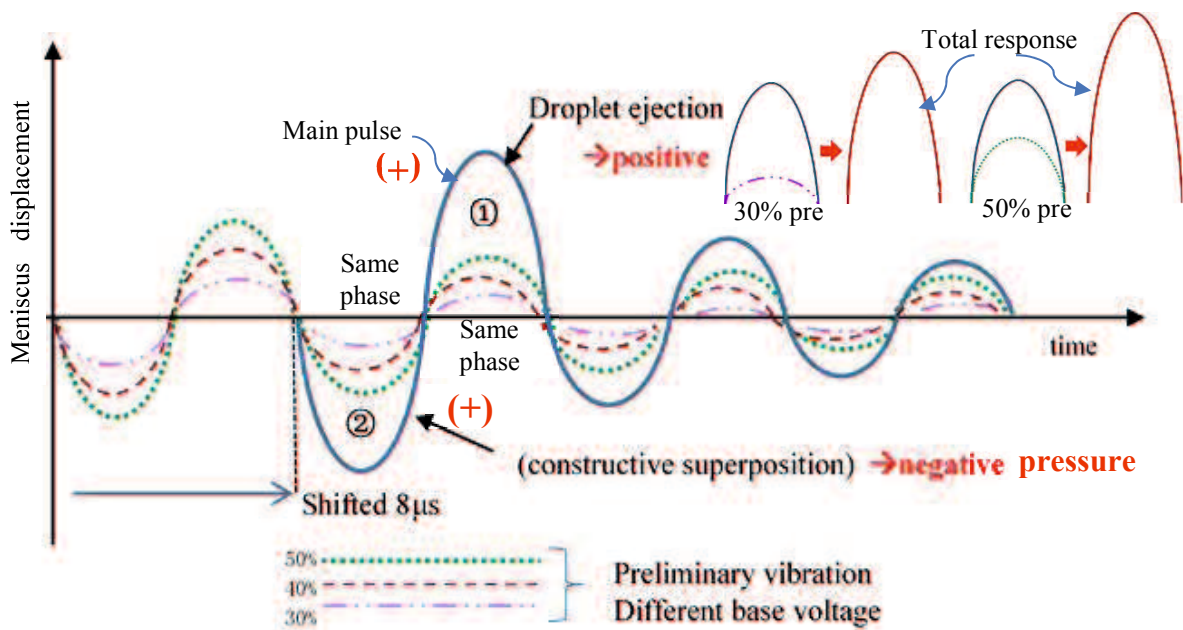
Fig. 4.2 The illustration of wave mechanism by different percentage of preliminary vibration

The preliminary vibration waveform consists of two waves and travel in the same direction. First wave is the preliminary vibration with small voltage so that there is no droplet ejection, whereas the second wave is acted as main pulse that supposed to generate the droplet. The exactly same phase of that two waves caused constructive superposition principle, produce a larger resultant at both positive and negative polar include in the residual vibration. The larger percentage of base voltage in preliminary vibration, cause the larger wave resultant in peak ① and generate larger droplet. The larger negative wave in peak ② will generate the larger back pressure such as restoring energy to "withstand" the droplet velocity and caused the lower velocity. The droplet velocity is tending to similar in base voltage percentage (40% and 50%) of preliminary vibration, and higher applied voltage (>15 V).

The correlation between base voltage and percentage of preliminary vibration, with the droplet velocity is shown in Fig. 4.3. Figure 4.3 presents that the actuating waveform with preliminary vibration by different voltage percentage gave the different effect. 30% of base voltage in the preliminary vibration at 14 -16 V generated the faster droplet than basic waveform. The velocity at 17V is similar but lower at 18V. 40% of preliminary vibration at 14 - 15 V generated the higher velocity than basic waveform and then significantly

decrease from 16 - 18V. On the other side, 50% preliminary vibration generates the droplet with lower velocity than basic waveform at all base voltage.
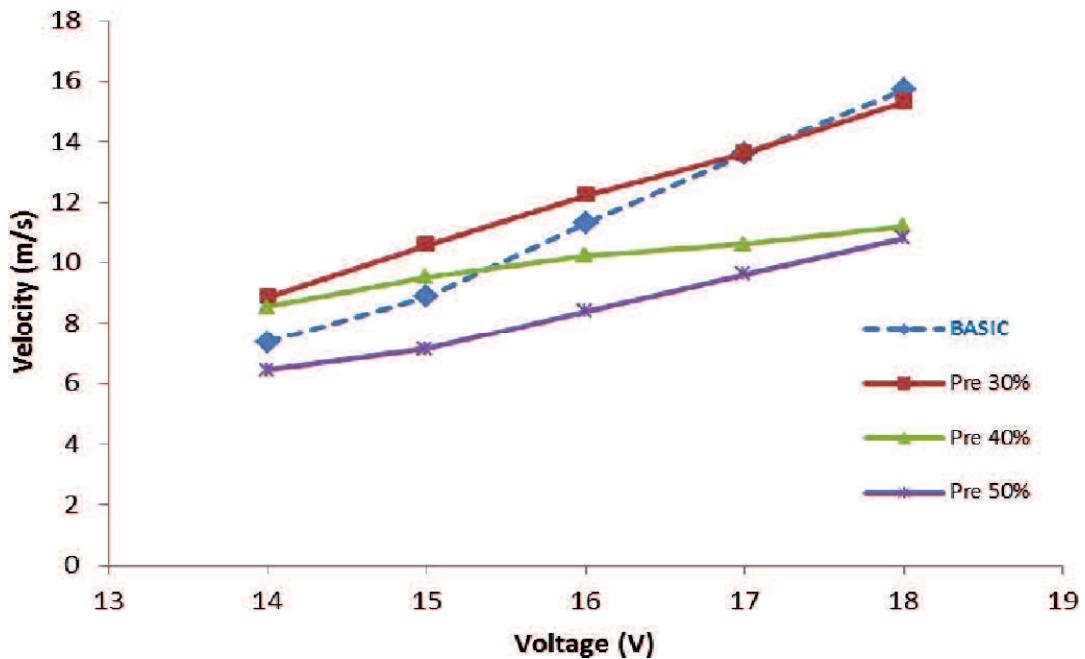
Fig. 4.3 Comparison of droplet velocity between basic waveform and preliminary vibration waveform

This phenomenon can be explained by reviewing the prior experiment to determine the percentage of base voltage as preliminary vibration. In the lower percentage (30%) at 14V and 15V, the low energy from low voltage that generated from the 30% preliminary vibration can only pull and push the ink inside the liquid chamber. The energy to "push" the ink from the orifice is not enough, until it returned to the standby position. The lower energy gives the lower or no residual vibration. The second pulse with higher energy supported caused the higher energy to "push" and ejects the ink, and generates the higher initial velocity and volume.

On the other hand, 50% preliminary vibration will make the droplet come out from the nozzle, and when it "forth" and "back" in to the nozzle. The "pull" energy from the main pulse, may overlapped with the larger residual vibration from preliminary vibration and combined, then subsequently "push" the ink from the nozzle. The energy to push the greater mass inside the liquid chamber, make the lower velocity of the droplet. The different trend of velocity for 40% and 50% of preliminary vibration may cause by the residual vibration and affect to the speed variation. This phenomenon is elucidated by

droplet shape in figure 4.4. Noted that the velocity curve shown in Figure 4.6 is the head droplet velocity.
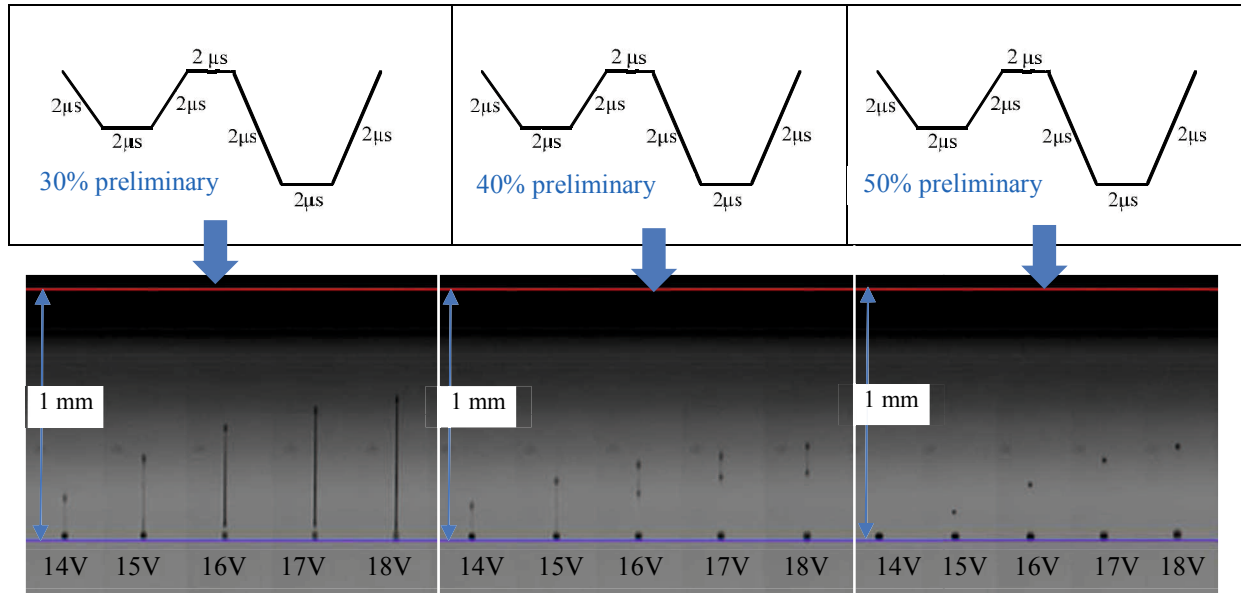
Fig. 4.4 The droplet shape of "preliminary vibration" waveform

Figure 4.4 shows the different droplet shape as result of different percentage of preliminary vibration. The smaller droplet head (main drop) with ligament was generated in 30% preliminary vibration. We can see that the higher voltage applied, will generate the longer ligament. If comparing to the basic waveform, 30% preliminary vibration generate the similar droplet behavior with "sharp" and long tail. It implies that the "water gun" effect are still existing.

With applied voltage at $14 - 15V$ for 40% of preliminary vibration shows the similar shape with 30% of preliminary vibration. Nevertheless, the different droplet shape appeared for $16 - 18V$ in 40% preliminary vibration. At $16 - 18V$, the droplet tail has pinched off from the main drop. Figure 4.3 shows that the velocity at those voltages is decreased. It indicates that when the tail is shrinking as it sweeps up the ink in the tail, it slows down the droplet. The correlation between velocity and shape is shown in Fig. 4.5. It is shown that the similar droplet shape and velocity at $16 - 18V$ applied voltage. The droplet pinched off and tail breakup process for 50% preliminary vibration can be seen more clearly in Fig. 4.6.
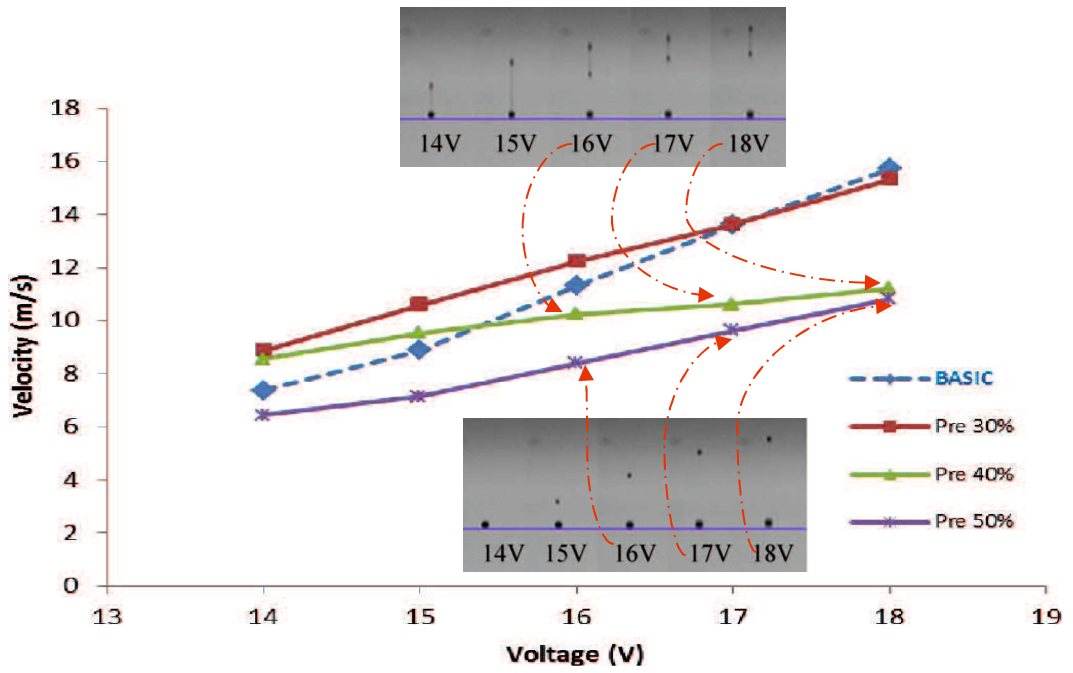
Fig. 4.5. The correlation between droplet velocity and shape (preliminary vibration)
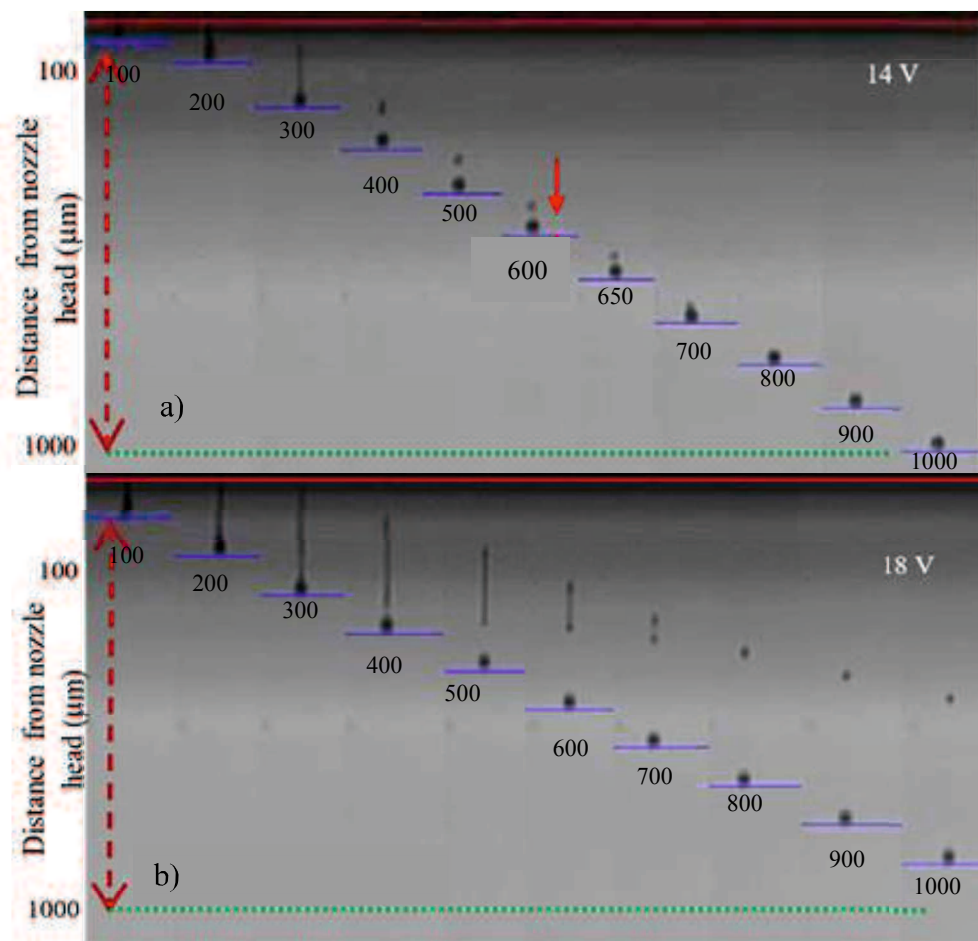
Fig. 4.6 The droplet pinched off and tail breakup process for 50% preliminary vibration

The real droplet pinched off and tail breakup process in Fig. 4.6. The droplet shape was captured at 100μm until 1000μm from the nozzle. This process then described in Fig. 4.7. The pinch off can be caused by many different effects. Driessen, et.al described the effects that can cause pinch off in the droplet formation process from the experiment [110]. The imbalance in the capillary tension after tail pinched off at the meniscus can causes the tail or ligament formation. The capillary tension pulls the droplet tail toward the droplet head. Concurrently, it sweeps up the ink in the tail and increase the tail mass or shrinking mode. It will slow down the droplet. In this study, we investigate the correlation of applied voltage with the pinch off and tail breakup process. We can see that the lower voltage allowed the satellite to reach and merged with the main droplet, become clear spherical droplet. For higher voltage (18V), the tail was starting the breakup process at 300μm from the nozzle. When the meniscus breakup from the nozzle and retracted again into the nozzle, the necking occurs then the ligament also pinched off with the main droplet or head droplet. The tails then shrinking and merged become a satellite at 800μm from the nozzle.
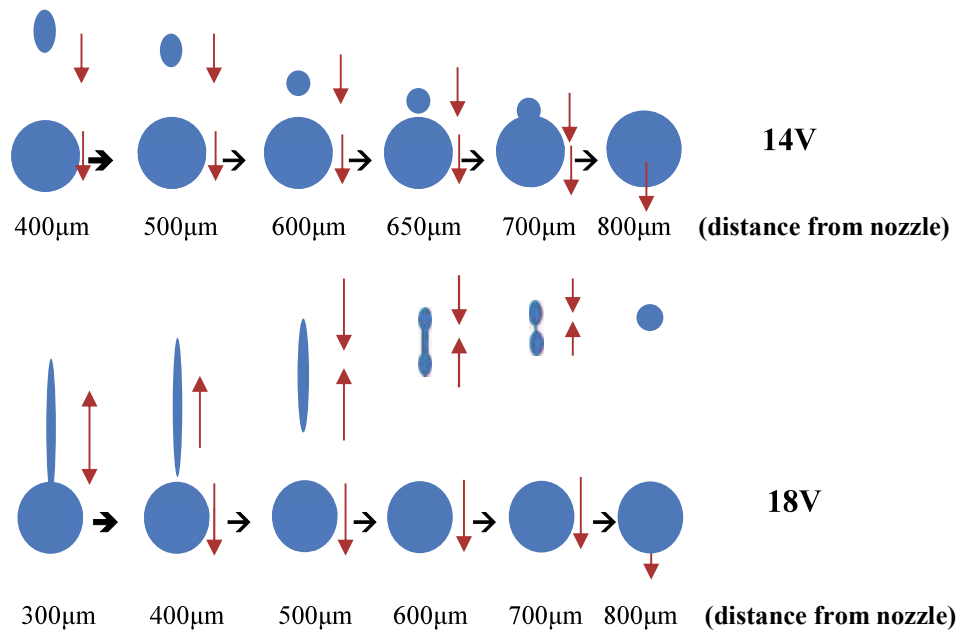
Fig. 4.7 The description of droplet pinched off and tail breakup process

The capillary tension that mentioned above can be described as the resultant of surface tension acting in curved menisci and is governed by the fundamental equation of capillarity known as the Young-Laplace equation in equation 4.1.

$$\Delta p = p - p_g = \sigma \left(\frac{1}{R_1} + \frac{1}{R_2} \right)$$

Where Δp is the Laplace pressure, represent the pressure drop across the interface, σ is the surface tension, and R_1 and R_2 are the principal radii of curvature on the interface. The pinch off will occur if R_1 is larger than R_2. A very thin thread liquid called as secondary tail (small R_2) generate a large pinching force. On the other side, the small R_1 generates the large restoring force and allowing to merge. The Laplace equation is described in Fig. 4.8.
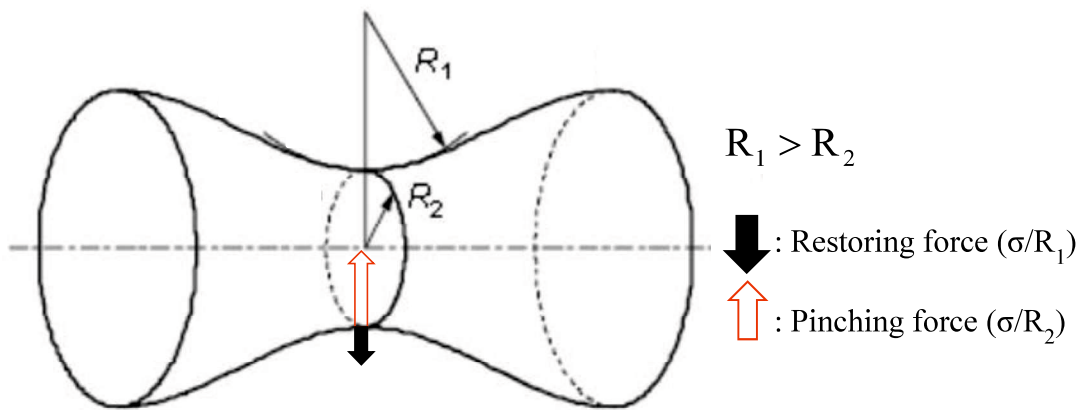
R_1: Minimum radius of curvature of a generator line

Fig. 4.8 Description of Laplace pressure law

The droplet volume of different % of preliminary vibration compared to basic waveform is shown in Fig. 4.9. From this figure, we can see that the larger base voltage percentage of preliminary vibration, the larger volume would be, and an increase of applied voltage, the droplet volume also increases. This phenomenon also can be explained with figure 4.2. The larger applied voltage means the larger wave resultant that could generate the larger droplet volume. In addition, the higher voltage applied, it would make the higher pressure give to the channel, the velocity of droplet increase and more fluid can be ejected from nozzle, generated the larger droplet volume.
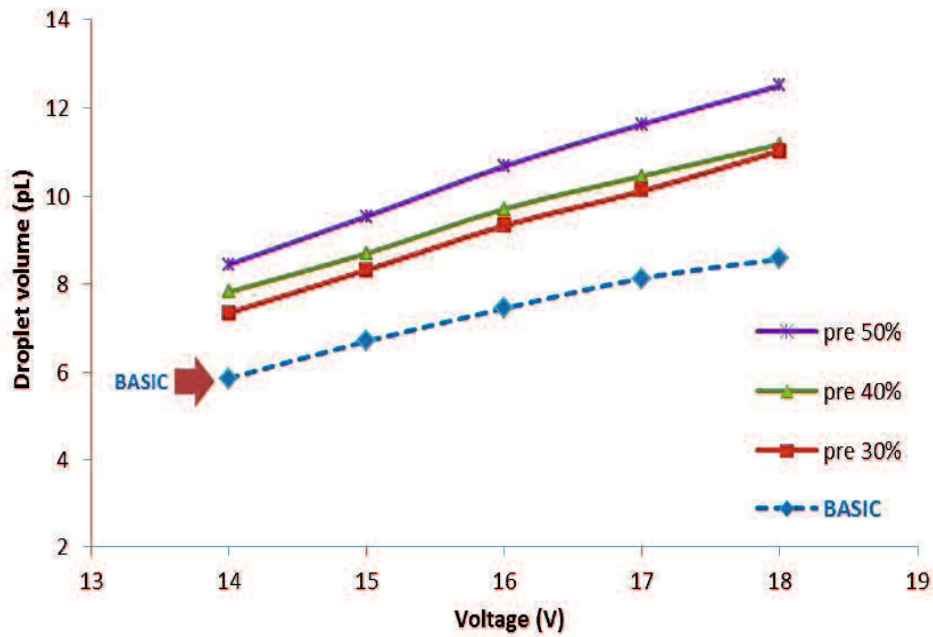
Fig. 4.9 The droplet volume comparison of preliminary vibration and basic waveform

4.3.2. Suppressing vibration

The function of suppressing vibration is to reduce the residual vibration and for suppressing the droplet volume and velocity by shifting the second pulse. The actuation waveform design can be made by considering the meniscus motion related to jetting behavior [6].

a. "Suppress A" (222_6_222) waveform

Pre-experiment result to decide the suppressing vibration percentage for next stage using input parameter of "suppress A" waveform is shown in Figure 4.10. The figure presents that different percentage of second pulse as suppressing vibration unless at 30% generated the larger droplet volume than basic waveform. This result depicts that the only effective waveform to reduce the residual vibration is at 30% suppressing vibration particularly in low voltage (14 and 15 V). There is a significant difference of volume for 100% suppressing at base voltage 17 and 18 V.
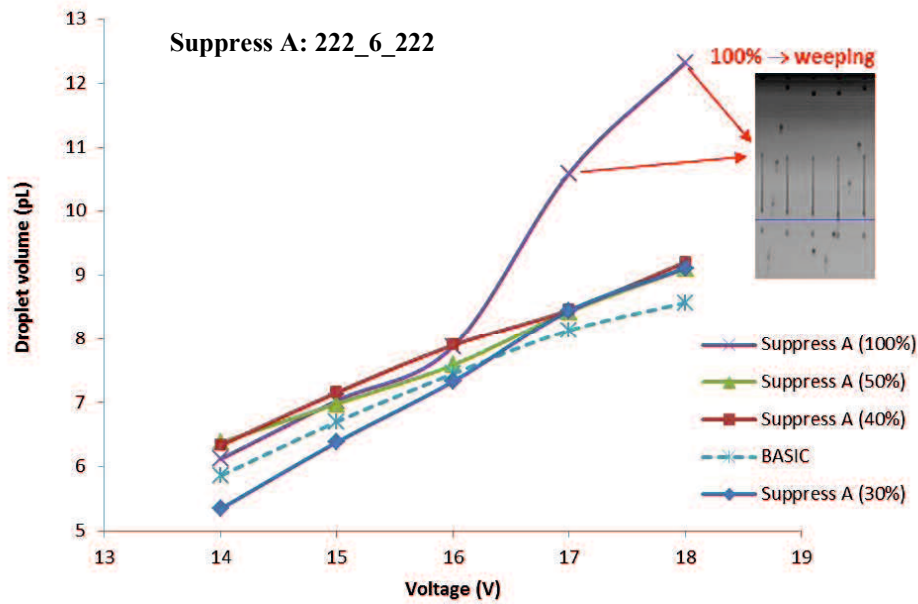
Fig. 4.10 Pre-experiment result for "Suppress A" 222_6_222 (different percentage of second pulse)

From monitor display of experiment device, we can see that in those applied voltage, ink weeping was occurred. It may cause by crosstalk effect and residual vibration in high voltage. Crosstalk in inkjet system is the phenomenon when the actuating waveform from one or more nozzles could unintentionally impact the other nozzles to eject the droplet. High voltage in second pulse could cause undesired pressure perturbations at the other nozzles [2]. The superposition principle to explain this phenomenon is described in Figs. 4.11 and 4.12.

Figures 4.11 and 4.12 present that the different percentage of base voltage will give the different effect. Appropriate small voltage supposed to reduce the residual vibration of the main pulse and generated the single peak only. The high voltage could generate new peaks such as multi-pulse that produce multi-drop and too high pressure caused weeping that must be avoid in inkjet system. Therefore, 30% suppressing vibration of "suppress A" waveform is proposed to reduce the residual vibration of main pulse, with applied voltage 14 – 15 V. Pre-experiment also shows that the droplet velocity and shape of this waveform is similar. There is no significant different of the experiment result using this waveform compared to basic waveform.
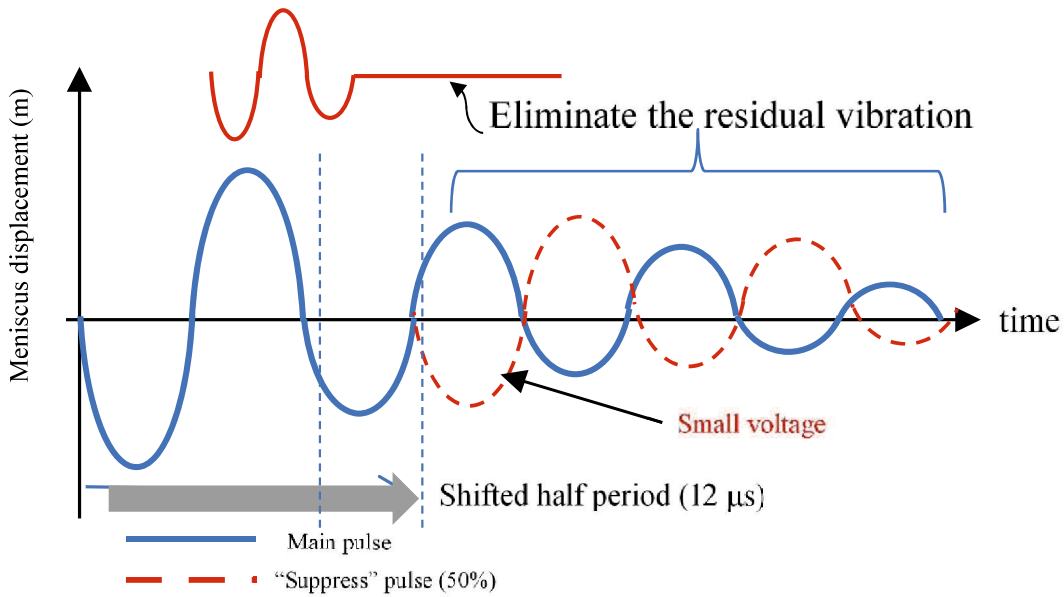
Fig. 4.11 Illustration of "Suppress A" (222_6_222) waveform output (small suitable voltage)
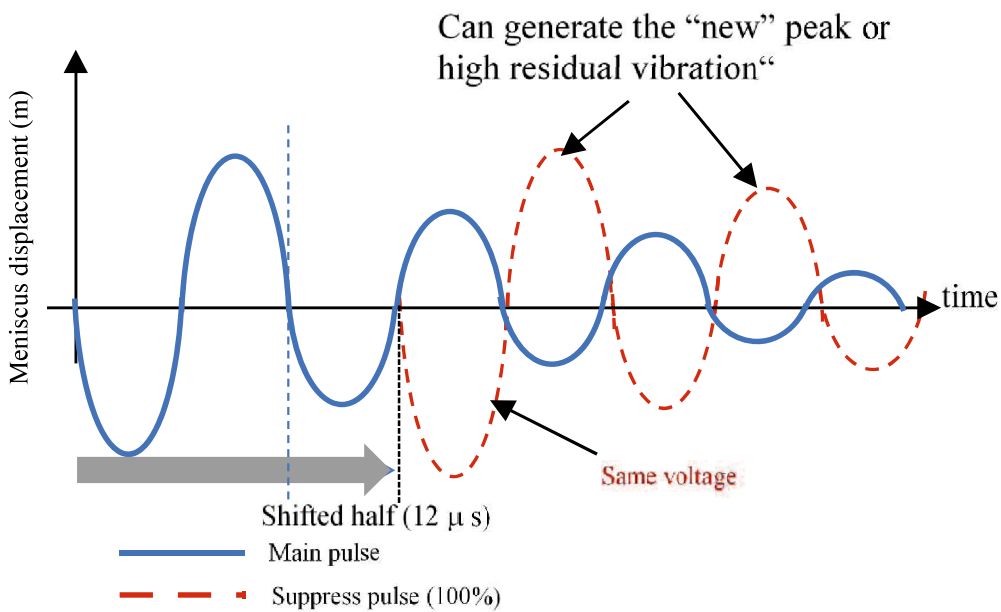
Fig. 4.12 Illustration of "Suppress A" (222_6_222) waveform output (same voltage)

The illustration in Figs. 4.11 and 4.12 are the prediction of wave superposition principle from two pulses with time separating 6μs. The response of those two pulses will be easier to explain by the conceptual model as shown in Fig. 4.13.
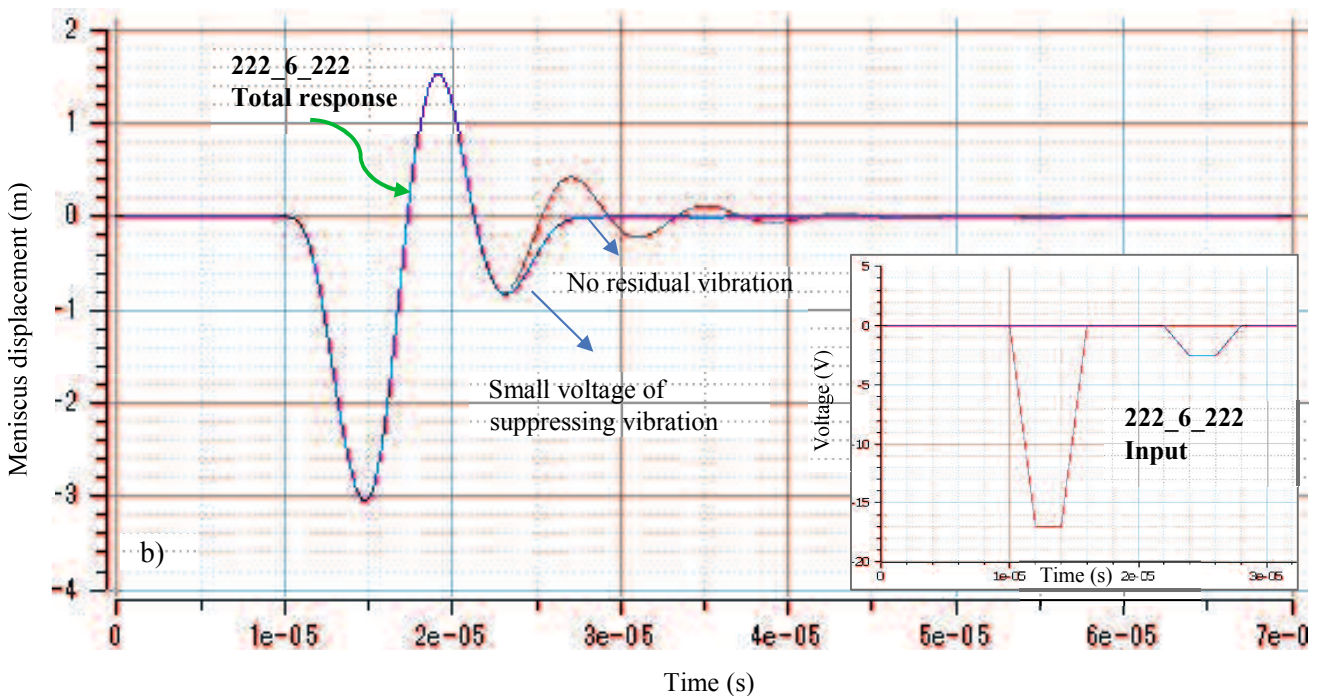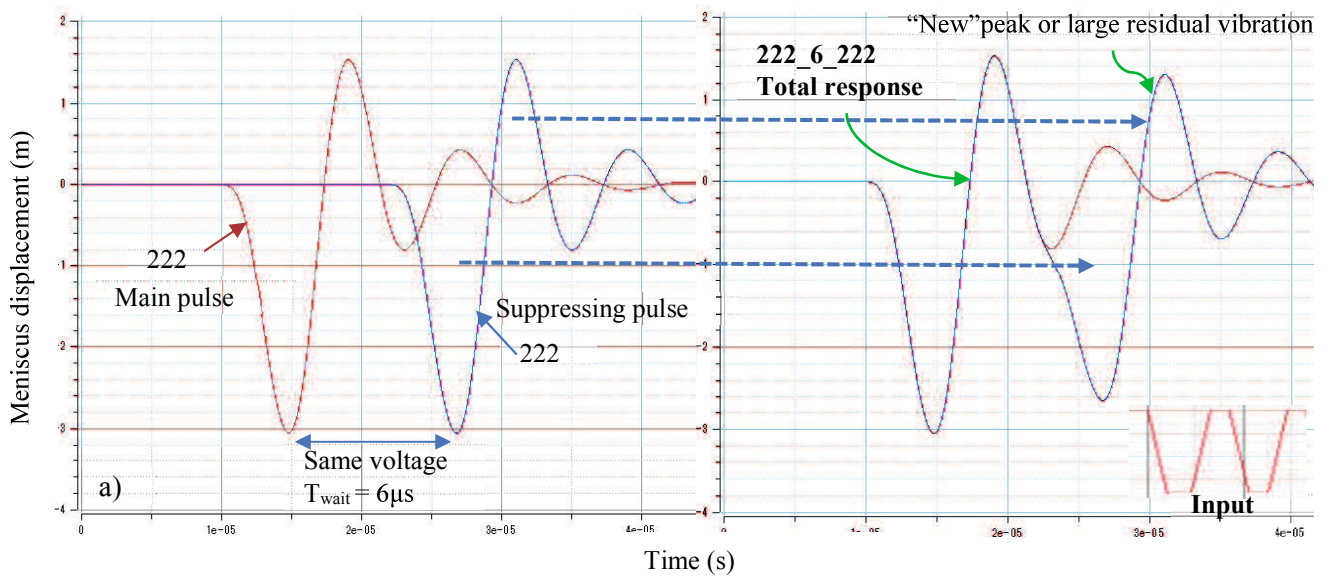
Fig. 4.13 Conceptual model of waveform 222_6_222
(a) Same voltage 222_6_222 (100%)
(b) Small voltage 222_6_222 (30%)

b. "Suppress B" (222_0_111) Waveform

The droplet shape and velocity in experiment result using "suppress B" waveform is shown in Figures 4.14 and 4.15. Fig. 4.14 gives the information that the suppressing vibration can effectively suppress the droplet velocity. The significant suppressed velocity was delivered by 50% suppressing vibration. The suitable voltage for obtaining a clear spherical droplet for single ejection method are 14V of 30 and 40% suppressing vibration and 14-15 V of 50% suppressing vibration.
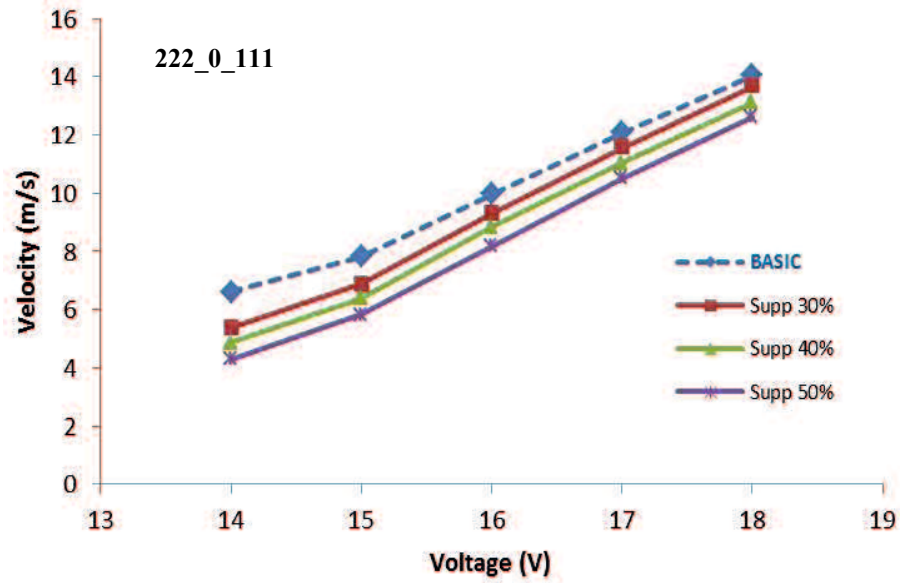
Fig. 4.14 Comparison of droplet velocity between basic waveform and "Suppress B" waveform
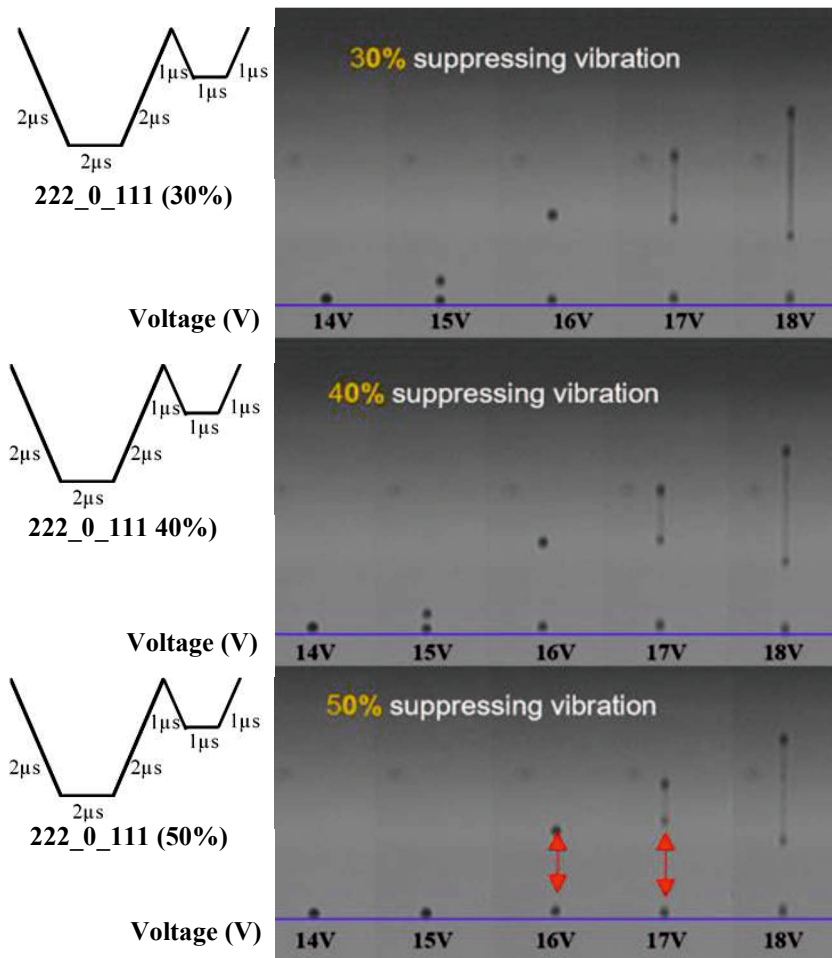
Fig. 4.15 Droplet shape for "suppress B" (222_0_111) waveform in different voltage

99

The explanation of suppressing vibration phenomenon is shown in Fig. 4.16 with the response shown in conceptual model in Fig. 4.17. The prediction of total response can be easier to understand by using the conceptual model. It shown that if using large voltage of suppressing pulse, the total response will suppress the peak from main pulse but can "create" the new peak or large residual vibration from suppressing pulse response. Hence, the suitable voltage must be determined.
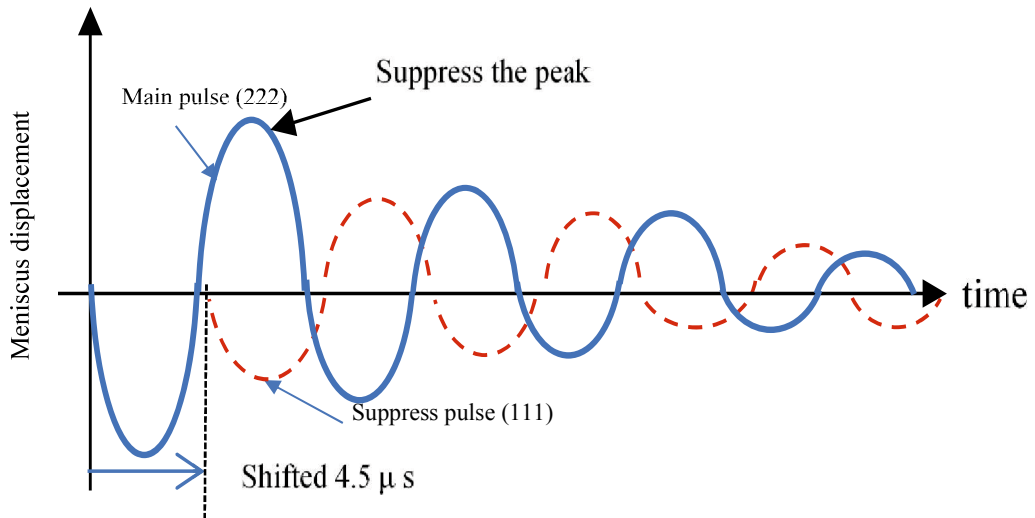
Fig. 4.16 The description of "Suppress B" (222_0_111) waveform output
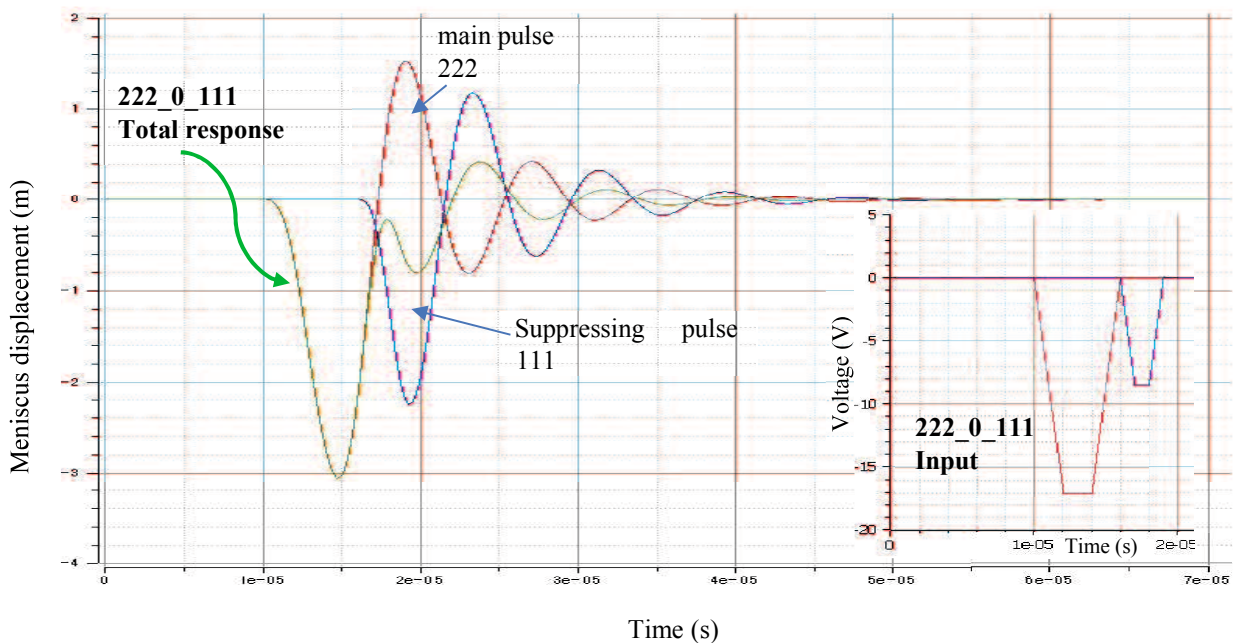
Fig. 4.17 Conceptual model for ""Suppress B" (222_0_111)

4.4 The Effect of Front and Back Suppressing Vibration

In this section, the effect of suppressing vibration pulse was investigated when we placed it before or after the main pulse. In the previous study, we used actuation waveform 222_6_222 so-called "Suppress A" and 222_0_111 so-called "Suppress B" as suppressing vibration with the profile shown in table 4.2 (c) and (d). The previous suppressing vibration is located after the main pulse so called back suppressing vibration, whereas this section used the actuation waveform with suppressing vibration that located before main pulse, hereafter called as front suppressing vibration. The profile of front suppressing vibration is shown in Fig. 4.18. The best result of base voltage percentage in the previous experiment (30% for "suppress A" and 50% for "suppress B" waveform) is used in this section. The experiment result of each input parameter is shown in Figure 4.18.
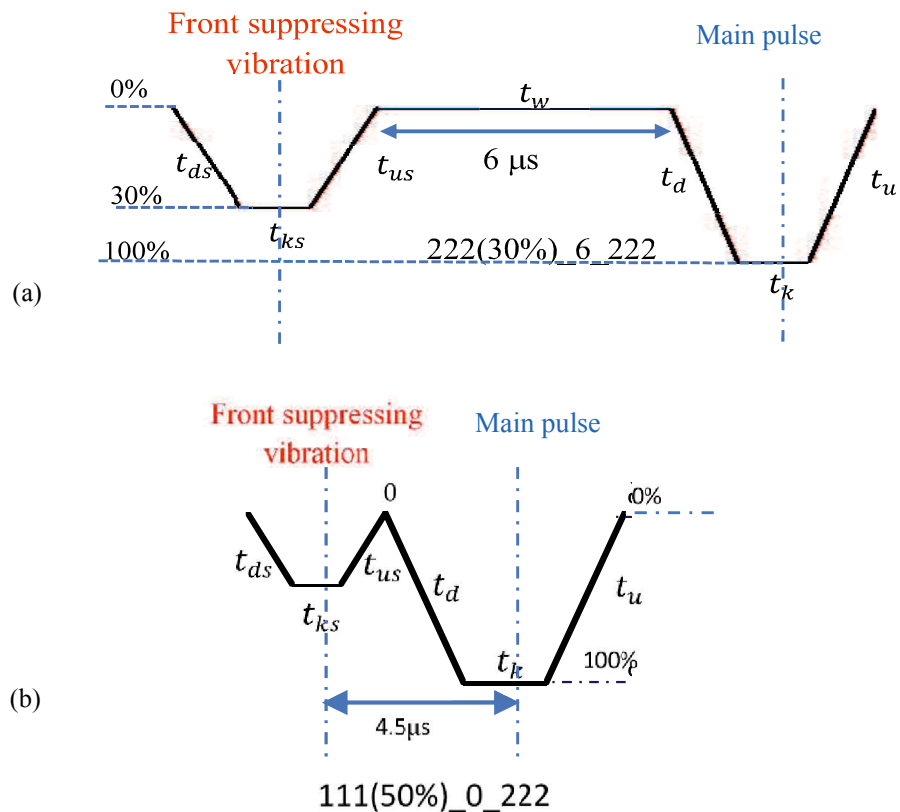
Fig. 4.18. The profiles of front suppressing vibration (a) Suppress A (b) Suppress B

Figure 4.19 present the droplet shape comparison of front and back suppressing vibration with basic waveform. We can see the similar droplet shape for basic waveform and back suppressing waveform of "Suppress A". Front "suppress A" generated the clear droplet at applied voltage $14 - 16$ V and droplet with ligament at $17 - 18$ V. The

comparison of front and back "Suppress B" shows that the clear spherical droplet was generated at 14-15 V only for back "suppress B", whereas front waveform generated clear droplet at all applied voltage.

The droplet shape is related to the droplet velocity particularly for back suppress A vibration, as shown in Figure 4.20. The figure shows that those waveforms also have similar velocity, with similar trend to back suppress B vibration. The front suppress A and B have similar velocity trend with smooth linearity, but in lower velocity. It also shows that the front suppress B has the lowest velocity than the other. This phenomenon can be explained by the conceptual model as shown in Fig. 4.21.
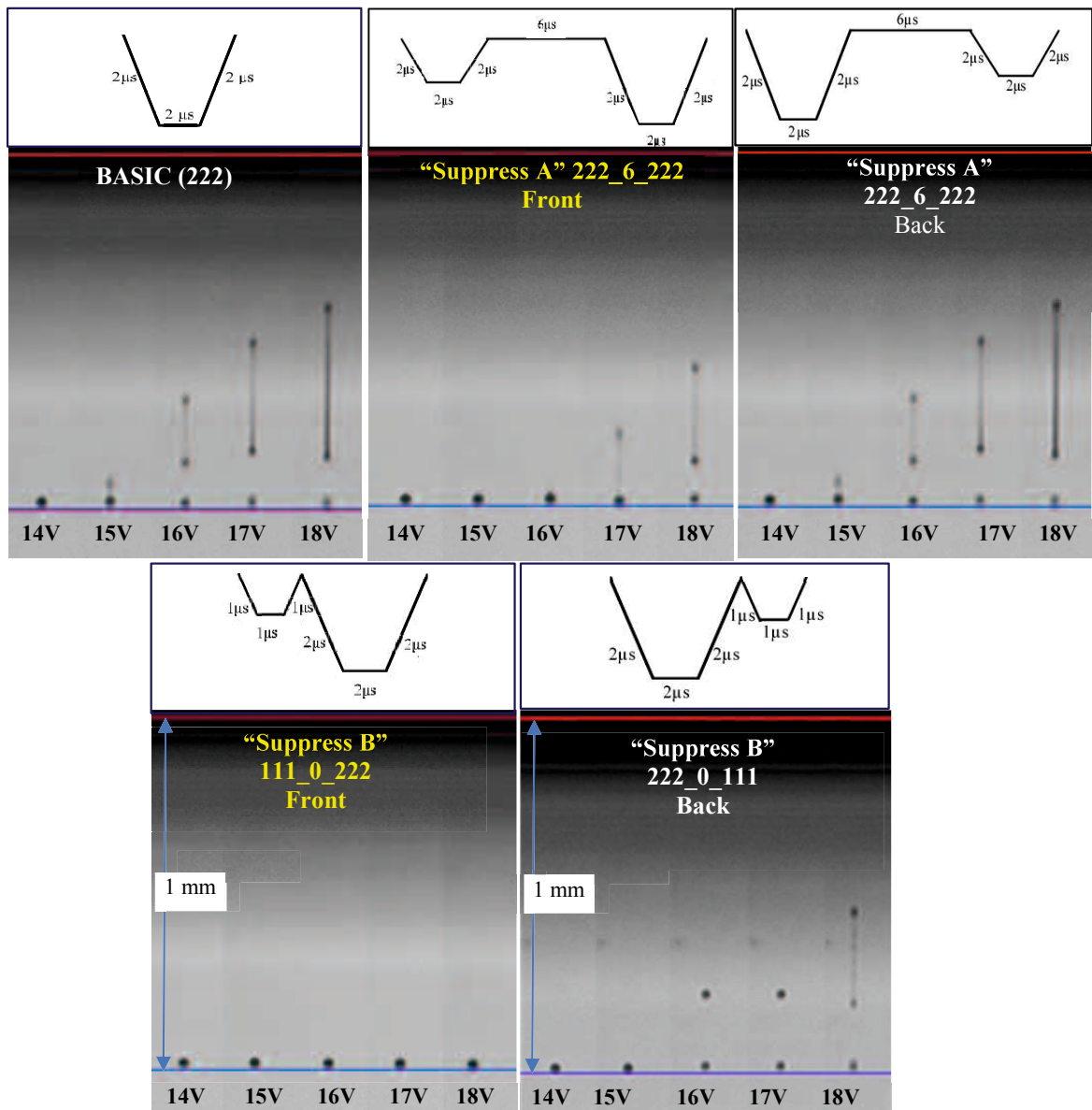
Fig. 4.19 The droplet shape comparison between basicwaveform with front and back suppressing vibration
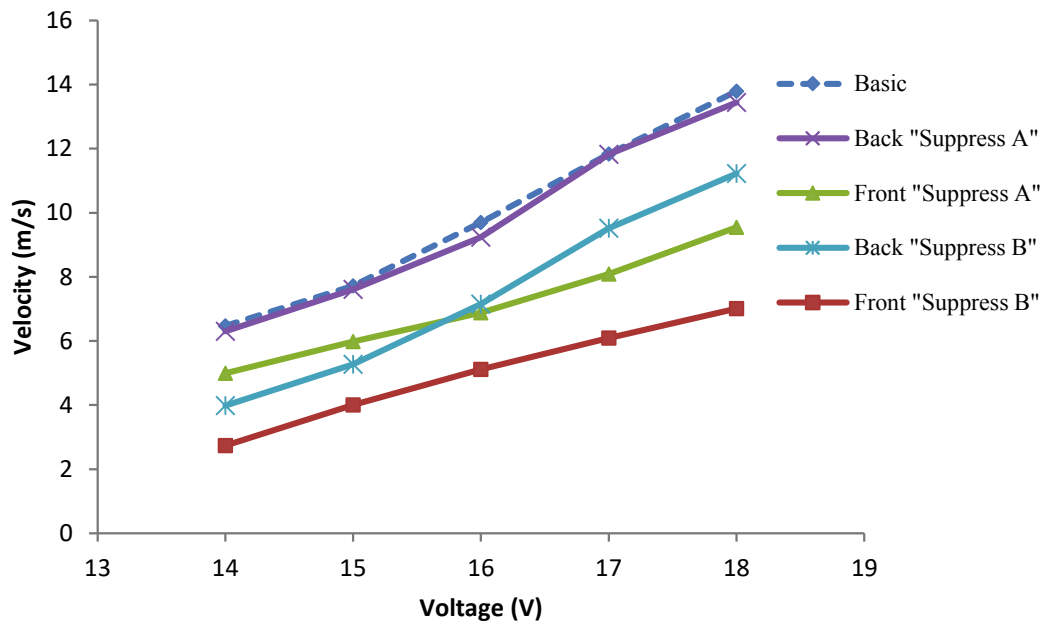
Fig. 4.20 The droplet velocity comparison between basicwaveform with front and back suppressing vibration

Figure 4.20 depicts that front "suppress B" (111_0_222) vibration has a different response than the others. The small pulse before main pulse without separating time as well preliminary vibration compose the wider negative pressure. It indicates that the "pull" mode that play a role in sucking the liquid thread into the liquid chamber take a longer time and the volume inside the nozzle become larger. With this additional pulse as a preliminary vibration, may generate the Helmholtz resonance inside the liquid chamber. Since the energy that used to "push" the ink out from the orifice is same, consequently the droplet velocity will be slower. This result then used for the next step in designing the actuation waveform for multi drop   method.
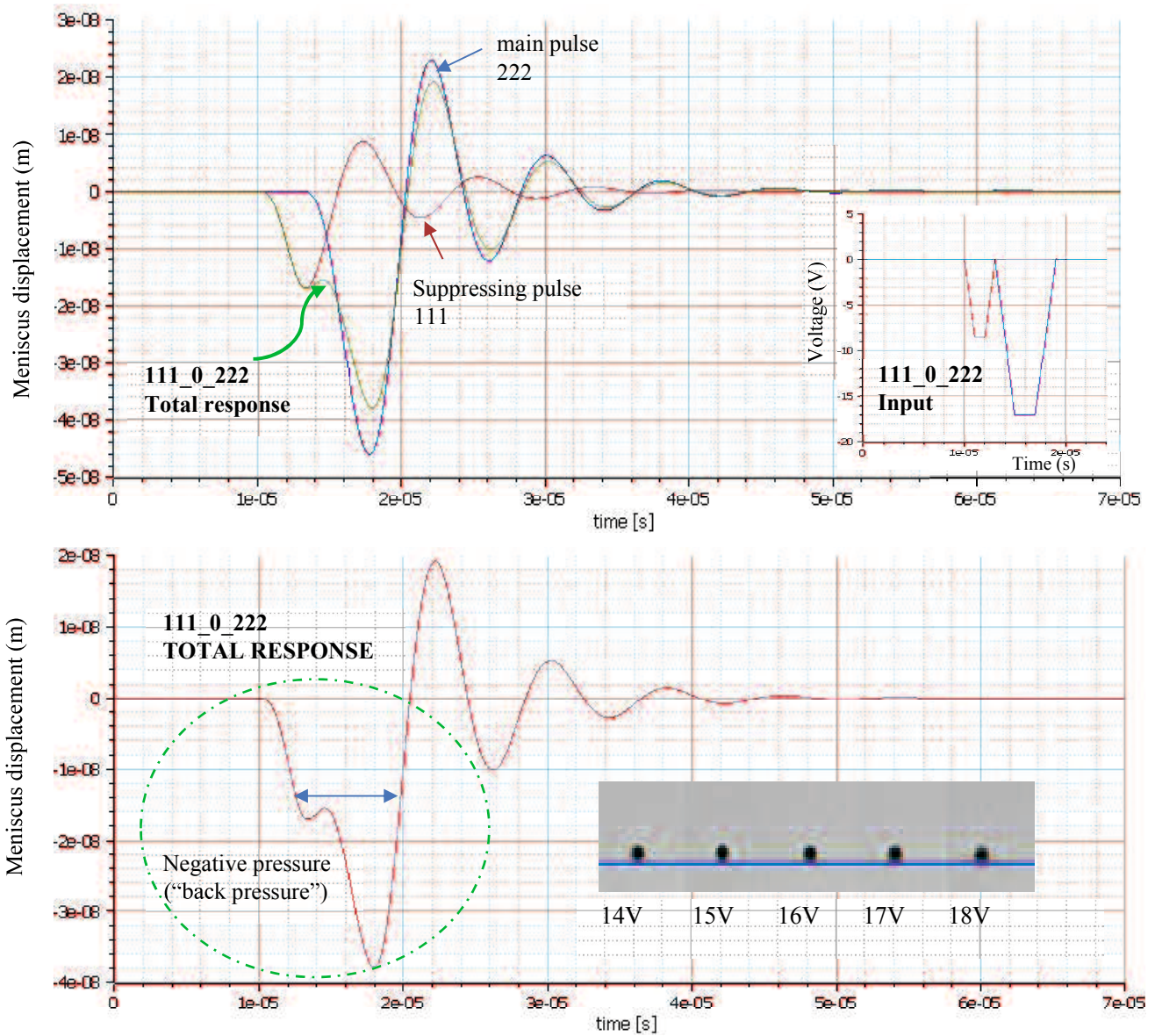
Fig. 4.21 Conceptual model for "Front Suppress B" (111_0_222)

4.5. The Effect of Head Temperature in Different Actuation Waveform on Droplet Volume and Velocity

The head temperature effect to droplet volume is shown in Fig. 4.22. It presents that the higher head temperature will lead the increasing the droplet volume. This phenomenon can be explained with the Andrade formula. The temperature of ink (T) is influenced the viscosity (η) of the liquid. The Andrade formula is as follow equation:

$$= A \exp \left(\frac{B}{T+C} \right)$$

4.1)

The studies described about relationships between temperature and viscosity using Andrade equation and the calculation of the viscosity as a function of temperature [84] & [85]. From that equation, it is determined that the higher temperature, make the lower viscosity. Viscosity of liquid is depending on temperature. Molecular cohesion in a liquid dominates the viscosity. In the higher temperature, the molecules in liquid become more energetic and separated. Therefore, when the cohesive force decreases, the viscosity will decrease too. Malcolm et al. in their study about inkjet fluid characterization stated that in DoD cases, the actuating waveform that generate droplet are affected by ink viscosity [54]. It is determined that for higher temperature of ink, means lower viscosity, will increase the droplet velocity.

Some studies observed the effect of ink viscosity to the droplet behavior [72], [76] - [80], [94] & [97]. It was stated by Shin, P. et.al. that by increasing the driving voltage and temperature, the size of single primary drop is increased due to the reduction in viscosity and contact angle of the operating liquid [109]. Jingmei et.al., with their research using edible ink stated that viscosity has big influence on the droplet formation, speed, ligament and volume. The higher viscosity of fluid will affect to the lower droplet speed [97]. The acoustic wave in DoD Inkjet printer are affected by ink properties such as ink viscosity. High viscosity will dampen the acoustic waves that used to generate the drop ejection. On the other side, low viscosity can reduce the damping factor [75] & [76]. Jang et.al. investigated the relationship between physical fluid properties and inkjet printability, stated that the low viscosity fluid is easier to eject the droplet without a significant viscous dissipation but the high surface tension will be detached the retreating filament from the main droplet, forming satellite [76].
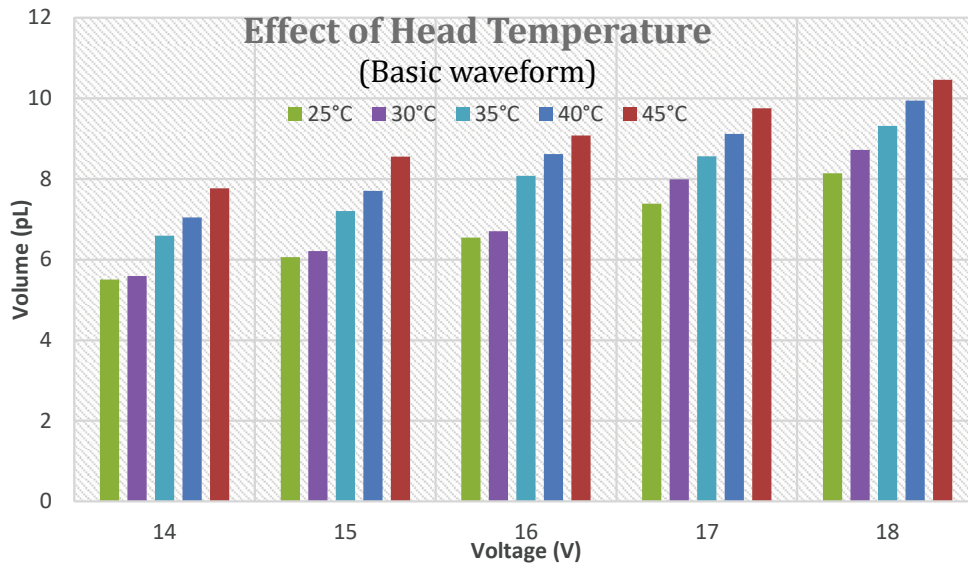
(a)
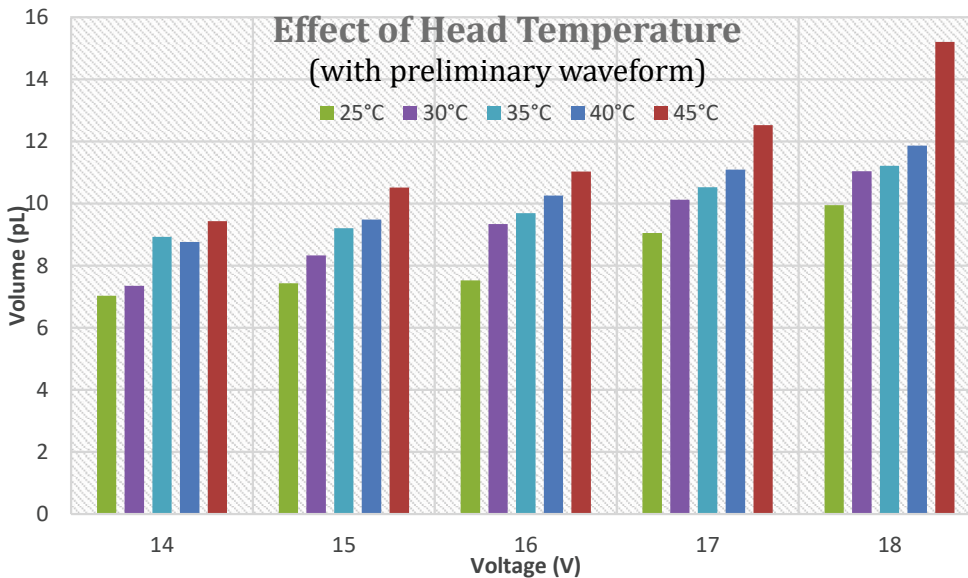
(b)

Fig. 4.22 Droplet volume as a function of head temperature (Dowanol)
(a) Basic waveform (222)
(b) with preliminary vibration (222_2_222)

The effect of head temperature to droplet velocity in different applied voltage is shown in Fig. 4.23. High head temperature will reduce the ink viscosity. Hence, the lower viscosity can be easier to eject and resulting the faster droplet. Noted that the velocity measurement is only for the main droplet and the satellite or ligament in this section is neglected. Therefore, this study also in agreement with previous studies, shows that the liquid viscosity will affect the droplet speed and volume.
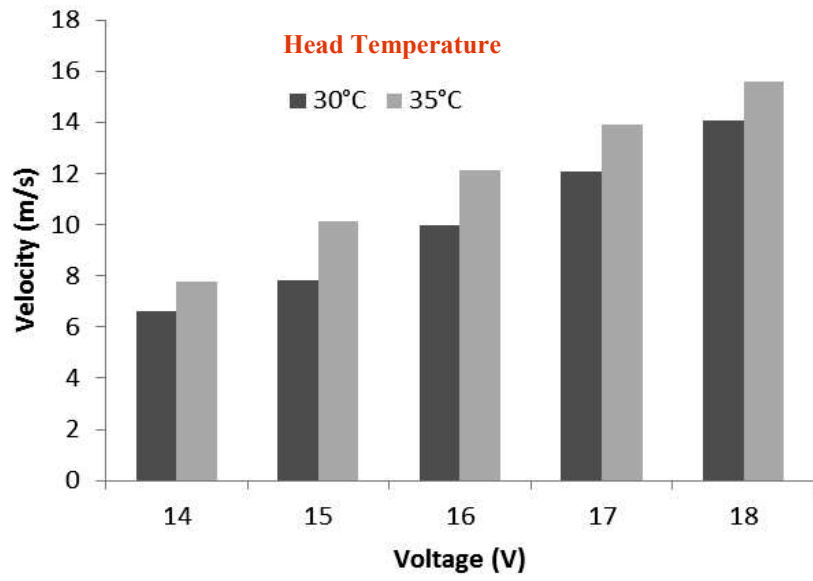
Fig. 4.23 Droplet velocity as a function of voltage in different head temperature (Basic waveform)

4.6 Conclusions

The investigation of preliminary and suppressing vibration effect shows that the waveform can be used to control the droplet size, volume, and velocity. The important point to adjust the droplet velocity and volume is in the voltage percentage of preliminary and suppressing vibration. The effect of voltage and head temperature is also in a good agreement with previous studies by other researchers, by considering the maximum voltage and head temperature to obtain the good result. The conclusions about controlling the droplet velocity and volume with clear droplet are as follows:

- Suppressing vibration & preliminary vibration is effective to control the droplet speed and volume. The suppressing vibration was proved to be an effective way to damp the residual vibration and reduce the droplet volume and speed. It was found that 30% of preliminary vibration with 14 – 15V applied voltage and 40% of preliminary vibration at 14 V are effective to increase the droplet speed and volume. 50% of preliminary vibration generated the larger volume but lower speed than basic waveform.

- 30% of suppressing vibration with input parameter 222_6_222 (suppress "A") can be utilized to reduce the residual vibration. 50% of suppressing vibration with input parameter 222_0_111 (suppress "B") also demonstrates its effectiveness to reduce the residual vibration, suppressing the droplet volume and speed. The significant improvement in droplet shape performance was shown by front suppressing vibration B with input parameter 111_0_222. This input waveform produced the clear spherical droplet for all applied voltage (14 – 18V).

- It is found that the good droplet shape performance from actuation waveform 111_0_222 have the different wave response in the simulation model. The conceptual simulation model by wave superposition principle can be used to improve the concept design in the next step.

- With an increase of applied voltage as well as the effect of head temperature, the droplet velocity and volume also increase. Furthermore, the ligament of droplet also longer with the higher applied voltage. This result is in a good agreement with other previous researches.

CHAPTER V

"U" AND "W" ACTUATION WAVEFORM DESIGN FOR SINGLE AND MULTI-DROPLET EJECTION METHOD

5.1 Introduction

Recently, some new approaches have been developed or are being developed to find a significant change in inkjet printer performance. The trend in inkjet printing is concerned to obtain the high image quality with high reliability. The other issue about the inkjet printing development is, for achieving the wider range of droplet volume, to improve its ability in market customization [1]. However, the customization of current print-head technology is still limited. There is a necessity to develop the print-head technology that can be much more tolerant with the fluid properties [111]. At present, it is necessary to substitute the print-head if using the different fluid. On the other side, for the different model of print-head, requiring the fluid formulation adjustment to get a good result. Therefore, without changing the print-head design, it is very challenging to find the best operating parameter that can be used in a wider range of fluid properties.

Most of commercial printer using binary technology that generate one droplet size. There are some inkjet printers that able to produce more than one size of droplet, but the range of drop size that ejected from the same nozzle is still small [2] & [5]. The technology of inkjet printing that generate the different droplet size from the same nozzle called as grey-scale technology. The implementation of multi-drop method that use in grey-scale technology is still limited. The constraint in this method is the difficulties to synchronize the multi-pulse for the optimum result in wave superposition to get the optimal droplet formation. The optimal droplet is the droplet without satellite [6], [13], [22] & [39] which is unacceptable in some inkjet printer application and necessary to eliminate for high print quality [7]. Many studies observed the satellite formation [8] − [16], [23] − [26], [31], [48] & [73]. However, research about eliminating the satellite is still limited. To get the optimum printing result with Drop on Demand (DoD) inkjet printer, the properly design of input waveform must be made [17], [19], [81] & [82]. Hence, it is necessary to determine the optimum design of actuating waveform for achieve the clear spherical droplet without satellite and ligament.

Numerous studies were conducted to design the actuating waveform [17], [19], [56] & [81]. The research concerning in reducing the residual vibration which caused satellite

were also reported [82] & [86]. Some other studies about controlling the droplet volume with different method were conducted [16], [17] & 19]. Most of the other studies using push-pull (positive waveform) and bipolar method as their actuating waveform [8] - [11], [14], [17], [20], [23], [25], [28], [29], [44], [47], [57], [58], [71], [72], [76], [81], [94], [95] & [108]. The common used method in commercial inkjet printer is pull-push method or negative waveform that can generate the smaller size of droplet with higher speed and narrow column of liquid droplet that correlated to the stability of drop ejection [53]. In this study, we use the negative waveform or pull-push mode of PZT driving pulse. The expected result to prevent the long ligament and droplet satellite by using this method hasn't be obtained.

In this study, the actuation waveform for driving PZT print-head was designed both in single or multi-drop generation method. The main target of the design is it ability in generating the good droplet performance without satellite, ligament and weeping occurrence. The effectiveness of this waveform design was examined by using Dowanol and UV ink as an operating liquid.

5.2 Limitation of Basic waveform

Currently, the basic waveform defined in Fig. 5.1 for single drop and multi-drop (2 and 3 pulses) was considered to drive the piezoelectric in the inkjet device. This waveform has very limited control capabilities particularly in multi-drop ejection method. The droplet shape generated from this waveform is shown in Fig. 5.2.

Figure 5.2 (a) depicts the droplet shape for single droplet (1 pulse). Figure 5.2 (b) shows the result for 2 and 3 pulses of the actuation waveform to generate multi-drop ejection. It presents that by using the basic waveform as an actuating waveform, the droplet shape was not as the expectation. The clear spherical droplet without satellite or ligament in single drop ejection was only generated from the applied voltage at 14V. It also shows that the higher applied voltage, the longer ligament will be generated.

The measurement result for droplet volume is 5.86pL with velocity 6.47m/s. The applied voltage more than 14V generated the higher velocity and volume. Yet, the droplet shape shown bad performance. In previous research, we investigated the effect of preliminary and suppressing vibration in the actuation waveform design. It was proved that the droplet volume and velocity can be controlled by preliminary and suppressing vibration. However, the expected result to prevent the ligament and satellite formation has not satisfied yet.
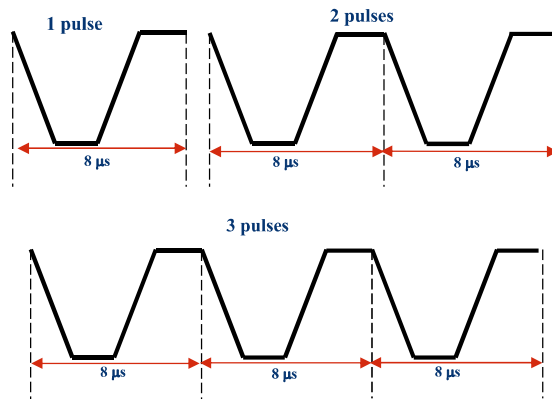
Fig. 5.1 Basic waveform profile (previous standard)
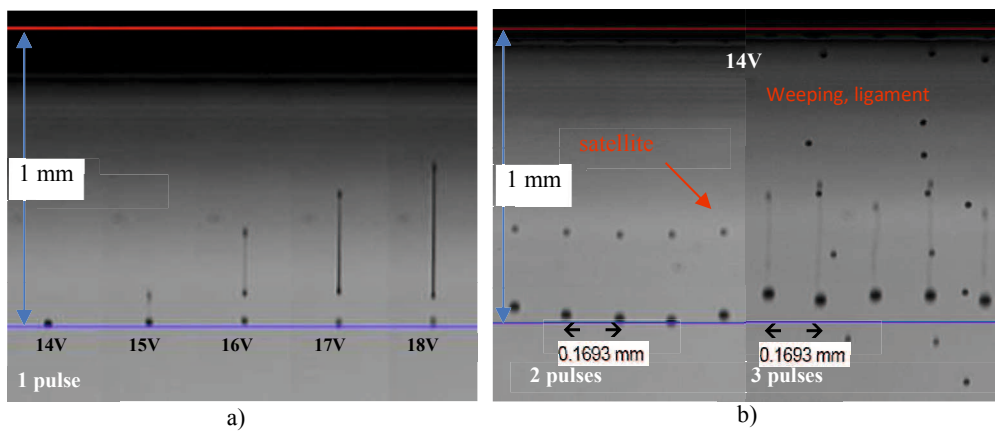
Fig. 5.2. Droplet shape from basic waveform (1- 3 pulse)

5.3. The Comparison of Pull-Push and Push-Pull Mode

The pull-push mode of piezo driving pulse that used in this study is tending to generate the long ligament with higher speed as shown in Fig. 5.2. It may cause by water gun effect due to the driving pulse mode. As stated before, this study was using pull-push mode or negative waveform as the actuation waveform to drive the PZT in the inkjet print-head. The other researcher made the comparison analysis of PZT driving pulse mode, namely pull-push and push-pull mode [53]. The comparison of those two driving pulse modes is shown in Fig. 5.3.

In Pull-Push method, the first stage is the pull mode. On this stage, when the signal to eject the droplet is received, the applied voltage becomes zero, and piezoelectric element return to its original condition. Then, the negative pressure is to increase the volume generated inside the liquid chamber. This pressure wave at sequent process will be reflected, become a positive pressure to eject the droplet. The second stage, push mode when in one cycle of its operation, the positive pressure wave reflected by the negative pressure that

generated inside the chamber, then overlapped with positive pressure wave to resonate and eject the droplet. The higher pressure that generate from the reflected negative pressure that combined with its positive pressure, produce the higher speed droplet with long and narrow tail (ligament).

In Push-Pull method, when the signal to eject the droplet is received, the applied voltage will enter the push mode, and the positive pressure will be generated to compress the liquid chamber, and directly eject the droplet. After the droplet ejection, the piezoelectric element is going to the pull mode, returning to the standby mode. In the pull stage, the breakup process of meniscus from the nozzle can be affected by this stage. There is an energy to retract the liquid inside the chamber, and slow down the droplet with a bigger size. The comparison of velocity distribution and the droplet size is shown in Fig. 5.4.
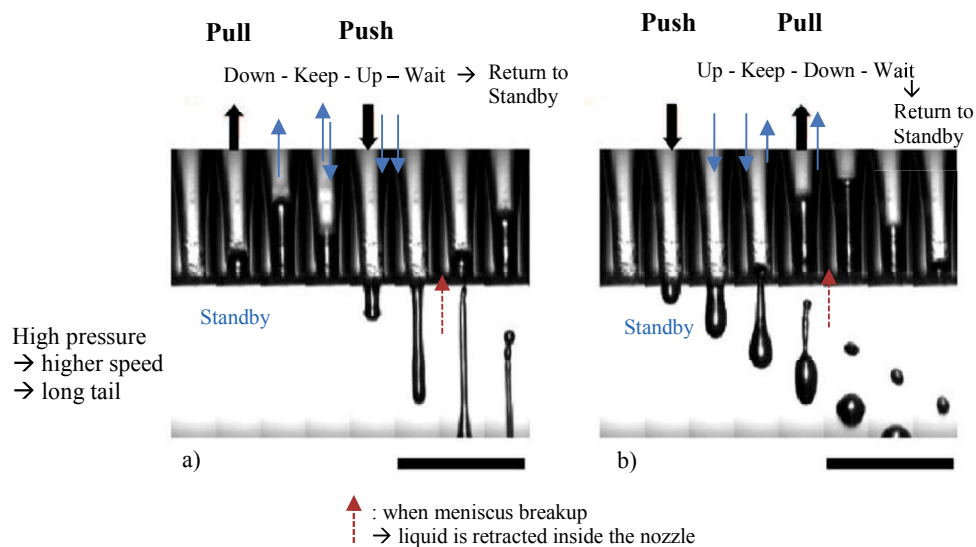
Fig. 5.3 The comparison of two driving pulse modes on PZT print-head
(a) Pull-Push mode   (b) Push-Pull mode
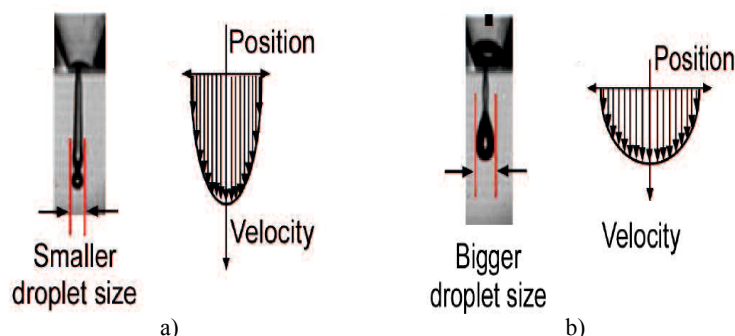
Fig. 5.4 The comparison of droplet result from two driving pulse modes on PZT print-head
(a) Pull-Push mode   (b) Push-Pull mode

In case of single drop, "water gun" effect with continuous flow indicate an absence of Helmholtz resonance that can generate the discrete flow and should be exist in the liquid

chamber. In Fig. 5.2 (b), the droplet that generated from 2 pulses input waveform is followed by satellite whereas 3 pulses ejected the droplet with ligament and weeping occurrence. The satellite generated because the last drop ejected cannot reach and merged to the prior drop before the observation distance (reach the substrate). This means that it is impossible to apply more than 2 pulses for high quality drops by using basic waveform. Furthermore, related to the droplet without satellite as an ideal droplet and become our target, this 2 pulses design is also not recommended.

5.4 Structural Concept for the Optimum Actuation Waveform Design

First step in designing new waveform with optimum result as the objective of this study is in finding the basic concept to eliminate the "water gun" effect for generating the multi-drop concept. Next step is determining how to reduce the residual vibration for prevent the satellite and weeping occurrence, particularly in the multi-drop concept. As explained in chapter 4, the preliminary vibration is the additional front pulse such as the main pulse with low voltage without droplet ejection, that is used to accelerate the droplet velocity and increase the volume. On another side, suppressing vibration is the small additional pulse after main pulse, to reduce the residual vibration and affect the reduction of droplet speed and volume. From previous experiment, it is determined that the applied voltage that effective to accelerate the droplet speed is 30% of base voltage. On the other side, the suppressing vibration is able reduce the droplet volume and speed, by reducing the residual vibration. The effective pulse as suppressing vibration is with the input parameter for t_{down}, t_{keep}, and t_{up} respectively 1μs with t_{wait} from main pulse 0 μs so called as suppress _0111.

The preliminary and suppressing vibration is effective to control the droplet volume and velocity but in low voltage only (14V) in single drop ejection. Many trial and error experiments were conducted to investigate the droplet behavior from different actuating waveform in single or multi-pulse. The example of droplet shape from preliminary experiment report is shown in Fig. 5.5. The figure depicts unexpected result from the input actuating waveform. Consequently, we must find the other idea for reach the research target.
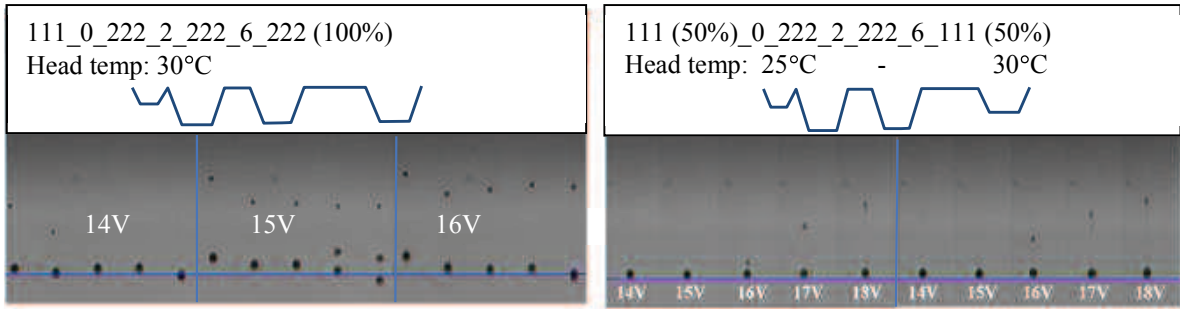
Fig. 5.5 The droplet shape of preliminary experiment result (example)

The literature study was conducted concurrently with the experimental study. Many previous relevant researches were conscientiously studied to understand the basic concept in controlling waveform. The theoretical approach especially in wave superposition concept was done to understand how to reduce the residual vibration.

Return to the main problem from previous waveform using basic waveform in Fig. 5.1 with the droplet shape result in Fig. 5.2, with the hypothesis gathered and concluded from the literature review, then summarized as follows:

1. Long ligament: higher voltage will generate longer ligament.

   Hypothesis: Pull-push mode of PZT driving pulse caused water gun effect.

2. Satellite: if latest ejected drop cannot reach and merged to the prior drop or main drop.

   Hypothesis: residual vibration, and the difference of each drop velocity

3. Weeping occurrence

   Hypothesis: Excessive pressure from high voltage or high pressure, and by residual vibration.

   Furthermore, the hypothesis how to overcome the cause of problems as stated above, was summarized as follows:

1. Caused: Water gun effect

   Solution: Create the preliminary vibration that able to be functioned as back pressure to "hold" or withstand the high pressure.

2. Caused: Residual vibration

   Solution:

   • Determine the suitable period from each pulse that able to reduce the residual vibration by wave superposition concept.

- Obtain the appropriate voltage for each drop to adjust the speed so then it can be merged before reach the substrate. Note that the larger voltage will generate the higher speed.

3. Weeping occurrence

Solution: Same solution as water gun effect and residual vibration, and determine the limit of applied voltage to prevent the excessive pressure.

The illustration of problem and hypothesis solution is shown in Figs. 5.6 and 5.7.
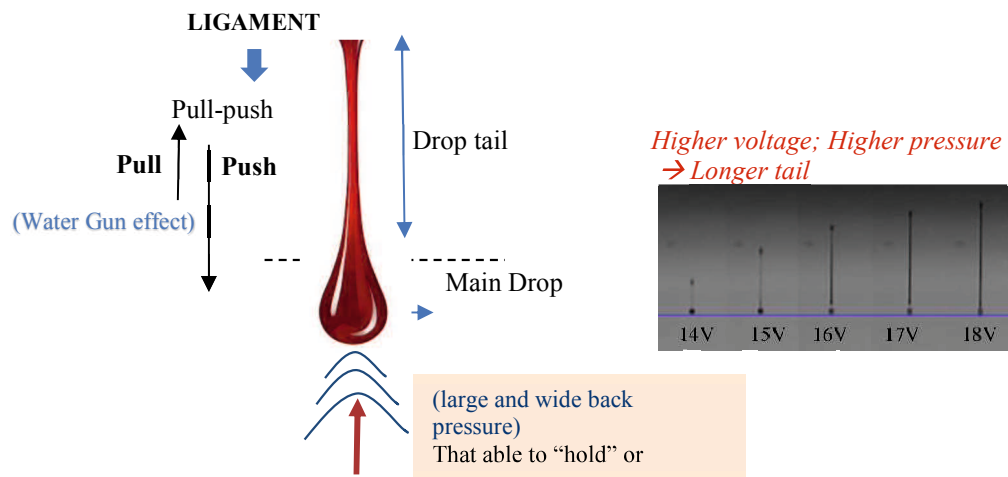
Fig. 5.6 Long ligament problem and hypothesis
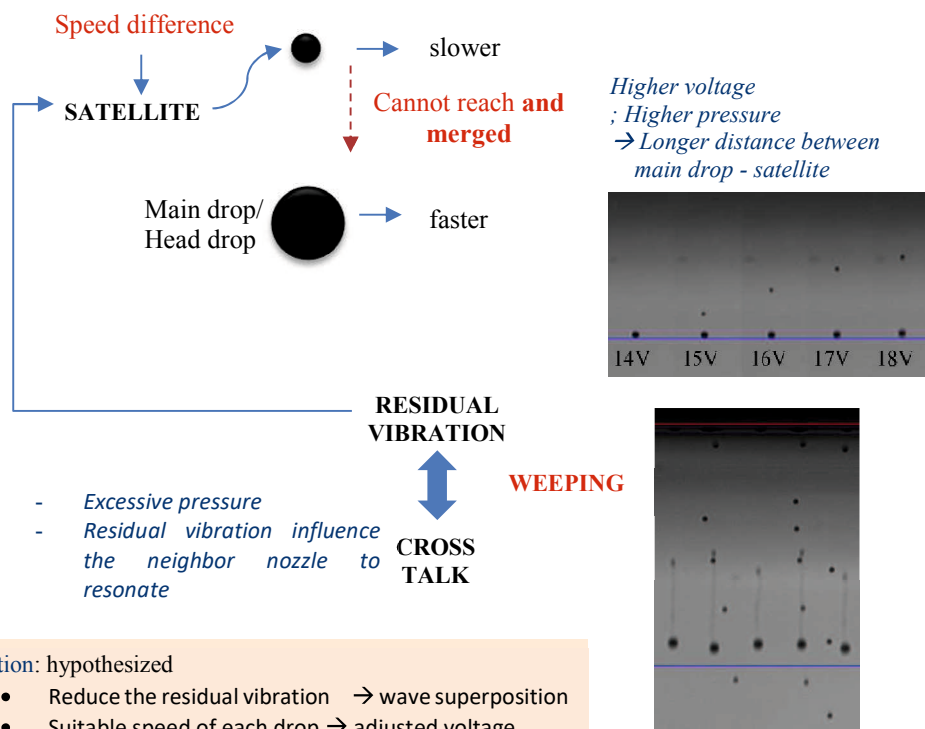
Fig. 5.7 Satellite and weeping problem

It was stated by other researcher that small negative pressure as preliminary vibration can prevent the weeping occurrence [81], but there is no explanation about the mechanism of how the negative waveform can avoid the weeping. Small pressure implies that there is no droplet ejection. It was also stated that the long dwell time (t_{keep}) can generate the large back pressure [81]. The same author in other study, concluded that the effective dwell time for suppressing the satellite effect is longer than efficient dwell time, but it may result in no jetting droplet [13]. The experiment result using the actuation waveform 111_0_222 that shown in chapter IV, strengthen the hypothesis that the preliminary vibration can avoid the satellite or weeping occurrence. It was found by the conceptual system model, that the effective preliminary vibration as an input waveform is the waveform that can generate the wider back pressure. Therefore, the first idea is to create the preliminary vibration that can generate the larger back pressure without droplet ejection using the long dwell time (t_{keep}) in the preliminary vibration.

The experiment using different dwell time (t_{keep}) was done to obtain t_{keep} without droplet ejection. The experiment result shown that there is no ejection with t_{keep} 5 - 8μs (See table 5.1).

Table 5.1 Experiment result of different t_{keep}

t_{Keep} (μs)		2.5	3	3.5	4	4.5	5	5.5	6	6.5	7	7.5	8	8.5	9	9.5	10
Ejection	Yes/No	Yes	Yes	Yes	Yes	Yes	No	No	No	No	No	No	No	Yes	Yes	Yes	Yes

It was found that by using the input parameter respectively 2μs - 6μs -2 μs (262) as the preliminary vibration give a better result in generating the clear spherical droplet. The profile of 262 pulse so called "U" waveform is shown in Fig. 5.8.
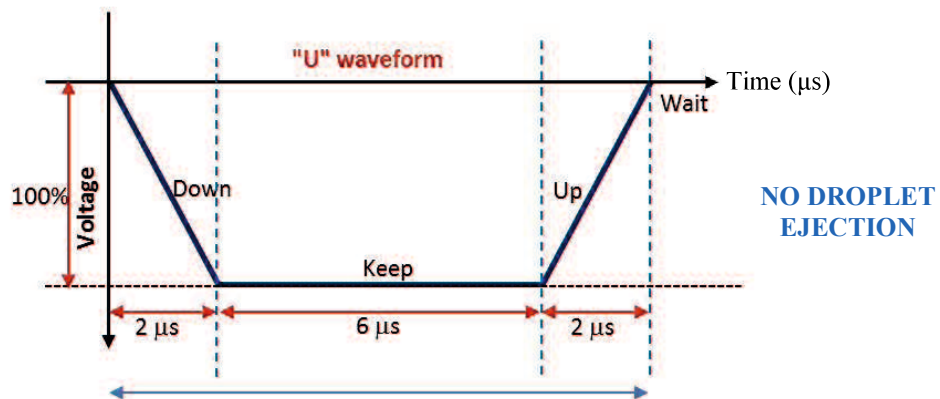
Fig. 5.8 "U" waveform profile as preliminary vibration

The other idea in creating the large back pressure is by combining the preliminary and suppressing vibration. By overlapping that two pulses and 4μs shifted period, then we

can create the large voltage without drop ejection. The concept generation of other preliminary vibration for creating the large back pressure is shown in Fig. 5.9. This waveform that generated from two overlapped pulses with input parameter t_{down} - t_{keep} - t_{up}; 221 (50%)_0_122, has the shape like alphabet "W" so called as "W" preliminary vibration for easier to write.
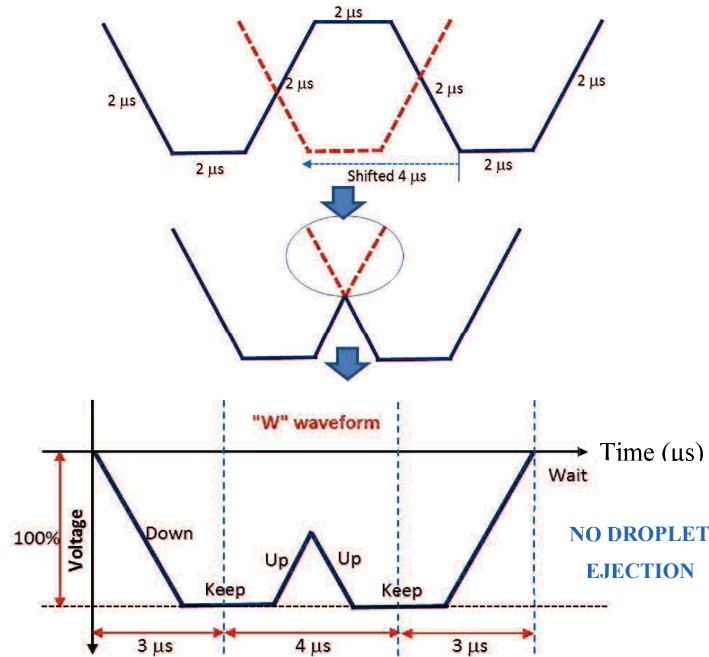
Fig. 5.9 "W" waveform profile as preliminary vibration

As discussed in section 5.2 particularly about pull-push mode, there are 2 stages in the droplet ejection process, namely "pull" stage and then "push" stage. Hence, we assume that the "U" and "W" waveform which long t_{keep} consist of two wave-ramp, namely front ramp and rear ramp. The first ramp namely front ramp is the "pull" mode to suction the ink inside the liquid chamber. The second ramp namely rear-ramp is the "push" mode to discharged ink from the nozzle. The response of each wave with phase difference 180° make the front-ramp response goes ahead one period to rear-ramp response, so then the second peak of rear-ramp is eliminated by destructive superposition of front-rear ramp. The total response of front and rear ramp from 262 natural periods will generate the single negative pulse response so called "soliton" without any residual vibration, as shown in Fig. 5.10. Noted that the complete soliton only can be reach for the system without damping. In real inkjet system, the existence of damping cannot be avoided because of liquid viscosity.
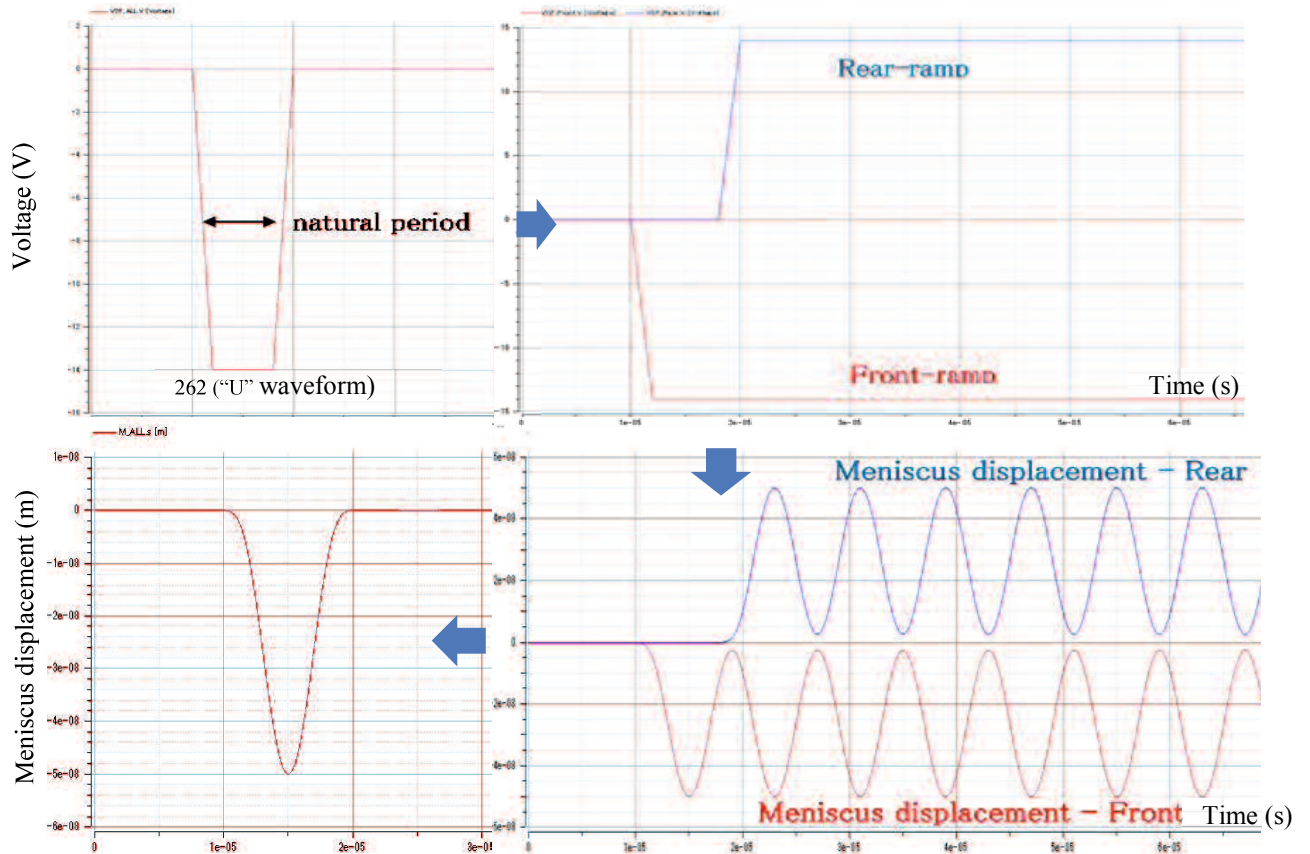
Fig. 5.10 Front-rear ramp concept of "U" waveform

The composite response of simulation model with viscosity consideration from front-back ramp wave with phase difference 180° of "U" waveform is shown in Fig. 5.11. The front-ramp response goes ahead one period to rear-ramp response, so then the first peak is reduced by second peak and damping the total residual vibration.
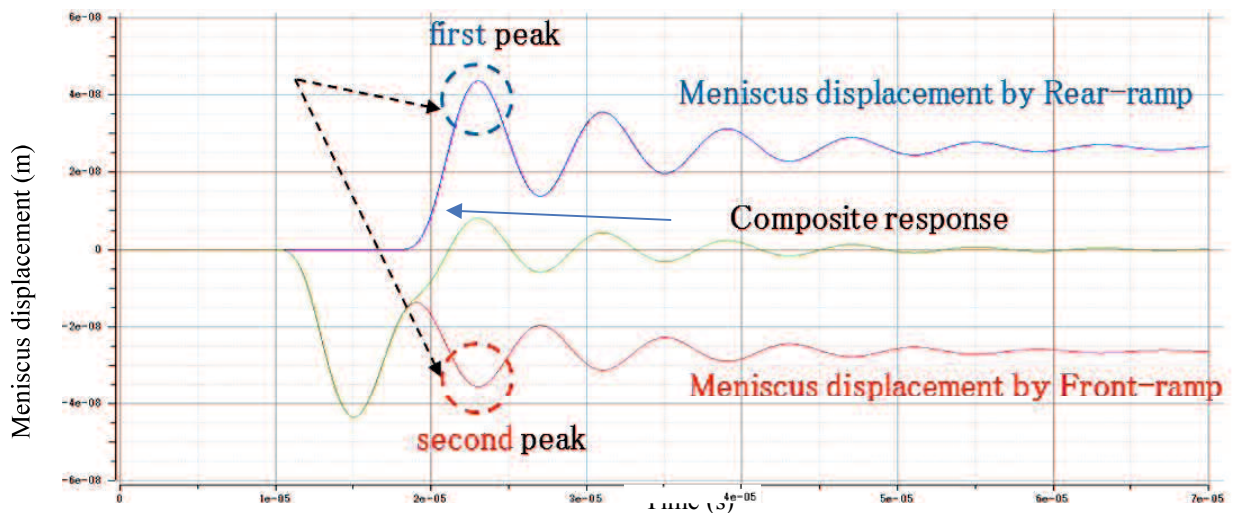
Fig. 5.11 The composite response of front and rear ramp (h = 0.2)

The comparison of simulation result by conceptual model of "U" and "W" waveform is shown in Fig. 5.12. It is shows that the difference between "U" and "W" waveform is very small.
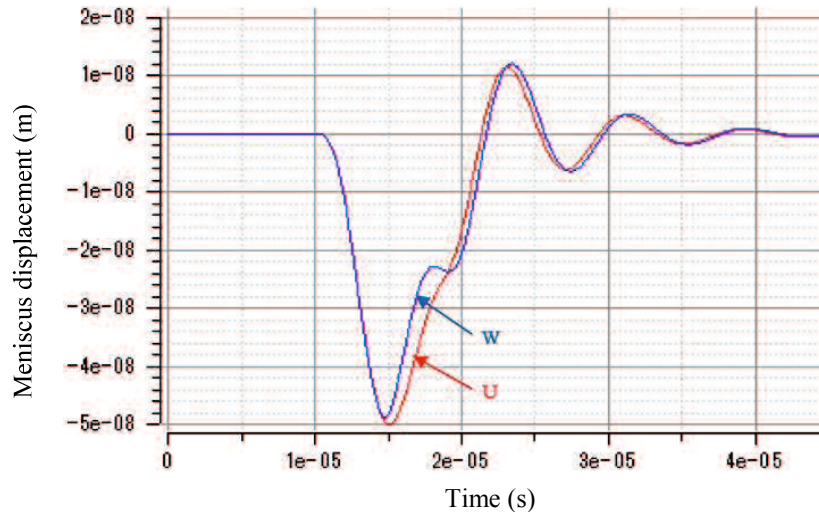
Fig. 5.12 "U" and "W" waveform response by conceptual system model

The next step with experimental approach then conducted for verify the hypothesis in single and multi-drop ejection, in the cycle such as PDCA (Plan-Do-Check-Action) cycle to continually improve the result. Figure 5.13 shows the PDCA cycle in design the optimum waveform by using "U" and "W" parameter as preliminary vibration in the single and multi-drop ejection. The waveforms have similar total period of 10 μs to generate large negative waveform. This waveform is deployed as preliminary vibration in single drop and multi-drops ejection (2 − 5 pulses) and examined with an experimental study.
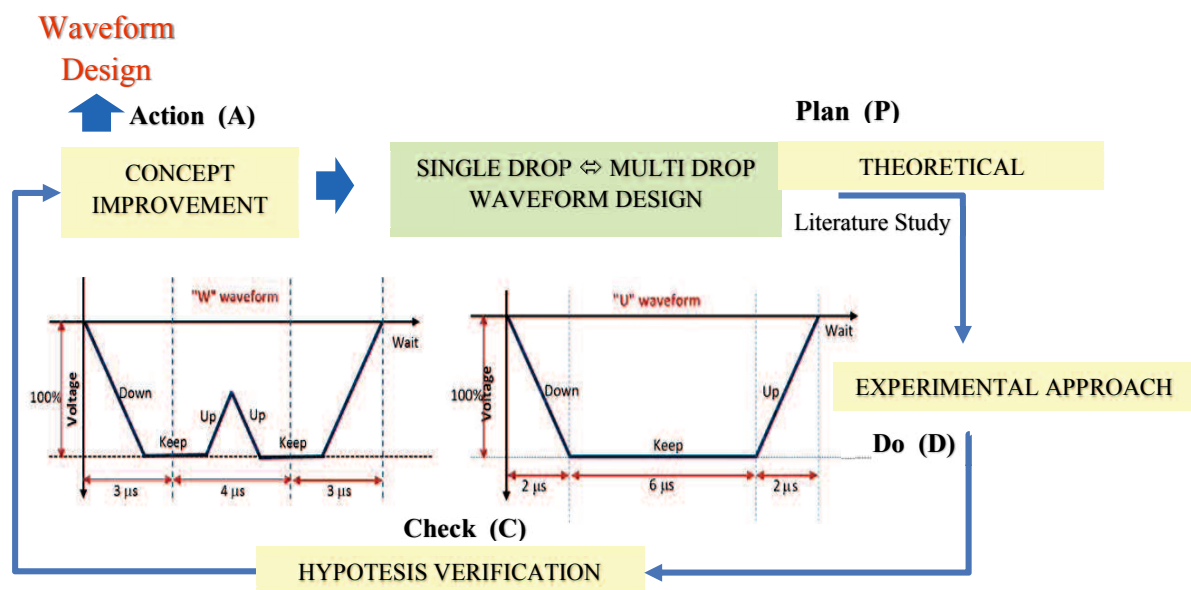
Fig. 5.13 Cycle process in waveform design with "U" & "W" preliminary vibration

5.5. New actuation waveform design

5.5.1 Single droplet waveform design

The pre-experiment was also conducted to find the suitable t_{wait}, or time between "U" or "W" as preliminary vibration with the main pulse. It is determined that the effective "wait" time, or t_w is zero. By using 2μs for t_{wait} such as previous preliminary vibration in chapter IV, it was found that the ejected droplet is not clear. Hence, the input waveform for single droplet as proposed waveform design is shown in Fig. 5.14.

The effective design that defined as the objective of this section is to determine waveform that able to generate the droplet with below requirements:

- Clear droplet (without satellite and ligament).
- Higher speed than basic waveform.
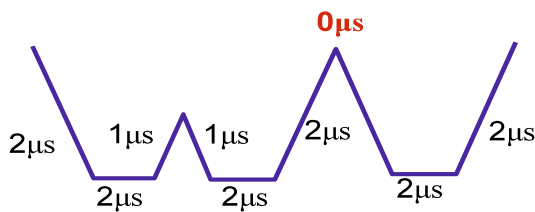
Fig. 5.14 (a) "W" single droplet waveform   Fig. 5.14 (b) "U" single droplet waveform
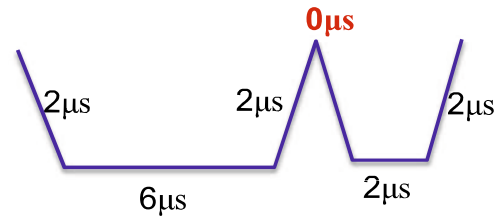
The conceptual model with simulation result shown in Fig. 5.15 is the comparison of 3 waveforms as follows:

- Independent "U" waveform (262)
- U_0_222 waveform; "U as preliminary vibration t_{wait} = 0 μs + main pulse (222)
- U_2_222 waveform; "U as preliminary vibration t_{wait} = 2 μs + main pulse (222)

The response of independent "U" waveform without followed by main pulse shows that "U" pulse itself will not ejects the droplet. Furthermore, the difference of response from the basic waveform and U_0_222 is only on the additional large-wide negative pulse as a response of "U" waveform, and very slight difference on its period. On the other hand, U_2_222 waveform had a different response because of the shifted period (t_{wait} = 2 μs).

The shifted period on U_2_222 will greatly impact the multi drop ejection. Therefore, the parameter of t_{wait} or time separation between 2 pulses is very important in designing the actuation waveform. The time interval (phase difference) of "U" waveform with t_{wait} = 0 μs from the following main pulse, are as follows:

- Front ramp pulse + main pulse → 10 = 8 + 2 (μs) with phase difference + π (rad)
- Rear ramp pulse + main pulse → 6 = 8 − 2 (μs) with phase difference - π (rad)
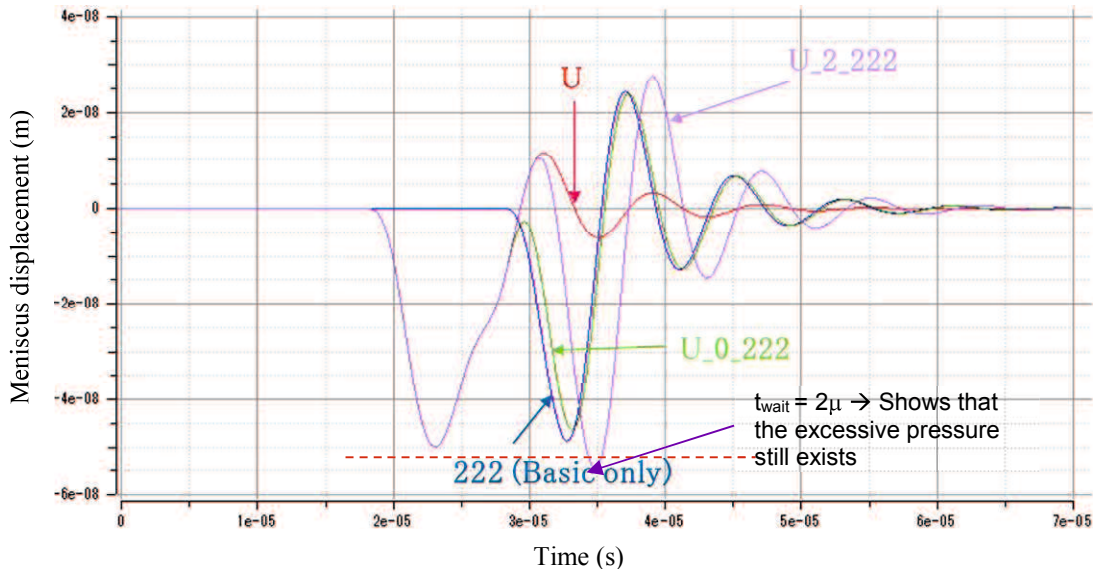
Fig. 5.15 The comparison of "U" waveform with different t$_{wait}$

5.5.2 Multi droplet waveform design

The similar velocity of each drop in multi-nozzle of inkjet printer is desirable for achieving the drop placement accuracy [10]. As stated in chapter I, the multi-drop method and clear ejected droplet is still become a big challenge in inkjet technology. Hence, the objective of this section is to determine waveform design that able to achieve below requirements:

- Wider range of droplet size or volume, using multi-drop method (multi-pulse)
- Clear droplet (without satellite and ligament)
- Similar velocity for each different size (maximum 2.5% deviation).
- Ganerated from the same applied voltage.

The basic concept that was discussed in section 5.2 then used to design the waveform in multi-drop method. The "U" and "W" pulse is also used as preliminary vibration to generate the large "back pressure to withstand the droplet until totally merged.

The other important point in designing the waveform for multi-drop concept beside t$_{wait}$ from "W" or "U" waveform is, t$_{wait}$ or the separating time between each pulse. First experiment was using waveform design as shown in Fig. 5.16 (t$_{wait}$ = 0µs), produced droplet volume with small increment. It was caused by the wave superposition in that waveform has canceled each other due to inappropriate phase difference. The droplet volume from waveform in Fig. 5.16 is shown in table 5.2. In same one pulse, we can see that the "W" waveform produced the larger droplet volume, and in 2 pulses produced the multiply volume

from 1 pulse of basic waveform. Starting at 3 and 4 pulses, the volume increment was not multiplication of previous pulse. Therefore, we must change the t_{wait} to get the optimum result.

Hence, t_{wait} = 2 μs is used for next experimental approach. With t_{wait} = 2 μs for each pulse without the voltage adjustment, the experiment result shown poor performance and tend to be weeping. Therefore, in order to produce the droplet with similar velocity at same base voltage and able to generate the clear droplet without satellite, we used voltage adjustment to generate the faster drop in the later ejection, compare to the previous drop. The adjustment was made by scaled up the base voltage percentage. The suitable pressure will generate the suitable velocity between drops so then the later droplet could reach and merged with the prior one. Therefore, the satellite will be eliminated. The voltage percentage adjustment that was determined from the experiment using Dowanol as an operating liquid is shown in Table 5.3. "Minus" symbol in table 5.3 means that the percentage of base voltage is deducted. Noted that the different liquid would give different characteristic so then the appropriate voltage adjustment should be determined.

In multi-drop waveform design, the additional suppressing vibration at the last pulse is also necessary to reduce the residual vibration and avoid the satellite particularly in 3-5 pulses. The recommended suppressing vibration in the first waveform design with Dowanol is using input parameter t (wait, down, keep, up); _0111 μs as suppressing vibration with voltage percentage 30% (small voltage). The profile of "W" for single and multi-drop was also designed in the same way with "U" waveform. The complete waveform profile in this study is shown in Fig. 5.17.
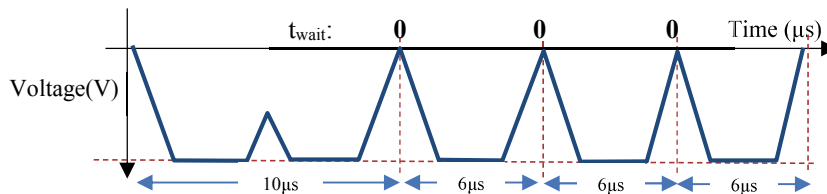
Fig. 5.16 "W" waveform with t_{wait} = 0μs

Table 5.2 Droplet volume for "W" waveform with t_{wait} = 0μs

Pulse number	Volume (pL)	
	Waveform W_0_2_0_2_ …	Basic waveform
1 main pulse	7.720	5.859
2 main pulses	10.701	-
3 main pulses	10.850	-
4 main pulses	11.729	-

Table 5.3 The percentage adjustment of base input voltage in generating the droplet with similar velocity at different droplet volume.

Drop Number	"U" waveform	"W" waveform
1	-7%	-7%
2	-10%, -3%	-5%, -0%
3	-18%, -16%, -14%	-16%, -14%, -12%
4	-24%, -22%, -20%, -18%	-24%, -20%, -18%, -16%
5	-28, -26%, -24%, -22%, -20%	-28%, -24%, -22%, -20%, -18%
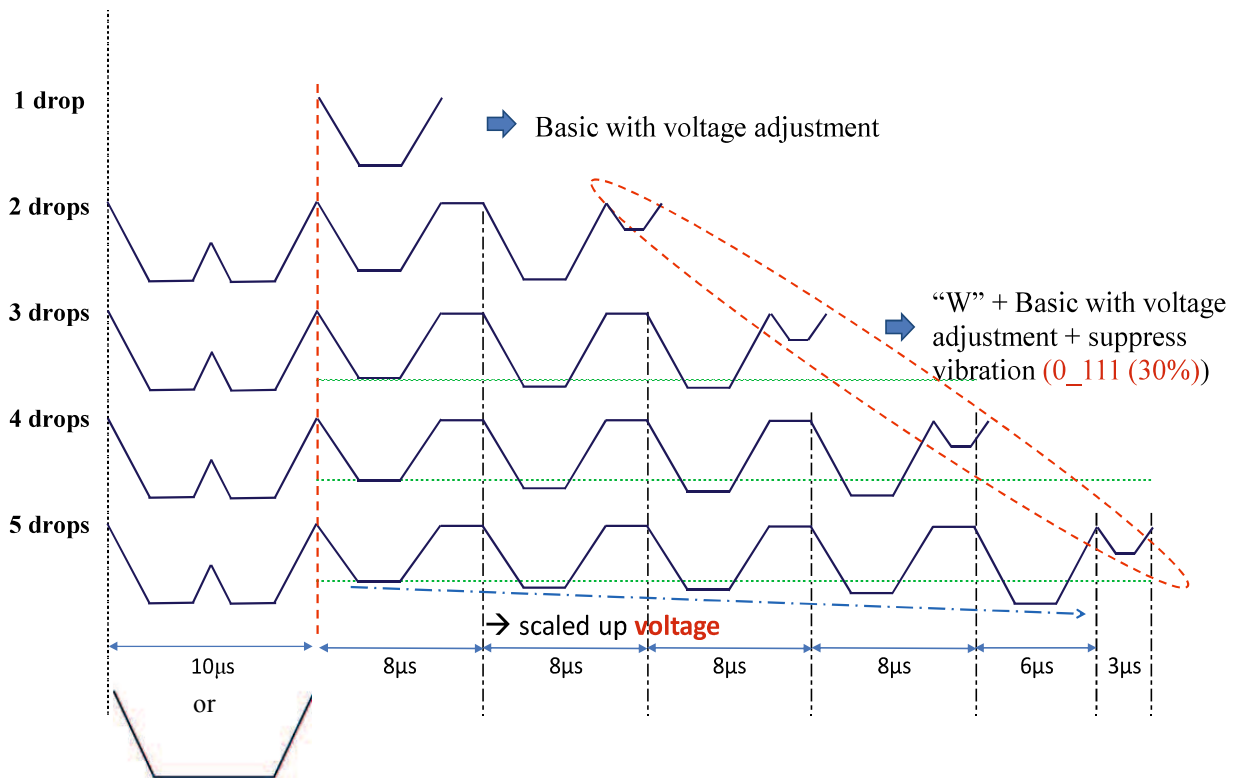
Fig. 5.17. The actuation waveform profiles for multi-drop method

The conceptual system model for the actuation waveform design in multi-drop method is shown in Fig. 5.18. This figure describes the comparison between input-response for unadjusted voltage (a) and adjusted voltage (b). It shows that the negative pressure response of preliminary vibration from unadjusted voltage that derived from the second, third and fourth pulse are more than soliton that derived from the wave "W" or "U". In the other side, the suitable adjusted voltage for the first, second and third pulse will generate the response with lower negative pressure than soliton, and similar for the fourth pulse. The comparison of multi-drop response of basic waveform with the new design in conceptual system model is shown in Fig. 5.19.
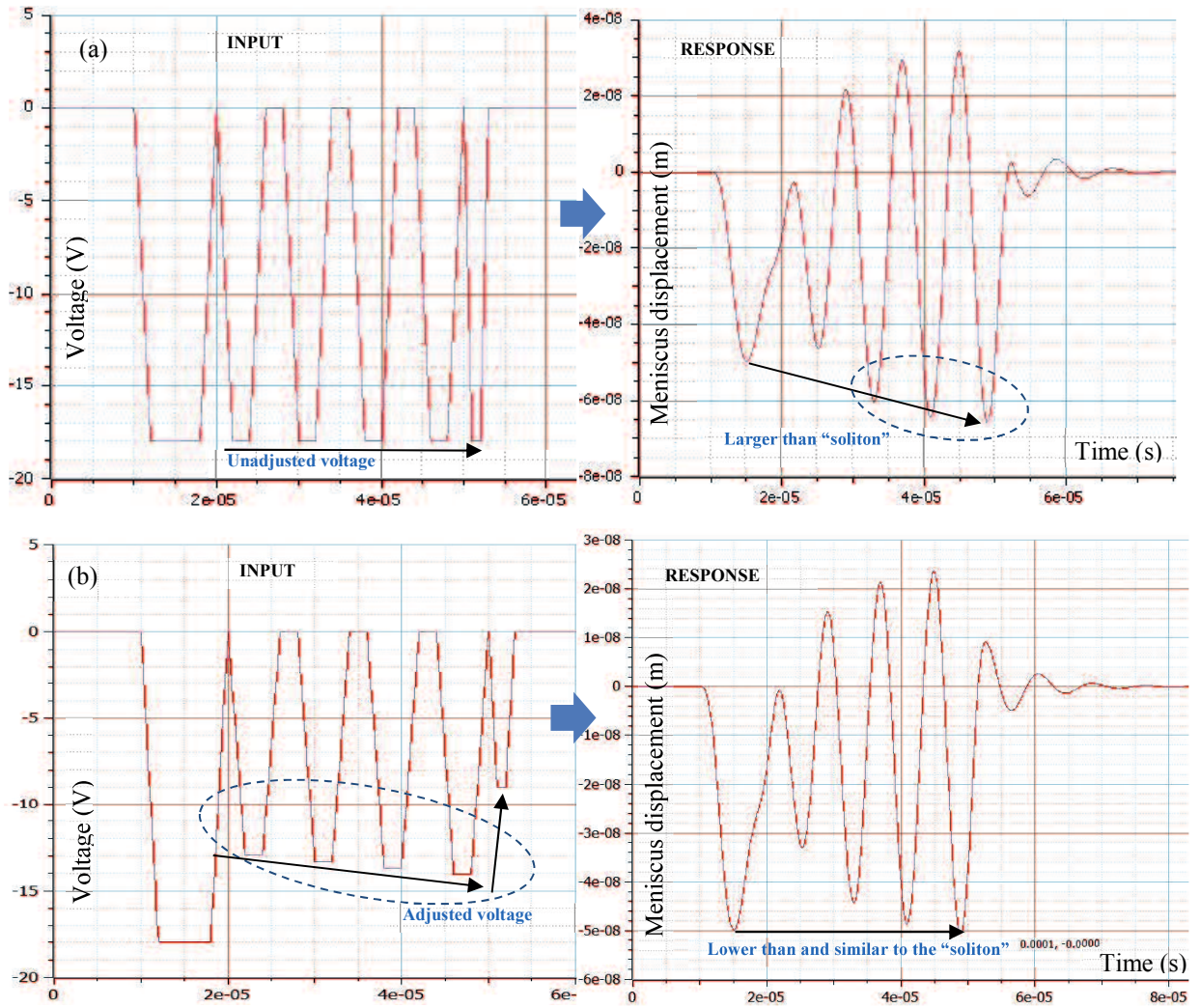
Fig. 5.18. Input-response of adjusted and adjusted voltage for multi-drop concept
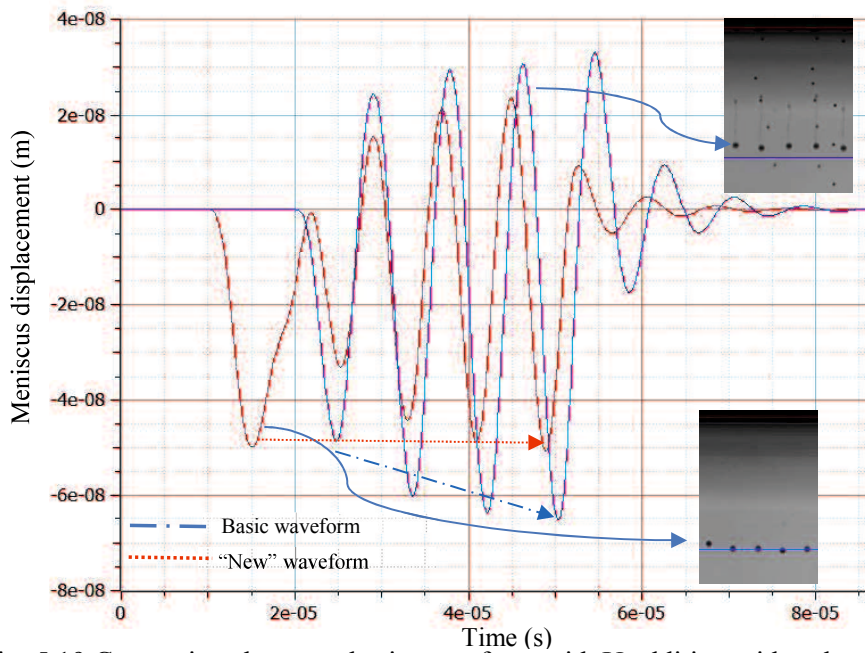
Fig. 5.19 Comparison between basic waveform with U addition with voltage adjustment

Fig. 5.19 depicts the comparison of the basic waveform without adjusted voltage and "W" waveform with adjusted voltage. It shows that the weeping occurred from the excessive pressure of constructive interference from multi-pulse. The waveform design with combination of soliton that derived from "W" waveform, suitable t_{keep}, adjusted voltage and suppressing vibration (0_111) could withstand those excessive pressures and avoiding the weeping occurrence until 5 drops ejection.

5.6 Experiment Result and Discussion
5.6.1 Single drop method

Of the prior experiment, it was revealed that "U" and "W" waveform without main pulse followed by, will not eject the droplet (at 14-18V). The comparison of basic waveform only with "U" and "W" additional pulse was examined in order to investigate its effect as preliminary vibration.

The comparison of droplet volume in single drop ejection for Basic, "U" and "W" waveform is shown in Fig. 5.20. Same condition with the experiment result shown in table 5.3, this figure presents that in the same applied voltage, both "U" and "W" waveform can generate the larger volume (bigger size).

The experiment result of single droplet with proposed waveform design is shown in Fig. 5.21 (a). We can see that the clear droplet in basic waveform was derived from applied voltage 14 V only whereas the others will generate the droplets with ligament. The additional "U" and "W" waveform as preliminary vibration was found to generates the clear and larger droplet that was derived at 14-17V for "W" whilst "U" waveform at 14-16V. This experiment result confirms that "W" and "U" waveform is effective to achieve the high performance of droplet.

The droplet speed that shown in Fig. 5.21 (b) at different applied voltage are consistent with previous research. It stated that the higher applied voltage, the faster of droplet speed. This result allows us to control the droplet speed, and obtain the larger droplet with the higher speed than basic waveform. By comparing the droplet volume and speed at the same applied voltage, it is determined that "U" and "W" waveform generate the larger volume or bigger size, with the lower speed of droplet. This characteristic is similar with the other mode of piezo driving pulse, namely push-pull. Therefore, "U" and "W" waveform (negative polar) can also generate the droplet as well push-pull mode (positive polar) so called push-pull reflection method.
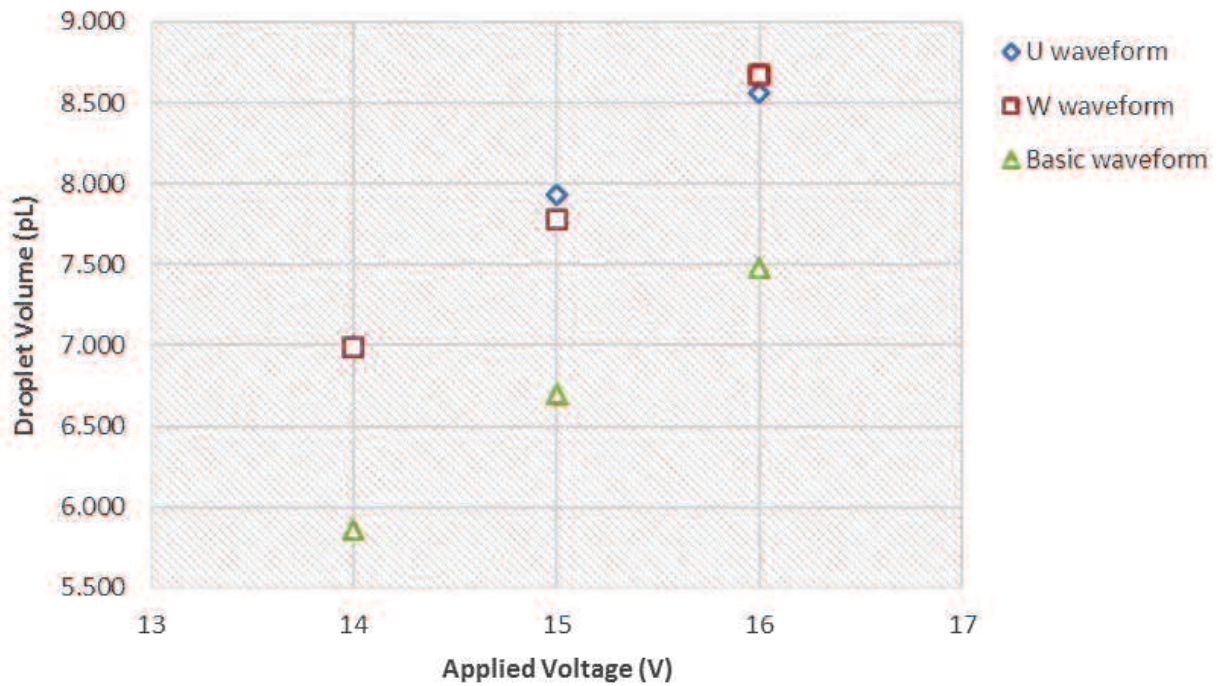
Fig. 5.20 Comparison of droplet volume in single drop ejection (U", "W" and basic waveform)

Figure 5.21 (b) shows that the velocity of clear droplet is almost similar at 14V basic waveform, 16 V by "W" and at 15V by "U" waveform addition. The higher velocity was achieved at 17 V by "W" and at 16 V by "U" waveform addition for single droplet ejection. The comparison of droplet velocity in detail is shown in table 5.4. The result also implies that the larger volume with similar higher speed can be derived by using appropriate voltage and "U" or "W" waveform as preliminary vibration is effective to eliminate satellite and ligament with larger volume.
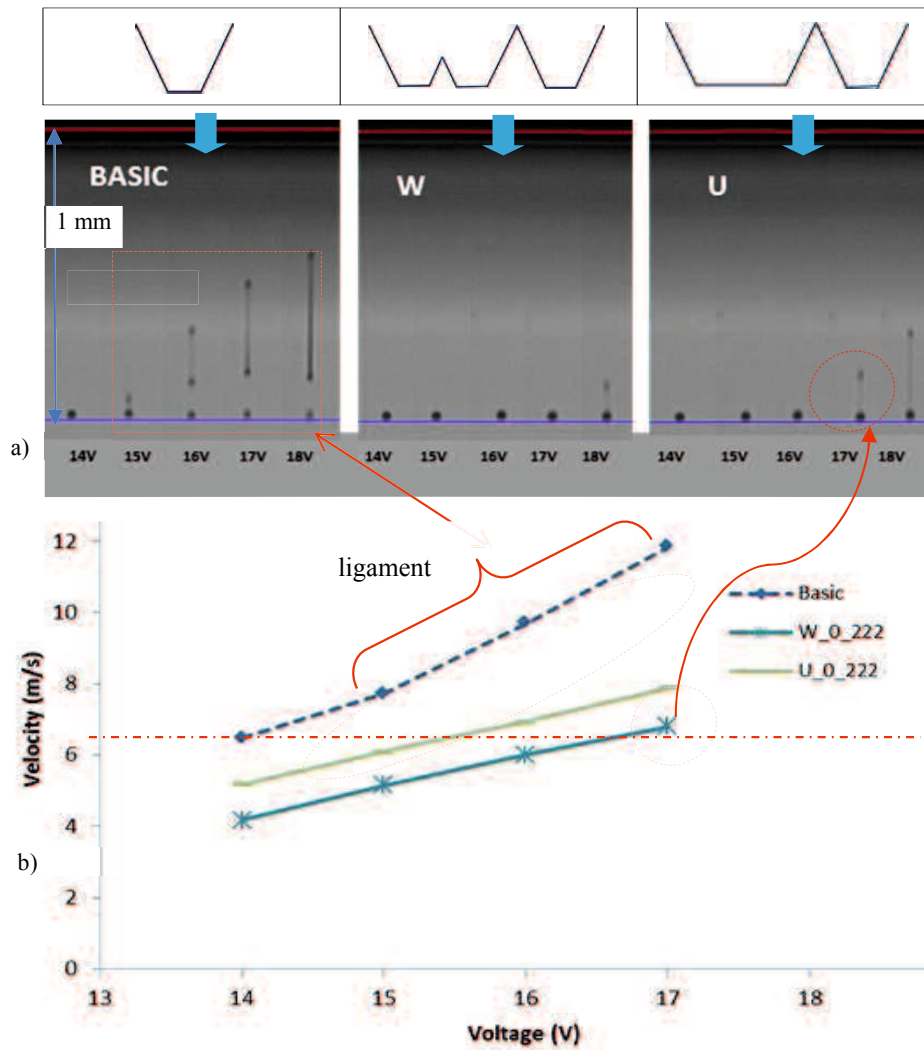
Fig. 5.21 The Comparison of droplet velocity (Basic, "U" and "W" wavefrom)

Table 5.4 Comparison of velocity for single droplet

Velocity (m/s)			
Voltage	BASIC	W	U
14 V	6.472	4.184	5.184
15 V	7.722	5.149	6.101
16 V	9.699	6.017	6.949
17 V	11.834	6.798	7.893

Note: Unclear droplet

5.6.2 Multi drop method

In previous section, the droplet shape from basic waveform input in single droplet showed that the only clear droplet could be obtained from applied voltage less than 15 V. The droplets with ligament were generated from applied voltage above 14 V in single drop. It is presumed that the chamber is not in the "compressive vibration state" but "in the flow state", so then it generated the droplet with long ligament.

It also has been demonstrated to be nonviable with basic waveform to apply the multi-drop. Therefore, we propose "Push-Pull reflection drive method (Resonance oscillation excavational pulse)" which has characteristics of solitary wave and propose a radical solution particularly in multi-drop concept. With this method, it is possible to realize a Helmholtz resonance box by uniformly and synchronously compressing and expanding the ink in the entire liquid chamber. It is important to be noted that the interference between the nozzles due to excessive (preliminary) vibration (suction at the meniscus) will caused the irregular vibration of the liquid chamber. The droplets from low voltage of main drive pulse (10 V to 14 V) are clear spherical droplets thus the small surface tension of the meniscus.

The droplet control by the multi-drop is "the method to control a droplet by a following droplet catching up with tip bubble discharged by a nozzle, and being united before it comes on the media surface". The other concept of multi-drop allows the droplet merge in the media surface. The multi-drop drawing concept for Dowanol ink in this study is shown in Figure 5.22. Soon after tip bubble was generated, the first diameter is small. Subsequently, by surface tension, the speed becomes slower than discharge speed and it grows up rapidly in the nozzle neighborhood. The speed of following droplet must be faster than to merge with the precedent bubble. Therefore, in multi-drop concept, it is necessary to adjust the drop speed for so that it able to merge without left the satellite or ligament. The droplet speed is adjusted by applied voltage adjustment to find a suitable speed for each pulse. The multi-drop capability allows the creation of a range of drop sizes enabling grey-scale printing. The mechanism of multi-drop method can be explained as follows:

- The first pulse using "W" waveform as preliminary vibration. The sloshing droplet (walk up and down droplet) without breakup are appeared if using this single pulse. The droplet returns to the liquid chamber. It may generate the Helmholtz resonance inside the liquid chamber. This pulse provides the large negative pressure or back pressure for withstanding the next firing droplet from the excessive pressure that could generate the ligament.

- The first ejection is from the first main pulse with period 8μs. The lower speed of droplet voltage due to the lower applied voltage and effect of preliminary vibration will be generated from this first pulse.
- The droplet ejection will continue from the subsequent main pulse, until 5pulse.
- The separating time between each pulse is important. It to control when the next droplet must be ejected, for synchronizing and obtain suitable wave superposition between each pulse for the optimal droplet formation.
- The next droplet must be using the larger applied voltage to generate the faster droplet, so then it can reach the prior droplet and be merged before it reaches 1 mm (observation distance and substrate distance standard from the nozzle)
- The last pulse using suppressing vibration for damp the residual vibration from all previous pulses.
- The final droplet will be spherical droplet without satellite and ligament.

The final droplet that reached the paper surface at 1 mm distance from the nozzle is totally a clear spherical droplet. Figure 5.23 shows the difference of droplet size from 1 main pulse until 5 pulses. We can see that the "U" and "W" waveform design was generated the clear droplet without ligament and satellite, and no "weeping" occurred until 5 pulses. This is a radical improvement compared to the results that shown from input actuating waveform using the basic waveform. The difference of droplet volume from each pulse is larger than the multiplication of single droplet, because of preliminary vibration effect. By this result, it is also confirmed the hypothesis that it is possible to create the real Helmholtz resonance by the additional of "W" or "U" waveform as preliminary vibration that can be compressing and expanding the liquid chamber uniformly and synchronously.

5.6.3 "W" And "U" waveform as Push-Pull reflection method

The droplet speed in different applied voltage are consistent with previous research which stated that the higher applied voltage, the faster of droplet speed. This result allows us to control the droplet speed, and obtain the larger droplet with the higher speed than basic waveform. By comparing the droplet volume and speed at the same applied voltage, it is determined that "U" and "W" waveform generate the larger volume or bigger size, with the lower speed of droplet. This characteristic is similar with the other mode of piezo driving pulse, namely push-pull mode. Therefore, "U" and "W" waveform (negative polar) can also generate the droplet as well push-pull mode (positive polar) so called push-pull reflection method.
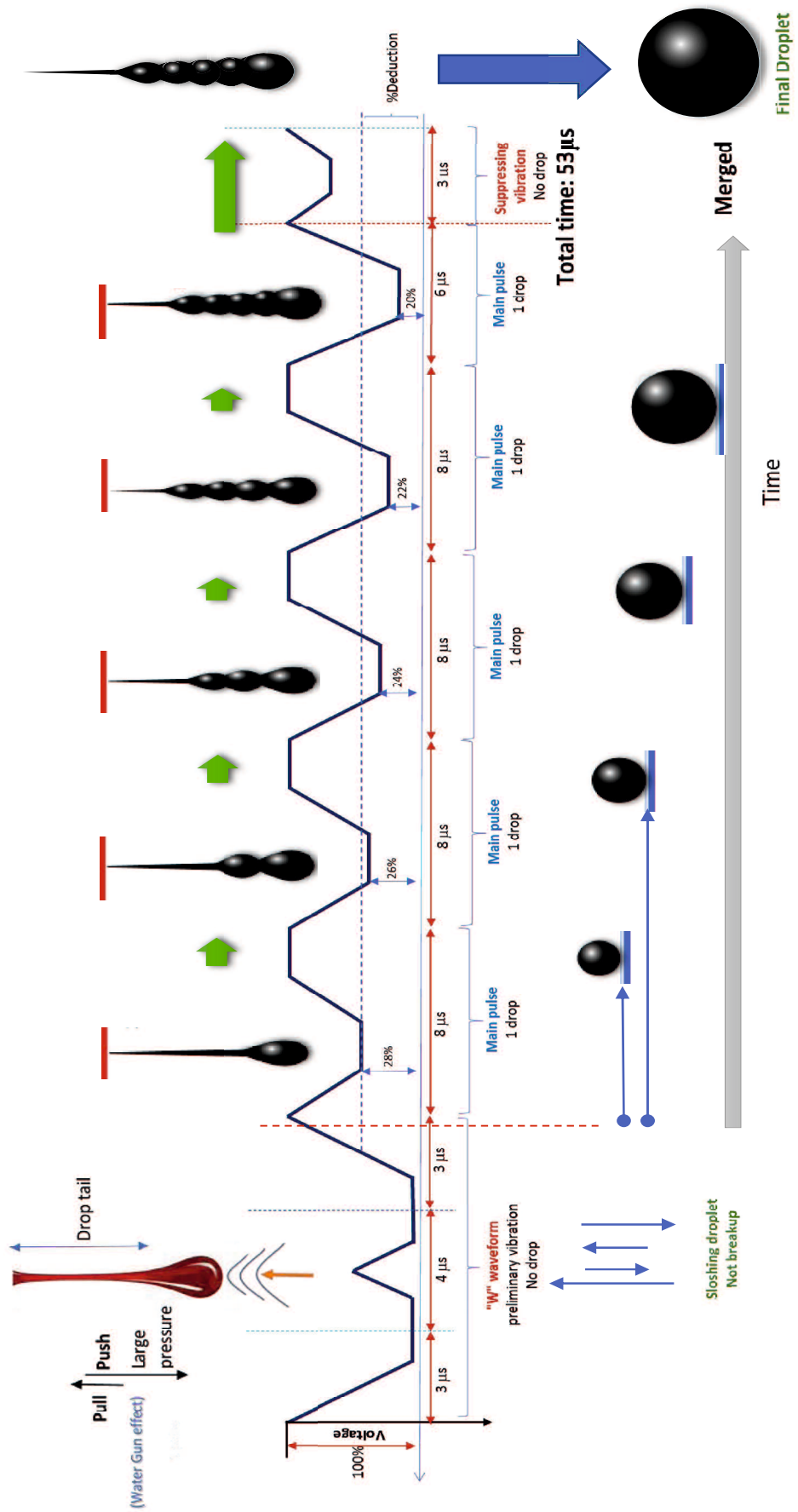
Figure 5.22 Conceptual drawing of multi-drop ejection (e.g. 5 pulses)
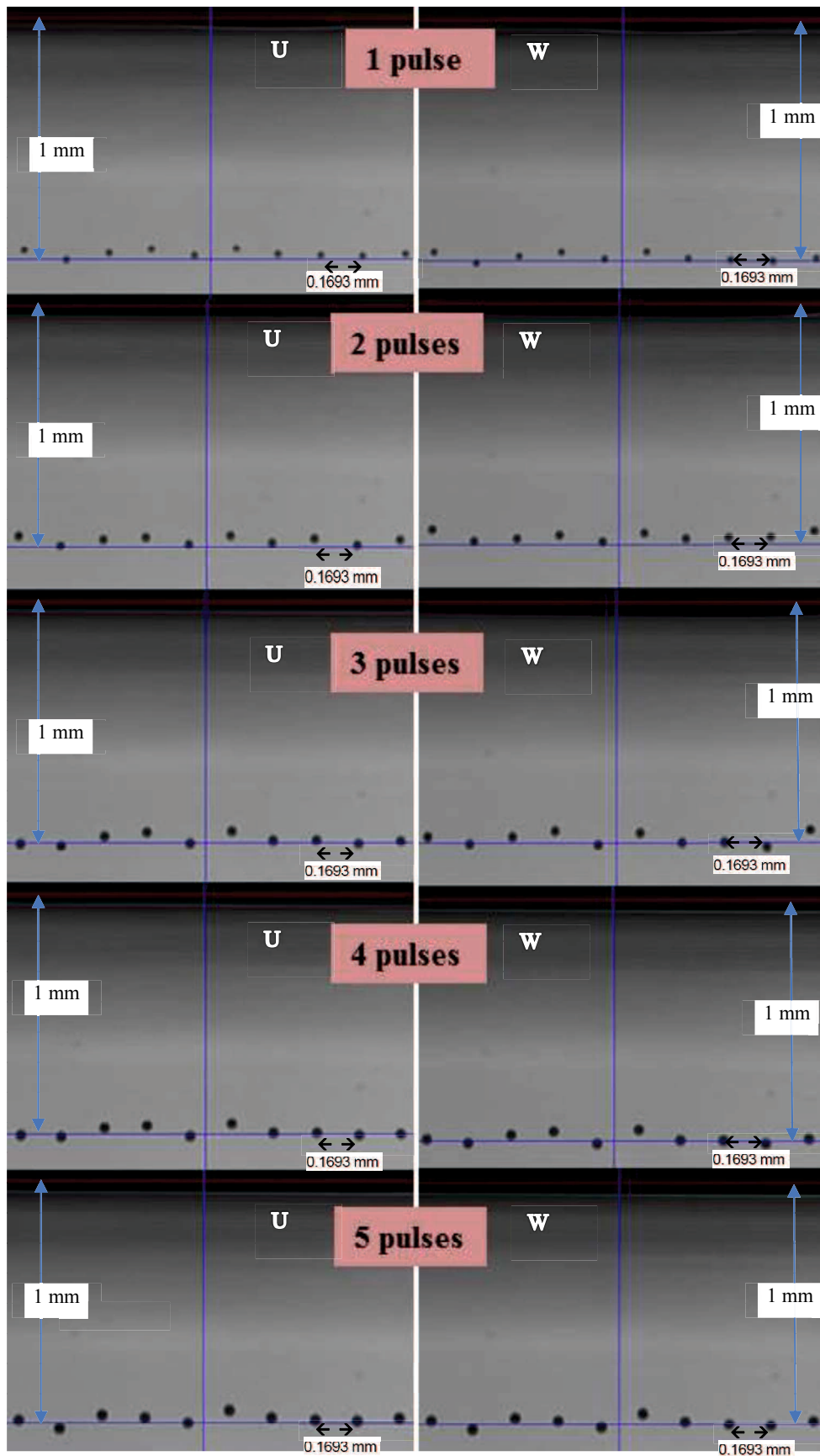
Fig. 5.23 The droplet shape with "U" and "W" preliminary vibration

5.7 Comparison of "U" and "W" Waveform Experiment Result

The comparison of droplet volume and velocity with "U" and "W" preliminary vibration is shown in Fig. 5.24. The similar velocity can be obtained by different voltage adjusment.
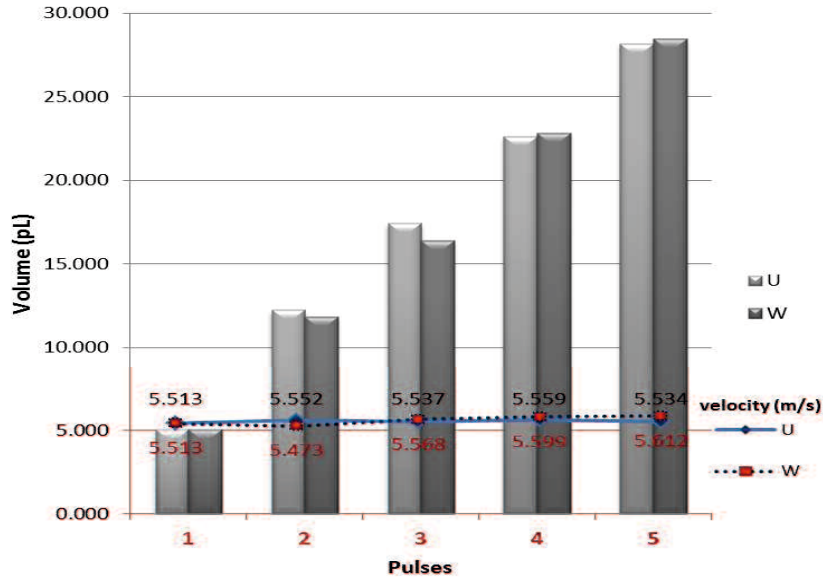
Fig. 5.24 The comparison of droplet volume and velocity with "U" and "W" preliminary vibration

Detail information of droplet volume, velocity and the deviation of each droplet velocity is shown in table 5.5, with the summary in table 5.6. The deviation of droplet velocity from 1 pulse until 5 pulses is shown in Fig. 5.25. It was stated that the limit of velocity deviation from each droplet to generate the high quality of grayscale effect in printing result is 2.5%. The figure shows that all of droplet speed has the difference less than 2.5%.

Table 5.5 Comparison of droplet volume, velocity and velocity deviation

	"U" waveform		"W" waveform	
Pulse	Volume [pL]	Velocity (m/s)	Volume (pL)	Velocity (m/s)
1	5.047	5.513	5.03	5.513
2	12.234	5.552	11.83	5.473
3	17.430	5.537	16.41	5.568
4	22.617	5.559	22.82	5.599
5	28.178	5.534	28.45	5.612
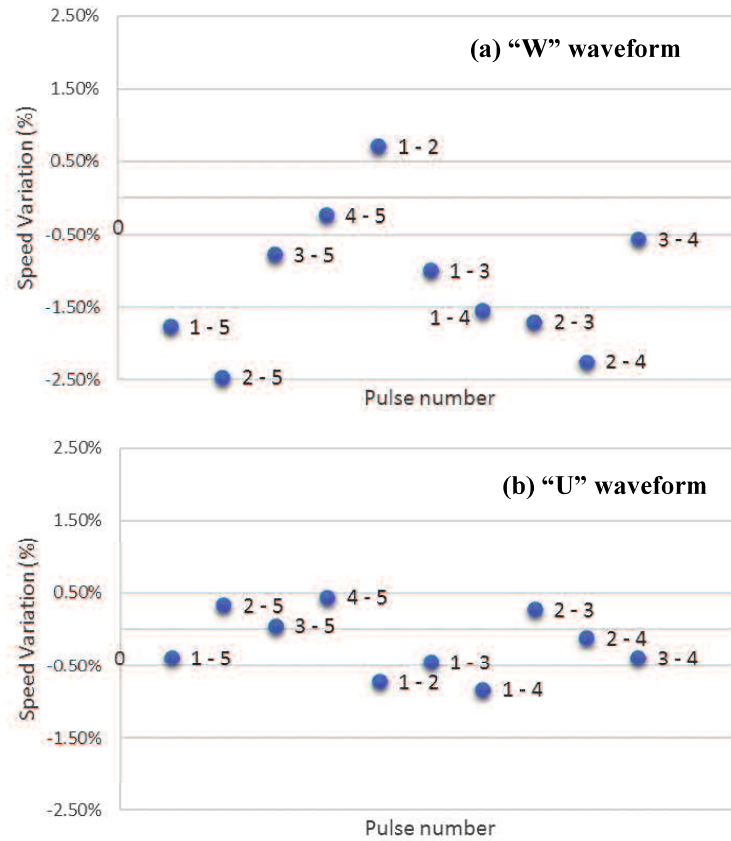
Fig. 5.25 The comparison of velocity deviation
(a) "U" preliminary vibration (b) "W" preliminary vibration

Table 5.6 The comparison of U and W waveform experiment result

waveform	U	W
Velocity	≈	
Volume	≈	
Total time	=	
Deviation	All √	All √
Main pulse limit	**6**	**5**

By this preliminary vibration, it is possible to create the real Helmholtz resonance box that can be compressing and expanding the liquid chamber uniformly and synchronously. In this study, an applied voltage to produce ideal droplet without satellite and ligament is 14 V with the droplet velocity ± 5.5 m/s. The higher velocity is still possible by determining the more suitable adjustment of base voltage. Table 5.6 also shows that the difference between U and W waveform is on the main pulse limit. U waveform has more pulse limit due to its simplicity.

5.8 The Verification of New Actuation Waveform Design by Using UV Ink

Some studies concluded the influence of fluid properties on droplet behavior [72], [76] - [80], [94], [97] & [99]. One of ink classification namely UV-curable ink [5]. UV ink is one of ink types that initially liquid, but becomes solid after the liquid polymerization process on the substrate so called as UV-curable ink. UV-Curable Ink in inkjet printer market have been used for many years [33]. Many application of printing industry using UV ink such as posters, golf balls printing, credit card, circuit boards, mobile phone, CDs, wood decor and textiles, etc. [37, 38]

In this section, we use UV ink as an operating liquid to investigate and validate the proposed waveform design by using "W" waveform as preliminary vibration. The viscosity of UV Ink compared to Dowanol is shown in table 5.7.

Table 5.7. Viscosity of operating liquid (Dowanol and UV Ink)

Head Temp.	VISCOSITY (mPa.s)	
	Dowanol (ρ: 1.013 g/cm^3)	UV Ink (ρ: 1.042 g/cm^3)
19°C	15.55	12.24
30°C	10.17	7.90
50°C	5.40	3.50

Table 5.7 shows that UV ink that used in this section has the lower viscosity but higher density than Dowanol in the previous section. The experiment was conducted for single and multi-drop concept with same design as Dowanol, with head temperature 35°C and 40°C and applied voltage 14V-20V. The different physical ink properties also influence the droplet behavior [72], [76] - [80], [94] & [97]. In UV ink which viscosity is lower than Dowanol, the ligament will be longer, as shown in Fig. 5.27 (a) for the droplet shape using basic waveform. The same result was come from the other study [97]. The study stated that the lower viscosity of operating liquid will lead to the longer ligament. That's why in the UV ink, we found that the ligament is still appear even in a very thin ligament.

From preliminary experiment observation data as shown in table 5.8, it was determined that the suppressing vibration 0_111 is effective to generate the clear droplet. 50% of suppressing vibration is still effective in 15V whereas the others not. Furthermore, the droplet speed from 50% of _111 waveform with 15V applied voltage is slightly higher than using 30% of suppressing vibration 0_111 with 14V applied voltage.

Therefore, this observation data used to improve the ability of proposed waveform design in single drop ejection with UV ink for implementing in the high voltage.

Table 5.8 Data observation of suppressing vibration _0111

Waveform : 222_0_111
Head Temp: 30 decel

% Suppress	Voltage	Speed	Remark
	14	4.312204	clear
	15	5.830904	clear
50%	16	8.203445	2 drops
	17	10.51525	short ligament
	18	12.64223	long ligament
	14	4.849661	clear
	15	6.35324	2 drops
40%	16	8.818342	2 drops
	17	11.17318	short ligament
	18	13.24503	long ligament
	14	5.376344	clear
	15	6.872852	2 drops
30%	16	9.354537	2 drops
	17	11.64144	short ligament
	18	13.73626	long ligament
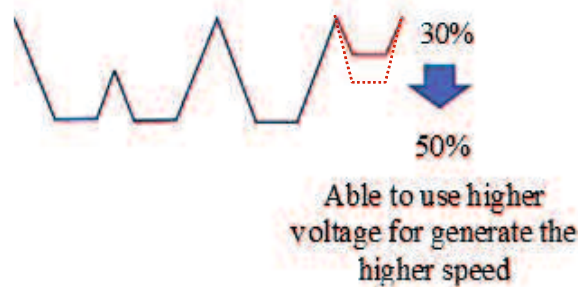
Fig. 5.26 waveform with suppressing vibration adjustment

5.8.1 Experiment result in single droplet ejection

The experiment results for single drop by using UV ink as an operating liquid is shown in Fig. 5.27. The actuating waveform with basic waveform shows the ejected drops with ligament (Fig. 5.27 a). In agreement with previous result by using Dowanol, we can see that the larger applied voltage also generated the longer ligament. In Fig. 5.21b, we can see that the "W" waveform without suppress vibration is effective until 16 V whereas 17-19V of applied voltage must be modified by an additional of suppressing vibration 0_111 with 30% of base voltage. 50% suppressing vibration 0_111 must be applied in 20V to eliminate the residual vibration that could generate the short ligament or satellite. We can see the clear droplet that could generated from 20V of applied voltage even in head temperature 40°C as shown in Fig. 5.20c. This result was using 50% base voltage in suppressing vibration.
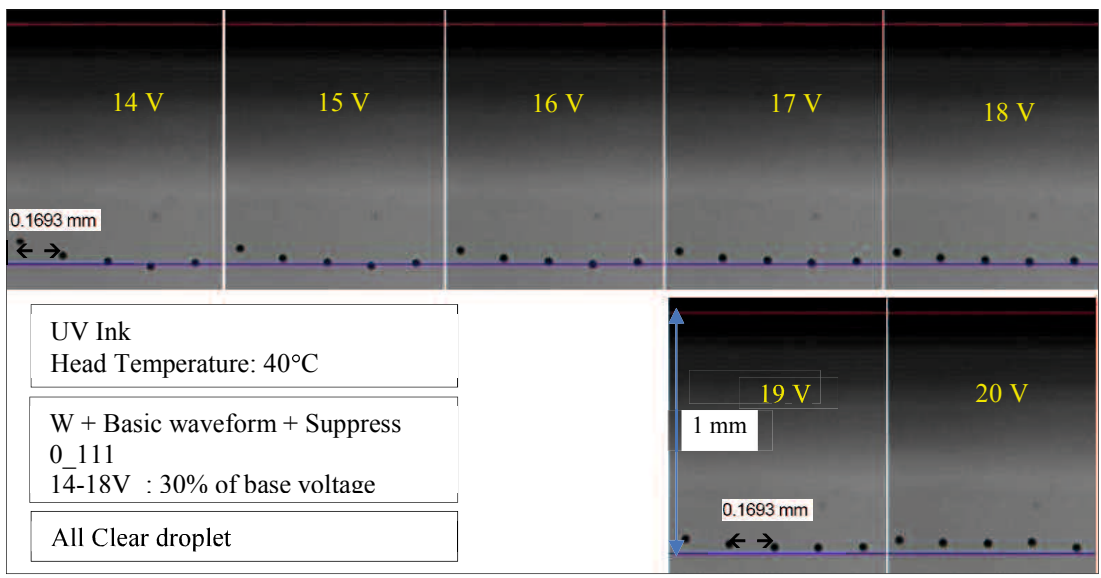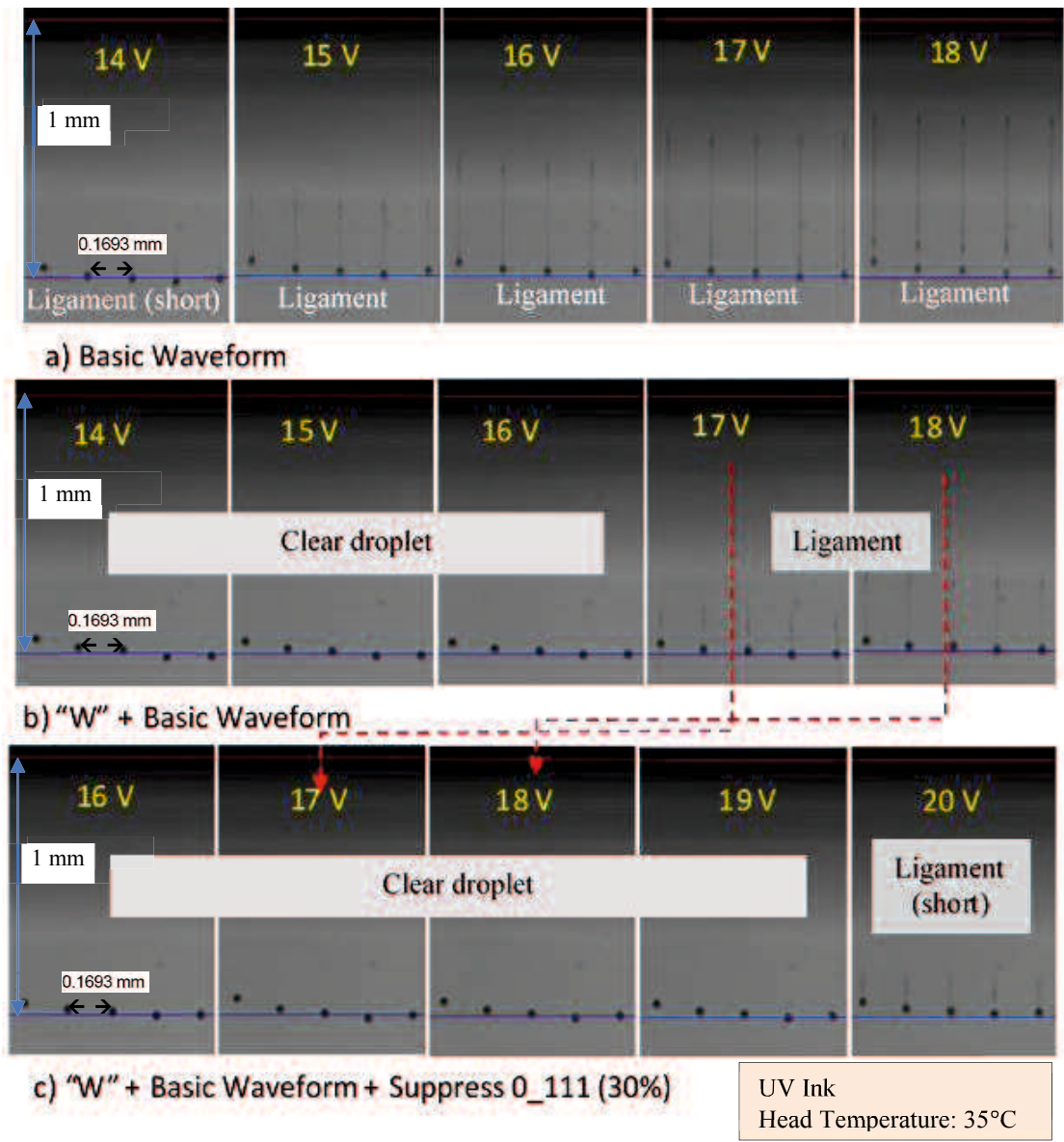
Fig. 5.27 Comparison of droplet shape for single drop (basic waveform and UV Ink)

Therefore, Fig. 5.27 presents that the larger voltage of suppressing vibration is effective to produce the clear droplet. If higher voltage applied in the actuating waveform, the higher voltage of suppressing vibration is also recommended for generate the clear droplet without ligament.

5.8.2 Experiment result in Multi drop ejection

The experiment result using UV ink as an operating waveform is shown in Fig. 5.28. In previous section of multi-drop concept by using Dowanol as operating liquid, we can see that it is nonviable even at 14V start for 3 pulses by using basic waveform. For UV Ink, the weeping also occurs start from 16V in 3 pulses actuating waveform, and 15V for 4 pulses actuating waveform, as shown in Fig. 5.28a.

From fig. 5.28b, it is confirmed that the proposed design of actuating waveform also effective to generate the droplet with good performance (without satellite and ligament), particularly with applied voltage 14V. For the other applied voltage, it is necessary to find the more suitable adjustment. For examples in 4 pulses, the percentage of scale up voltage we used is 16%, 14%, 12% and 10% that still too large and generate the excessive pressure that caused the thin ligament. It should more adjusted and deployed the lower scale of voltage such as in Dowanol (using 24%, 22%, 20% and 18%). This phenomenon will be explained more clearly with the simulation model using modelica on chapter VII. The excessive pressure will be run into the ejection process if the response of multi-pulse input waveform is larger than the negative pressure (back pressure) from the "W" waveform as the preliminary waveform.

Therefore, it is proved that the suitable adjusted voltage is an important factor for controlling the droplet behavior in multi-drop ejection method to generate the clear droplet. In case of the large printing area, the very thin ligament could be neglected. The resume of experiment results of droplet shape behavior in single and multi-drop with a comparison between basic waveform (only) and waveform with "W" pulse as preliminary vibration and 0_111 as suppressing vibration is shown in table 5.9. The result in multi-drop strengthen the conclusion in the single droplet ejection about the importance of suppressing vibration percentage (applied voltage) in the droplet control.
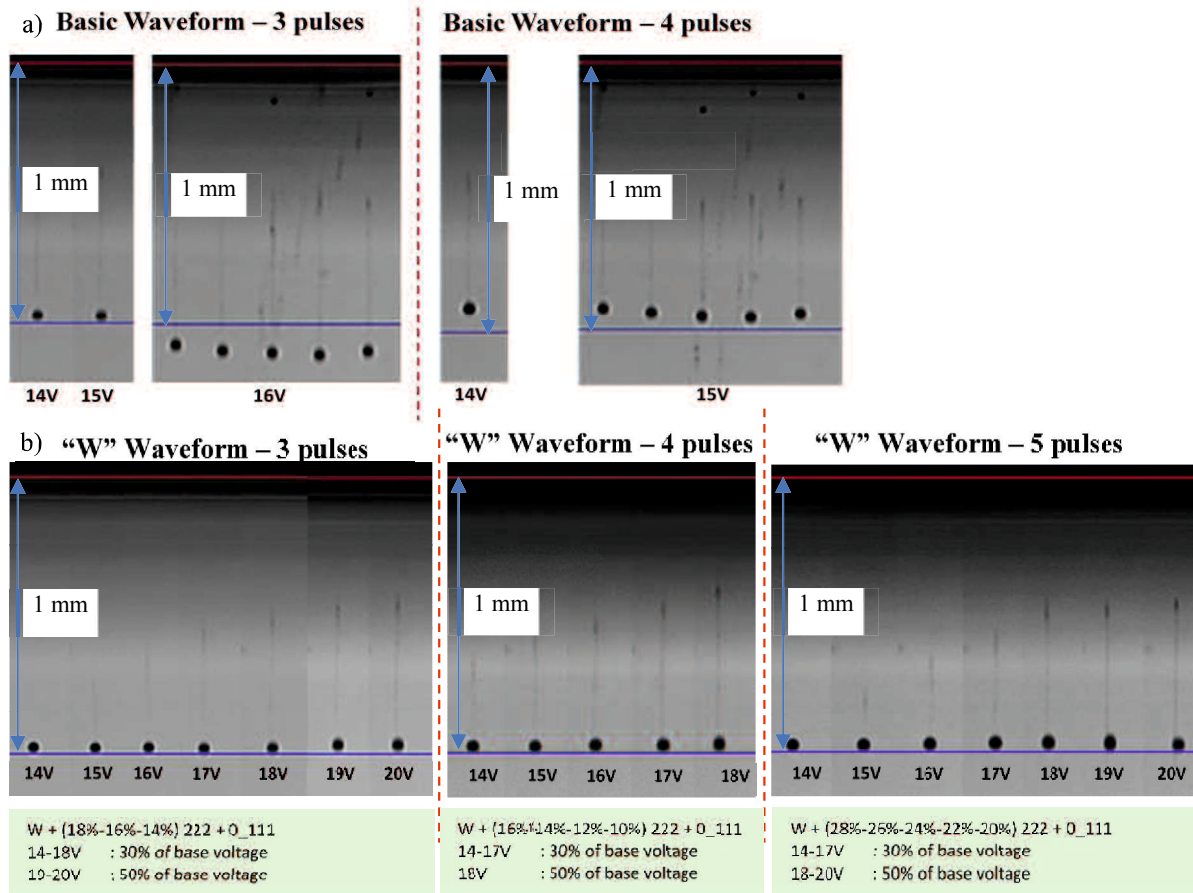
Fig. 5.28. Droplet shape for multi-drop concept with UV Ink

Table 5.9. Resume of droplet performance (basic and W waveform)
("W" Design) in single and multi-drop concept.

Voltage	Single Drop		Multi drop					
			3 pulses		4 pulses		5 pulses	
	Basic	W Design	Basic	W Design	Basic	W Design	Basic	W Design
14	L	●	L	●	L	L	X	●
15	L	●	L	L	X	L	X	L
16	L	●	X	L	X	L	X	L
17	L	●	X	L	X	L	X	L
18	L	●	X	L	X	L	X	L
19	L	●	X	L	X	L	X	L
20	L	L	X	L	X	L	X	L

Note: ●   Clear droplet
Head Temperature: 35 °C L   Droplet with thin ligament
                  X   Weeping

      The experiment results show the important implication in controlling the droplet performance of inkjet print-head particularly in multi-drop ejection without satellite and ligament, and avoid the "weeping" occurrence. The addition of suppressing vibration with small voltage is necessary to prevent satellite or ligament because of residual vibration

particularly in more than 2 drops ejection. The voltage adjustment technique demonstrates the velocity controlling for each drop in the multi-drop concept, for generating the grey-scale technology of inkjet printing with high quality. The higher voltage of suppressing vibration is also recommended for higher voltage of main pulse. It also revealed that the physical properties such as density and viscosity influence the droplet behavior. In low voltage using 14V, the generated droplet is clear, whereas in UV ink the generated droplet is with thin ligament.

Hence, it is verified that the "W" waveform is also effective for generating the good performance of droplet in multi-drop concept, with different operating liquid (UV Ink and Dowanol). The higher speed is still possible by determining the suitable adjusted base voltage of each sequence pulse.

Figures 5.29 the different droplet performance from each waveform design with single ejection method. Figure 5.30 described that by using W waveform as the design of input parameter to drive the PZT inkjet printer, the multi-drop method was applicable with a good performance of droplet shape. The droplet velocity and volume is also controllable.
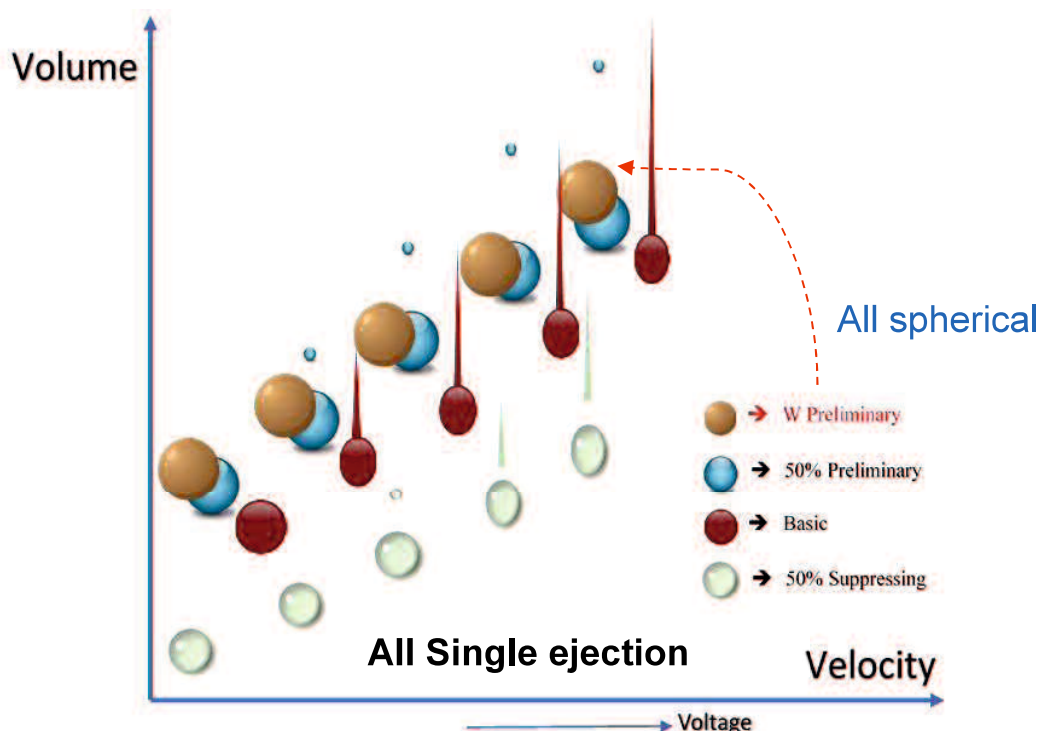
Fig. 5.29 The illustration of droplet shape with different waveform design in single ejection method
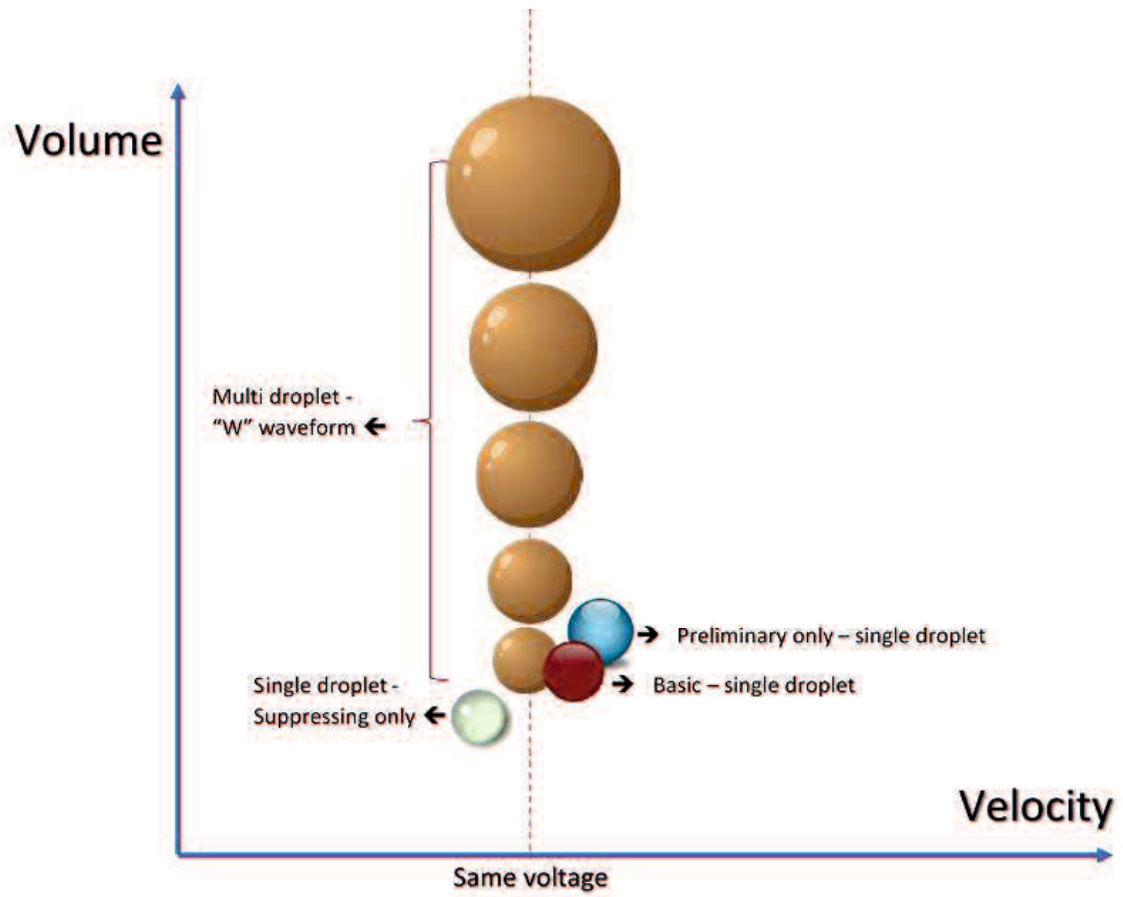
Fig. 5.30 The comparison of single and multi-drop ejection method

5.9 Conclusion

1. It is impossible to generate multi-drop with clear spherical droplet by using basic waveform. It was determined that "U" and W" waveform as a new waveform design are effective to be utilized in eliminating the "water gun effect" and reduced the residual vibration.

2. It is to be proved that "U" and W" waveform significantly improve the droplet performance, by generating the droplet without satellite, ligament and weeping occurrence even in the multi drop concept. The larger drop and lower speed (compared to basic waveform in same applied voltage) for single drop ejection shown that the inkjet printer with pull-push system that used in this study, can generate the droplet such as push-pull system (therefore, the waveform design called as push-pull reflection waveform method). The higher speed with clear droplet can be obtained by using the larger applied voltage with "W" or "U" waveform.

3. The different droplet size in multi-drop ejection method with similar velocity and clear droplet can be obtained by appropriate voltage adjustment. The suitable voltage adjustment of each pulse is important to prevent the excessive pressure that can generate the ligament. The higher speed is also possible by suitable adjusted voltage of each sequence pulse.

4. The different operating liquid will represent some different behaviors related to its viscosity. From the experiment result by using Dowanol and UV ink, the additional concept to create the "tuning factor" was determined. An additional "W" waveform + suppressing vibration (0_111) to reduce residual vibration and avoid weeping accurrence is effective in single drop with:

- 30% suppress vibration at 17-18V.
- 50% suppress vibration at 19-20V.

The higher base voltage that applied in the actuating waveform need a higher percentage suppressing vibration is also recommended for generate the clear spherical droplet without ligament.

CHAPTER VI

MODIFIED "W" WAVEFORM DESIGN ON SINGLE AND MULTI-DROP CONCEPT FOR EDIBLE INK

6.1 Introduction

As stated in chapter V, the current necessity in inkjet printing technology is determining the print-head that have higher flexibility with fluid properties. The more flexible print-head versus fluid formulation can be reached by the design of print-head itself or by the design of the operating parameter to actuate the print-head. In this study, we investigated the new waveform design effectiveness by using W waveform with another operating fluid, namely edible ink. Edible ink is the liquid with edible food colors that use for creating preprinted images onto various confectionery products such as cakes or cookies. Designs made with edible ink can either be preprinted or created with an edible printer, a specialty device which transfers an image onto a thin, edible paper. Edible paper is made of starches and sugars and printed on with edible food colors.

The joint research company has main customer that using edible ink as their operating liquid. This liquid has a lower viscosity so then it is more difficult to control. The comparison of viscosity with Dowanol and UV ink is shown in table 6.1. Therefore, in this section, we also use Edible ink as an operating liquid to investigate and validate the proposed waveform design by using unmodified "W" waveform as preliminary vibration. As initial experiment, we used basic waveform design from print-head supplier with edible ink (black), with applied voltage 14 -18V and head temperature 25°C. The droplet shape by using actuating waveform (basic waveform) is shown in Fig. 6.1.

Table 6.1 Viscosity of the operating liquid

Head Temp (°C)	DOWANOL η(mPa)	UV INK η(mPa)	EDIBLE INK η(mPa)
19	15.55	12.24	-
25	-	-	7.60
30	10.17	7.90	-
50	5.40	3.50	-

Figure 6.1 presents the droplet shape with poor performance. Even in low voltages the actuating waveform couldn't generate the clear droplet. In 14 V for single drop, the droplet separated into 2 drops, whereas the others produce a droplet with a clearly visible

tail. For multi-drop concept, it also found that the satellite will be generated in low voltage and the higher applied voltage will cause weeping.
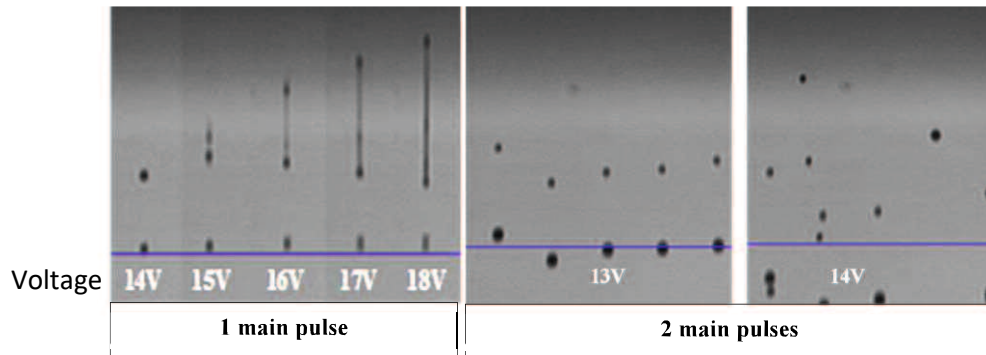
Fig. 6.1 The droplet shape for edible ink using basic waveform

The effectiveness of unmodified "W" waveform by using edible ink as an operating liquid is shown in figure 6.2. It presence that the unmodified "W" waveform can control the droplet behavior in single drop which produce a clear droplet until 14V if using 30% additional suppressing vibration (_0111). For 2 main pulses, the unmodified "W" waveform is effective until 16V of base voltage by using 50% additional suppressing vibration (_0111). Those results are in a good agreement with the result in previous chapter using UV ink. The unmodified "W" waveform are only effective to produce the clear droplet without any satellite and weeping occurrence until 3 main pulses. Therefore, for gaining the wider range in droplet size, the concept in "W" waveform as preliminary vibration must be improved.

Unmodified W waveform
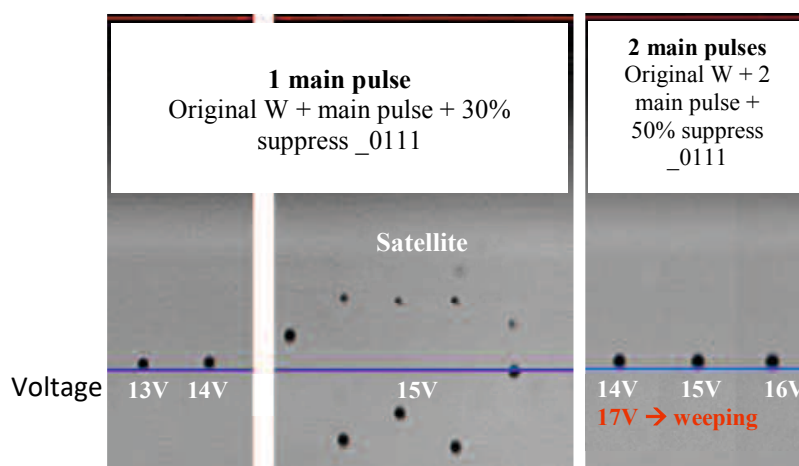
Fig. 6.2 The droplet shape for edible ink using "unmodified W" waveform in single and multi-drop

6.2 Concept Improvement of "W" Waveform

As stated at chapter V, it was assumed that "W" waveform is consisting of 2 ramps, namely front-ramp and rear-ramp. The illustration of this assumption is shown in Fig. 6.3. The liquid viscosity will cause the residual vibration that is generated both from the front or rear-ramp. The residual vibration from front-ramp will be damped by the rear-ramp. Nevertheless, the first peak from the rear ramp will generate the residual vibration in the total composite response of front-rear ramp. Therefore, for damping the first "peak" from the rear-ramp, the unmodified "W" waveform is modified by deducting applied voltage in rear-ramp. It will reduce the residual vibration that was hypothesized may avoid the satellite and weeping occurrence. The concept improvement with "modified W" waveform is shown in Fig. 6.4.
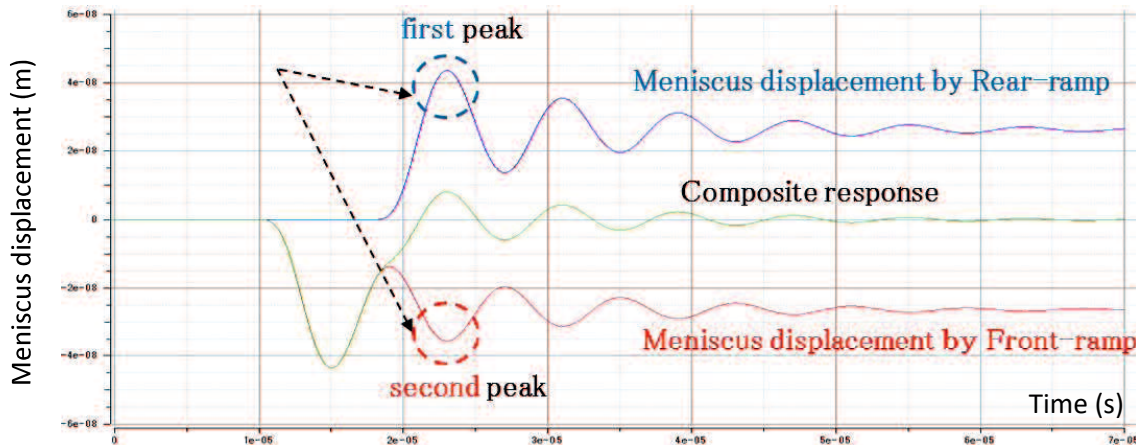
Fig. 6.3 Residual vibration of rear-ramp wave
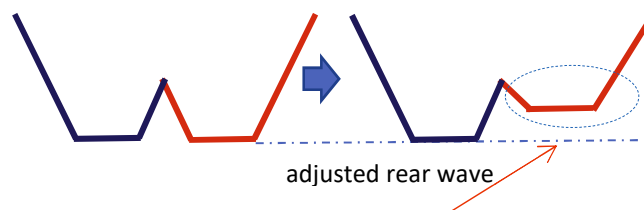
Fig. 6.4 Profile of "Modified W" waveform

Conceptually, both waveform ("U" and "W") were assumed as a waveform that consists of two wave ramps namely front-ramp and rear-ramp. However, in a real experiment with the input parameter, only "W" waveform that can be modified. The comparison of conceptual model between "unmodified W" and "modified W" waveform is shown in Fig. 6.5. We can see that the residual vibration from W waveform can be reduced by rear ramp adjustment. The optimum percentage of voltage adjustment was obtained from experimental

study. The experiment result from different input parameter is shown in table 6.2. It shows that 40% deduction of rear-ramp is more recommended for generating the clear spherical droplet. Hence, we use 40% deduction for the next design of modified W waveform.
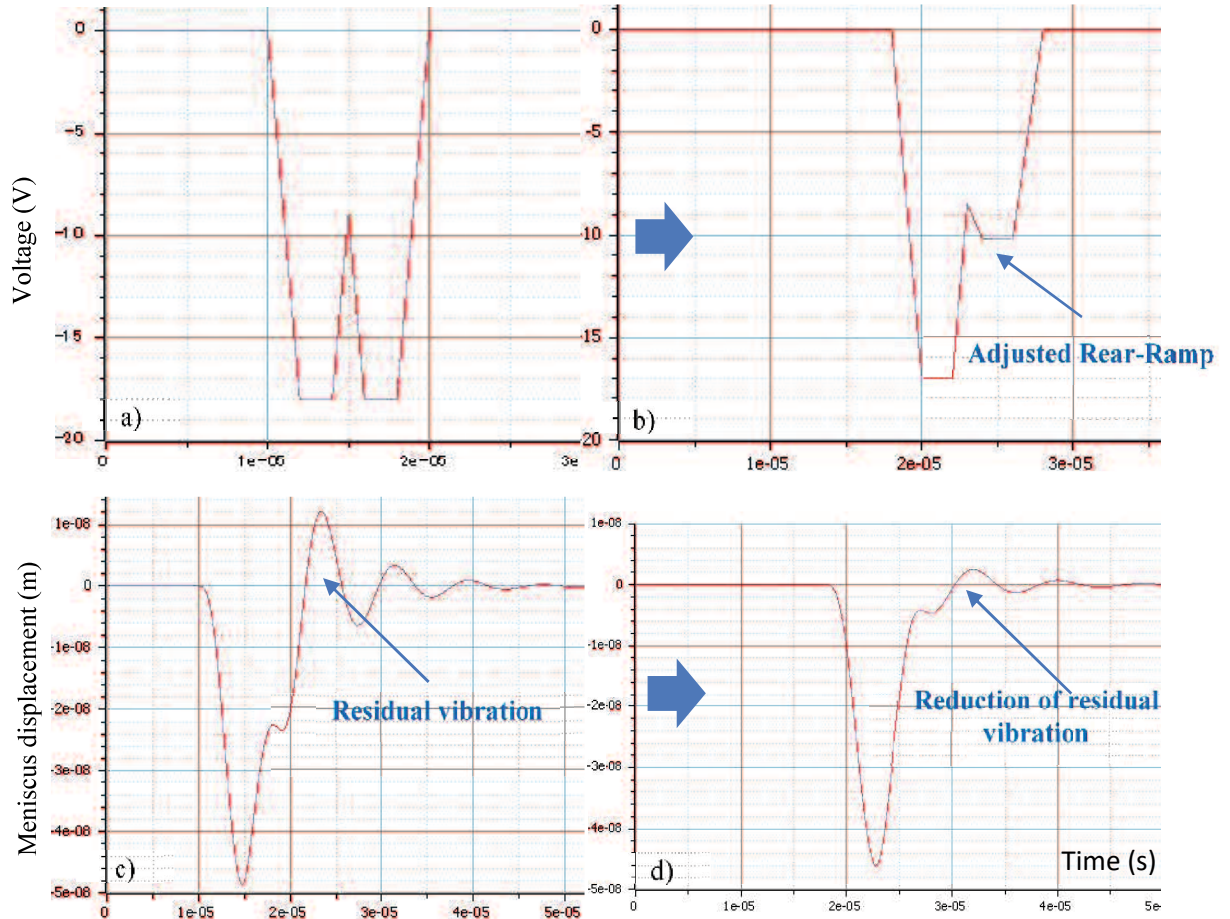
Fig. 6.5 Comparison of unmodified and modified W waveform
a) input unmodified "W" waveform   b) input of modified "W" waveform with adjusted rear-ramp
c) response unmodified "W" waveform   d) response of modified "W" waveform with adjusted rear-ramp

Table 6.2. The experiment results from different input parameter

Edible ink	1 main pulses		2 main pulses		3 main pulses	4 main pulses	5 main pulses			
Rear ramp adjustment	40%		40%		40%	40%	20%	40%	20%	40%
Voltage	Unadjusted voltage		Unadjusted voltage	Adjusted voltage	Adjusted voltage					
	No Suppress	Suppress 30%	Suppress 30%		Suppress 30%		No Suppress		Suppress 30%	
13	●	●	●	●	●	●	●	●	●	●
14	●*	●	●	●	●	S	S	●	S	●
15	S	●	W	●	●	W	-	S	-	S
16	-	●	-	●	W	-	-	-	-	-
17	-	S	-	●	-	-	-	-	-	-
18	-	S	-	S	-	-	-	-	-	-

The experiment results by using edible ink at applied voltage 14V $(1-5$ main pulses) is shown in Figure 6.6. It presence the droplet shape as expected performance with no satellite, ligament and weeping occurrence.
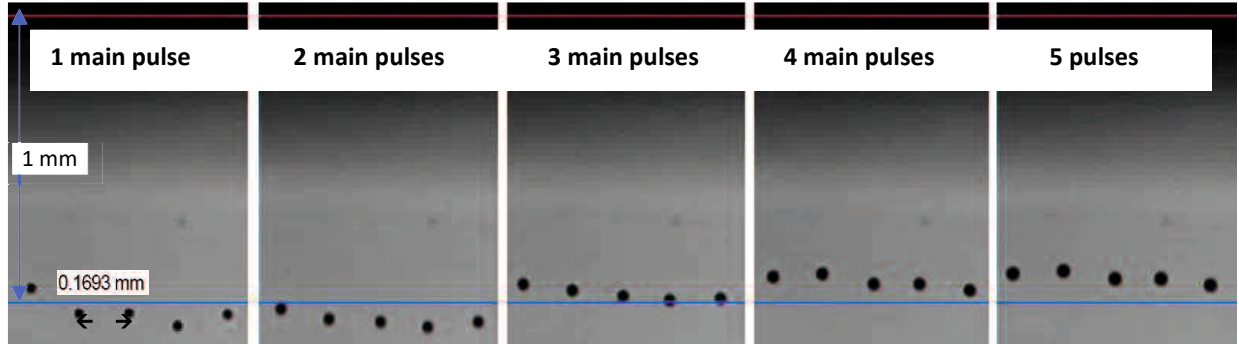
Fig. 6.6 The droplet shape for edible ink using "modified W" waveform

The comparison table of generated droplet with different waveform design (basic, unmodified W and modified W) is shown in table 6.3. It shows the effectiveness of modified W in controlling the droplet behavior until 5 pulse for getting a wider range of droplet size in multi-drop concept (grey-scale technique). It is possible to improve the performance on 4 main pulses with applied voltage 14 V by adjusting the percentage of each pulse to get the optimum condition in reducing the residual vibration and eliminate the satellite.

Table 6.3 The comparison table of generated droplet with different waveform design
(Basic, unmodified W and modified W)

| Voltage | SINGLE DROP | | | MULTI-DROP | | | | | | | | | | | |
| | | | | 2 main pulses | | | 3 main pulses | | | 4 main pulses | | | 5 main pulses | | |
	Basic	Original W	Modified W	Basic	Original W	Modified W	Basic	Original W	Modified W	Basic	Original W	Modified W	Basic	Original W	Modified W
13	S	●	●	S	●	●	X	●	●	X	S	●	X	S	●
14	S	●	●	X	●	●	X	●	●	X	S	S	X	X	●
15	L	●	●	X	X	●	X	X	●	X	X	X	X	X	S
16	L	S	S	X	X	●	X	X	X	X	X	X	X	X	X
17	L	S	S	X	X	●	X	X	X	X	X	X	X	X	X
18	L	S	S	X	X	S	X	X	X	X	X	X	X	X	X

- ● : Clear droplet
- S : Satellite
- L : Ligament
- X : Weeping

The complete concept generation of waveform design process is shown in Fig. 6.7. The process was starting from caused-effect analysis with literature and experimental study that was established to arrange the hypothesis as the proposed solution to solved the problem.
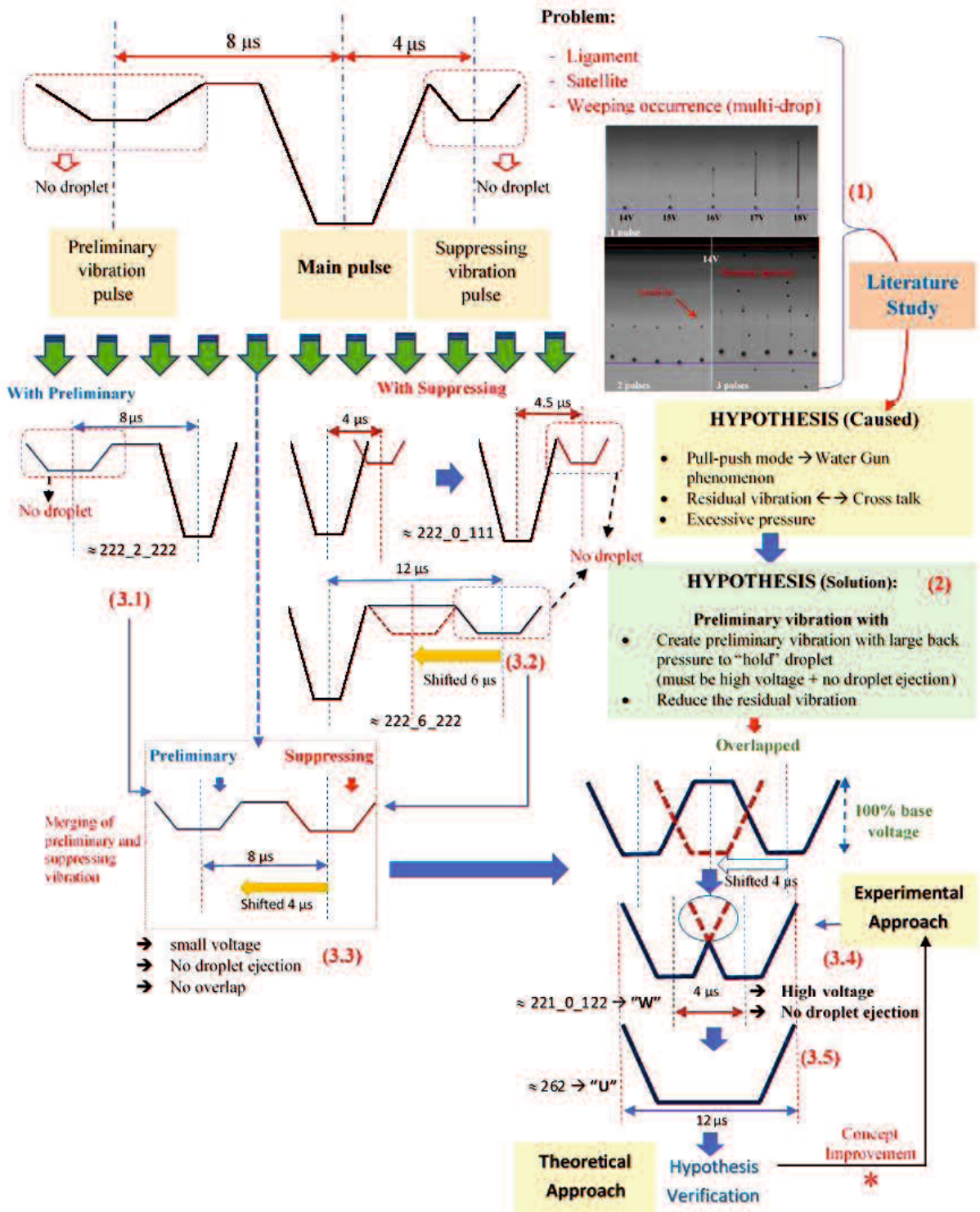
Fig. 6.7 Concept generation for New Actuation Waveform Design
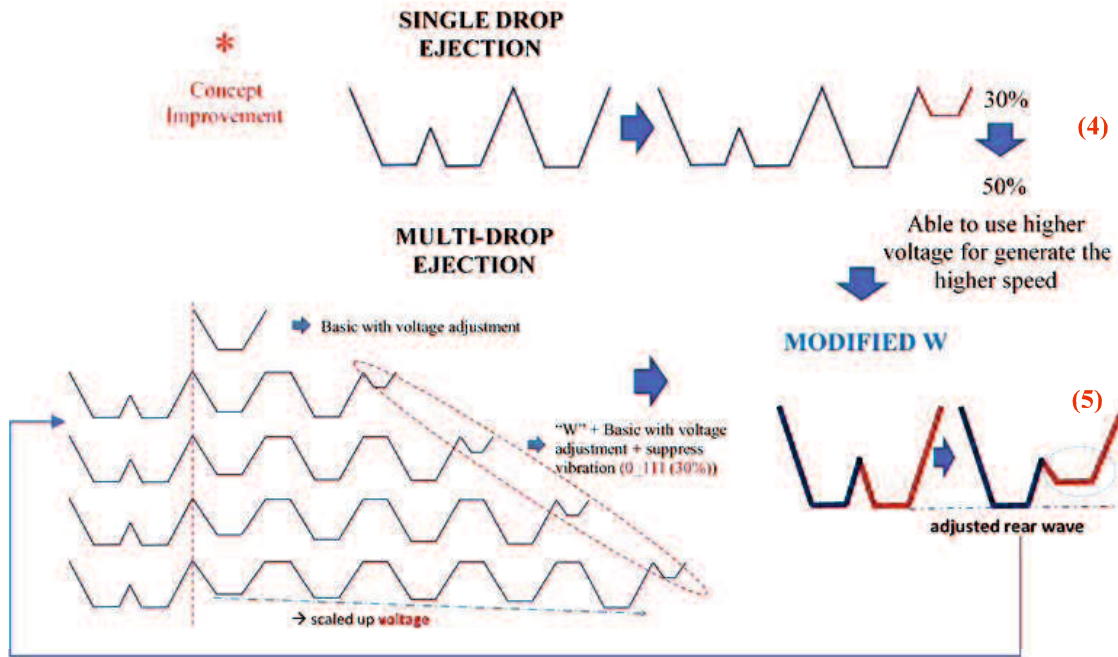
Fig. 6.8 Concept generation for New Actuation Waveform Design (improvement)

The investigation was starting from the droplet performance evaluation using basic waveform. It resulted a poor performance of droplet shape (with satellite, ligament and weeping occurrence using more than 2 pulses).

(1) Previous concept for control the droplet volume and speed using preliminary and suppressing vibration. It was determined that the preliminary and suppressing vibration able to control the droplet volume and speed). However, the performance of droplet was not as expectation (Ligament, satellite and still weeping occurrence in over than 2 pulses).

Hypothesis of Caused:

- Long ligament: higher voltage will generate longer ligament.
    - Hypothesis: Pull-push method caused water gun effect.
- Satellite: if latest ejected drop cannot reach and merged to the prior drop or main drop.
    - Hypothesis: residual vibration, and the difference of each drop velocity
- Weeping occurrence
    - Hypothesis: Excessive pressure from high voltage or high pressure, and by residual vibration.

148

(2) Hypothesis for Solution:

Furthermore, the hypothesis how to overcome the cause of problems as stated above, was summarized as follows:

- Water gun effect

  - Solution: Create the preliminary vibration that able to be functioned as back pressure to "hold" or withstand the high pressure.

- Residual vibration

  - Determine the suitable period and t_{wait} for each pulse and that able to reduce the residual vibration by wave superposition concept.

  - Obtain the appropriate voltage for each drop to adjust the speed so then it can be merged before reach the substrate. Note that the larger voltage will generate the higher speed.

- Weeping occurrence

  - Solution: Same solution as water gun effect and residual vibration, and determine the limit of applied voltage to prevent the excessive pressure.

(3) Concept preliminary and suppressing vibration

3.1 Preliminary vibration

The prior pulse before the main pulse. There is no drop ejection from this pulse only. Using input parameter t_{down}, t_{keep}, t_{up}, t_{wait} respectively 2μs before main pulse (222_2_222) with small voltage.

3.2 Suppressing vibration

The pulse that following the main pulse for suppress the residual vibration. There are 2 waveforms used in this study; 222_6_222 and 222_0_111 with small voltage of suppressing vibration so then there is no drop ejection from this pulse.

3.3. Combination of preliminary and suppressing vibration. Small voltage, no drop ejection, no overlapping.

3.4. The overlapping and large voltage of preliminary and suppressing vibration, creating the new pulse as preliminary vibration, with input parameter 221(50%)_0_122 so called "W" pulse. The theoretical and experimental approach proposed the other pulse with similar concept (long dwell time) with input parameter 262 so called "U" waveform

(4) Design the waveform for single drop ejection with input parameter 221221(50%)_0_122_0_222_0_111 and concept improvement by adjust the

suppressing vibration (0_111) from 30% in low voltage to 50% in higher voltage (18-20V)

(5) Design the waveform for multi-drop ejection with "W" or "U" pulse as preliminary vibration, then t_{wait} = 0, main pulses, t_{wait} = 0, and the additional of suppressing vibration (_0111) at the last pulse.

The modified "W" made by 40% voltage deduction at rear-ramp.

6.3. Conclusion

The influence of fluid properties on droplet performance from inkjet printer is inevitable. Hence, it is necessary to have a flexible waveform design for different fluid formulation. In the previous chapter, we use Dowanol and UV ink as the operating liquid. In this chapter, edible ink with a lower viscosity was used for verifying the effectiveness of W waveform design. From the experiment study, it was found that the unmodified "W" waveform (without adjusted rear wave) is effective to generate the clear spherical droplet until 3 main pulses. As an improvement of W waveform design, we proposed the modified "W" by rear-ramp adjusment. It is to be prooved that the modified W waveform is effective until 5 main pulses in the multi-drop ejection method. Therefore, the modified W waveform is more recommended for edible ink with a lower viscosity than Dowanol and UV ink.

The rear-ramp adjusment was done by voltage deduction, for more suitable wave superposition in reducing the residual vibration. The optimum adjustment of rear-ramp is 40% deduction from base voltage for edible ink. The rear-ramp adjustment can reduce the residual vibration. It shown by the simple conceptual simulation model using modelica.

CHAPTER VII

CONCLUSIONS

7.1 Summary of the Results

This dissertation gives the contributions to inkjet printing technology by new actuation waveform design that simpler and easier to modified for different operating liquid. By using the modified waveform design, it proved to be effective for liquid with lower viscosity than print-head specification (optimum viscosity range). It means that without changing the print-head design, the wider range of application can be reached. The new actuation waveform design in this study can control the droplet velocity and volume with a good shape for enhancing print quality. The small speed variation (< 2.5%) also can be obtained by voltage adjustment. The big challenge for applying the multi-drop method to get the wider range of droplet size from the same printhead also achieved in this study.

This dissertation is divided into 4 big conclusions which provide the results as follows:

1. The estimated actual natural period of the device (IJ-DOT-R5) in this study is 8.2643μs and 2.066 μs is proposed as the input parameter of t_d, t_k, t_u, t_w to obtain the higher droplet speed with basic waveform. The recommendation of fire limitation number standard is 100.000 drops for droplet weight measurement and 1000 μm distance from the nozzle for droplet velocity measurement. This standard is necessary to be implemented for improve the inkjet printer experiment system.

2. The small voltage pulse as preliminary vibration with 30% of base voltage 14 – 15V and 40% of base voltage 14V are effective to increase the droplet velocity and volume whereas 50% of base voltage 14 – 18V will generate the lower velocity but in a greater volume than basic waveform. On the other hand, 30% of base voltage on suppressing vibration for "Suppress A" (222_6_222) waveform can be utilized to reduce the residual vibration with the same velocity as basic waveform. 50% of suppressing vibration with front and back "Suppress B" (222_0_111) waveform demonstrates its effectiveness to reduce the residual vibration. All clear droplet was generated from "front suppress B" waveform. With an increase of applied voltage as well as the effect of head temperature, the droplet velocity and volume also increase. Furthermore, the ligament of droplet also longer with the higher applied voltage because of the higher pressure. The optimum

applied voltage with preliminary and suppressing vibration is 14 V only similar to the basic waveform. Hence, the concept design was developed to improve the droplet performance.

3. The actuation waveform design that was developed in this study is to be proved effectively to improve the droplet performance, by generating the droplet without satellite, ligament and weeping occurrence even in the multi drop concept. The larger drop and lower speed (compared to basic waveform in same applied voltage) for single drop ejection shown that the inkjet printer with pull-push system that used in this study, can generate the droplet such as push-pull system (therefore, the waveform design called as push-pull reflection waveform method). However, it is possible to increase the droplet speed by using the higher voltage than basic waveform to generate the clear droplet. The different droplet size with similar velocity and clear droplet can be obtained by appropriate voltage adjustment. The higher speed is also possible by suitable adjusted voltage of each sequence pulse. The different operating liquid will represent some different behavior related to its physical properties. From the experiment result by using Dowanol, UV ink and edible ink, the additional concept to create "tuning factor", for controlling droplet in the proposed waveform design using "W waveform" are as follows:

   - An additional "W" waveform + suppressing vibration (0_111) to reduce residual vibration and avoid weeping occurrence is effective with:
     - 30% suppress vibration at 17-18V.
     - 50% suppress vibration at 19-20V.
   - The modified "W" waveform (adjusted rear wave) is more recommended for edible ink. The rear wave adjusment was done by scaled down or deduction of the voltage, to get the more suitable wave superposition in reducing the residual vibration. The optimum adjustment of rear wave is 40% scaled down from base voltage for edible ink.

4. The effect of input parameter in the actuation waveform design to the droplet behavior could be predicted with the simulation model using modelica. The mechanism of wave superposition particularly in creating the large "back pressure" and reducing the residual vibration is easier to understand. With the inkjet simulation model, the optimization of waveform design in the future will be easier.

The illustration of the multi-drop actuation waveform design mechanism is described in Fig. 7.1.
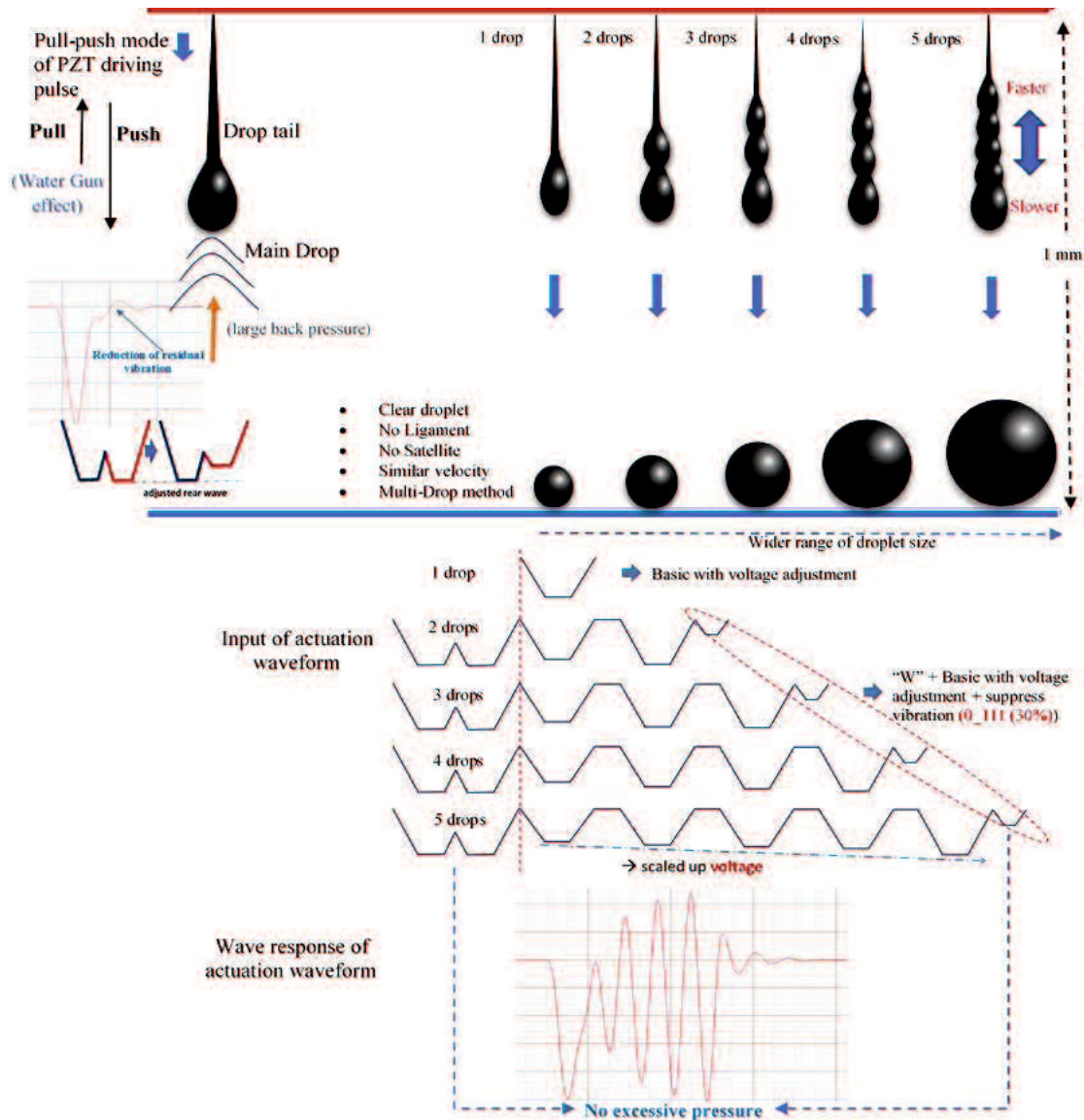
Fig. 7.1 Illustration of the actuation waveform design mechanism

7.2 Future Consideration

The suggestion for future studies are:

1. Using the similar waveform design in different voltage direction (polar) namely positive waveform such as "M" waveform to create the better performance in push-pull mode of Piezoelectric driving pulse.

2. Apply the concept of waveform design to the apparatus that provide more than 8 pulses of actuating waveform.

3. Add the preliminary vibration before "W" or "U waveform for increase the droplet speed and get the larger volume.

REFERENCE

[1] Van der Meulen, M.J., PhD thesis, "Meniscus motion and drop formation in inkjet printing", Physics of Fluids, University of Twente, P.O. Box 217, 7500 AE Enschede, The Netherlands, 2014

[2] Hoath, S.D., "Fundamentals of Inkjet Printing, The Science of Inkjet and Droplets", book published by Wiley-VCH, 2016

[3] N.F. Morrison and O.G. Harlen, in Proc 27th Int. Conf. on Digital Printing Technologies, NIP27, Minneapolis, MN, USA, 2011, 360-364, 'Inkjet printing of non-Newtonian fluids'.

[4] Mishra, S., et.al., "High-Speed and Drop-On-Demand Printing with a Pulsed Electrohydrodynamic Jet", Journal of Micromechanics and Microengineering, 20, 8pp, 2010

[5] Hutching, I.M., and Martin, G.D., "Inkjet Technology for Digital Fabrication, John Wiley & Sons, Ltd., Publication, 2013

[6] Holthoff, E.L, et al., "Standardized Sample Preparation Using a Drop-on-Demand Printing Platform", *Sensors* journal, *13*, 5814-5825, 2013

[7] Meinhart C.D. and Zhang, H., "The Flow Structure Inside a Microfabricated Inkjet Printhead", Journal of Microelectromechanical System, Vol. 9, No. 1, IEEE, 2000

[8] Hsiu M. and Hwang W.S., "Effects of Pulse Voltage on the Droplet Formation of Alcohol and Ethylene Glycol in a Piezoelectric Inkjet Printing Process with Bipolar Pulse", Material Transactions, Vol. 49, No. 2, pp. 331-338, 2008

[9] Liou, T.M., et. al., "Effects of actuating waveform, ink property, and nozzle size on piezoelectrically driven inkjet droplets", Microfluid Nanofluid, pp 575-586, Springer, 2010

[10] Jo, B.W. et. al., "Evaluation of jet performance in drop-on-demand (DOD) inkjet printing", Korean J. Chem. Eng., 26 (2), pp 339-348, 2009

[11] Xu, C et al., "Study of Droplet Formation Process during Drop-on-Demand Inkjetting of Living Cell-Laden Bioink", American Chemical Society, pp 9130 − 9138, 2014

[12] Yang, G. and Liburdy J.A., "Droplet Formation from a Pulsed Vibrating Micro-Nozzle", Journal of Fluids and Structures 24, pp 576-588, © Elsevier, 2008

[13] Kwon K.S., "Experimental analysis of waveform effects on satellite and ligament behavior via *in situ* measurement of the drop-on-demand drop formation curve and the Instantaneous jetting speed curve", Journal of Micromechanics and Microengineering, 20, 115005 (14 pp), 2010

[14] Khalate, A.A., et. al., "Performance improvement of a drop-on-demand inkjet printhead using an optimization-based feedforward control method", Control Engineering Practice, 19, pp 771-781, 2011

[15] Kim, B.H et al., "Dynamic characteristics of a piezoelectric driven inkjet printhead fabricated using MEMS technology", Sensors and Actuators A 173, pp 244-253, Elsevier, 2011

[16] Chung Wu, H ert. Al., "Effect of Actuating Pressure Waveform on the Droplet Behavior in a Piezoelectric Inkjet", Material Transaction Vol. 51 No. 12 pp 2269 − 2276, 2010

[17] Khalate, A.A., et al, "A Waveform Design Method for a Piezo Inkjet Print-head Based on Robust Feedforward Control", Journal of Microelectromechanical Systems, Vol. 21No. 6, pp 1365-1374, 2012

[18] Korvink, J.G., et.al., "Inkjet-based Micromanufacturing, Wiley-VCH, 2012

[19] Kwon, K.S. & Kim, W.,"A Waveform design method for high speed inkjet printing based on self-sensing measurement", Sensor and Actuators A 140, pp 75-83, 2007

[20] Gan et al., "Reduction of droplet volume by controlling actuating waveforms in inkjet printing for micro-pattern formation", J. Micromech. Microeng. **19** (2009) 055010 (8pp)

[21] Casterjòn-Pita, A.A. et.al.,"A Novel Method to Produce Small Droplet from Large Nozzles", Review of Scientific Instrument, 83, 115105, 2012

[22] Martin, G.D., et.al., "Inkjet Printing – The Physic of Manipulating Liquid Jets and Drops", Journal of Physics: Conference Series 105, IOP Publishing Ltd, 2008

[23] Shin, P. et.al., "Control of Droplet Formation for Low Viscosity Fluid by Double Waveforms Applied to a Piezoelectric Inkjet Nozzle", Microelectronics Reliability 51, pp 797-804, Elsevier Ltd, 2011

[24] Chung Wu, H. et.al., "Simulation of Droplet Ejection for a Piezoelectric Inkjet Printing Device, Material Transaction Vol. 45 No. 3 pp 893 − 899, 2004

[25] Chung Wu, H. et.al., "Development of a Three-Dimensional Simulation System for Micro-Inkjet and Its Experimental Verification", Material Science and Engineering A 373, pp 268 − 278, Elsevier, 2004

[26] Jo, B.W. et.al., "Evaluation of Jet Performance in Drop-on-Demand (DoD) Inkjet Printing", Korean J. Chem. Eng., 26(2), pp 339 − 348, 2009

[27] Hoath, S.D., et.al., "Drop Speeds from Drop-on-Demand Ink-jet Print Heads", Journal of Imaging Science and Technology, 57 (1), 2013

[28] Lin Tsai, H., et.al, "Fabrication of Microdots Using Piezoelectric Dispensing Technique for Viscous Fluids", Material Journals, Vol 8 (10), 2015

[29] Jiuan Lin, H., et al., "The Effects of Operating Parameters on Micro-Droplet Formation in a Piezoelectric Inkjet Printhead Using Double Pulses Voltage Pattern, Material Transactions, Vol. 47, No. 2, pp 375 − 382, Japan Institute of Metal, 2006

[30] Shyng Leu, T., et.al., "Experimental Study of Meniscus Dynamic Behaviors in Squeeze-Mode Piezoelectric Inkjet Printhead", Material Science Forum Vol. 594, pp 155-162, Trans Tech Publication, 2008

[31] Poozesh, S., "Inkjet Printing: Facing Challenges and Its New Applications in Coating Industry", Doctoral Dissertation of Mechanical Engineering, paper 72., University of Kentucky, 2015

[32] Magdassi, S, "The Chemistry of Inkjet Inks", World Scientific Publishing Co. Pte.Ltd., 2009

[33] Jan G. et.a., "Inkjet-based Micromanufacturing" Wiley-VCH Verlag & Co., 2012

[34] Bogy, D & Talke, F.E., "Experimental and Theoretical Study of Wave Propagation Phenomena in Drop-on-Demand Ink Jet Devices", Ibm Journal of Research and Development, 1984, published on line at: https://www.researchgate.net/publication/224103962

[35] Wijshoff, "The Dynamics of the Piezo Inkjet Printheads Operation", Physics Reports , 491, pp 77-177,2010

[36] Le, H.P., "Progress and Trends in Ink-jet Printing Technology", Journal of Imaging Science and Technology 42: 49—62, 1998

[37] J.R. Castrej´on-Pita, et.al "Future, Opportunities and Challenges of Inkjet Technologies", Atomozation and Sprays, 2013

[38] Grant, A., "UV Ink-jet Inks Evolve to Meet Applications", European Coating Journal, 05, pp 44-52, 2004

[39] Ezzeldin M. et al, "Experimental-based feedforward control for a DoD inkjet printhead", Control Engineering Practice 2, pp 940–952, 2013

[40] Ezzeldin, M. et.al, "Improving the Performance of an Inkjet Print-head using Model Predictive Control", 18th IFAC World Congress, 2011

[41] Wassink, M.B., "Inkjet Print-Head Performance Enhancement by Feedforward Input Design Based on Two-Port Modeling, PhD. thesis, Delft University of Technology, The Netherlands, 2007

[42] Chen, A.U., and Basara, O.A," A New Method for Significantly Reducing Drop Radius without Reducing Nozzle Radius in Drop-on-Demand Drop Production", Physics of Fluids Vol. 14 No. 1, 2002

[43] Ono, Y., et.al., "Simulation of a Liquid Droplet Ejection Device using Multi-Actuator", Japanese Journal of Applied Physics 55, 2016

[44] Xu, C., et.al." Electric Field-assisted Droplet Formation using Piezoactuation-based Drop-on-Demand Inkjet Printing", Journal of Micromechanics and Microengineering. 24, 9 pp, 2014

[45] Liou, T.M.,"Three-Dimensional Simulations of the Droplet Formation during the Inkjet Printing Process", Int.Comm.Heat Mass Transfer, Vol. 29, No. 8, pp. 1109-1118, 2002

[46] Zeng, L., et.al., "Multi-Diciplinary Simulation of Piezoelectric Driven Microfluidic Inkjet", Proceeding of the ASME, IDETC/CIE, 2009

[47] Herran,L., "Jet Instability and Droplet Formation for Bio-Printing Application", PhD Dissertation, Clemson University, 2013, accessed from http://tigerprints.clemson.edu/all_dissertations

[48] Zhang, H., et.al.," Numerical Investigation of the Influence of Companion Drops on Drop-on-Demand Ink Jetting", Journal of Zhejiang University-SCIENCE A (Applied Physics & Engineering) No. 13, pp 584-595, 2012

[49] He, M., et. al., "Drop-on-Demand Inkjet Performance Enhancement by Dynamic Lumped Element Modeling for Printable Electronics Fabrication", Hindawi Publishing Corporation, Mathematical Problems in Engineerivng, 16 pp, 2014, http://dx.doi.org/10.1155/2014/270679

[50] Le, H.P.,"Progress and Trends in Ink-jet Printing Technology, Journal of Imaging Science Technology, 42, 1998

[51] R. The et.al.,"Piezoelectric Inkjet-based Single-cells Printing by Image Processing for High Efficiency and Automatic Cell Printing, 17th International Conference on Miniaturized Systems for Chemistry and Life Sciences 27-31, 2013

[52] Jalili, N., "Piezoelectric-based Vibration Control from Macro/Nano Scale Systems", Science Business Media, LLC, © Springer, 2010

[53] Yamaguchi, S., et.al.," Cell Patterning Through Inkjet Printing of One Cell Per Droplet", Biofabrication 4, 045005 (8pp), IOP Publishing, 2012

[54] Furlani, E.P., "Fluid Mechanics for Inkjet Printing," Fundamentals of Inkjet Printing: The Science of Inkjet and Droplets, ed. Hoath, SD., Wiley pp 13- 56, 2016

[55] Morita, N., et.al., "Inkjet Printheads," Fundamentals of Inkjet Printing: The Science of Inkjet and Droplets, ed. Hoath, SD., Wiley pp 57- 89, 2016

[56] Wei, H., et.al.,"A Waveform Design Method for High DPI Piezoelectric Inkjet Print-head Based on Numerical Simulation", Microsyst Technology, published online © Springer, 2017

[57] Xu, J. and Attinger, D., "Drop on Demand in a Microfluidic Chip", Journal of Micromechanics and Microengineering, 18, 065020, 10 pp, IOP Publishing, 2008

[58] Tsai, M.H., et.al, "The Micro-droplet Behavior of a Molten Lead-free Solder in an Inkjet Printuing Process", Journal of Micromechanics and Microengineering, 19, 125021, 10 pp, IOP Publishing, 2009

[59] Joseph, A., et.al, "Advantage of Black-Box of Mixed-Signal Integrated Circuit", International Journal of Scientific Development Research, Vol. 1, pp 763 − 771, 2016

[60] Fritzson P., Bunus P., "Modelica − A General Object-Oriented Language for Continuous and Discrete-Event System Modeling and Simulation", In Proc. Annual Simulation Symposium (2002): 365-380.

[61] Fritzson P., "Introduction to Modeling and Simulation of Technical and Physical Systems with Modelica", A John Wiley & Sons, Inc., Publication, 2011.

[62] Kousa J. A., "Virtual Computational Test bed for Building Integrated Renewable Energy Solutions", Thesis report of Eindhoven University of Technology, 2014.

[63] Otter M., "Modeling, Simulation & Control with Modelica 3.0 & Dymola 7", 2009.

[64] Elmqvist H., et al, "Object Oriented & Hybrid Modeling in Modelica", Journal Europeen des Systemes Automaties, AP II-JESA, volume 35, 2001.

[65] Zupančič B., Sodja A.," Computer-aided Physical Multi-domain Modelling: Seome Experiences from Education and Industrial Applications", Simulation Modelling Practice and Theory 33, (2013): 45-67.

[66] Liu G. R., et al, "The Finite Element Method, A Practical Course", Els evier Science Ltd. All rights reserve, 2003.

[67] Oktavianty, O., et.al, "Acausal and Causal Model Construction with FEM Approach Using Modelica", International Journal of Medical, Health, Biomedical, Bioengineering and Pharmaceutical Engineering Vol.10, No. 3, 2016

[68] Kaneko, J., et.al, Proposal of Design Method in the Semi-Acausal System Model", International Journal of Electrical, Computer, Electronics and Communication Engineering Vol. 9, No.2, 2015

[69] Kwon, K.S., et.al, "Visualisation and Measurement", in Fundamentals of Inkjet Printing: The Science of Inkjet and Droplets, (S.D. Hoath (Ed), Wiley-VCH (2016)

[70] Hoath, S.D.," Standardization Inkjet Drop Speed Measurement Methods for Printed Electronics", Digital Fabrication Conference, No.1, Vol. 2015

[71] Tsai, M.H.," Effect of Pulse Voltage on Inkjet Printing of a Silver Nanopowder Suspension", Nanotechnology, Vol. 19 No. 33, IOP Publishing, 2008

[72] Dong, H. and Carr, W.W., "An Experimental Study of Drop-on-Demand Drop Formation", Physics of Fluids 18, 072102, 2006

[73] Smith, P.J. and Stringer, J., "Application in Inkjet Printing"," Fundamentals of Inkjet Printing: The Science of Inkjet and Droplets, ed. Hoath, SD., Wiley pp 397- 414, 2016

[74] Dijksman, J.F., and Pierik, A., "Dynamic of Piezoelectric Print-head", "Inkjet Technology for Digital Fabrication, Ed. By Hutching, I.M., and Martin, G.D., pp 45-86, John Wiley & Sons, Ltd., Publication, 2013

[75] Mackley, M.R., et.al,"Inkjet Fluid Characterization", in Fundamentals of Inkjet Printing: The Science of Inkjet and Droplets, (S.D. Hoath (Ed), pp 339-364, Wiley-VCH (2016)

[76] Jang, D., et.al., "Influence of Fluid Physical Properties on Ink-Jet Printability", Langmuir 25 (5), pp 2629-2635, ACS Publications, 2009. Downloaded from http://pubs.acs.org

[77] Tirtaatmadja, V et.al.,"Drop Formation and Breakup of Low Viscosity Elastic Fluids: Effects of Molecular Weight and Concentration", Physics of Fluids 18, 043101, 2006 view online: http://dx.doi.org/10.1063/1.2190469

[78] Moon, J.H., et.al.,"Spreading and Receding Characteristics of a non-Newtonian Droplet Impinging on a Heated Surface", Experimental Thermal and Fluid Science 57, pp 94-101, © Elsevier Inc., 2014

[79] Morrison, N.F., and Harlen, O.G., "Viscoelasticity in Inkjet Printing", Proceedings of PACAM XI, American Congress of Applied Mechanics, 2010

[80] Delrot, P., et.al.,"Inkjet Printing of Viscous Monodisperse Microdroplets by Laser-Induced Flow Focusing", Physical Review Applied 6, 024003, 2016

[81] Kwon, K.S.,"Waveform Design Method for Piezo Inkjet Dispenser Based on Measured Meniscus Motion", Journal of Microelectromechanical Systems, Vol. 18 No. 5, 2009.

[82] Szczech et al., "Fine-Line Conductor Manufacturing Using Drop-On-Demand PZT Printing Technology" IEEE Transactions on Electronics Packaging Manufacturing, vol. 25, no. 1, 2002

[83] Wijshoff, H., "Drop Formation Mechanism in Piezo-acoustic Inkjet", NSTI-Nanotech Vol. 3, 2007

[84] Ioana S., "A New Viscosity-Temperature Relationship for Vegetable Oil" Journal of Petroleum Technology and Alternative Fuels Vol. 3(2), pp. 19-23, 2012

[85] Singh, R.N., and Sommer, F., "Viscosity of Liquid Alloys: Generalization of Andrade's Equation" Monatsh Chem., 143:1235–1242 Springer-Verlag, 2012

[86] Khalate, A.A. et al., "Minimization of cross-talk in a piezo inkjet printhead based on system identification and feedforward control, Journal of Micromechanics and Microengineering 22, 115035 (21pp), 2012

[87] Raymond, M. "Waveform and Drop Optimization", Tech Talk in Ink Jet Printing Conference, 2016

[88] Kwon, K.S., "Vision Monitoring", in "Inkjet-based Micromanufacturing, pp127-144, Wiley-VCH, 2012

[89] Toshiaki, N., et.al., "Study on Clarification of the Core Technology in a Monozukuri Company", proceeding of International Conference on Industrial Engineering and Management (ICIEM), pp 1780-1786, 2017

[90] Xiao, Y., "A Cell Patterning System Based on Thermal Ink-jet Technology", Dissertations, published online at: http://preserve.lehigh.edu/etd

[91] Yamaguchi, et.al., "Stable ejection of micro droplets containing microbeads by a piezoelectric inkjet head", J. Micro-Nano Mech., 7 pp 87–95, © Springer, 2012

[92] Lie, J., "Numerical simulation of breakup of a viscous drop in simple shear flow through a volume-of-fluid method", Physics of Fluids Volume 12, No.2, 2002

[93] Hoath, S.D., et.al, "Jetting of Complex Fluids", Journal of Imaging Technology, 2013

[94] published on line at: http://eprints.whiterose.ac.uk/id/eprint/76408

[95] Jung, S., "Fluid Characterisation and Drop Impact in Inkjet Printing for Organic Semiconductor Devices", University of Cambridge, 2011

[96] Chung Wu, H., et. al., "Study of Micro-Droplet Behavior for a Piezoelectric Inkjet Printing Device Using a Single Pulse Voltage Pattern", Materials Transactions, Vol. 45, No. 5, pp. 1794 − 1801, The Japan Institute of Metals, 2004

[97] Khalate, A.A.,"Model-based Feedforward Control for Inkjet Printheads, PhD thesis, ISBN: 978-94-6186-245-7, 2013

[98] Jingmei, S., et.al.," The Influence of the Viscosity of Edible Ink to Ink-jet Printing Drop State", Advanced Materials Research, ISSN: 1662-8985, Vols. 535-537, pp 2559-2562, 2012

[99] Reis, N., et.al.,"Inkjet-Delivery of Particle Suspensions by Piezoelectric Droplet Ejectors", Journal of Applied Physics, 97, 094903, AIP Publishing, 2005, published on line at: http://aip.scitation.org/doi/full/10.1063/1.1888026

[100] Derby, B. "Inkjet Printing of Functional and Structural Materials: Fluid Property Requirements, Feature Stability, and Resolution", Annual Review of Material Research, 40, pp 395-414,2010

[101] Fujii, M," Issues and Approaches Imposed on Ink Jet Technologiues for the Progress of Printed Electronics", Transacsions of the japan Institute of Electronics Packaging, Vol. 3, No. 1, 2010

[102] Ozawa, K., et.al.,"Development of a Femtoliter Piezo Ink-jet Head for High Resolution Printing", proceeding of 23th International Conference on Digital Printing Technologies, pp 898-901, 2007

[103] Kwon, K.S et.al., "Jetting Frequency and Evaporation Effects on the Measurement Accuracy of Inkjet Droplet Amount", Journal of Imaging Science and Technology, 59 (2), 2015

[104] Hoath, S.D. et.al.," How PEDOT: PSS Solutions Produce Satellite-Free Inkjets", Organics Electronics 13, pp3259-3362, © Elsevier, 2012

[105] Verkouteren, R.M. et.al., "Inkjet Metrology: High Accuracy Mass Measurement of Microdroplets Produced by Drop-on-Demand Dispenser", Analytical Chemistry, Vol. 81, No. 20, pp 8577-8584, 2009

[106] Brünahl, J. and Grishin, A.M., "Piezoelectric Shear Mode Drop-on-Demand Inkjet Actuator", Sensors and Actuators A 101, pp 371-382, ©Elsevier, 2002

[107] Wijshoff, "Structure and Fluid-Dynamics in Piezo Inkjet Printheads", Herman Wijshoff dissertation, Océ Technologies B.V, 2008

[108] Ezzeldin, M.,"Performance Improvement of Professional Printing Systems: from theory to practice", dissertation, Océ Technologies B.V, 2012

[109] Herran, C.L., et.al., "Performance Evaluation of Bipolar and Tripolar Excitations during Nozzle-jetting-based Alginate Microsphere Fabrication", Journal of Micromechanics and Microengineering. 22, 2012.

[110] Published on line at:

[111] http://iopscience.iop.org/article/10.1088/0960-1317/22/085025/pdf.

[112] Shin, P. et.al., "Operability diagram of drop formation and its response to temperature variation in a piezoelectric inkjet nozzle", Microelectronics ReliabilityMicroelectronics Reliability 51, pp 437–444, 2011.

[113] Driessen, T and Jeurissen, R., "Drop Formation in Inkjet Printing" in Fundamentals of Inkjet Printing: The Science of Inkjet and Droplets, (S.D. Hoath (Ed), pp 93-115, Wiley-VCH (2016)

[114] Martin, G.D., and Willis, M., "Inkjet Technologies: What Next?" in Fundamentals of Inkjet Printing: The Science of Inkjet and Droplets, (S.D. Hoath (Ed), pp 419-444, Wiley-VCH (2016)